Research Department

Technical Report No. 65

The ECMWF Analysis-Forecast System during AMEX

by

Kamal Puri*, Peter Lönnberg** and Martin Miller

May 1990

* On leave from Bureau of Meteorology Research Centre, Melbourne, Australia
** Current affiliation Finnish Meteorological Service, Helsinki, Finland

CONTENTS

INTRODUCTION

Although the performance of numerical weather prediction (NWP) models in the tropics considerably lags the performance in the extratropics, significant progress has been made in the recent years. For example, the systematic errors of the ECMWF model in the tropics have been considerably reduced (see Tiedtke et al., 1988) when compared to errors in the earlier version of the model reported by Kanamitsu (1985) and Heckley (1985). A number of factors such as increased horizontal and vertical resolution and improvements in analysis have been partly responsible for this. However, the major impact on model performance in the tropics has resulted from improvements in the parametrization of cumulus convection, interactive clouds and the radiation scheme and (perhaps most importantly) through the inclusion of shallow convection in the model (see Mohanty et al., 1985).

In spite of the progress made in tropical NWP several problems still remain. Inadequate parametrization of physical processes, particularly cumulus convection, leads to large systematic errors in model forecasts in the tropics. The Kuo cumulus parametrization remains the most widely used parametrization of cumulus convection and considerable attention has focused on improving its performance by attempting to obtain an optimum value of the moistening parameter b which partitions moisture supply between moistening and heating and by refining the definition of the cloud base used in the scheme. In recent years at ECMWF much attention has been focused on alternative convection schemes namely the Betts-Miller adjustment scheme (Betts, 1986; Betts and Miller, 1986) and a massflux scheme (Tiedtke, 1989); an assessment of the former scheme with respect to tropical cyclones will be given in Part II of this report. In spite of recent improvements there are a number of aspects of cumulus parametrization which are not well understood and remain poorly parametrized. Cumulus momentum transport and interaction between cumulus convection and boundary layer flow are just two examples of aspects of cumulus convection which are poorly understood. The parametrization of radiative processes also has an impact on model forecasts in the tropics as was shown for the ECMWF model by Mohanty et al. (1985), for example. The radiation scheme in use at ECMWF in 1987 has a systematic error in that it underestimates the outgoing longwave radiation near the top of the model. Preliminary work with an improved radiation scheme shows encouraging impact on the model circulation in the tropics (Morcrette, 1988, private communication). Thus a considerable amount of theoretical, modelling and observational work needs to be carried out in order to properly understand the role of different physical processes in order to improve their parametrization in numerical models.

Apart from physical parametrizations, deficiencies in analyses also contribute to forecast errors. The analysis of even the primary variable in the tropics poses special problems. Firstly, the data base for key variables such as wind field (particularly divergent wind)

and moisture is inadequate. Secondly, deficiencies in forecast models have a deleterious effect on analyses, particularly in a four dimensional data assimilation system. Furthermore, some analysis systems have a midlatitude bias which is imposed through the use of assumptions such as nondivergence or geostrophy in the analysis increments. Some recent developments in analysis in the tropics include the implementation of divergent structure functions in optimum interpolation (Undén, 1989) and attempts to use outgoing longwave radiation (or satellite) data as proxy data in analysing the divergence field and to specify heating rates in normal mode initialization (Julian, 1984; Puri and Miller, 1989). The initialization step is also being extended to include adjustment of the moisture field in order to obtain better agreement between model rainfall in the early stages of the integration and observed rainfall data (Krishnamurti et al., 1983; Puri and Miller, 1989).

Although model performance for large scale quasi-stationary systems in the tropics displays large systematic errors, the performance with respect to transient disturbances is more promising. For example, Kanamitsu (1985) found that the ECMWF analysis scheme is capable of detecting transient disturbances such as easterly waves. An objective verification of the forecasts using correlations between time filtered analyses and forecasts showed that these waves are well predicted up to about four days indicating that the model deficiencies at the very large scales have a relatively small impact on the properties of the transient disturbances. Similarly Reed et al. (1988) carried out a study based on a later version of the ECMWF analysis-forecast system to evaluate its performance in analysing and forecasting easterly waves and their related tropical storms during a two month period in the summer of 1985. They concluded that the system has an impressive capability for forecasting tropical wave disturbances and other synoptic-scale circulation features.

The ability of current models to predict transient waves in the tropics is very encouraging as it suggests that improved prediction of tropical cyclones with these models may be possible. Models such as those in use at ECMWF, the U.K. Meteorological Office (UKMO) and NMC, United States have now attained resolutions where the outer circulations of small scale systems such as tropical cyclones are beginning to be resolved. However, it should be noted that these models are still not at a stage where they can resolve the inner structure and thus cannot simulate details of the structure of the cyclones. However, the motion of cyclones is believed to be strongly influenced by the large scale flow and therefore prediction of motion by such models might be possible. Hall (1987) has carried out a study of the performance of the UKMO model in handling the motion of all major tropical cyclones in the North Atlantic and North Pacific during 1986. In all, 169 cyclones were considered. Hall concluded that the model provides useful skill in predicting the movement of tropical cyclones, especially when they engage upper level troughs in the middle latitude flow. This is particularly evident for 48 and 72 hour forecasts when persistence and climatology can lead to large errors.

During the period January 10 to February 15 1987 an extensive observation program was carried out in the Australian region corresponding to phase II, the major field phase, of the Australian Monsoon Experiment (AMEX, see Holland et al., 1986). AMEX was carried out by the Bureau of Meteorology Research Centre (BMRC) in collaboration with Monash University. Phase II was designed specifically to provide a research data base of sufficient resolution to document the basic structure of the monsoon circulation in the Australian tropics and to diagnose the effects of the interaction between the convective and large scale flow. The AMEX atmospheric sounding array shown in Fig. 1 (taken from Holland et al., 1986) was designed to take advantage of the existing Australian, Indonesian and Papua New Guinea network and to concentrate on the climatologically active region in the Gulf of Carpentaria. The routine atmospheric sounding network is shown by squares and open circles in Fig. 1 and the upgraded AMEX component by solid circles. The core of the network is a group of six stations upgraded or established around the Gulf taking wind and thermal soundings at six hourly intervals. Additionally an outer array of seven existing Bureau of Meteorology stations were upgraded to the same frequency. In addition to the upper air network, radars with remote sensing capability to monitor four-dimensional structure of precipitation were an integral part of the experiment.

The period covered by phase II of AMEX spanned the onset of the Australian summer monsoon which occurred on January 14 (as indicated by a number of indices). There was a weak break from about January 24 to January 31 followed by an active period. The whole AMEX period was characterized by a high level of convective activity in the north of Australia. Four tropical cyclones (TC's) formed during the period covered by AMEX namely TC's Irma (Jan 19 to Jan 21), Connie (Jan 17 to Jan 21), Damien (Feb 1 to Feb 5) and Jason Feb 7 to Feb 13). Two of the cyclones (Irma and Jason) occurred in the Gulf of Carpenteria within the enhanced AMEX network and were therefore well observed. Further details of observations taken and significant weather events during AMEX can be found in Gunn et al. (1989) and details of the torpical cyclones have been documented by Manchur (1987). Thus the AMEX data provide a good base for performing numerical weather prediction (NWP) studies on the onset and subsequent development of the monsoon and tropical cyclones.

The additional sounding and SYNOP data collected during AMEX were transmitted in real time to ECMWF and were included in the data base to produce the operational ECMWF analyses of this period. However, the amount of AMEX data received was highly variable. In January only a small percentage of the data was received and although reception improved in February, the amount of data received was still incomplete.

The aim of part I of this paper is to document the performance of the ECMWF analysis-forecast system in depicting the main features of the circulation in the Australian

DIGITISED RADAR

▲ AMEX OBSERVATION SITE
UPPER AIR WIND & THERMAL
OBSERVATIONS 4 TIMES PER
DAY.
WINDS TRACKED BY OMEGA
NAVIGATION.

● AMEX OBSERVATION SITE
UPPER AIR WIND & THERMAL
OBSERVATIONS 4 TIMES
PER DAY
WINDS TRACKED BY RADAR

⊠ ROUTINE UPPER AIR
OBSERVATION SITE
GENERALLY THERMAL
OBSERVATIONS 1-2 TIMES
PER DAY
WINDS 4 TIMES PER DAY
WINDS TRACKED BY RADAR

□ ROUTINE UPPER AIR
OBSERVATION SITE
GENERALLY THERMAL
OBSERVATIONS ONCE
PER DAY
WINDS 2-4 TIMES PER DAY
WINDS TRACKED BY
THEODOLITE

⊘ ROUTINE PILOT BALLOON
OBSERVATION SITE.
WIND OBSERVATIONS 2-4
TIMES PER DAY
WINDS TRACKED BY RADAR

○ ROUTINE PILOT BALLOON
OBSERVATION SITE
WIND OBSERVATIONS 2-4
TIMES PER DAY
WINDS TRACKED BY
THEODOLITE

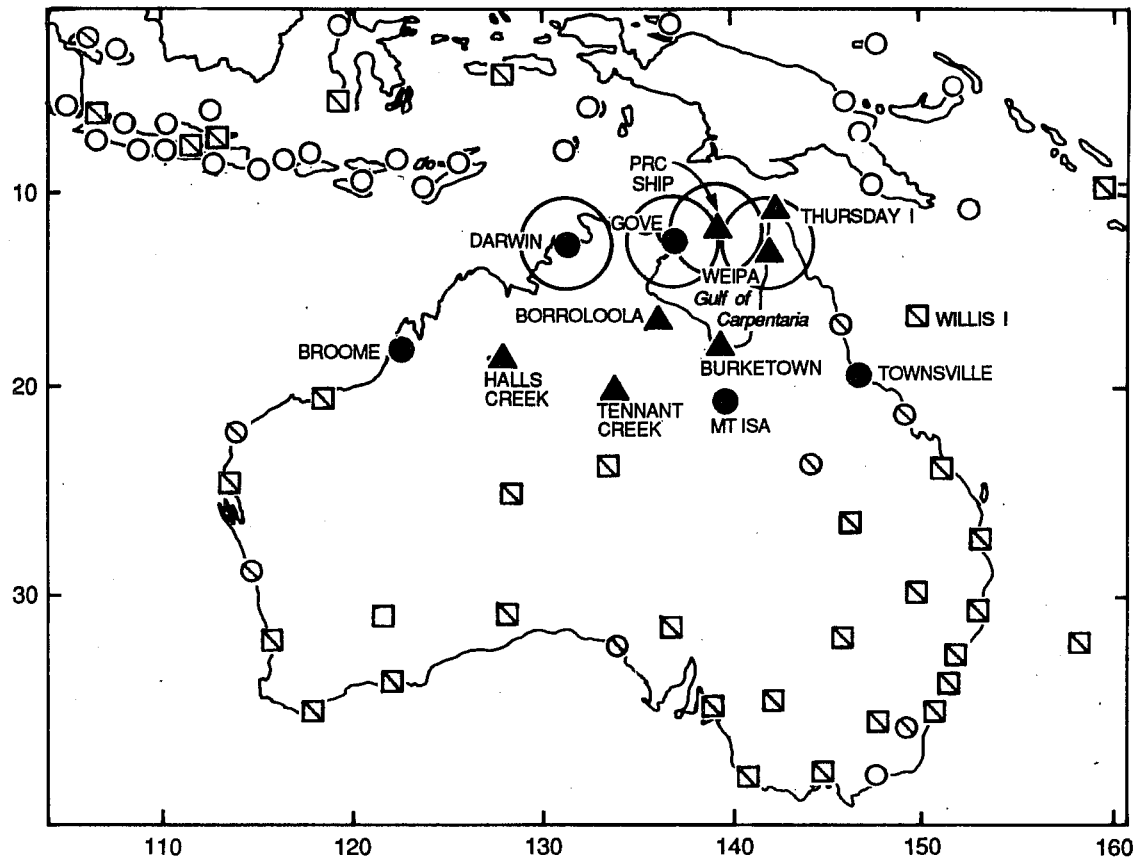

Fig. 1 The atmosphere sounding network for AMEX Phase II.

region in the period January 10 to February 15 1987 during which AMEX was conducted. The features include the onset of the Australian summer monsoon and the active and break periods in the monsoon and four tropical cyclones, two of which occurred within the AMEX network.

Part II of the paper describes the sensitivity of analysis-forecasts of the tropical cyclones to convective parametrizations used in the model. Two convective schemes, the Kuo parametrization in use until Spring 1989 and the Betts-Miller adjustment scheme are compared. Some forecasts using the mass flux scheme of Tiedtke, which became operational in Spring 1989, will also be described. Part II also shows two forecasts for tropical cyclones Irma and Jason with a higher resolution forecast model.

Part III describes experiments aimed at reducing the problem of data rejection in the analysis of tropical cyclones which results in considerable errors in locating the centre of the cyclones. Results of these experiments have application to bogusing of tropical cyclone data.

The model used in these studies is the operational ECMWF model (as in Feb 1987) which has 19 levels in the vertical and is truncated at triangular wave number 106 (T106) in the horizontal. The model includes all the revised parametrizations implemented in May 1985. The revised parametrizations which include shallow convection, a more effective representation of deep convection, a new cloud scheme and improvements in the radiation scheme resulted in significant improvements in the representation of quasi-stationary flow in the tropics. A gravity-wave drag formulation and improvements in the analysis scheme have also been implemented which have resulted in further improvements in the performance of the analysis-forecast system.

Acknowledgements

The authors are grateful to M. Tiedtke for performing the forecasts using his mass flux cumulus parametrization scheme, A. Simmons for performing the T159 integrations, W. Heckley for providing the code to plot figures 3 and 4 in Part I of the report and A. Hollingsworth, J. Pailleux, N. Davidson and J. McBride for the comments on the manuscripts. The authors are also grateful to H.M. Wong of BMRC for preparing the final versions of the figures. One of us (K.P.) is grateful to members of the Research and Operations Departments of ECMWF for their help with various problems. In particular he is grateful to D. Dent, A. Simmons, G. Kelly, P. Undén, W. Heckley and K. Arpe for their help with the ECMWF model and data assimilation system, the diagnostic package and graphics, and to P. O'Sullivan for his help with graphics.

PART I: PERFORMANCE OF THE ECMWF ANALYSIS-FORECAST SYSTEM DURING AMEX

Kamal Puri

Abstract

The main aim of this part is to document the performance of the ECMWF analysis-forecast system in depicting the mean features of the Australian monsoon circulation during AMEX and some individual features such as the onset of the monsoon, the active and break periods in the monsoon and the four tropical cyclones, two of which formed within the AMEX network. In most cases only forecasts up to 72 hours will be considered as the model skill in the tropics beyond this period falls off rapidly.

1. AUSTRALIAN SUMMER* MONSOON - ONSET AND ACTIVE/BREAK PERIODS

The summer monsoon which locally affects regions of Southeast Asia and Australasia can have an influence which extends to global scales. Thus when fully developed, the summer monsoon convection drives large scale circulations both in the east-west and north-south direction (Krishnamurti et al., 1973). As noted by Lau and Chang (1987), the summer monsoon exhibits distinct characteristics that differ considerably from its winter counterpart (i.e. the Indian monsoon). The basic difference is that during the summer monsoon the major convection is over the maritime continent while the monsoon heat low in winter is entirely over land. Another difference is in the location of the heat sources. For the winter monsoon the major heat source is situated between 15°N to 30°N where the Coriolis effect gives rise to highly rotational planetary scale circulation. The summer monsoon on the other hand has its main heat source situated over the equatorial belt where the divergent component of motion reveals itself more prominently (Lau and Chang, 1987).

In the Southeast Asian region the summer monsoon arrives in the north about November and retreats from this region around March/April. During December or early January a dramatic southward shift occurs in the location of the major heat source accompanied by the sudden establishment of lower tropospheric westerlies between the equator and 10°S. This is known as the onset of the Australian summer monsoon. A review on this subject is given by McBride (1987). The Australian Monsoon can last from 10 days to 100 days (see Holland, 1986) and is marked by active/break periods which are associated with strengthening/weakening of the low level westerly winds. Tropical cyclones form an important component of the Southern Hemisphere monsoon circulation. In the Australian region McBride and Keenan (1982) in a case by case study of tropical cyclone development

*Winter and summer monsoon refer to the southern hemisphere season

for five years have found that in 84% of cases the precyclone cloud cluster when it first appeared was embedded in the monsoon trough. At the time the cluster was actually classified as having reached tropical cyclone intensity, 97% were in the trough. Thus the summer monsoon encompasses a wide spectrum of phenomena which span scales ranging from subsynoptic to global scales and time scales ranging from hours to several months or years.

In this section the ability of the ECMWF analysis-forecast system in handling various aspects of the Australian summer monsoon for the AMEX period will be described. Although the performance of the system for the Indian monsoon has been documented (Mohanty et al., 1985) no detailed studies for the Australian monsoon have been carried out so far. The onset of the monsoon during AMEX can be seen in Fig. 2 (provided by B. Gunn), which shows the vertical section of zonal wind as a function of time and averaged over the domain 5°S to 15°S, 110°E to 140°E. The wind data are obtained from the Australian univariate optimum interpolation analysis system. The monsoon onset clearly occurs on Jan 14 with a weak break from around Jan 25 to 29 followed by a further active period. Fig. 3 shows the vertical section of the zonal wind as analysed at ECMWF as a function of time. The time frequency of the analysis is six hours. Apart from differences in the intensities of the low level wind, there is good agreement with the height-time section shown in Fig. 2. The ECMWF analyses also indicate monsoon onset occurring around Jan 14 with a weak break from Jan 25 to Jan 30 followed by a mainly active period. Fig. 4 shows similar height-time sections for the 24 and 48 hour forecasts respectively. The 24 hour forecasts show an impressive skill in predicting most of the features of the monsoon present in the analyses. Particularly impressive is the accurate prediction of the onset date and the active/break periods. The 48 hour forecast does not predict the onset date which in fact only shows up in the 48 hour forecast valid for Jan 15. However, the 48 hour forecasts provide a reasonable guidance for the following break and active periods. The onset of the Australian monsoon is accompanied by a rapid increase in convective activity over the northern regions of Australia. Fig. 5 shows the 24 hour forecast area averaged precipitation (5°S to 15°S, 110°E to 140°E) as a function of time from Jan 10 to Feb 15 1987. Although the intensity of precipitation is difficult to verify, the model displays an impressive capability in forecasting the rapid increase in precipitation with the onset of monsoon followed by a decrease in the break period and then increased precipitation in the following active period. The precipitation in the latter period of February is forecast too low and is possibly related to the failure of the model in handling tropical cyclone Jason which formed in the Gulf of Carpenteria. The capability of the model in predicting the increase in precipitation over northern Australia with the onset of the monsoon is better indicated in Figs. 6(a) and (b) which, respectively, show the rainfall for two 24 hour forecasts prior to onset and two forecast on and after the onset.

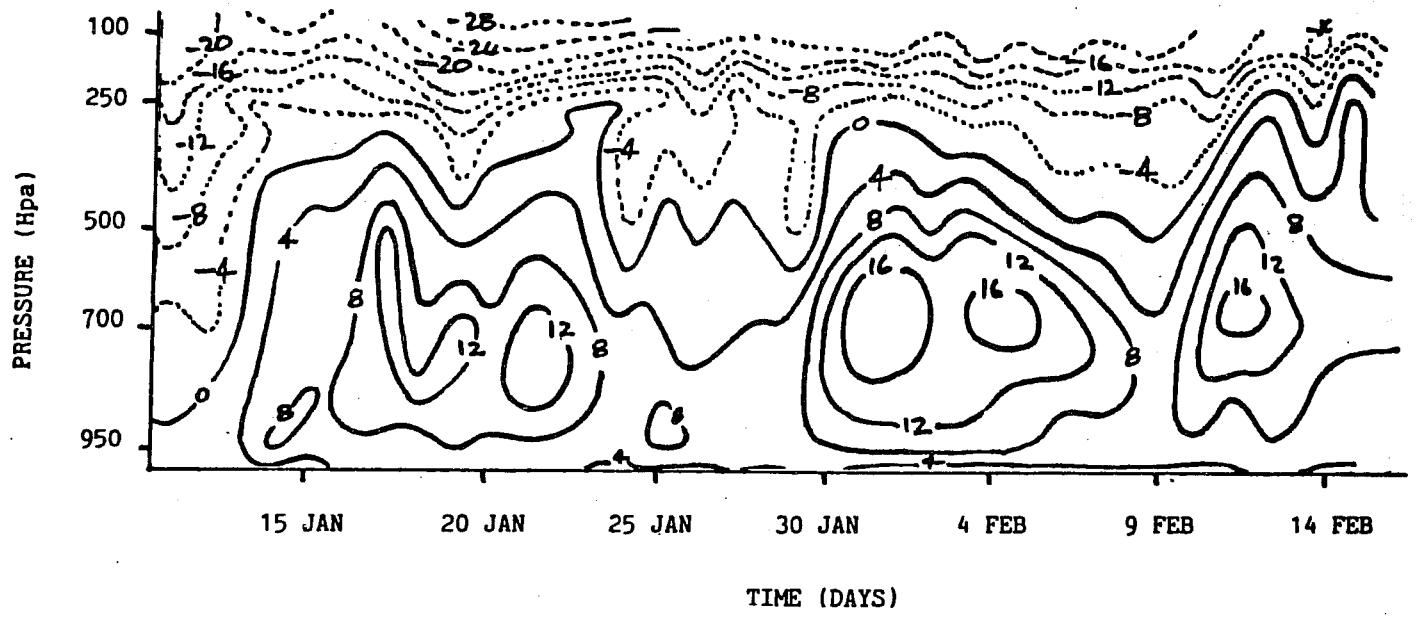

Fig. 2 Vertical cross section of area mean (5°S to 15°S, 110°E to 140°E) zonal wind as analysed by Bureau of Meteorology (BOM) as a function of time. Full (dashed) lines denote positive (negative values). Units are ms^{-1} and contour interval is 4 ms^{-1}.

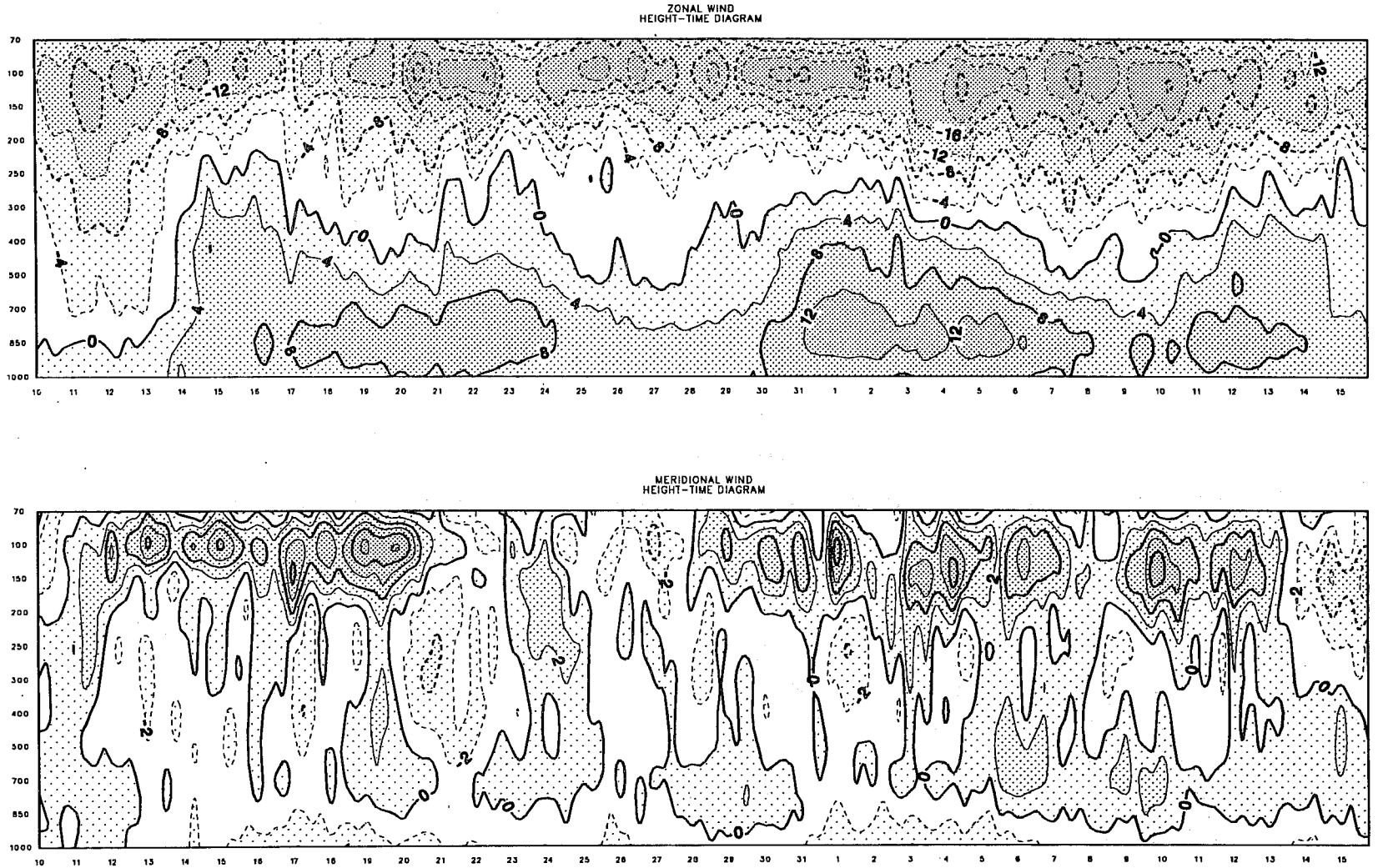

Fig. 3 As in Fig. 2 but zonal wind (top) and meridional wind (bottom) as analysed at ECMWF. The time frequency is 6 hours and contour intervals are 4 ms^{-1} and 2 ms^{-1} respectively for zonal and meridonal winds.

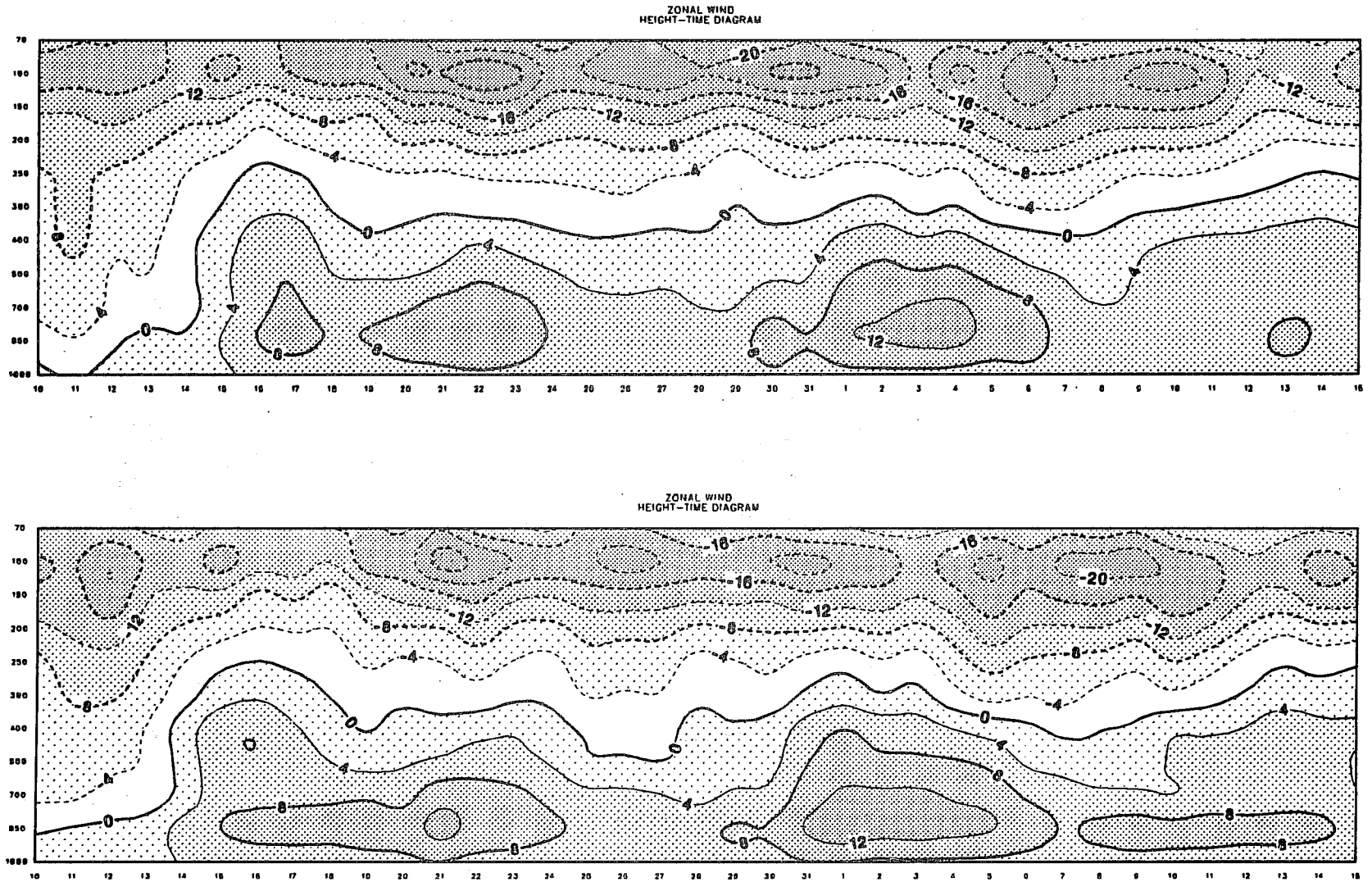

Fig. 4 As in Fig. 2 but 24 hr (bottom) and 48 hr (top) ECMWF forecasts for zonal wind. Contours intervals are 4ms^{-1}.

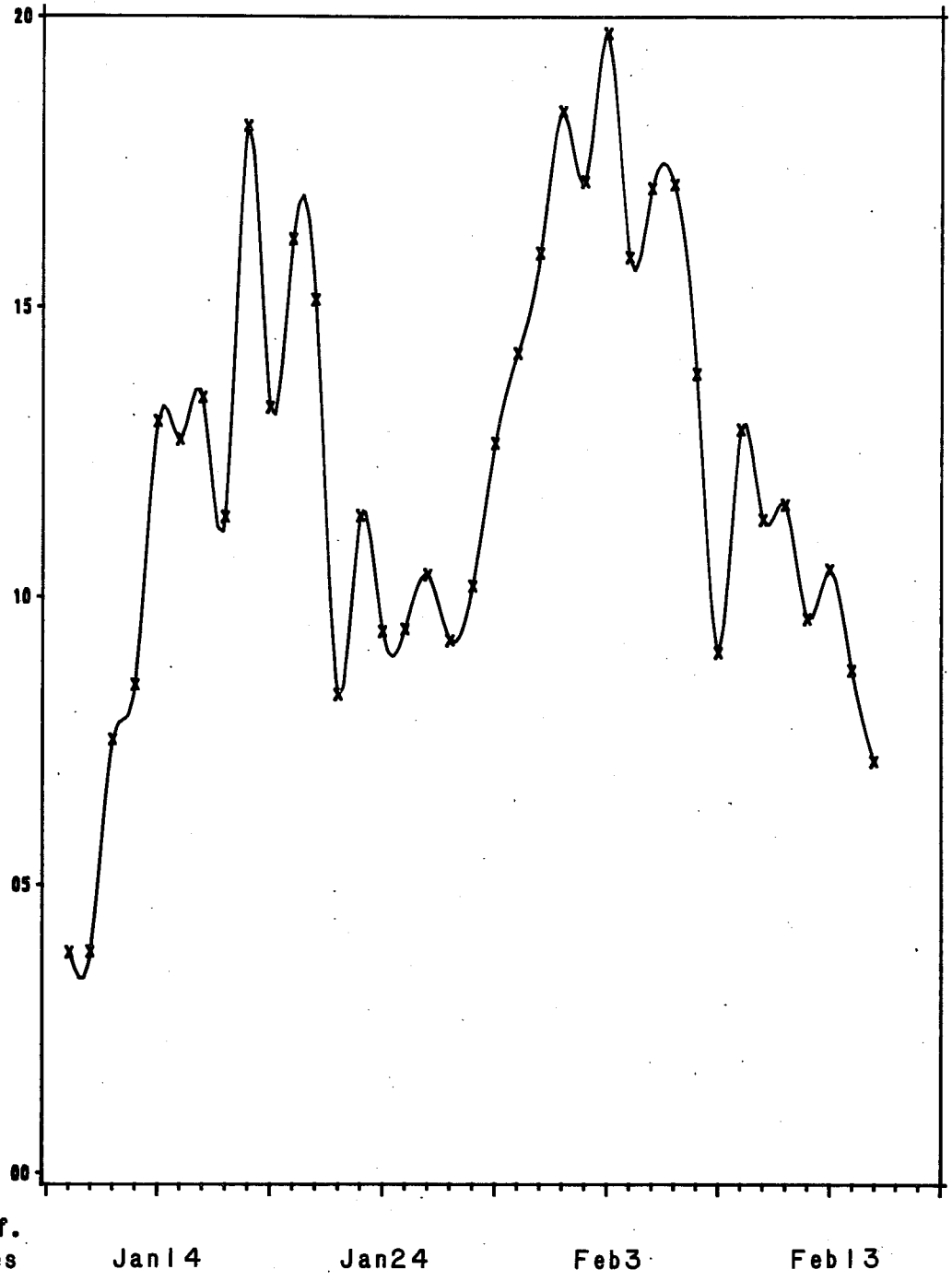

Fig. 5 Area averaged (5° to 15°S, 110°E to 140°E) 24 hr forecast precipitation (in mm) as a function of time from Jan 10 to Feb 15 1987.

Close inspection of Figs 3 and 4 around January 14 indicates the model fails to capture the monsoon onset until some low level westerlies are established in the initial conditions. This is better illustrated in Figs. 7(a) to (c) which show the 24 and 48 hour forecasts for the 850 hPa wind field starting from Jan 12 to Jan 14 together with the starting and verifying analyses. The main feature to note in the analyses from Jan 12 to Jan 16 is the marked southward shift in low level westerlies around Jan 14 together with an increase in the westerly winds over the region to the north of northern Australia. The 24 and 48 hour forecasts from Jan 12 (Fig. 7(a)) fail to capture any of these changes. The 24 hour forecast from Jan 13 (Fig. 7(b) predicts the strengthening of the westerlies (and therefore the monsoon onset); however the 48 hour forecast fails to retain the strong westerlies. Both the 24 and 48 hour forecasts from Jan 14 (Fig. 7(c)) which start with strong westerlies in the initial conditions provide impressive forecasts of the winds although the strong cross-equatorial flow near 125°E is poorly predicted. However, the above results indicate the inability of the model to retain low level westerlies unless they are well established initially. The reason for this is not clear and is probably linked to the marked reduction in the convective activity in the model with time as will be shown below.

There was a weak break in the monsoon from around Jan 25 to Jan 29 which was marked by a weakening of the low level westerlies to the north of northern Australia. The weakening of the westerlies is well depicted by the ECMWF analyses as shown in Fig. 8 which presents the 850 hPa winds from 1200 GMT Jan 23 to 1200 GMT Jan 26. The 24 hour and 48 hour forecasts from 1200 GMT on Jan 23 and Jan 24 shown in Fig. 9 show that the forecasts also indicate this weakening of winds; however for the 48 hour forecast winds, although verifying well with the analyses, the weakening could partly be due to the systematic weakening of low level westerlies in the model with time.

The subsequent strengthening of the winds around January 30 is again well depicted by the analyses as shown in Fig. 10 for Jan 30 to Feb 1 and 24 hour and 48 hour forecasts from Jan 29 and Jan 30 as shown in Fig. 11. The contrast in the 850 hPa winds for the two periods shown in Figs. 8 and 10 (for analyses) and Figs. 9 and 11 (for forecasts) is quite marked and it is encouraging that the model is able to simulate some of these features although as indicated above the weakening of the winds in Fig. 9 could be partly due to the systematic error in the model.

Apart from the differences in the low level winds, the precipitation to the north of Australia in the two periods considered above are also very different with much greater rainfall in the active period. The model has some skill in forecasting these sharp differences as indicated in Fig. 12 which shows 24 hour forecast rainfall from Jan 25 (break period) and Jan 30 (active period). The GMS IR imagery for 1200 GMT Jan 26 and 1200 GMT Jan 31 are shown

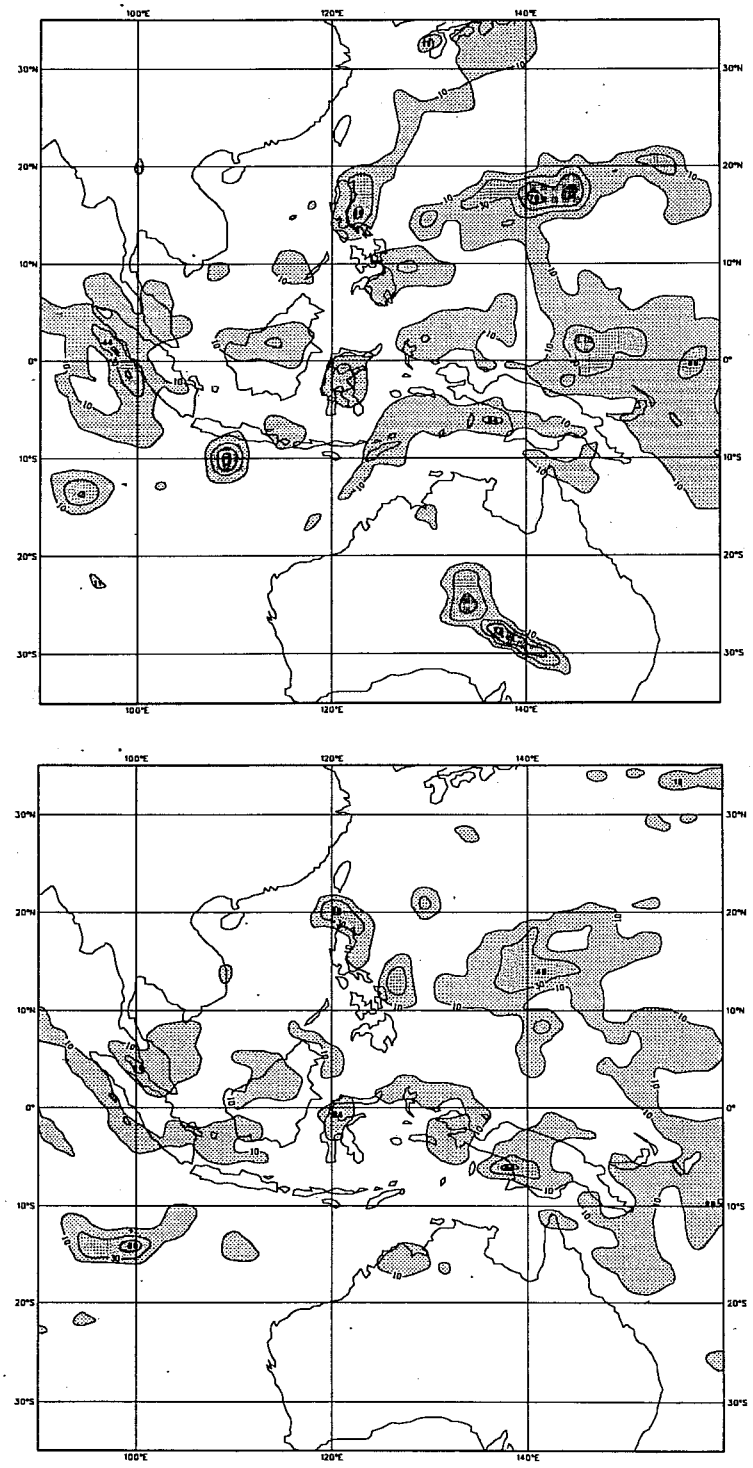

Fig. 6a Precipitation (in mm) for 24 hr forecasts from 1200 GMT Jan 10 (bottom) and Jan 11 (top).

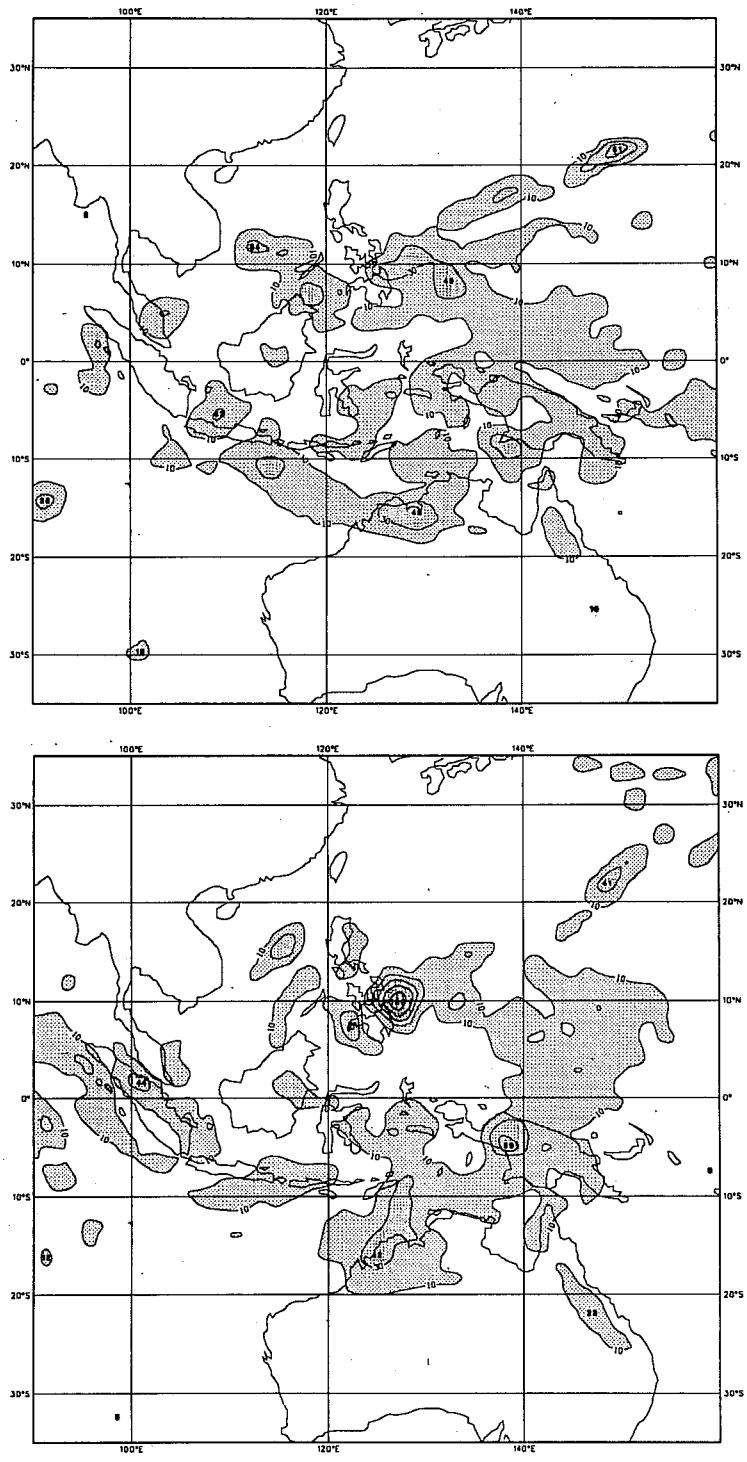

Fig. 6b As in Fig. 6a but for forecasts from 1200 GMT Jan 13 and Jan 14.

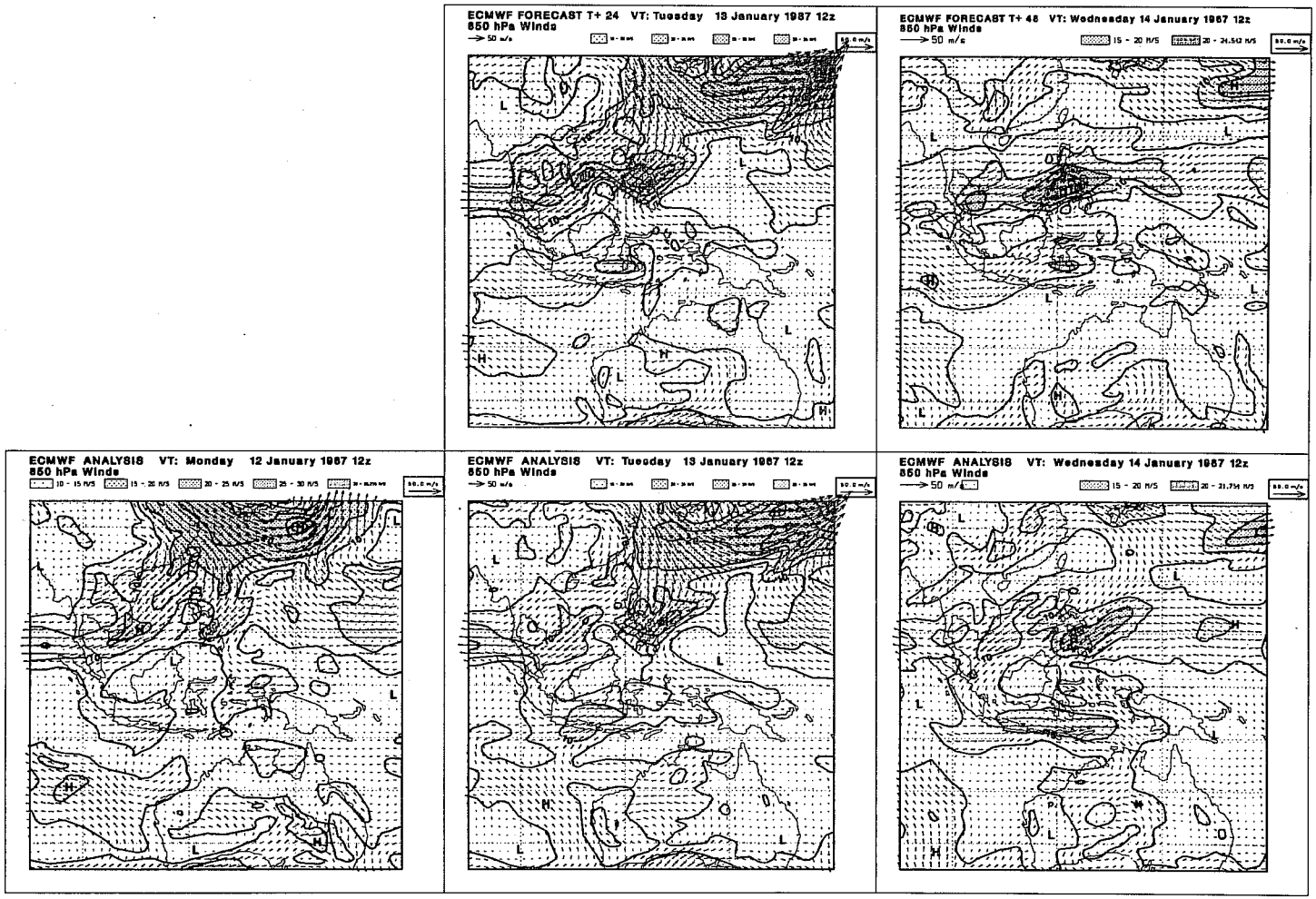

Fig. 7a 24 hr and 48 hr forecasts for 850 hPa vector wind starting from 1200 GMT Jan 12, 1987 together with starting and verifying analyses. Units are ms^{-1} and contour interval for isotachs is 5 ms^{-1}.

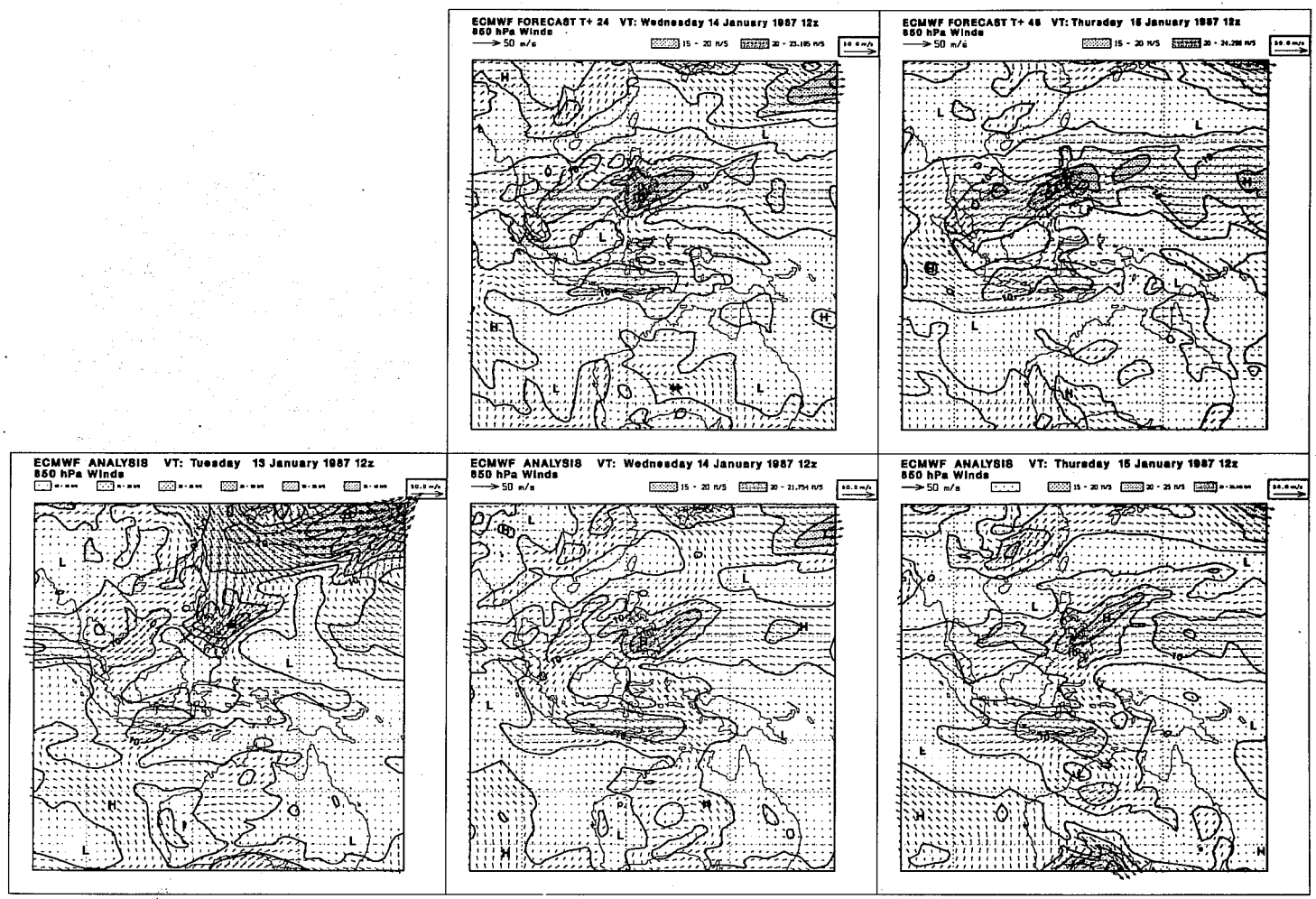

Fig. 7b As in Fig. 7a but for forecasts from 1200 GMT Jan 13.

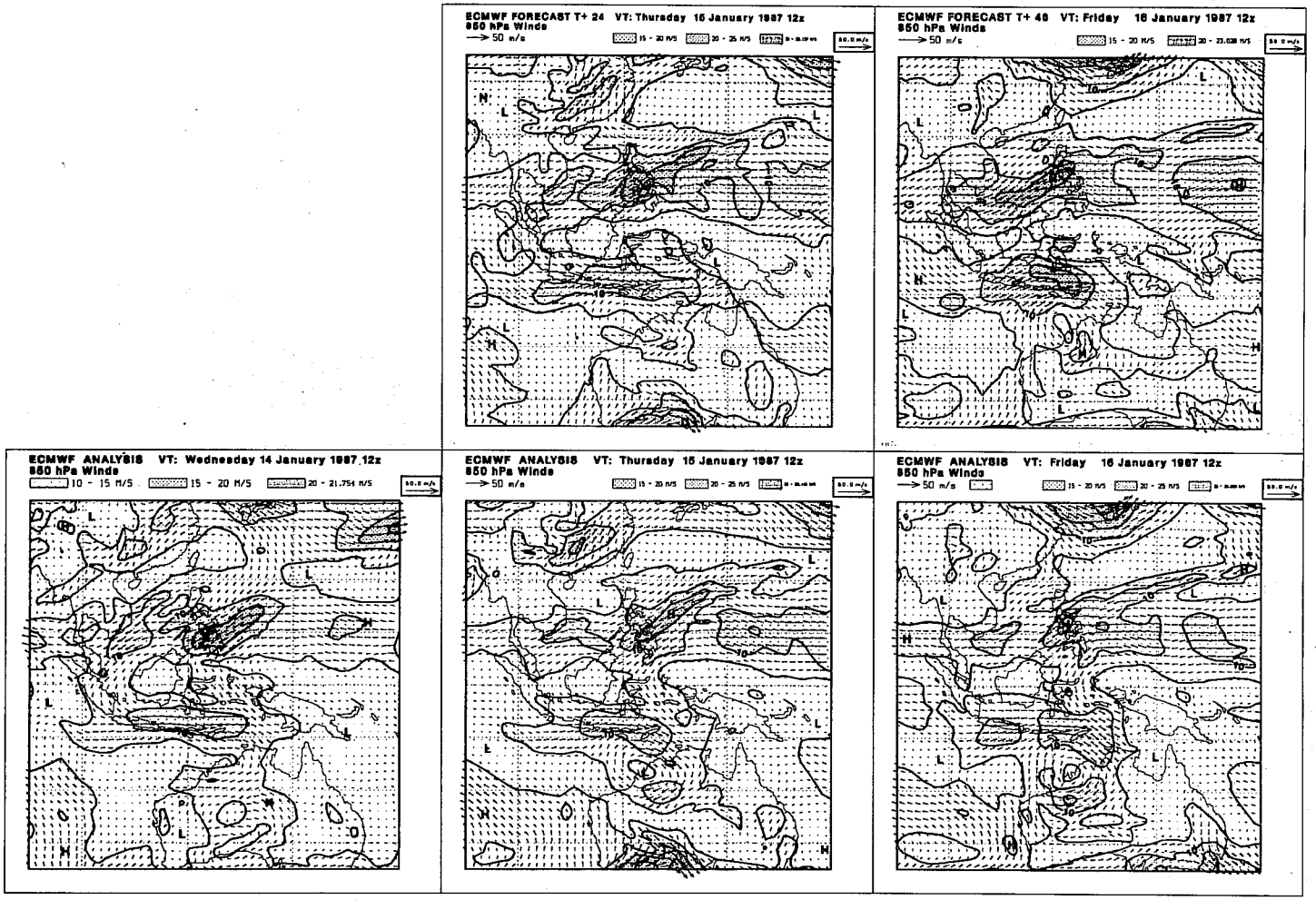

Fig. 7c As in Fig. 7c but for forecasts from 1200 GMT Jan 14.

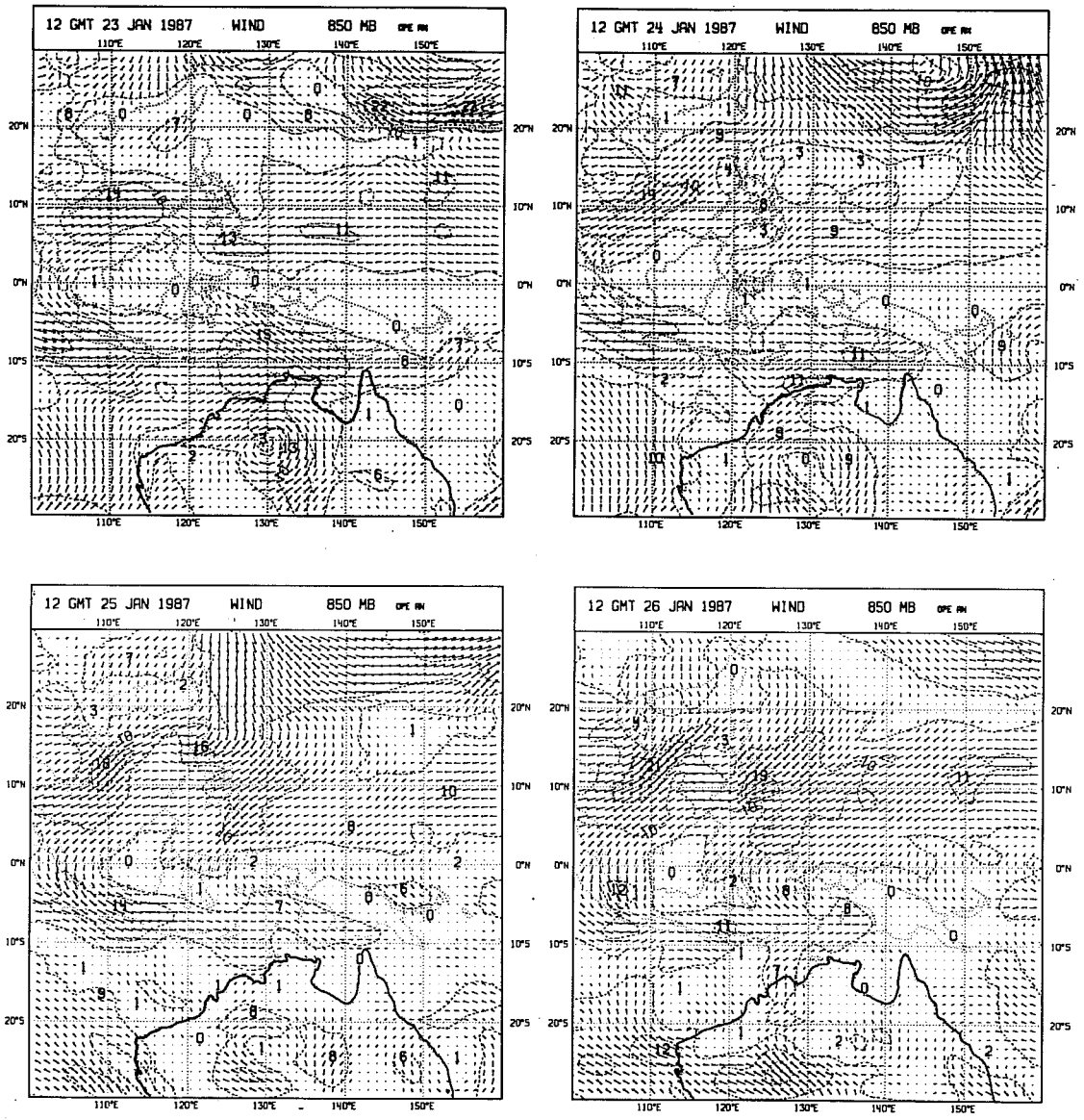

Fig. 8 850 hPa vector wind analyses from 1200 GMT Jan 23 to Jan 26, 1987. Units are ms^{-1} and contour interval for isotachs is 5 ms^{-1}.

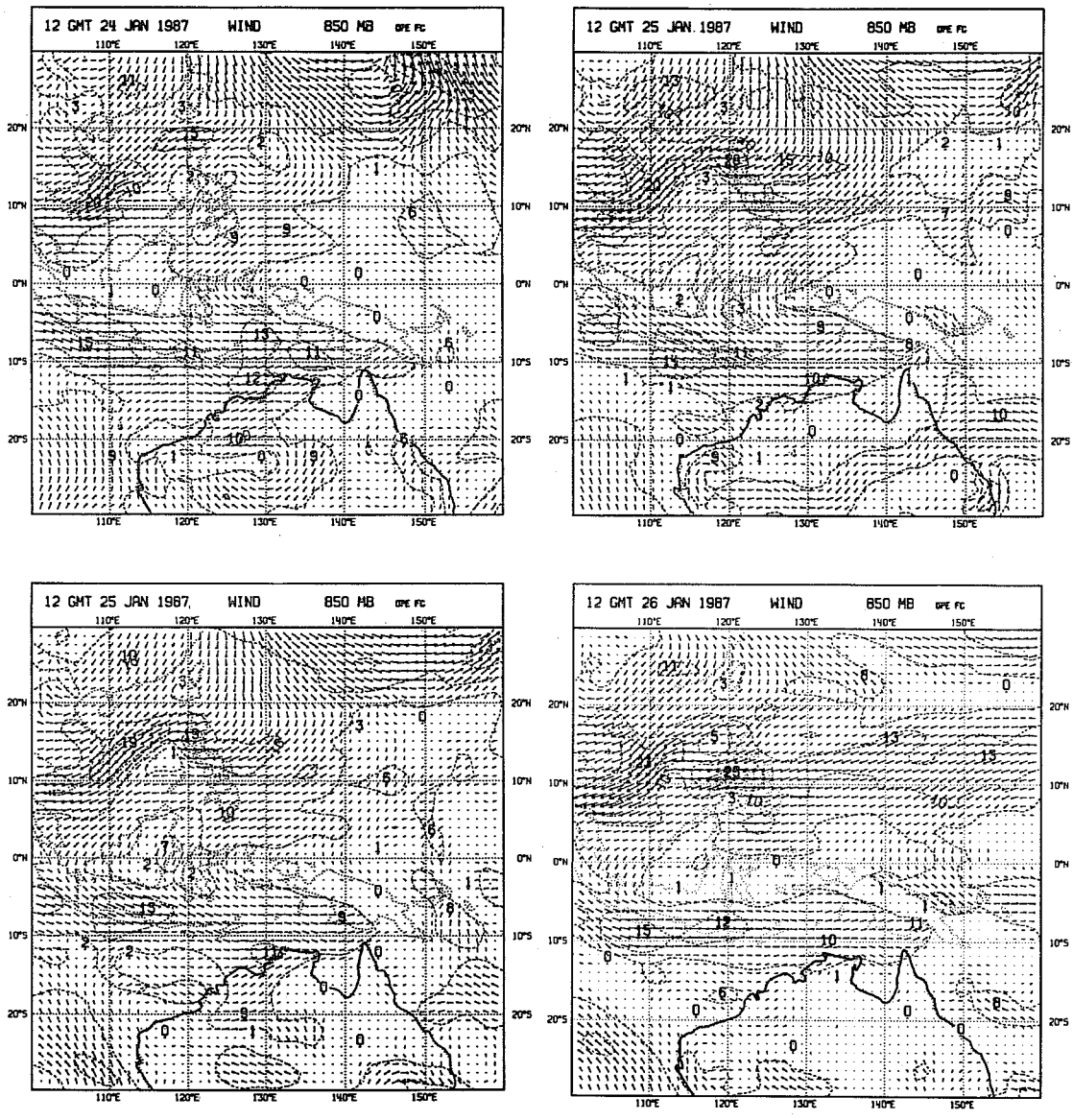

Fig. 9 24 and 48 hr forecasts for 850 hPa vector wind starting from 1200 GMT Jan 23 (top) and Jan 24 (bottom). Units are ms^{-1} and contour interval for isotachs is 5 m^{-1}.

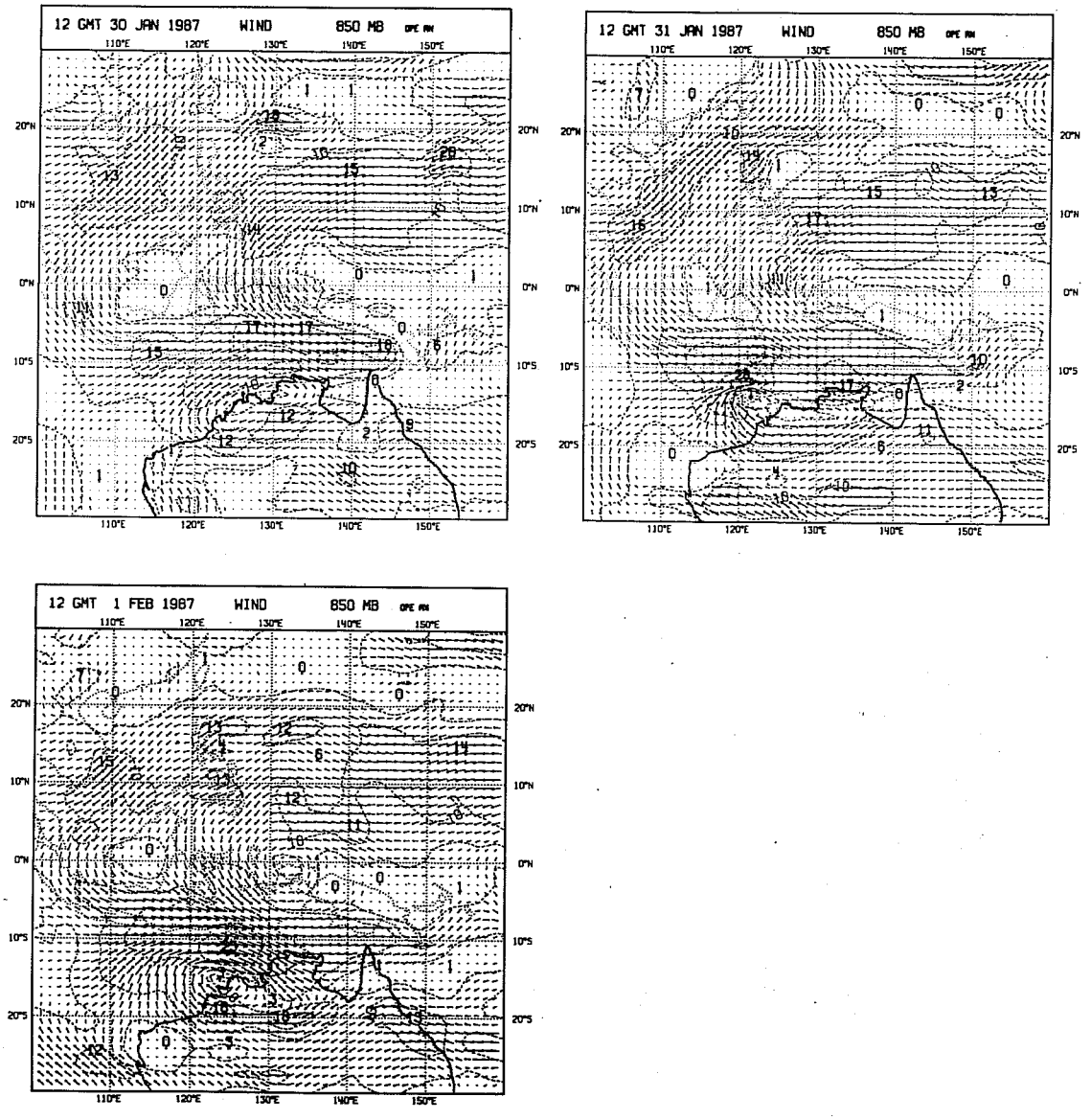

Fig. 10 As in Fig. 8 but for analyses from 1200 GMT Jan 30 to Feb 1.

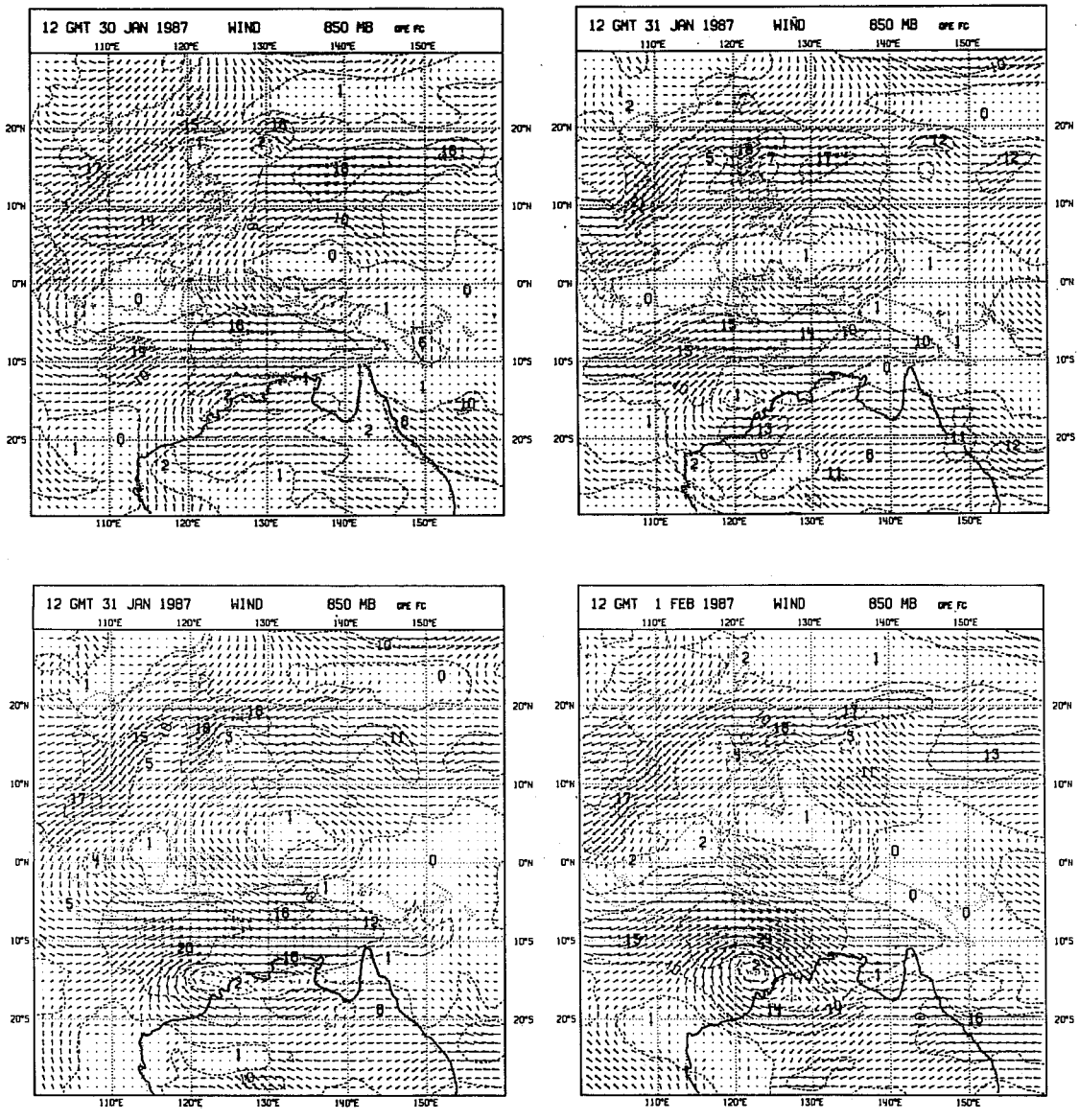

Fig. 11 As in Fig. 9 but for forecasts from Jan 29 (top) and Jan 30 (bottom).

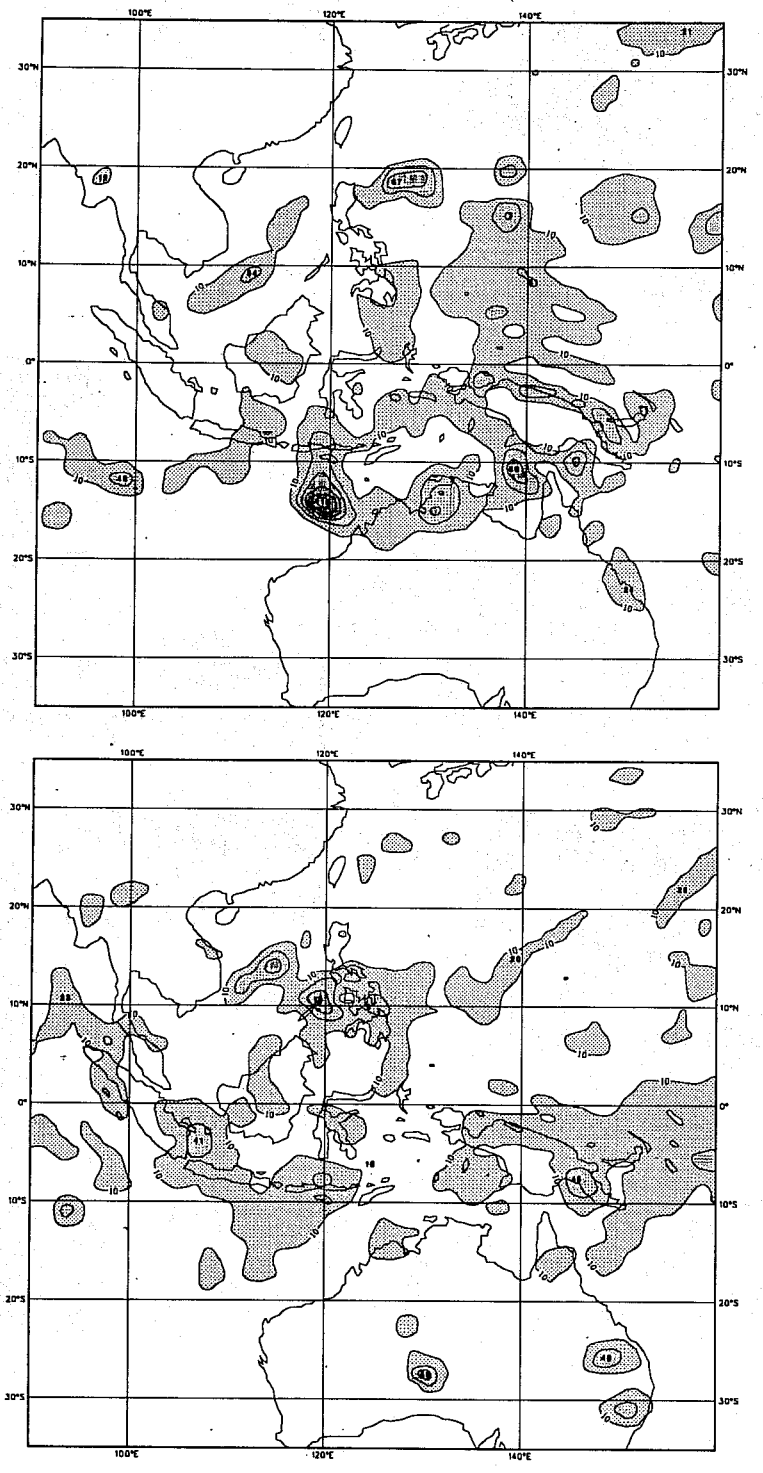

Fig. 12 Precipitation (in mm) for 24 hr forecasts from 1200 GMT Jan 25 (bottom) and Jan 30 (top).

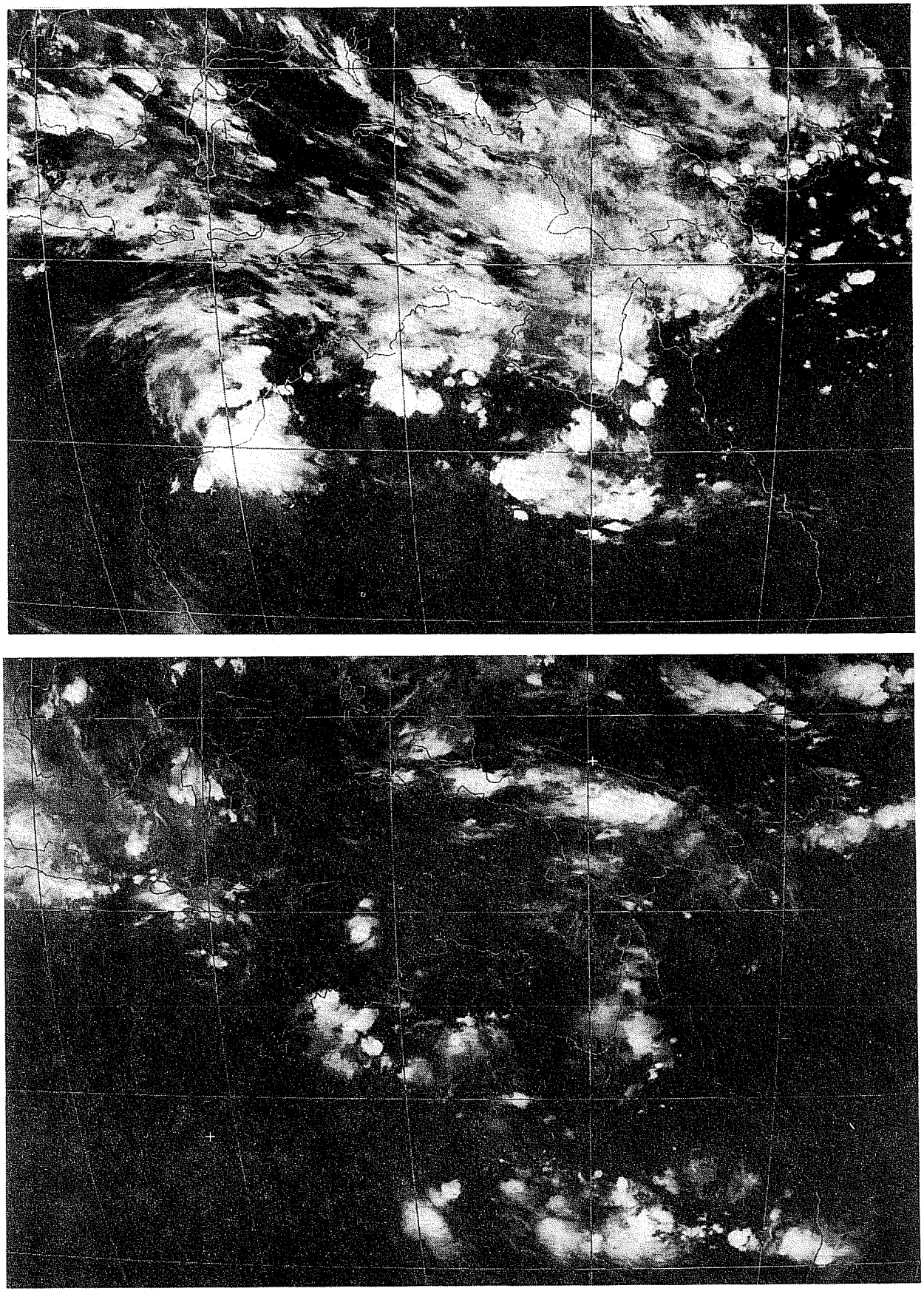

Fig. 13 GMS IR-imagery for 1200 GMT Jan 26 (bottom) and Jan 31 (top).

in Fig. 13 to indicate the dramatic changes in the convective activity for the two periods. Although there are significant differences of detail between the forecast precipitation and the GMS imagery, the model is able to forecast the major difference, namely the level of convective activity between the two periods. With increasing interest in obtaining improved estimates of precipitation, particularly in the tropics, the result is encouraging as it suggests that the data assimilation system is capable of providing useful information on precipitation based essentially on mass and wind data combined with the physical parametrizations. Such information could be of considerable interest for GEWEX (Global Energy and Water Cycle Experiment) and GPCP (Global Precipitation Climatology Project) which have been set up to provide best estimates of precipitation. Thus model based precipitation could be used to provide estimates of precipitation in data void regions and also to have some influence in regions with data.

2. MEAN CIRCULATION IN ANALYSES AND FORECASTS

Fig. 14(a) shows the mean 850 hPa and 200 hPa wind analyses for the period Jan 10 to Feb 15 1987. The period was marked by strong low level westerly flow over and to the north of northern Australia which is typical of the Australian monsoon circulation. There is cyclonic circulation in the Gulf of Carpentaria and off the West Australian coast. Another feature of note is the strong cross-equatorial flow from the northern to the southern hemisphere in the regions around 100°E and 125°E. The ECMWF analysis of the mean circulation agrees with the mean obtained from the Australian Bureau of Meteorology's tropical analysis scheme (not shown). The agreement between the two independent analyses with respect to the main features of the monsoon circulation is very encouraging. Fig. 14(b) shows the mean 48 hour forecasts verifying for the analysis period shown in Fig. 14(a). The low level westerly flow to the north of Australia is well handled in the mean at 48 hours although the westerlies are weaker than analysed and the underestimate increases with time. The cyclonic circulations in the Gulf of Carpentaria and off western Australia are well forecast at 48 hours. The circulation in the Gulf has weakened by day 3 and is located too far to the east over western Australia (not shown). The cross-equatorial flow at both 48 hours and 72 hours, although occurring at the correct locations, is much weaker than the analysed flow. Many of the features of the 850 hPa wind are reflected at 200 hPa.

In order to indicate the performance of the analysis-forecast system with respect to divergent circulation, Figs. 15(a) and (b) show the mean analyses and 48 hour forecasts for velocity potential at 850 hPa and 200 hPa. Although the forecasts for the velocity potential are consistent with each other, the agreement with the analysis is not as good as for the streamfunction (not shown) which shows reasonable agreement with the verifying analysis. This is particularly the case at 200 hPa where there is a marked weakening of the divergent circulation with time. The vertical velocity ($\omega=dp/dt$) is closely related to the divergent circulation in the tropics. The mean verifying analysis and the 48 and 72 hour forecasts for the vertical velocity are shown in Figs. 16(a) and (b). Although comparison of forecasts with the analysis of this field can be misleading as the analysis will have substantial errors for a number of reasons such as lack of data, errors in the first guess and considerable gravity wave noise, there is a reasonable agreement between analysis and forecasts and for the location of significant vertical motion. The forecasts also show the general weakening trend with time noted for the velocity potential. The weakening trend in the divergence and vertical velocity is particularly evident in the vertical section of the area mean (5°S to 15°S, 110°E to 140°E) of these fields. These vertical sections for the analyses and 48 and 72 hour forecasts are shown in Fig. 17. Note the marked weakening for both fields in the upper troposphere. This systematic weakening of the upper level divergent circulation is a consistent feature of the ECMWF analysis-forecast system which has not been altered by significant improvements in various

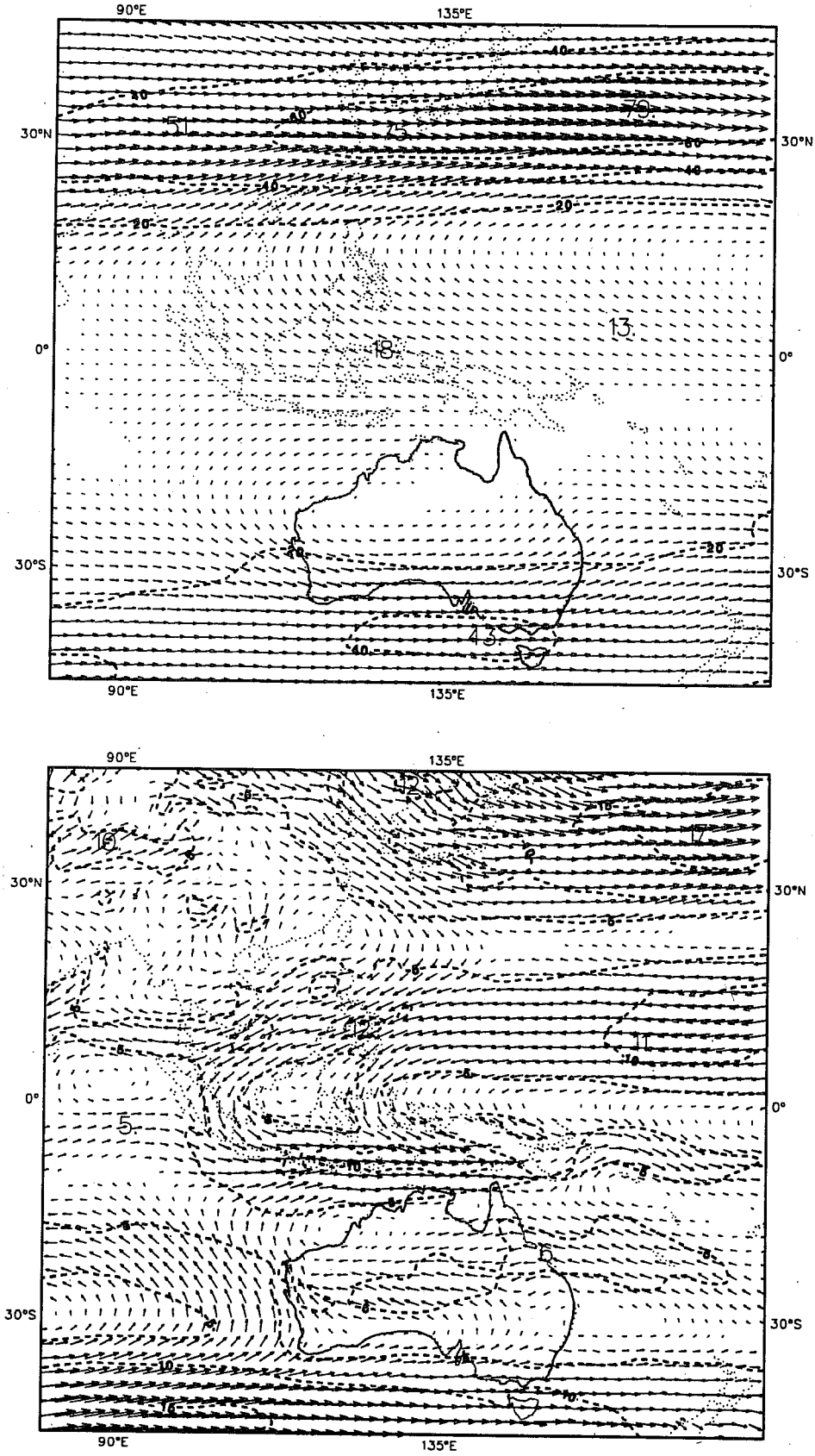

Fig. 14a Mean 850 hPa (bottom) and 200 hPa (top) vector wind analyses for the period Jan 10 to Feb 15, 1987. Units are ms^{-1} and contour interval for isotachs at 850 hPa and 200 hPa are 5 ms^{-1} respectively.

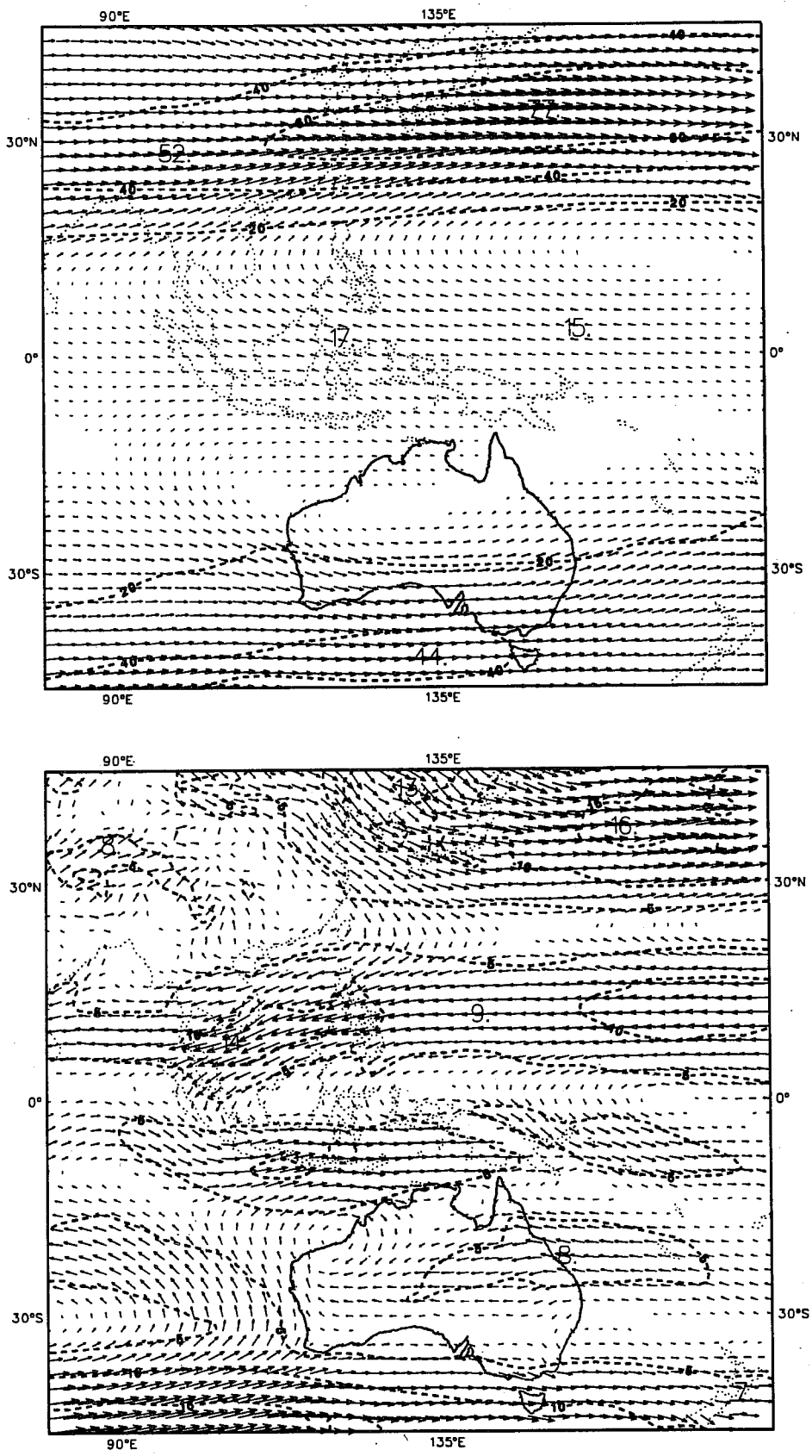

Fig. 14b As in Fig. 14a but for 48 hr forecasts.

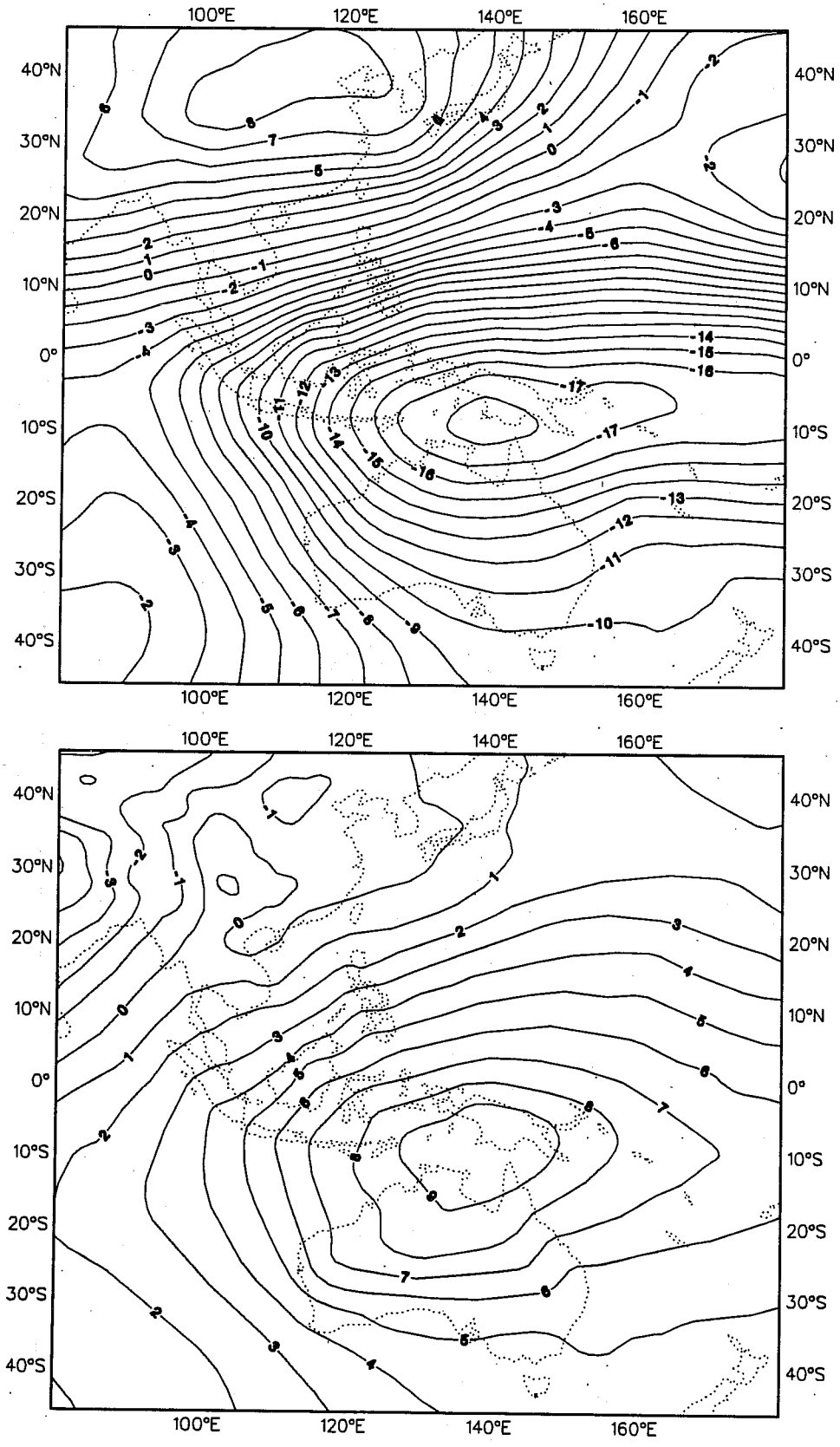

Fig. 15a As in Fig. 14a but for velocity potential. Units are 10^6 x m^2s^{-1} and contour intervals for both 850 hPa and 200 hPa are 1 x 10^6 m^2s^{-1}.

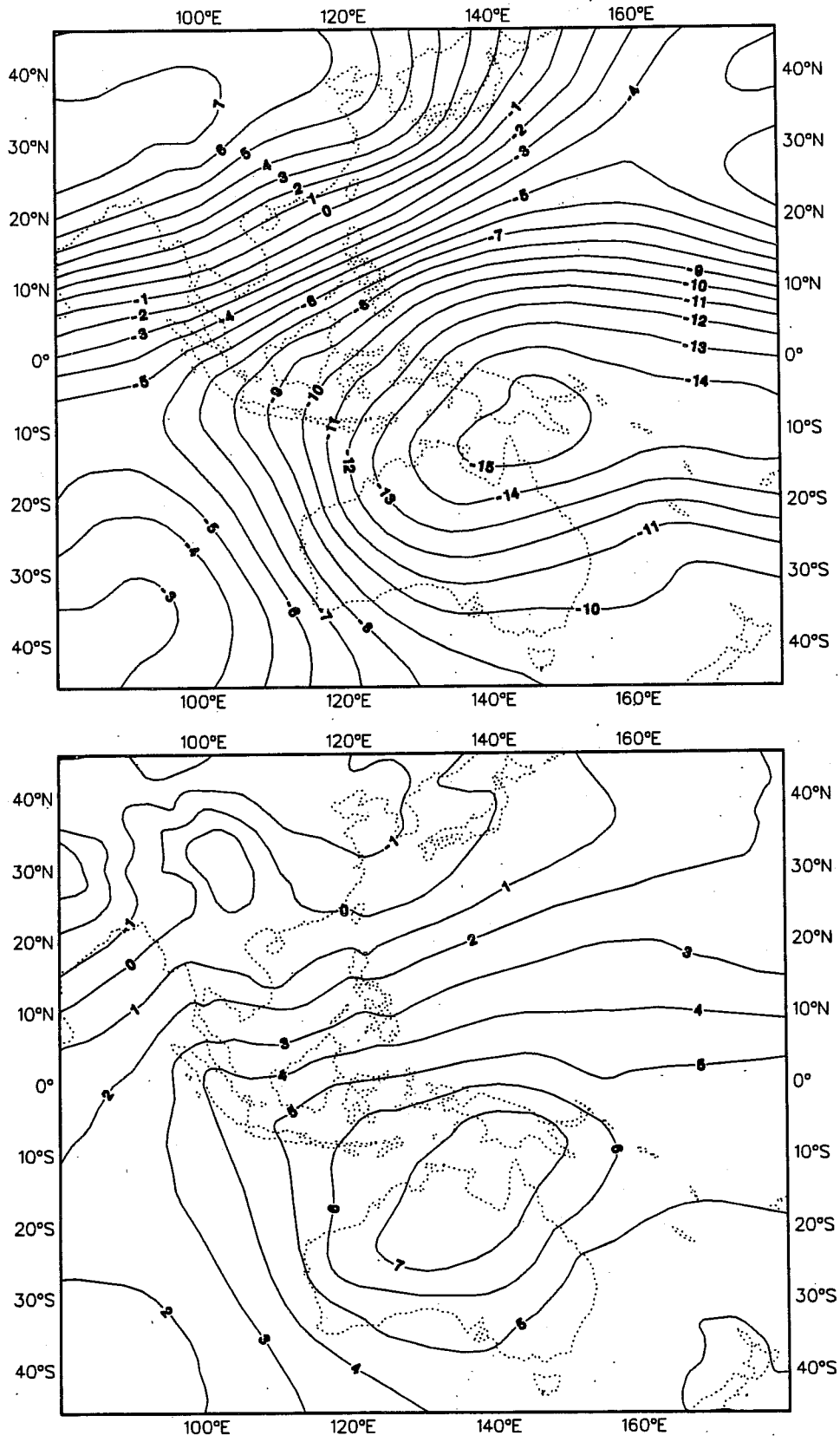

Fig. 15b As in Fig. 15a but for 48 hr forecasts.

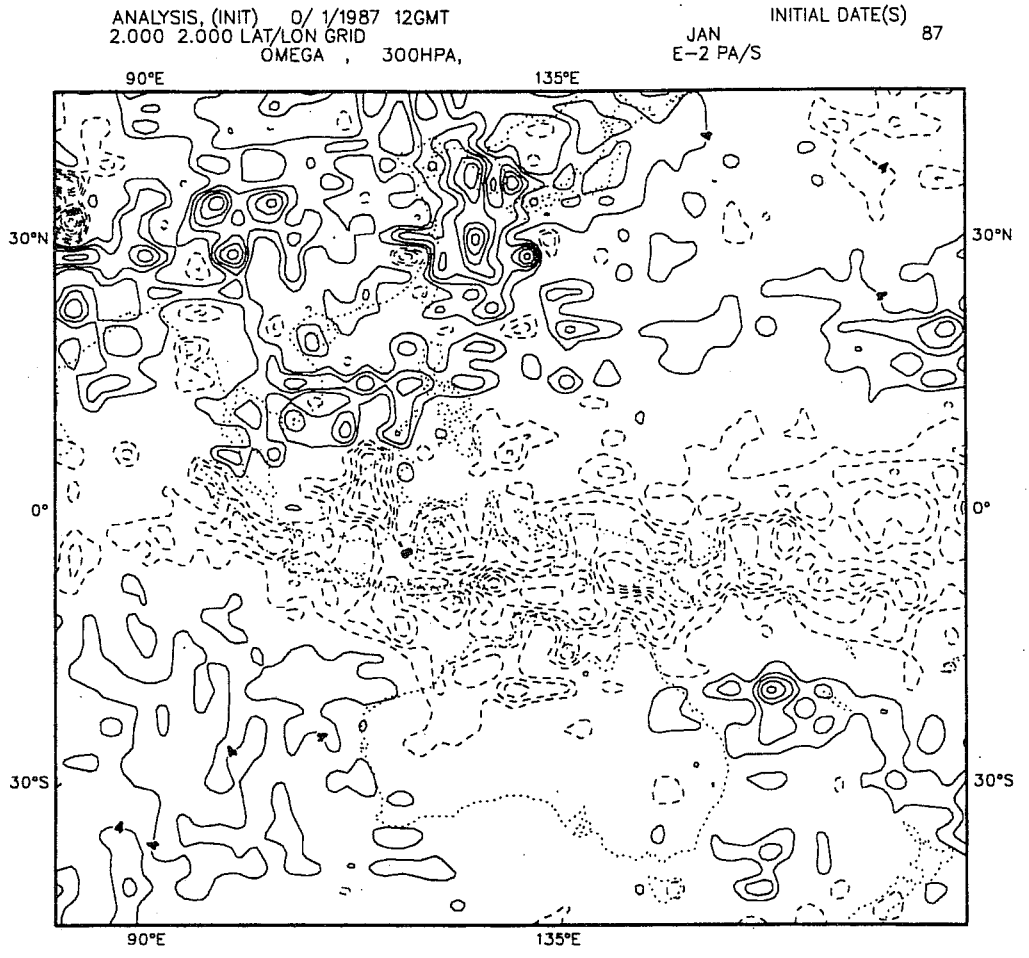

Fig. 16a As in Fig. 14a but for vertical velocity at 300 hPa. Units are 10^{-2} Pas^{-1} and contour interval is 4 x 10^{-2} Pas^{-1}.

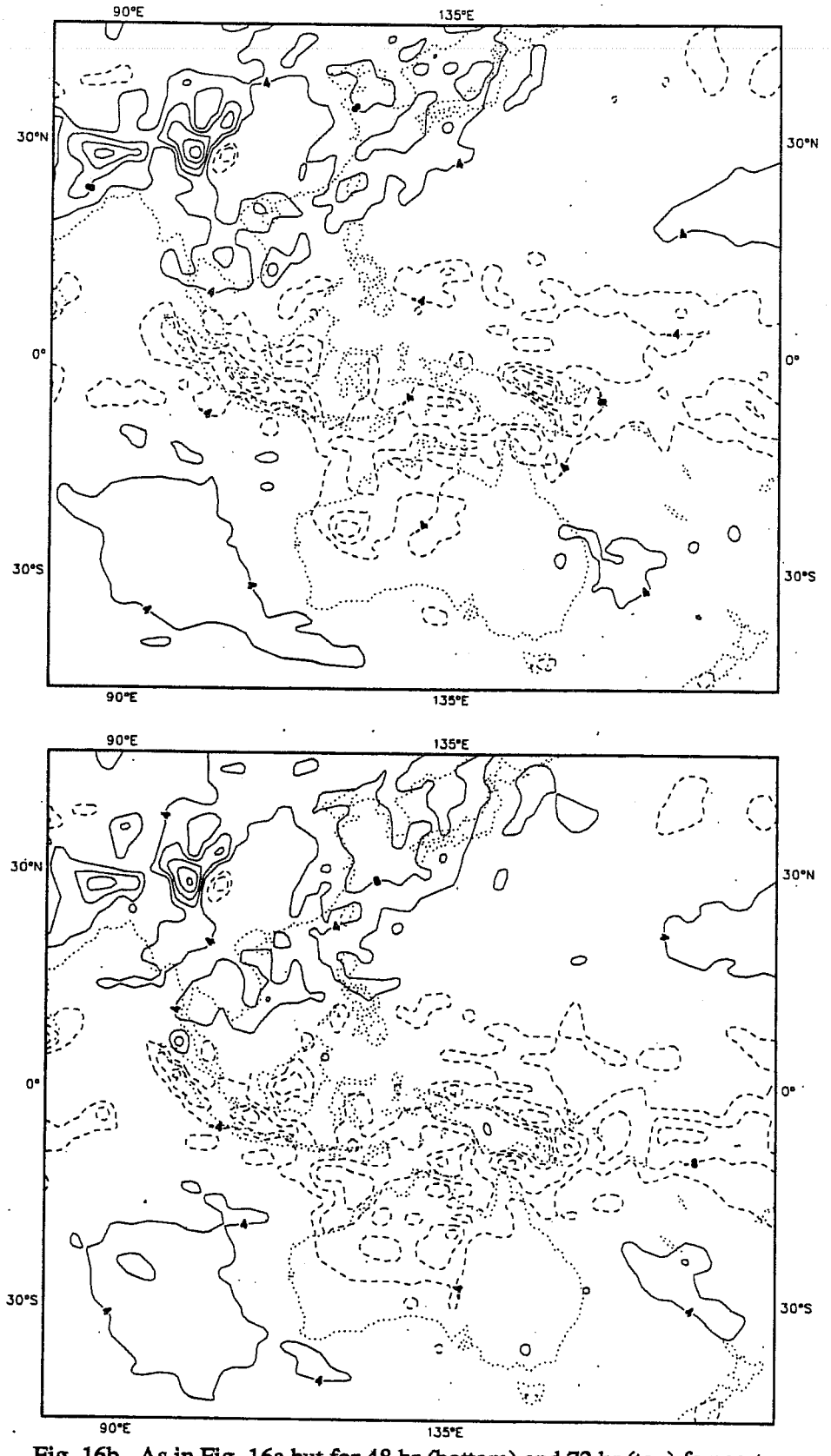

Fig. 16b As in Fig. 16a but for 48 hr (bottom) and 72 hr (top) forecasts.

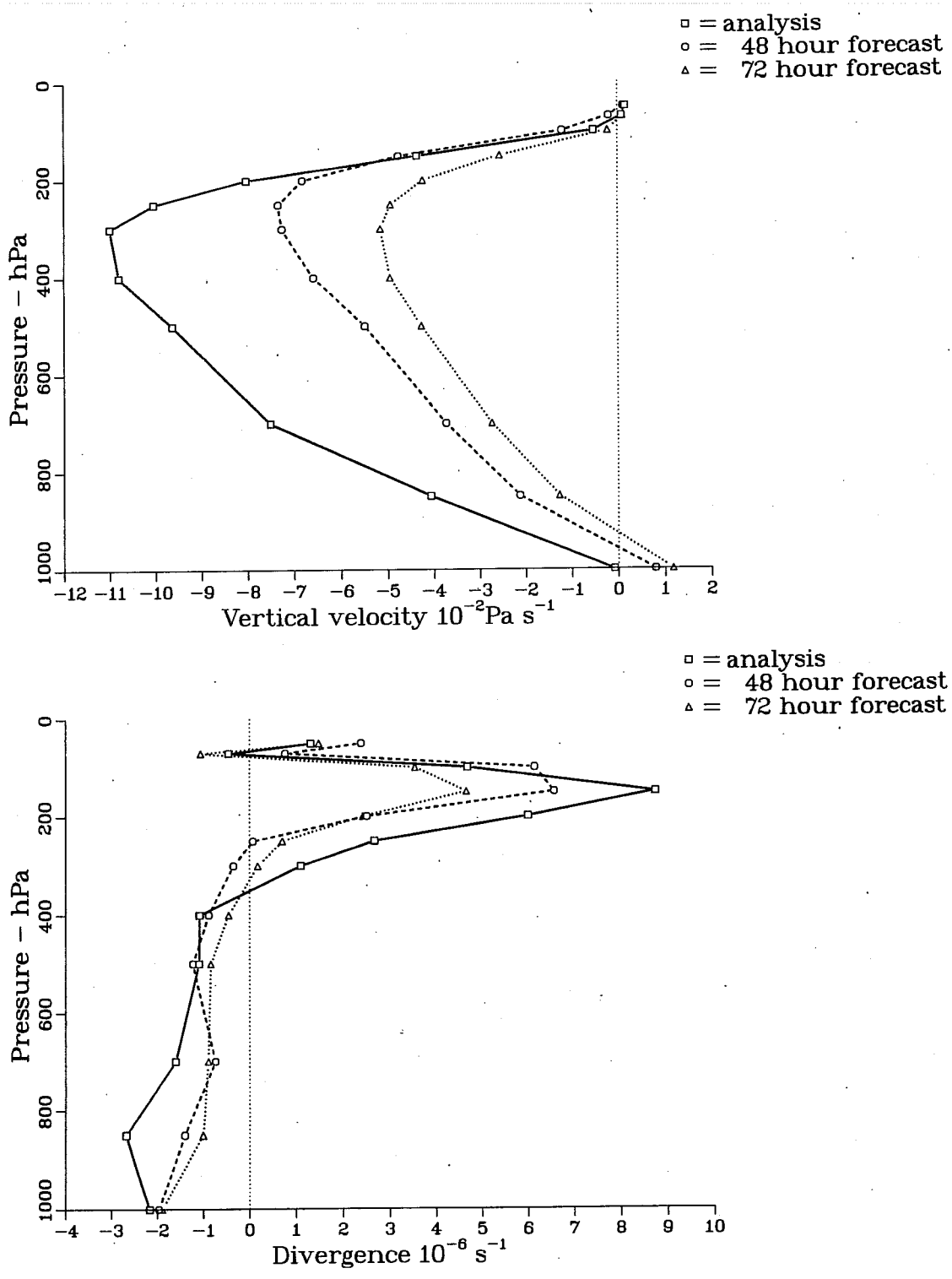

Fig. 17 Vertical cross sections of area mean 5°S to 15°S, 110°E to 140°E) divergence (bottom) and vertical velocity (top). Units of divergence and vertical velocity are $10^{-6}s^{-1}$ and 10^{-2} Pas^{-1} respectively.

components of the system. The error is now considered to be related to the underestimation of the outgoing longwave radiation flux by the radiative parametrization in the model which results in insufficient cooling (see Arpe, 1988). An example of this deficiency for the AMEX period is given in Fig. 18 which shows the longwave radiation at the top of the model for the 48 hour forecasts. Also shown is the mean (Jan 18 to Feb 15 1987) outgoing longwave radiation (OLR) flux from NOAA-9 satellite. There are differences of larger than 60 watts m^{-2} in the tropics which are indicative of higher black body temperatures in the model.

The weakening of the divergent circulation in the tropics is also closely related to the precipitation and cloud cover in the model. The 24 hour cumulative rainfall amounts for the 24, 48 and 72 hour forecasts (now shown) indicate a marked weakening in the precipitation with time. The weakening is much more dramatic for the convective cloud cover which is shown in Fig. 19 for the 24, 48 and 72 hour forecasts. By 72 hours the convective activity in the model has substantially weakened. A direct verification of the precipitation and convective cloud cover is difficult because of lack of data. However, an indirect measure of both quantities is provided by the OLR fluxes shown in Fig. 18. The shaded region in this figure are for OLR fluxes less than 200 watts m^{-2} which are regions of deep convection. The 24 hour forecast convective clouds show reasonable agreement with regions of strong convection indicated by the OLR data.

An indication of the model performance in predicting the mass field in the tropics is given in Figs. 20(a) and (b) which show the analysis and 48 hour forecasts of the geopotential field at 1000 hPa and 500 hPa. As with the wind field the main feature is the good consistency between the 48 and 72 hour forecasts (not shown) and the good agreement between the analyses and forecasts. The main error at 1000 hPa is the underestimation of the geopotential over north and north-west regions of Australia. This deficiency is related to underestimation by the model of the intensity of four tropical cyclones which occurred in this region.

In summary, results for the mean performance of the model indicate that progress has been made in the tropics with recent improvements in the physical parametrization, increased model resolution and improvements in analysis. The 48 and 72 hour forecasts of the wind and mass fields show good consistency with each other and a reasonable agreement with analysis. However a number of problems remain, the main one being the weakening of tropical divergent circulation with time and a related weakening in the convective activity in the model. Another systematic problem which could cause the above problem is the underestimation of the outgoing radiative flux by the radiative parametrization in the model.

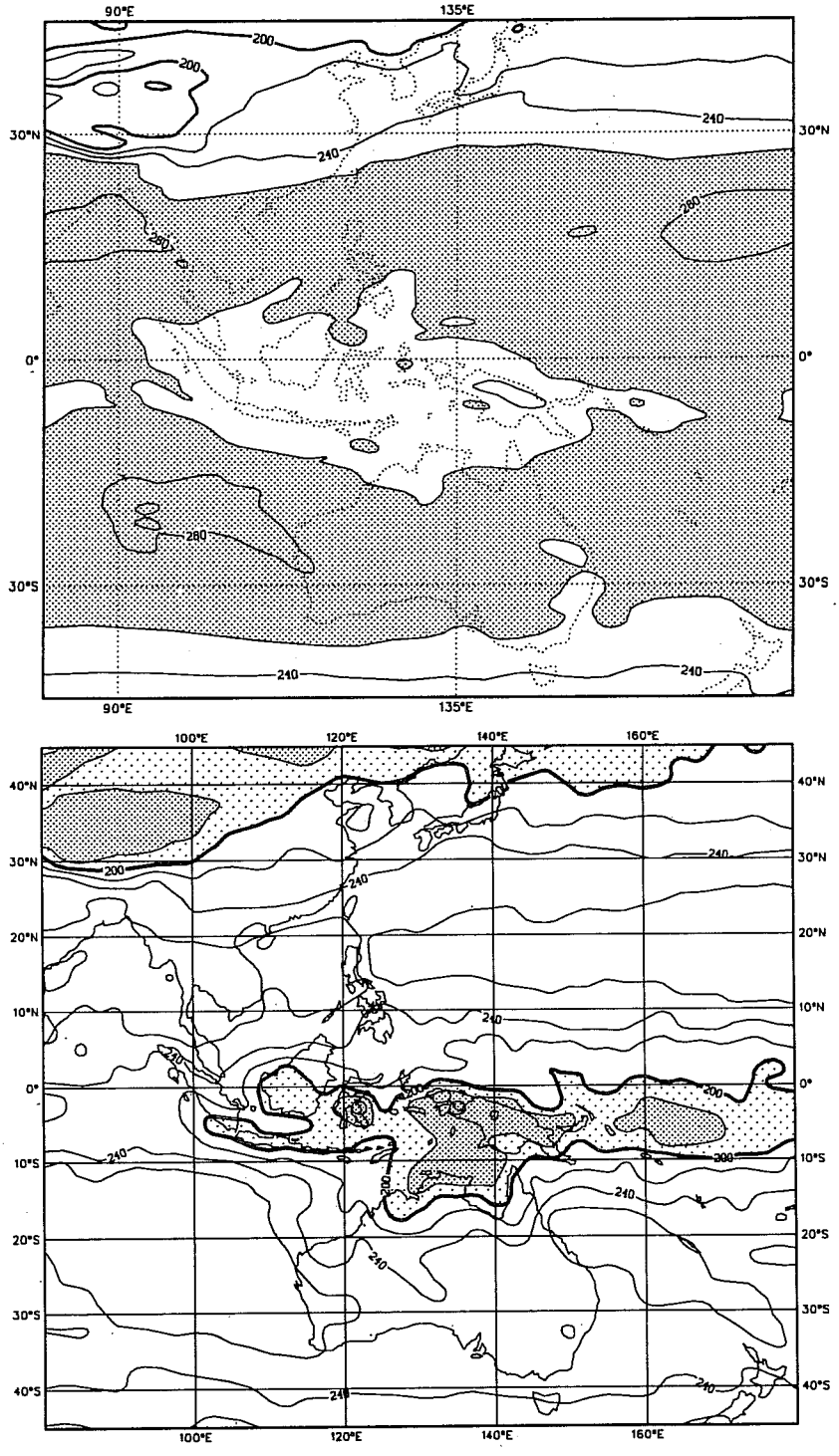

Fig. 18 Mean long wave radiation for 48 hr forecasts at the top of model (top) and mean outgoing longwave radiation flux from NOAA-9 for the period Jan 18 to Feb 15, 1987 (bottom). Units are watts in m^{-2} and contour intervals are 20 watts m^{-2}.

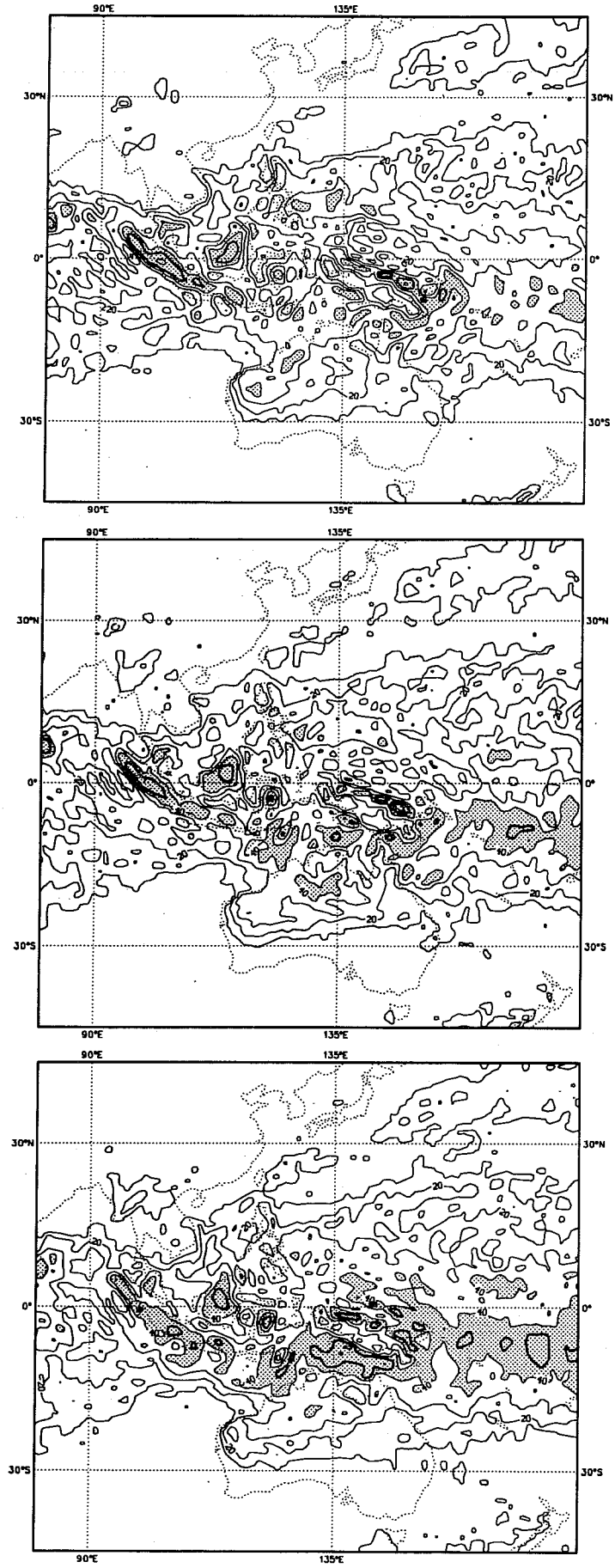

Fig. 19 24 hr (bottom), 48 hr (middle) and 72 hr (top) forecast convective cloud cover. Units are in % and contour interval is 10%.

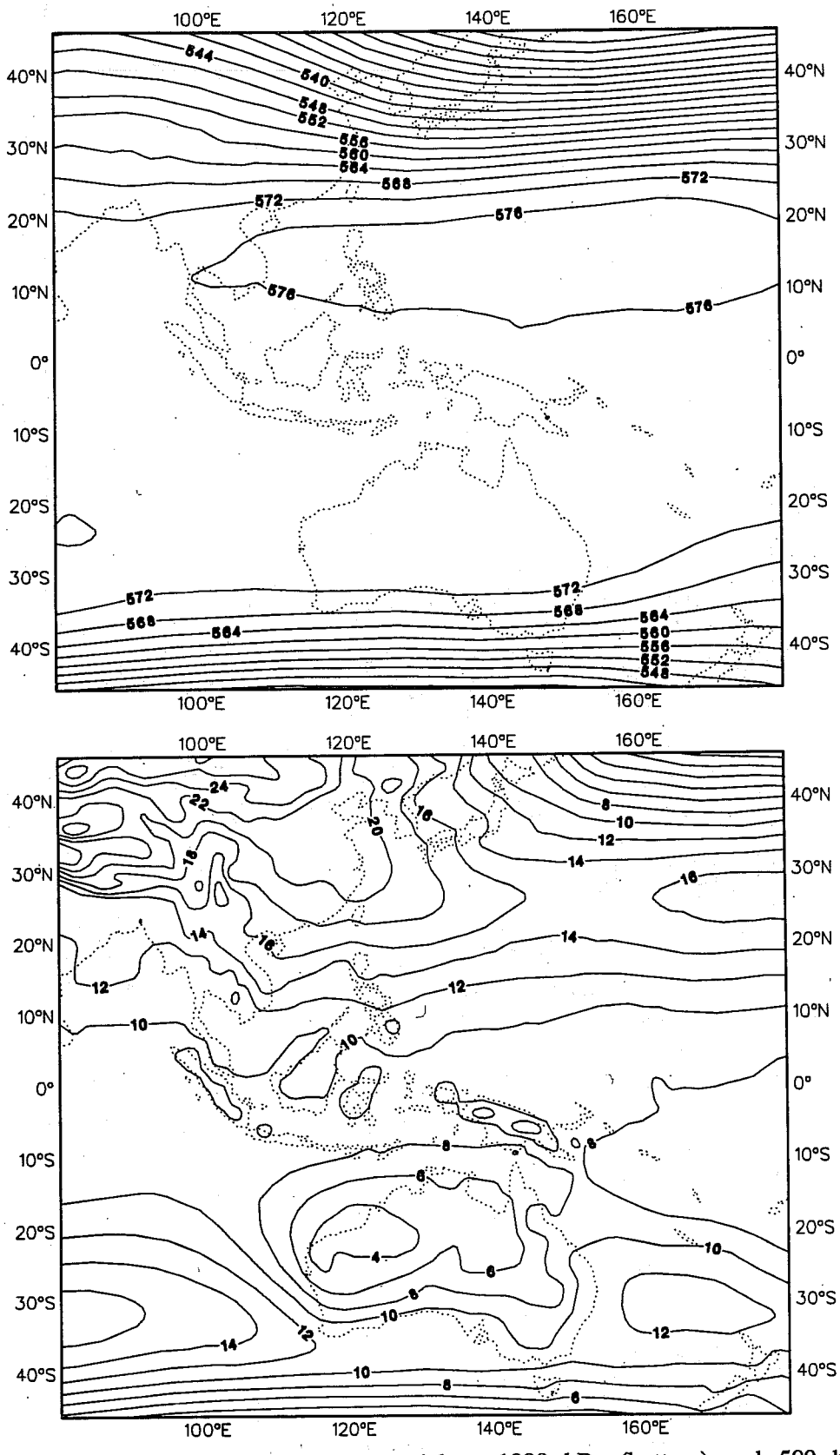

Fig. 20a As in Fig. 8a but for the geopotential at 1000 hPa (bottom) and 500 hPa (top). Units are in $10^2 m^2 s^{-2}$ and contour intervals at 1000 hPa and 500 hPa are $2x10^2 m^2 s^{-2}$ and $4x10^2 m^2 s^{-2}$ respectively.

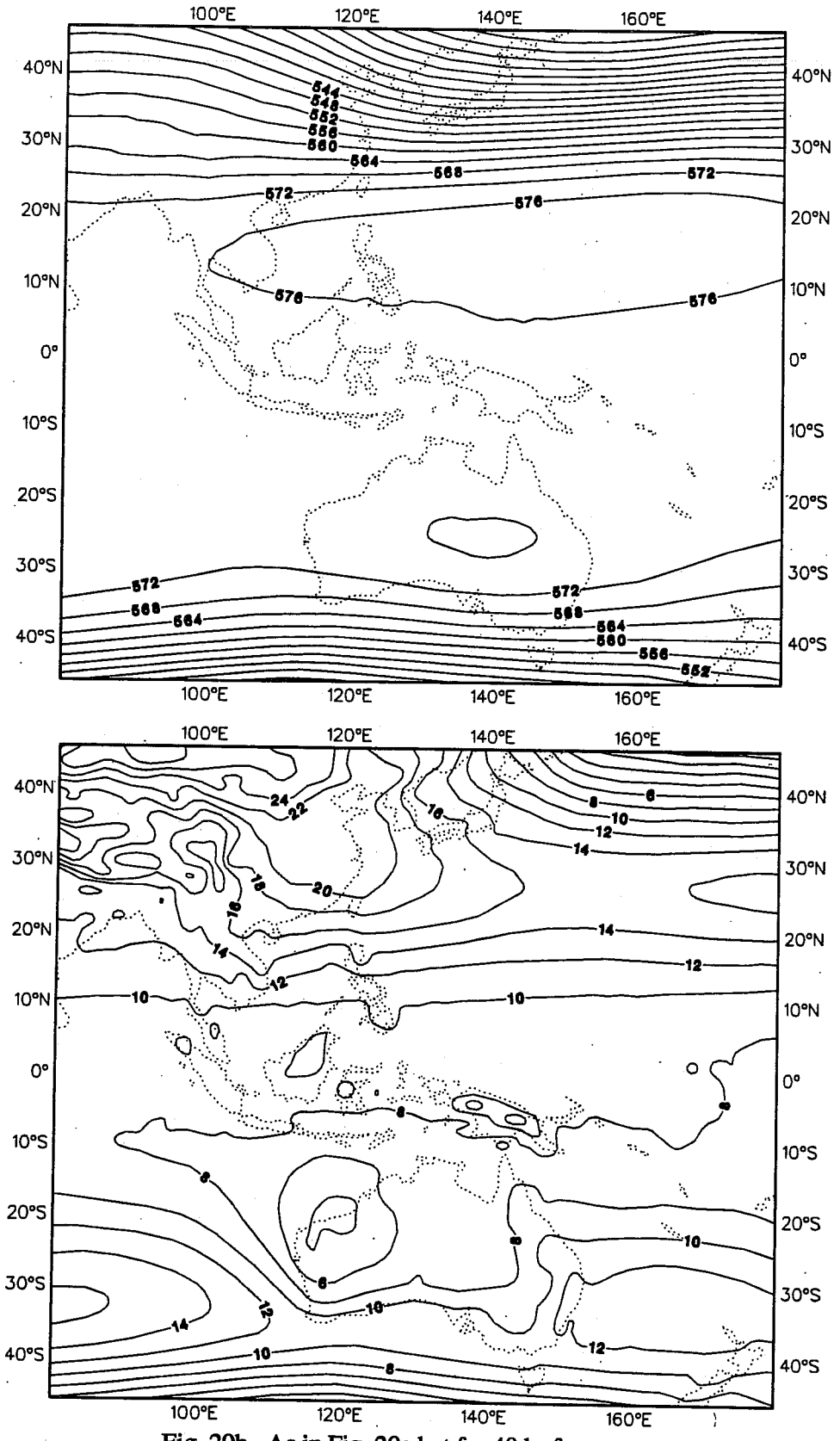

Fig. 20b As in Fig. 20a but for 48 hr forecasts.

3. TROPICAL CYCLONES

Numerical weather prediction models such as the one used at ECMWF have attained resolutions where small scale atmospheric features such as tropical cyclones are beginning to be resolved. During the period considered in this study four tropical cyclones, Irma, Connie, Damien and Jason, formed in the Australian tropics. The tracks followed by the cyclones as obtained from BOM are shown in Fig. 21. Two of the cyclones, Irma and Jason formed within the enhanced AMEX network around the Gulf of Carpentaria. The aim of this section is to consider the performance of the ECMWF analysis - forecast system in handling these tropical cyclones. Analyses and forecasts for each cyclone will be considered separately. Our main attention will be focused on the location of the cyclones and their gross features, as the ECMWF model and analysis scheme cannot resolve the inner structure and finer details of the cyclones. TC's Irma and Jason will be considered in more detail as these cyclones formed within the AMEX network and were therefore well observed.

3.1 Analyses of tropical cyclones

(i) Tropical cyclone Connie

Tropical cyclone Connie formed from a low which originated over land, intensified rapidly and reached tropical cyclone intensity around 1200 GMT 17 Jan 1987. Connie then moved southwest, intensifying to a maximum intensity of around 950 hPa. It crossed the coast at 20.3°S, 118.5°E around 0900 GMT Jan 19 and continued inland on a southerly track weakening slowly. Further details of the cyclones considered here can be found in Manchur (1987). The track followed by Connie as obtained from BOM is shown in Fig. 21 and the position and intensity as a function of time as determined by the Bureau of Meteorology (BOM) are shown in Table 1. The location of the cyclones are determined by the Bureau from GMS imagery and radar if the cyclone is within range of a radar station. The intensity, in terms of central pressure and maximum wind speed is estimated using the Dvorak technique and could be in considerable error. The strongest wind recorded during the cyclone was a wind gust of 171 km h^{-1} (48 ms^{-1}) at Port Hedland at 191147 GMT when the mean wind speed was 93 km h^{-1} (26 ms^{-1}). Figs. 22(a) to (e) show the ECMWF sea level pressure and 850 hPa wind analyses of TC Connie at 12 hour intervals. The figures also show the observations that were accepted by the analyses. The location of the cyclone as determined from the minimum sea level pressure and the central pressure are also shown in Table 1 and the cyclone track as obtained from the ECMWF analyses is shown in Fig. 23 at 12 hour intervals. In general the cyclone is located with 1° to 1.5° of the Bureau's fix with a maximum error of around 2° in longitude at 0000 GMT on Jan 18. The analysed central pressures are generally much weaker than the estimates shown in Table 1. Although the BOM estimates are liable to have considerable error, there were some observations which indicate that the central pressures were much deeper than the ECMWF analysed values and closer to the Bureau's estimates. This can be seen in Fig. 24 which

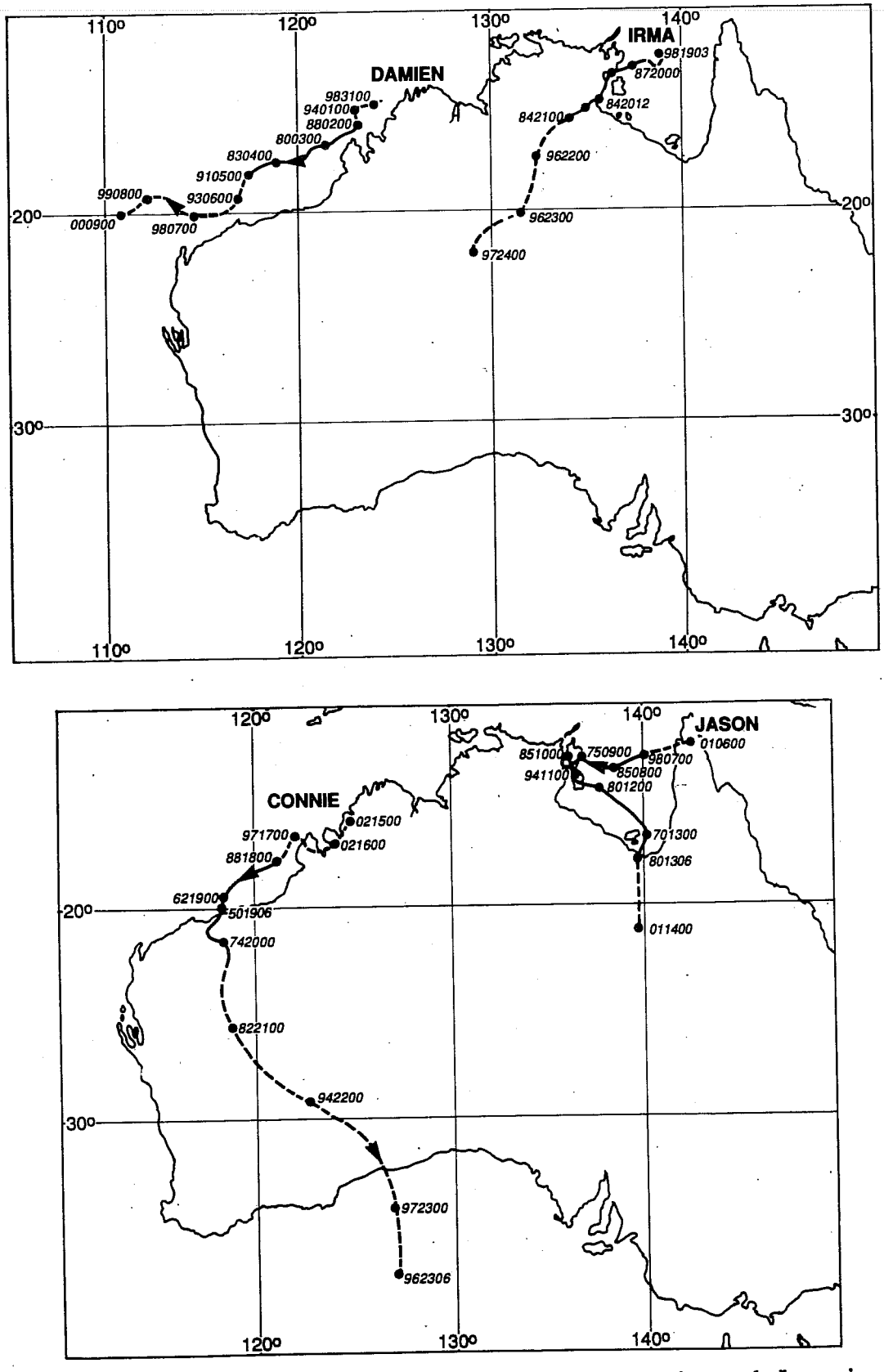

Fig. 21 Best tracks and intensities for TCs Irma, Connie, Damien and Jason issued by BOM.

TROPICAL CYCLONE CONNIE - TRACKS

Jan	BOM			Ops Analysis		
	Lat (S)	Long (E)	Press (hPa)	Lat (S)	Long (E)	Press (hPa)
17/1200	17.1	121.9	994	17.4	121.9	997
18/0000	17.8	121.0	988	16.2	119.2	993
18/1200	18.5	119.2	976	17.3	120.4	990
19/0000	19.5	118.6	962	18.5	119.5	991
19/1200	20.5	118.4	955	19.6	119.2	994
20/0000	22.0	118.4	974	20.7	119.4	994
20/1200	23.5	118.2	980	23.0	118.1	995
21/0000	25.9	118.9	982	25.2	119.3	994

Table 1 Locations and central pressures for TC Connie obtained from BOM best estimates and the ECMWF operational (ops) analyses.

TROPICAL CYCLONE IRMA - TRACKS

Jan	BOM			Ops Analysis		
	Lat (S)	Long (E)	Press (hPa)	Lat (S)	Long (E)	Press (hPa)
19/0000	12.5	138.6	994	14.2	137.0	1004
20/0000	12.8	137.4	987	13.0	137.0	1002
20/1200	13.6	135.9	984	15.4	135.9	1002
21/0000	15.4	134.1	984	16.5	134.5	999

Table 2 As in Table 1 but for TC Irma.

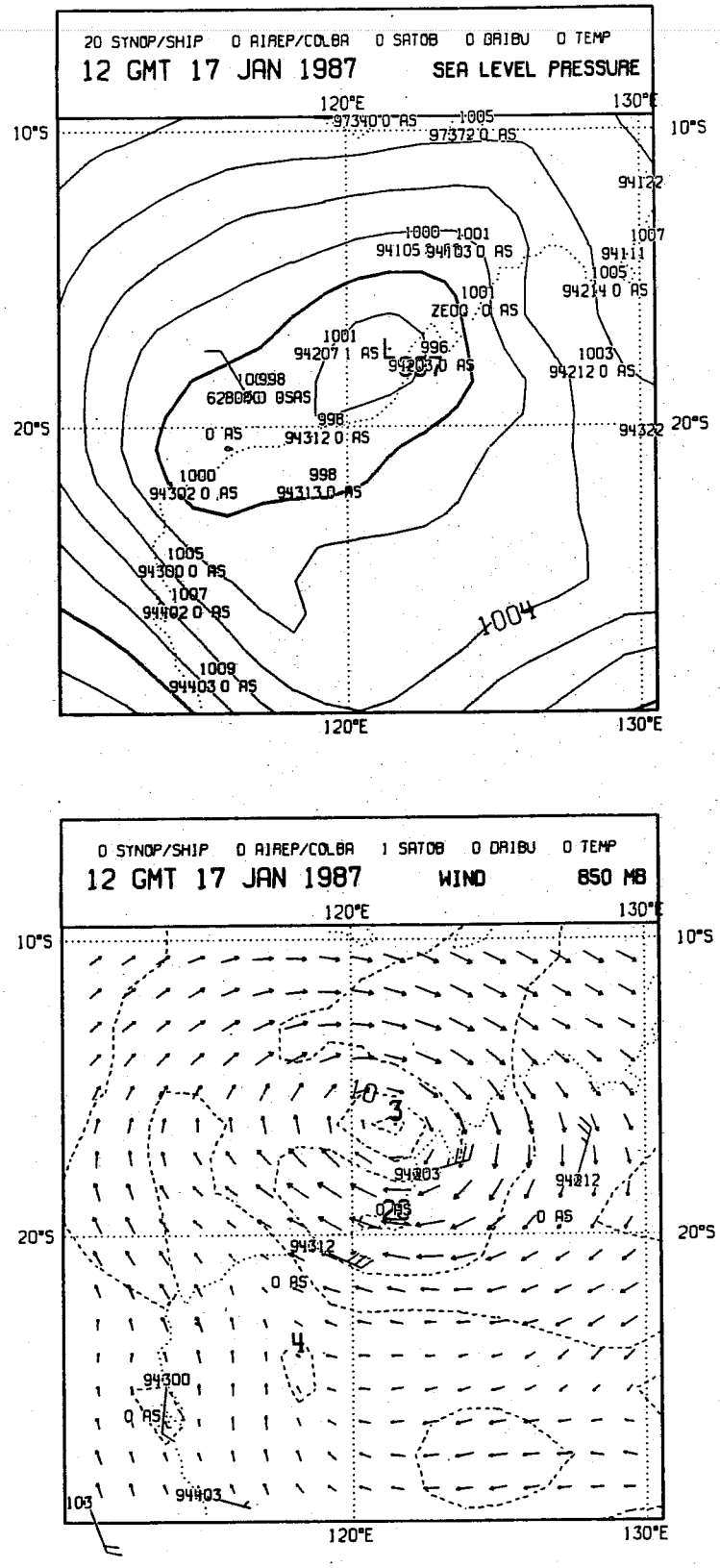

Fig. 22a MSLP (top in hPa) and 850 hPa vector wind (bottom in ms^{-1}) ECMWF analyses for TC Connie at 1200 GMT Jan 17. Contour intervals are 2 hPa and 5ms^{-1} respectively for MSLP and isotachs. The observations used by the analyses are also shown.

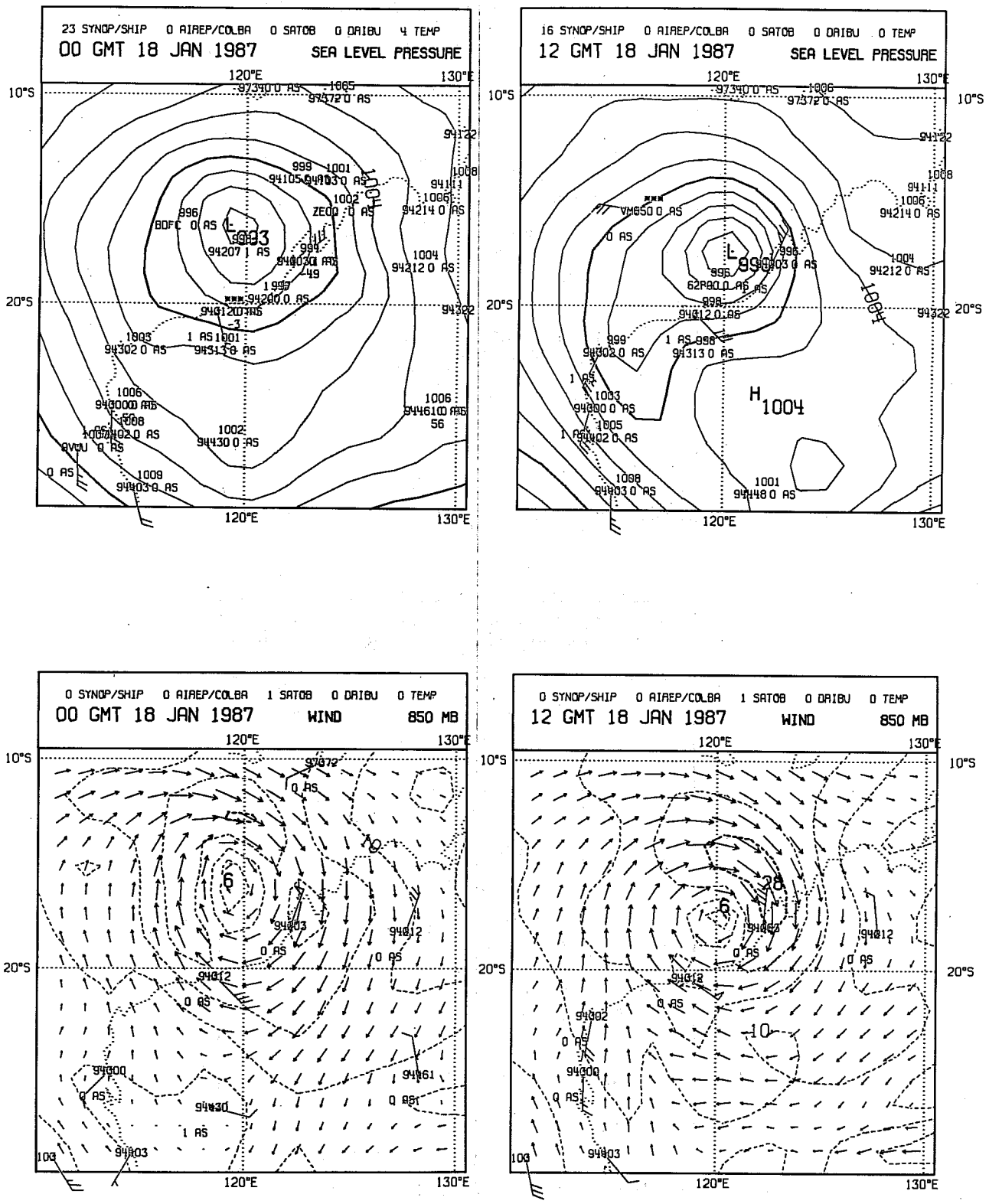

Fig. 22b As in Fig. 22a but for analyses at 0000 and 1200 GMT Jan 18 for TC Connie.

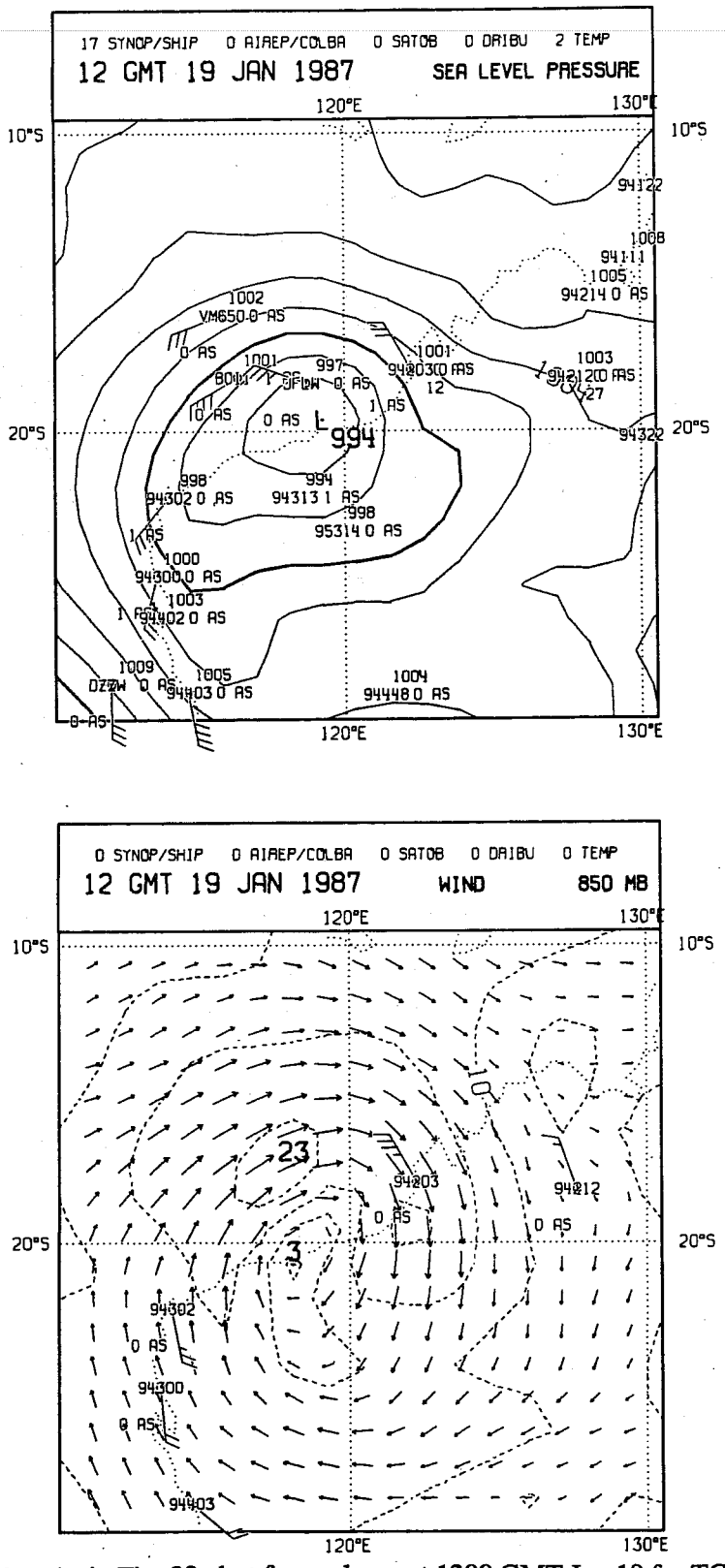

Fig. 22c As in Fig. 22a but for analyses at 1200 GMT Jan 19 for TC Connie.

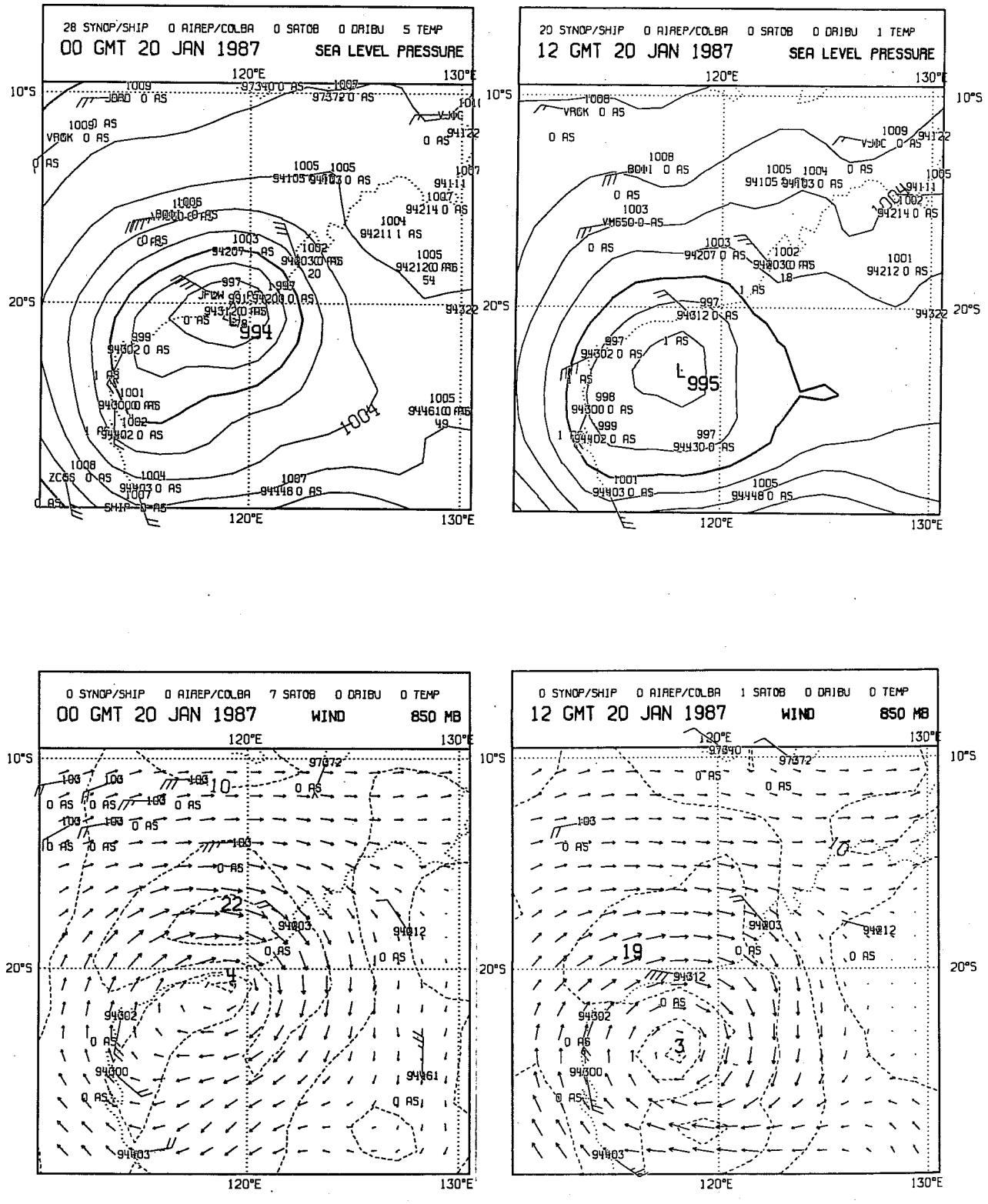

Fig. 22d As in Fig. 22a but for analyses at 0000 and 1200 GMT Jan 20 for TC Connie.

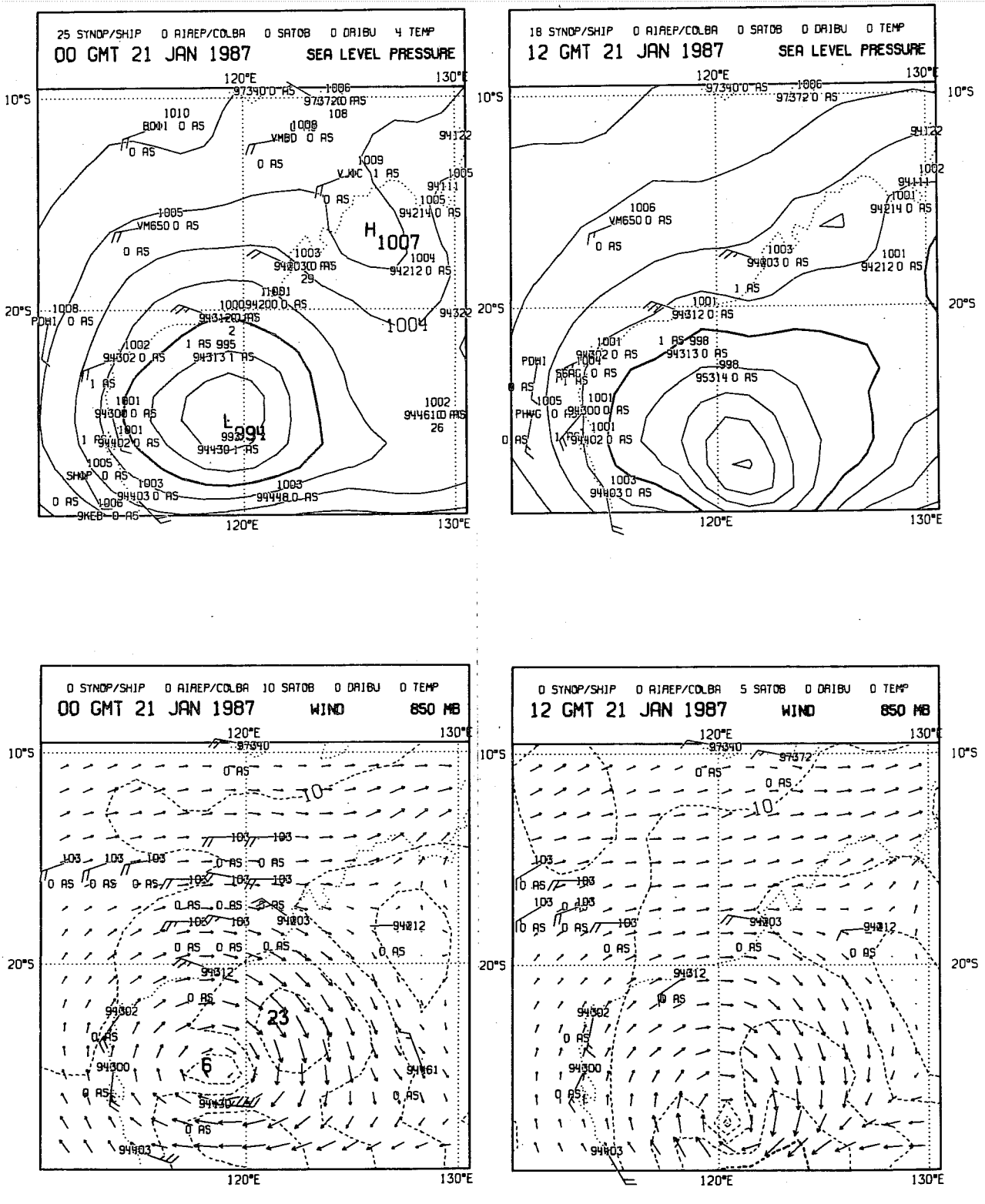

Fig. 22e As in Fig. 22a but for analyses at 0000 and 1200 GMT Jan 21 for TC Connie.

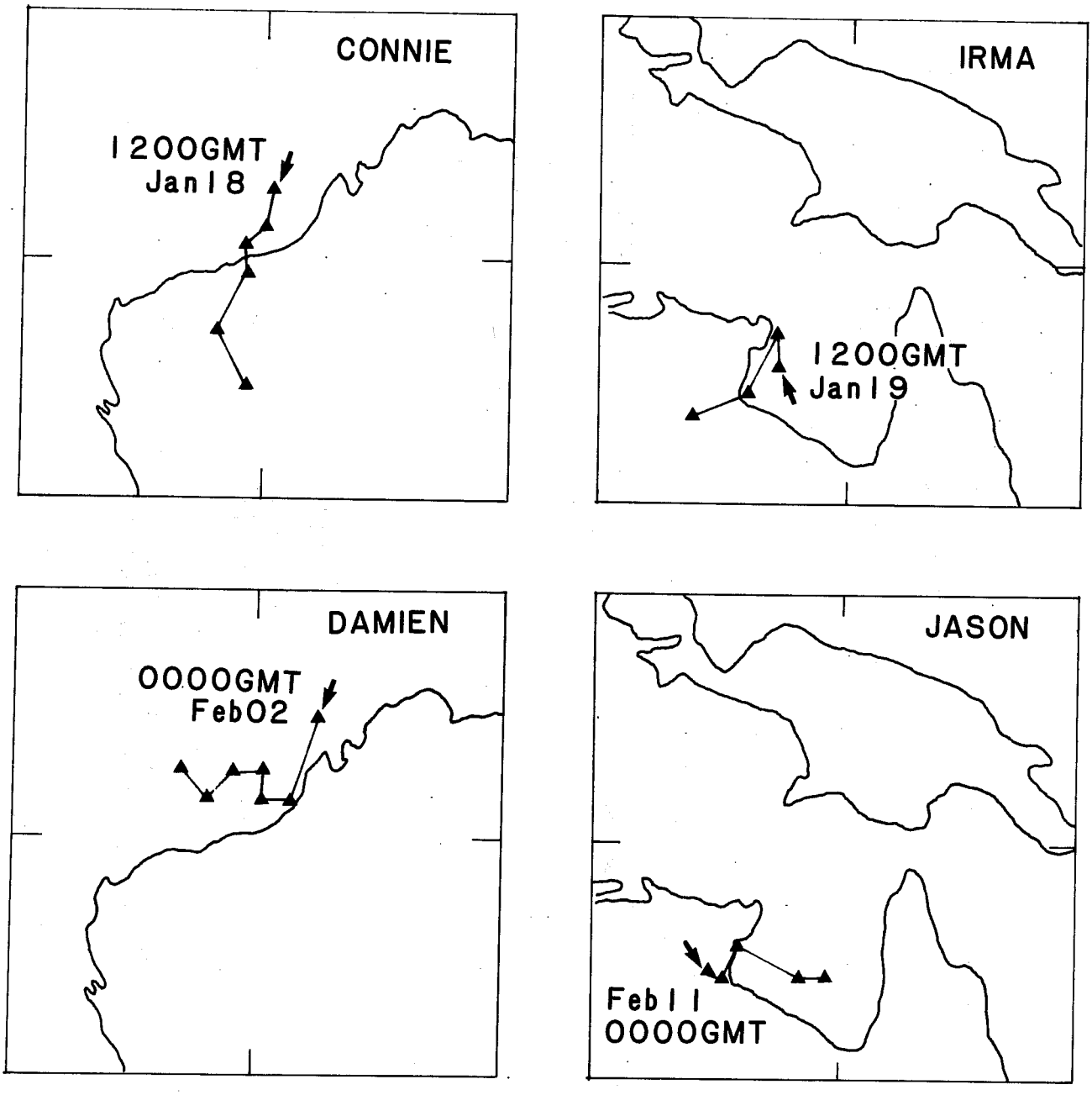

Fig. 23 Track for TCs Connie, Irma, Damien and Jason at 12 hr intervals as obtained from ECMWF analyses.

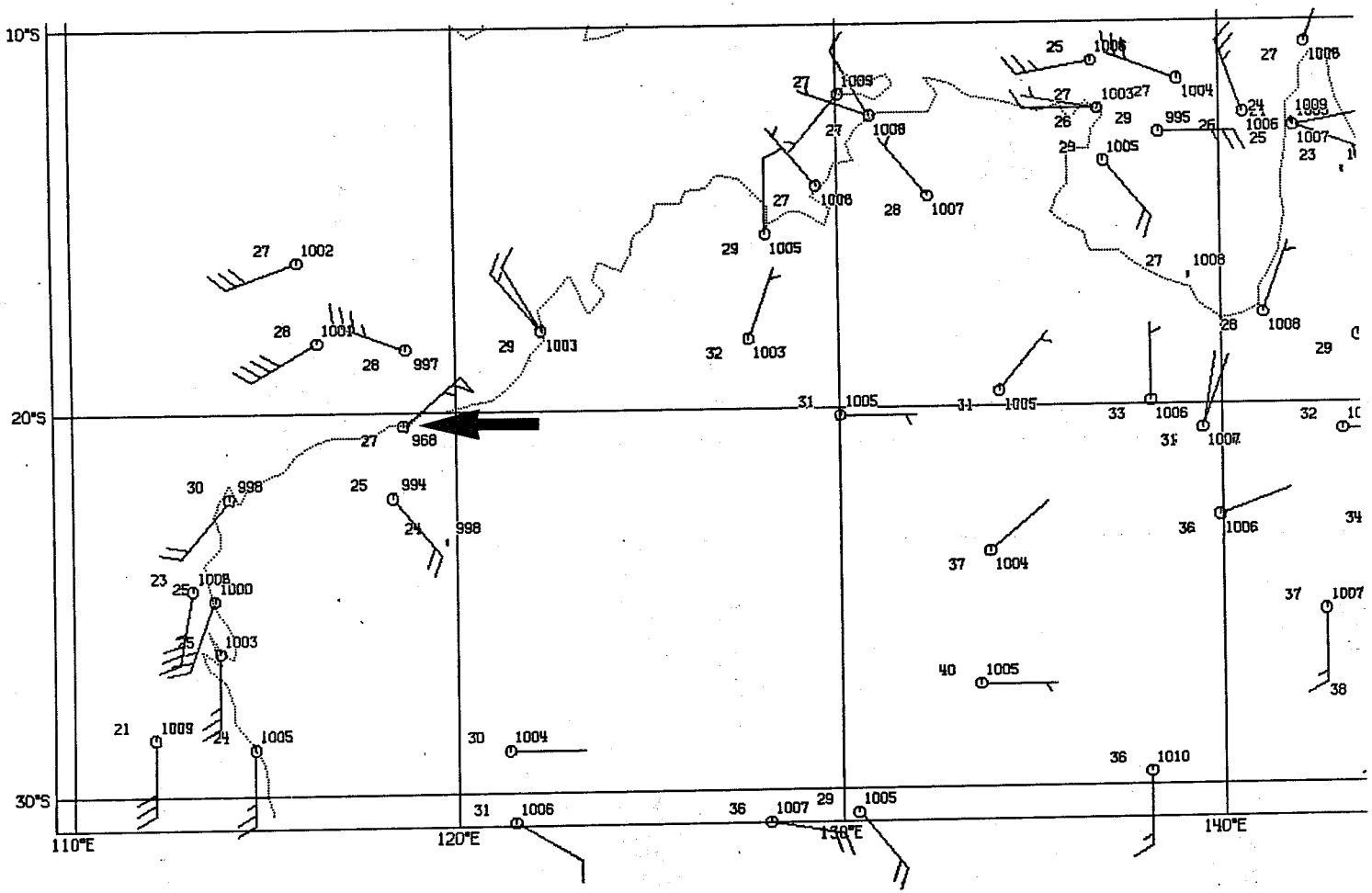

Fig. 24 All surface observations available for analysis at 1200 GMT Jan 19 in the region of TC Connie. Observation of 968 hPa is indicated by the arrow.

shows all the surface observations available at 1200 GMT Jan 19 when the cyclone was at its most intense stage. Note the observation of 968 hPa at station 94312 (Port Hedland). This observation was in fact rejected by the ECMWF analysis system as indicated in Fig. 25 which shows all observations that were rejected at this time. Fig. 25 also shows another example of a key observation within the cyclone that was rejected by the analysis system for 0000 GMT Jan 20. This observation also indicates that the cyclone at this stage was considerably deeper than analysed. Further evidence that the ECMWF analysis system leads to central pressures that are too weak can be seen in Fig. 26 which shows the UKMO analyses for the sea level pressure and 850 hPa wind at 1200 GMT Jan 19. Note that the central pressure of 983 hPa is significantly deeper than the corresponding ECMWF analysis.

(ii) Tropical cyclone Irma

Tropical cyclone Irma developed from an area of deep convection in the northern Gulf of Carpentaria that had persisted for several days prior to January 19. The low continued to intensify and was upgraded to a cyclone at 1200 GMT Jan 19. Irma moved in a southwesterly direction and crossed the coast around 1200 GMT Jan 20. The lowest pressure recorded was 989.9 hPa and strongest wind reported was 111 km h^{-1} (31 ms^{-1}). It should be noted that Irma formed within the enhanced data network of AMEX and was therefore relatively well observed. The track followed by Irma as obtained from BOM is shown in Fig. 21 and the position and intensity as a function of time are shown in Table 2. Figs. 27(a) to (c) show the ECMWF sea level pressure and 850 hPa wind analysis of TC Irma at 12 hour intervals together with observations that were accepted by the analysis system. Fig. 28 shows observations that were rejected for two analysis times. The location of the cyclone and the central pressure as obtained from the ECMWF analyses are also shown in Table 2 and the cyclone track according to these analyses is shown in Fig. 23. The analysed cyclone locations are within 1° to 2° of the BOM's locations and the analysis system correctly located landfall around 1200 GMT Jan 20. As with TC Connie the analysed central pressures are much weaker than the BOM estimates. Figure 28 shows that the rejected surface observations are those which indicate lower surface pressures. Further evidence for the ECMWF sea level pressure analyses being too weak is given by the UKMO sea level pressure analyses for 1200 GMT Jan 20 in Figure 29 which shows a central pressure of 996 hPa compared to 1002 in the ECMWF analysis. Note however that the UKMO analysis places the cyclone too far to the north. The UKMO operationally use manually generated TC bogus data but no bogus data were used for TC Irma.

(iii) Tropical cyclone Damien

Tropical cyclone Damien formed from al monsoonal low and attained tropical cyclone at 2100 GMT February 1. TC Damien was a maritime cyclone throughout its life cycle. The strongest observed wind was about 83 km h^{-1} (23 ms^{-1}) to the north of the cyclone at 1200

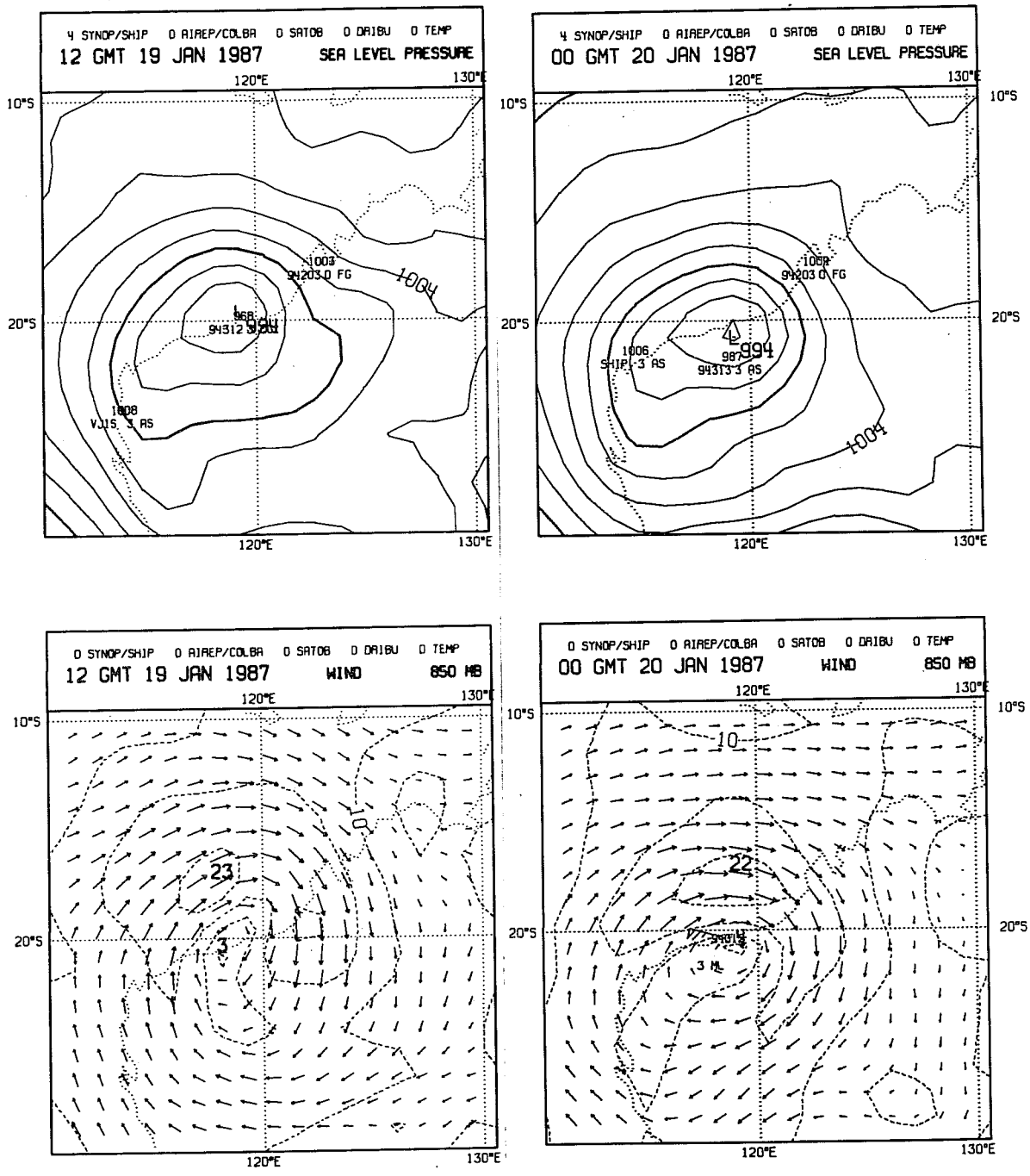

Fig. 25 As in Fig. 22c,d for analysis at 1200 GMT Jan 19 and 0000 GMT Jan 20 but showing observations rejected by the analysis.

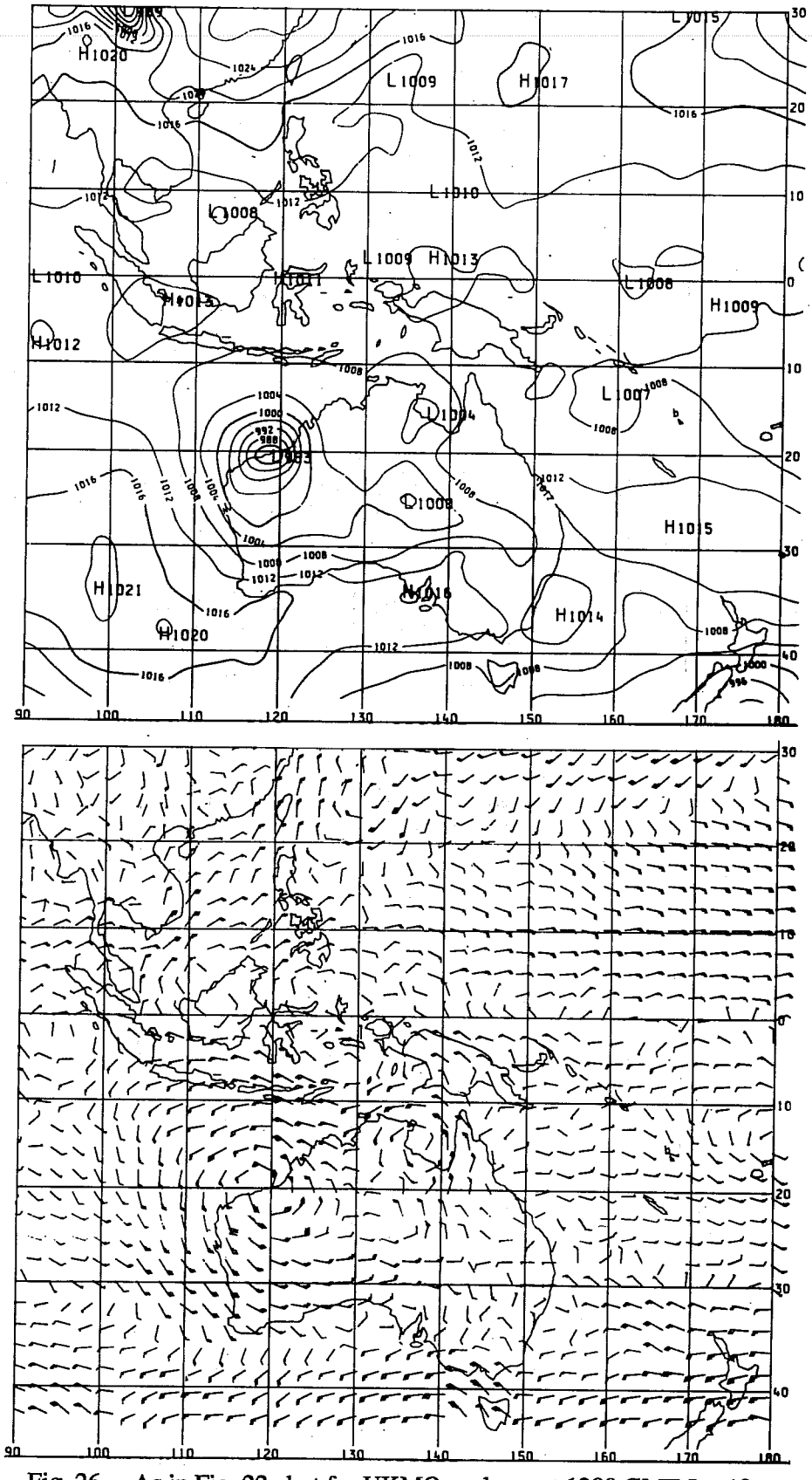

Fig. 26 As in Fig. 22a but for UKMO analyses at 1200 GMT Jan 19.

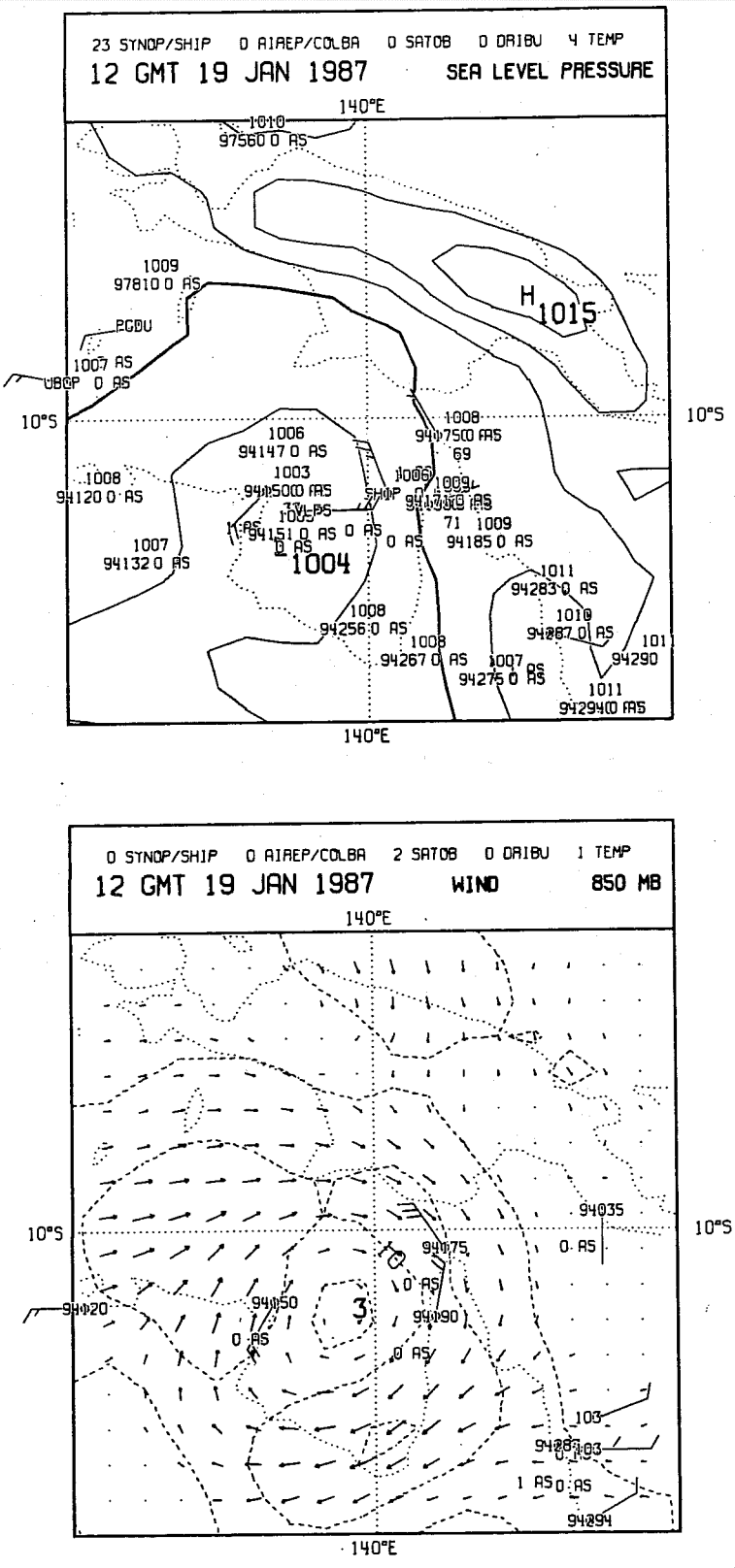

Fig. 27a As in Fig. 22a but for analyses at 1200 GMT Jan 19 for TC Irma.

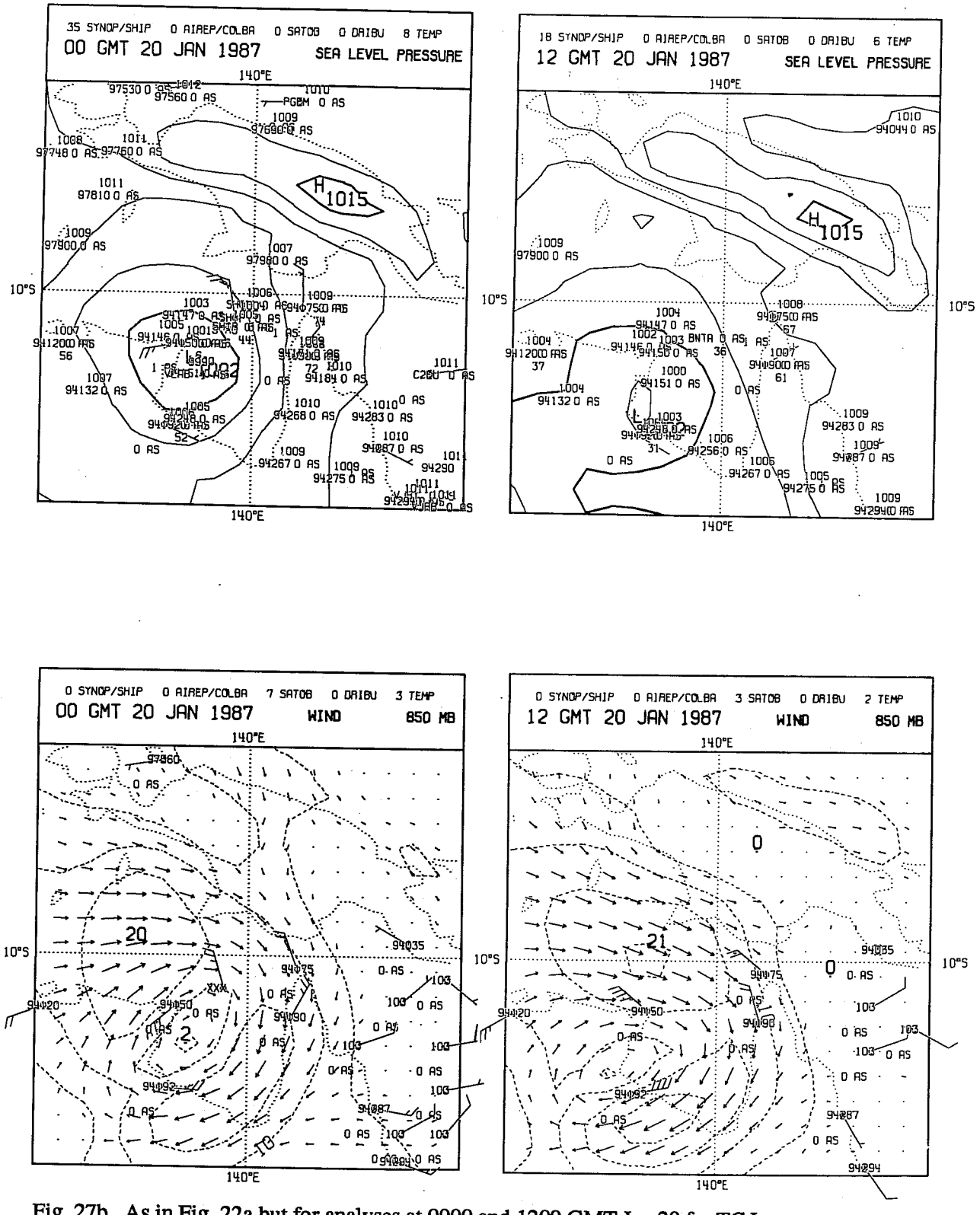

Fig. 27b As in Fig. 22a but for analyses at 0000 and 1200 GMT Jan 20 for TC Irma.

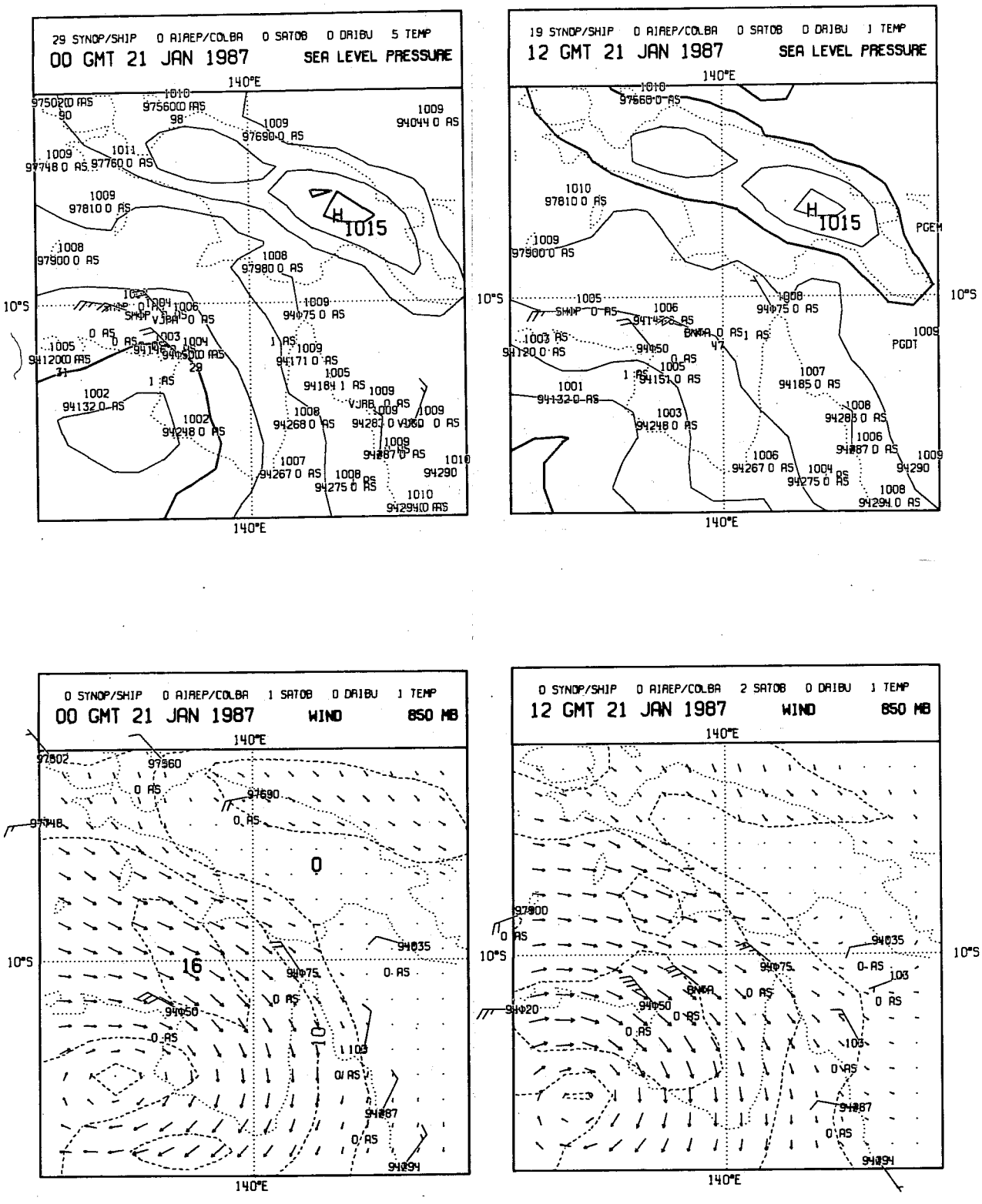

Fig. 27c As in Fig. 22a but for analyses at 0000 and 12 GMT Jan 21 for for TC Irma.

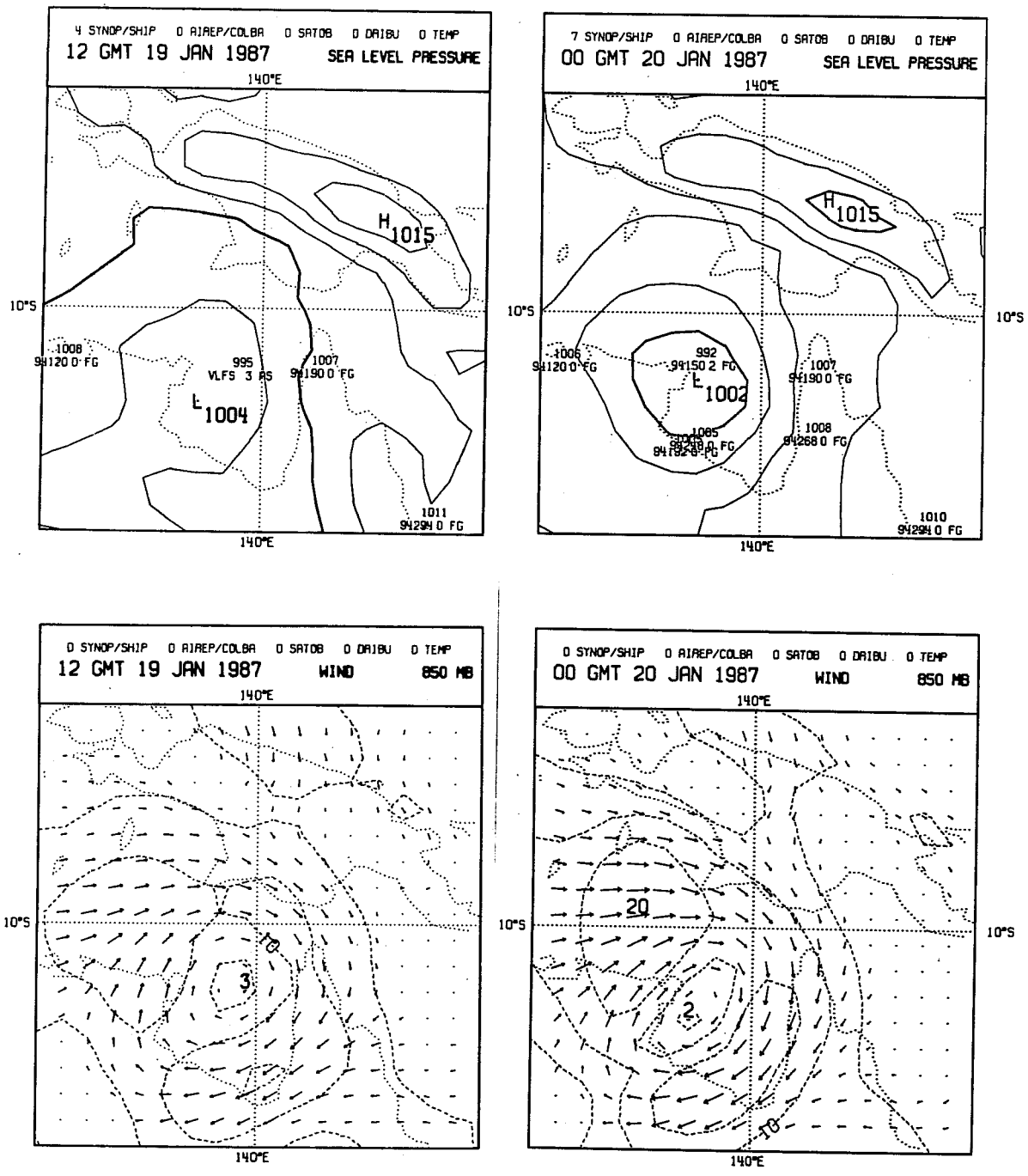

Fig. 28 As in Fig. 25 but for analyses at 12 GMT Jan 19 and 0000 GMT Jan 20 for TC Irma.

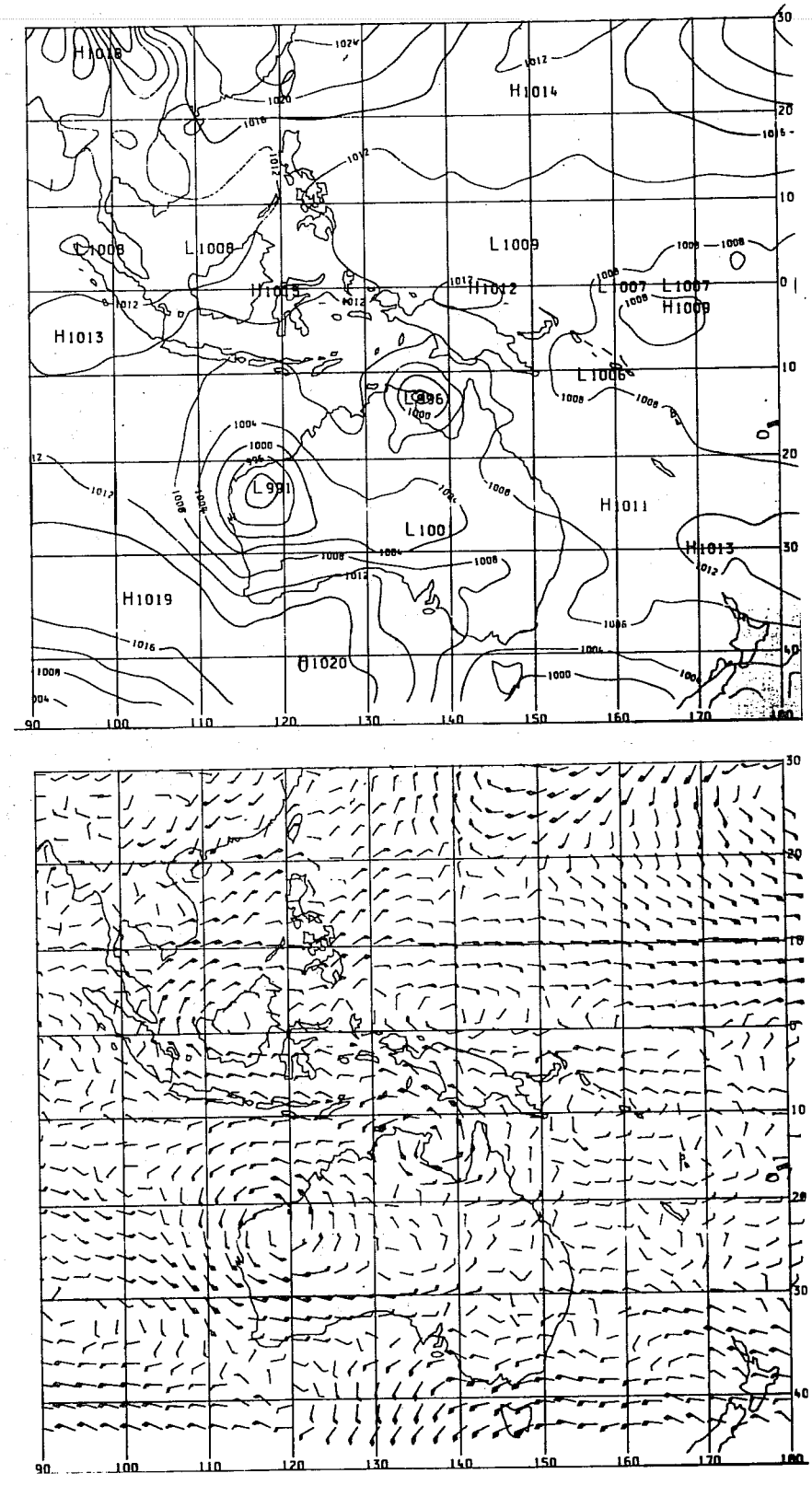

Fig. 29 As in Fig. 26 but 0000 GMT Jan 20.

GMT Feb 3 and the strongest estimated winds were 97 km/h (27 ms^{-1}) from 0000 GMT to 0600 GMT on Feb 3. The lowest central pressure was estimated to be 980 hPa at 0000 GMT Feb 3.

The track followed by Damien as obtained from BOM is shown in Fig. 21 and the position and intensity as a function of time as determined by BOM are shown in Table 3. Figs. 30(a) to (d) show the ECMWF sea level pressure and 850 hPa wind analyses for TC Damien at 12 hour intervals for part of its life cycle together with observations accepted by the system. The location of the cyclone and the central pressure as obtained from the ECMWF analyses are shown in Table 3 and the cyclone track according to these analyses is shown in Fig. 23. Although the location error in the early stages of the cyclone was 1.5° to 2°, the cyclone locations in the later stages (1200 GMT Feb 3 to 1200 GMT Feb 5) were well analysed with errors of less than 1°. The low level wind analyses also reflected most of the observed features. As with the previous cyclones the analysed central pressures are much weaker than the BOM estimates. However, in contrast to the other cyclones, no observations in the vicinity of the cyclone were rejected; closer inspection of the observations used in Fig. 30 shows that the analyses are consistent with observations, none of which reach the lower values of BOM estimates. Lack of observations close to the centre of the cyclones suggest that bogusing of data in the vicinity of the cyclone could be useful to improve the analysis of the intensity of tropical cyclones in addition to improving their location.

(iv) Tropical cyclone Jason

TC Jason developed from a tropical low which formed near the northeastern part of the Gulf of Carpentaria. The low moved west southwest, intensified and reached cyclonic intensity at around 0600 GMT Feb 7. The cyclone continued to move west southwest and crossed the coast at around 0000 GMT. It then weakened and drifted southward and moved over water again around 0000 GMT Feb 11. Jason initially moved eastward and then southeast and continued to intensify until it became a severe cyclone at about 1800 GMT Feb 12. It eventually made landfall near Burketown. The maximum intensity was reached at about 1800 GMT Feb 12 with a central pressure of 970 hPa. The highest reported wind speed was 159 km h^{-1} (44 ms^{-1}) at Burketown at 0520 GMT Feb 13 and the lowest recorded pressure was 981 hPa at 0030 GMT Feb 13. The track followed by Jason as obtained from BOM is shown in Fig. 21 and the position and intensity as a function of time is given in Table 4. Figs. 31(a) to (e) show the ECMWF sea level pressure and 850 hPa wind analyses for part of the life cycle of TC Jason together with the observations accepted by the analysis system while Fig. 32 shows the observations rejected for two for the analysis times. The cyclone location and the central pressure as obtained from the ECMWF analyses are shown in Table 4 and the cyclone track obtained from these analyses is shown in Fig. 23.

TROPICAL CYCLONE DAMIEN - TRACKS

Feb	BOM			Ops Analysis		
	Lat (S)	Long (E)	Press (hPa)	Lat (S)	Long (E)	Press (hPa)
02/0000	15.6	123.3	988	15.1	122.6	999
02/1200	16.3	122.5	984	18.4	121.6	997
03/0000	16.7	121.5	980	18.4	120.4	993
03/1200	17.4	120.6	982	17.4	120.4	997
04/0000	17.5	118.9	983	17.3	119.2	997
04/1200	17.8	117.8	987	18.4	118.1	996
05/0000	18.1	117.6	991	17.3	117.0	998
05/1200	18.7	117.2	992	18.4	118.1	998

Table 3 As in Table 1 but for TC Damien.

TROPICAL CYCLONE JASON - TRACKS

Feb	BOM			KUO Analysis		
	Lat (S)	Long (E)	Press (hPa)	Lat (S)	Long (E)	Press (hPa)
09/0000	12.9	136.8	977	13.1	135.9	1004
09/1200	13.0	136.2	984	14.3	137.1	1003
10/0000	12.6	136.1	990	14.3	137.2	1005
10/1200	13.1	136.2	992	*	*	*
11/0000	13.6	136.3	992	15.4	134.7	1003
11/1200	14.0	136.7	990	15.4	134.5	1002
12/0000	14.2	137.8	980	14.2	135.9	1002
12/1200	15.5	139.0	965	15.4	138.3	1002

Table 4 As in Table 1 but for TC Jason.

* Centre not well defined

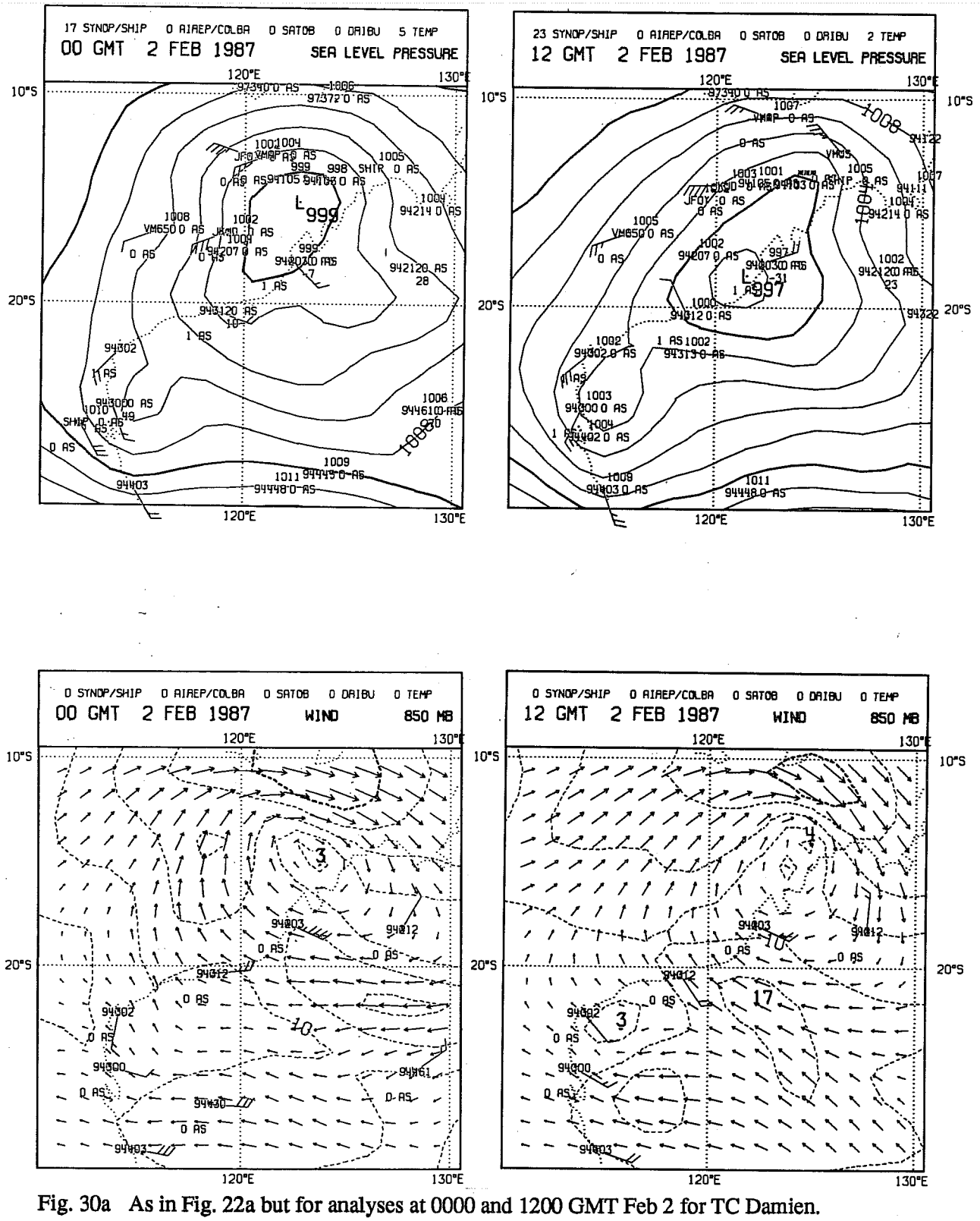

Fig. 30a As in Fig. 22a but for analyses at 0000 and 1200 GMT Feb 2 for TC Damien.

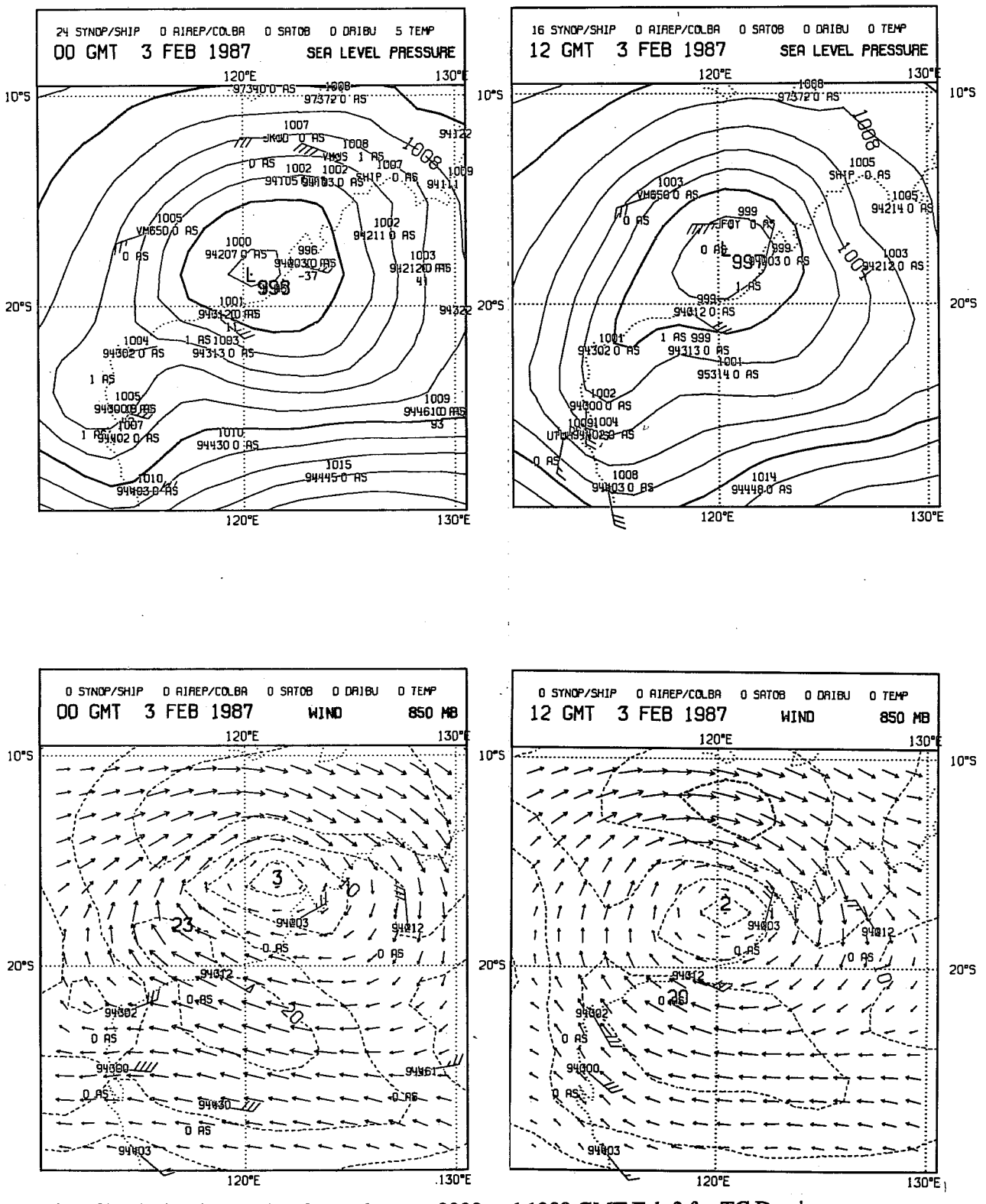

Fig. 30b As in Fig. 22a but for analyses at 0000 and 1200 GMT Feb 3 for TC Damien.

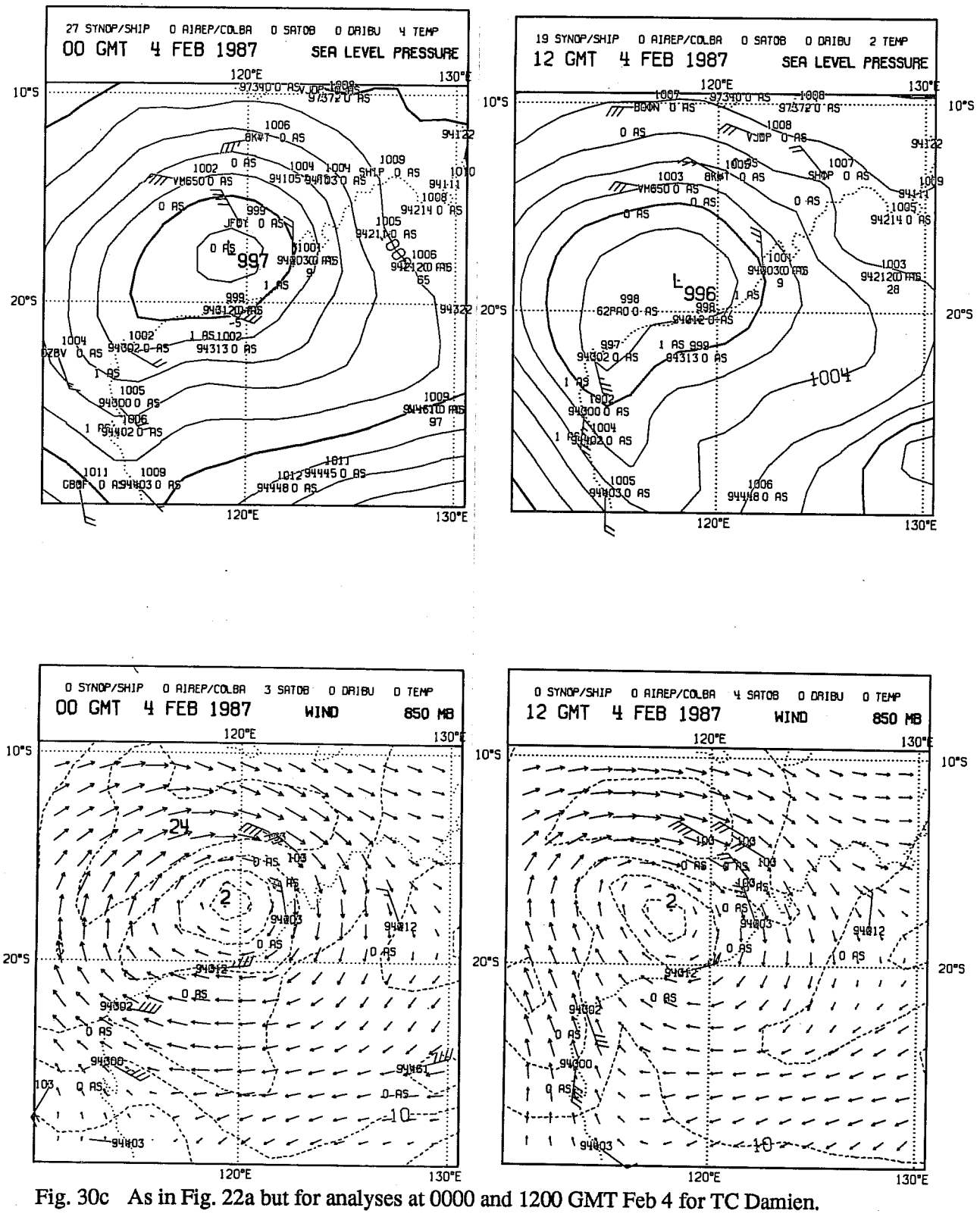

Fig. 30c As in Fig. 22a but for analyses at 0000 and 1200 GMT Feb 4 for TC Damien.

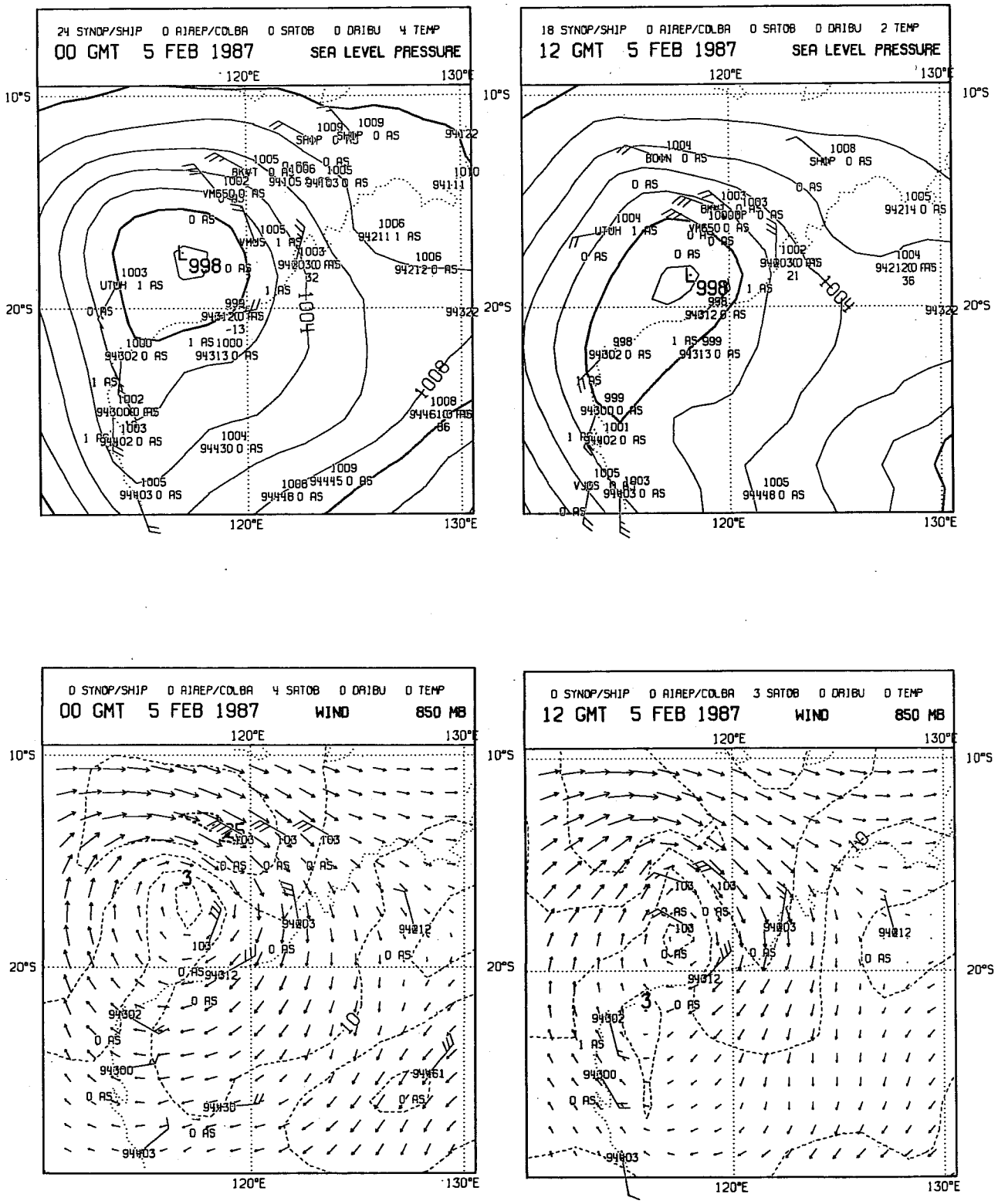

Fig. 30d As in Fig. 22a but for analyses at 0000 and 1200 GMT Feb 5 for TC Damien.

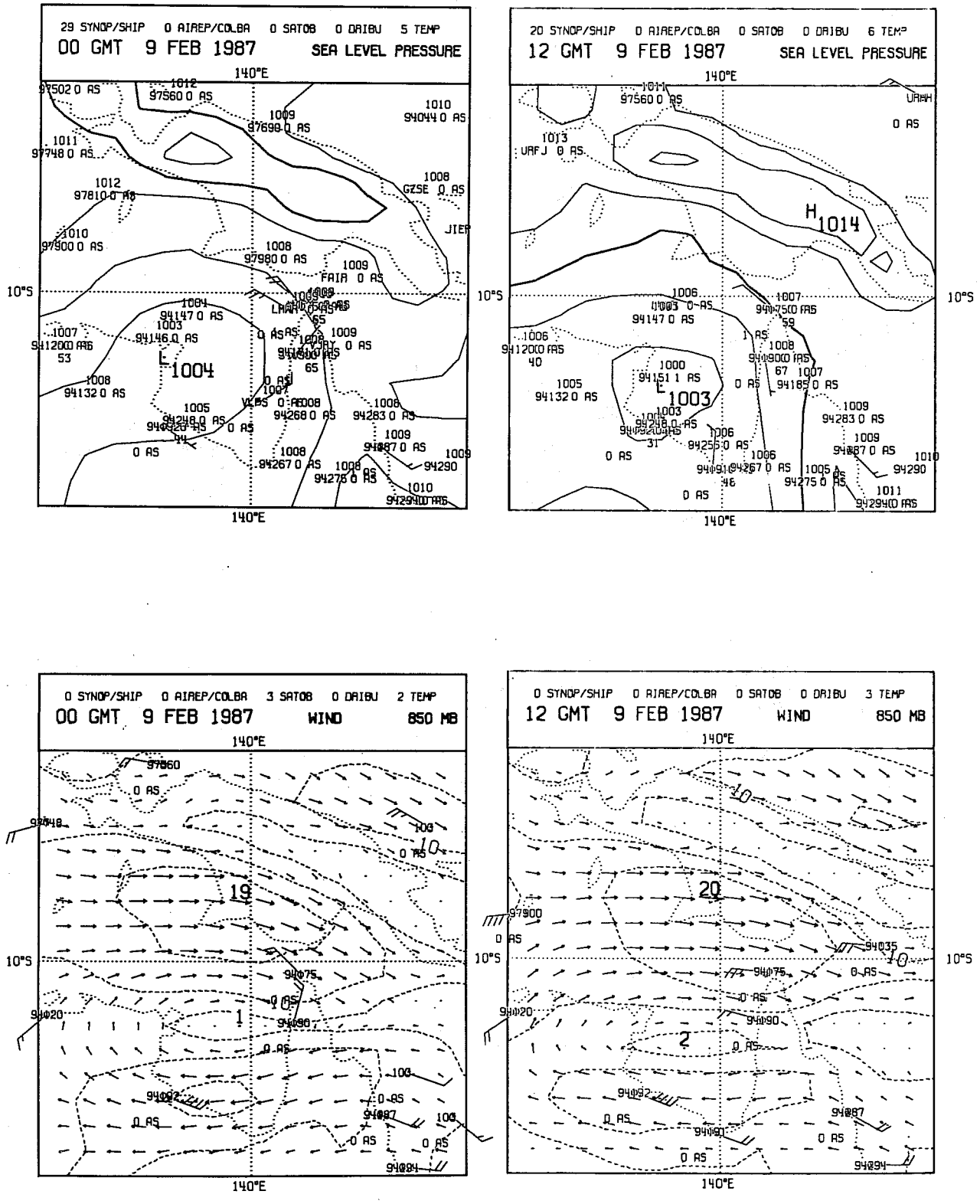

Fig. 31a As in Fig. 22a but for analyses at 0000 and 1200 GMT Feb 9 for TC Jason.

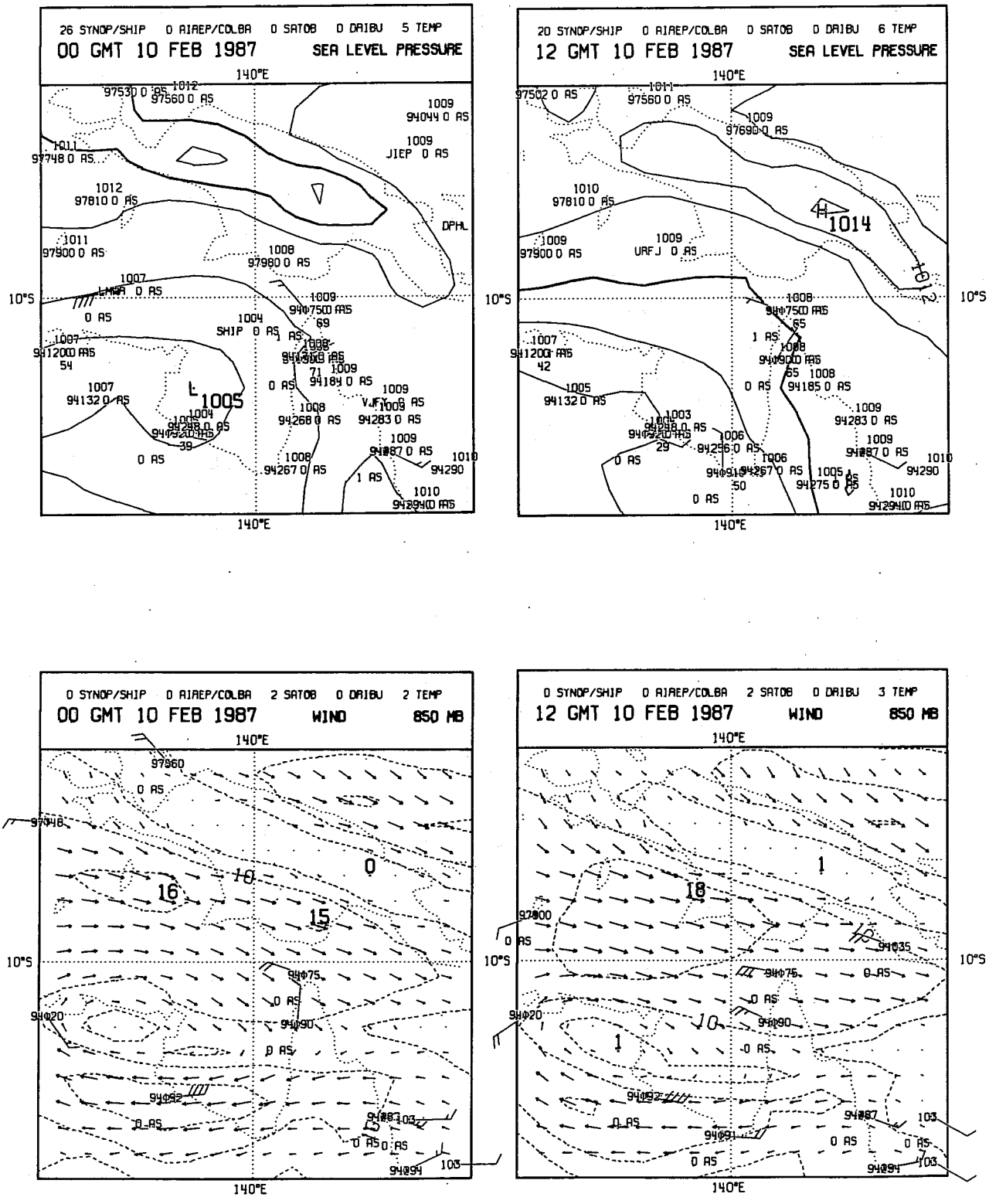

Fig. 31b As in Fig. 22a but for analyses at 0000 and 1200 GMT Feb 10 for TC Jason.

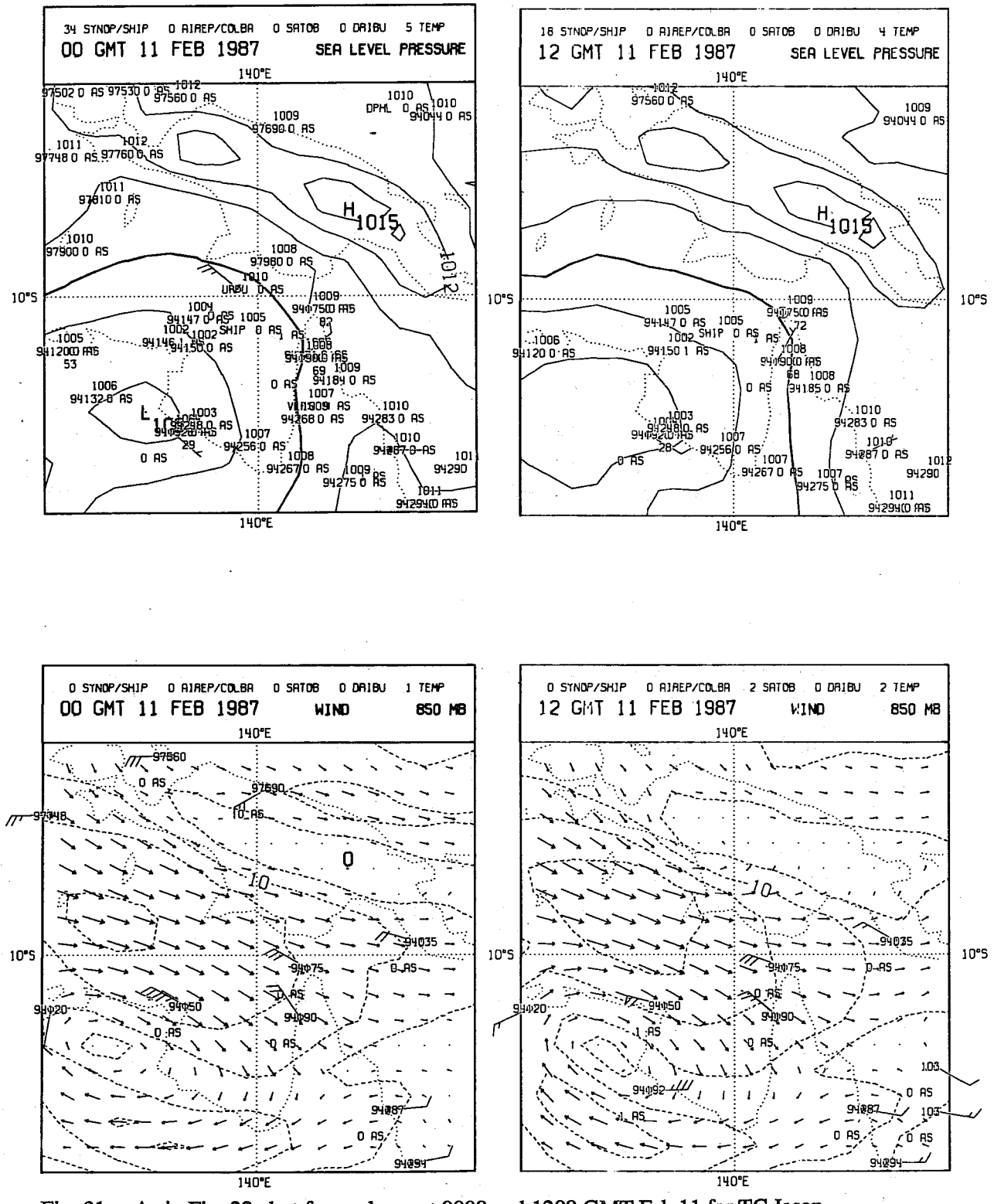

Fig. 31c As in Fig. 22a but for analyses at 0000 and 1200 GMT Feb 11 for TC Jason.

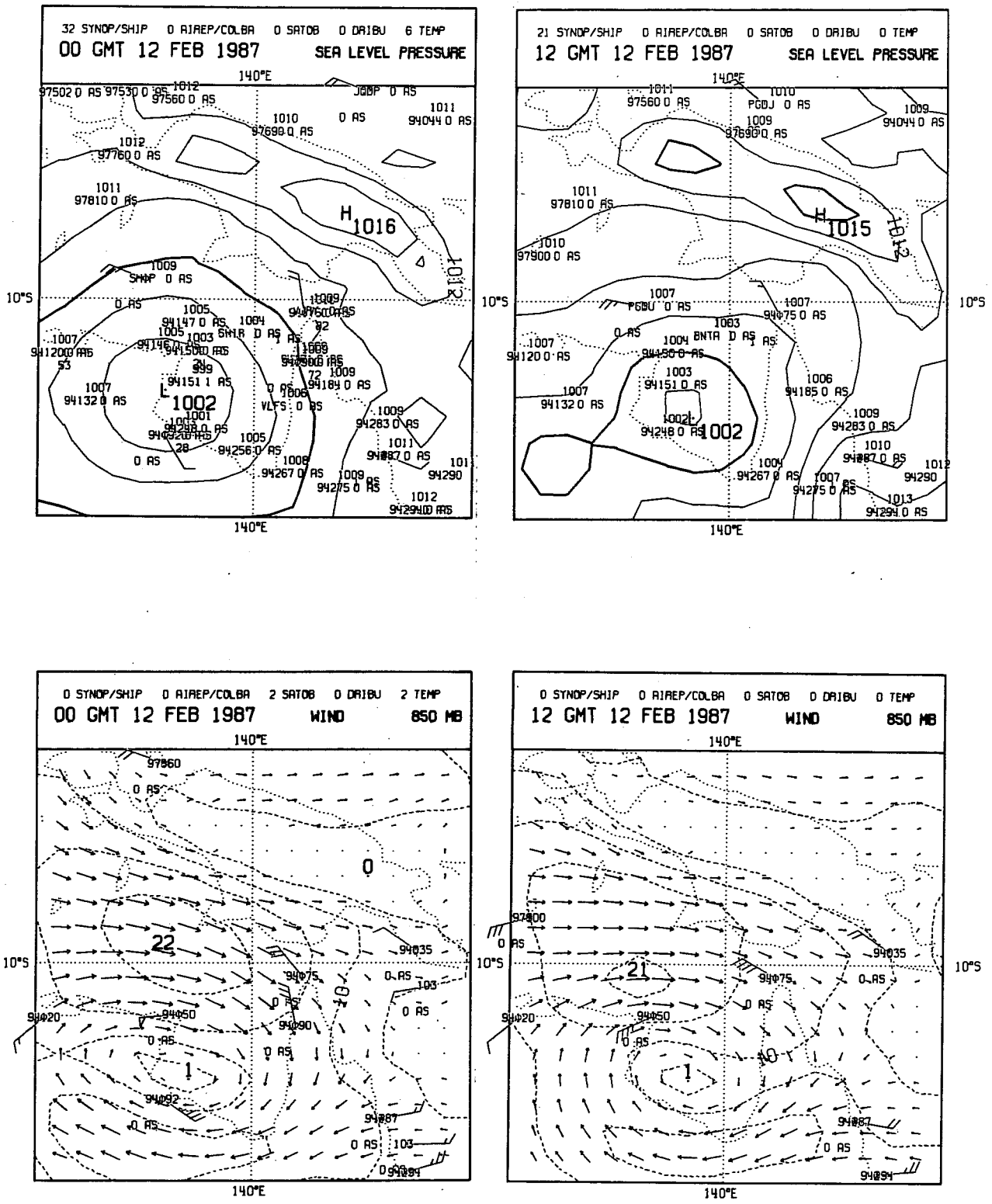

Fig. 31d As in Fig. 22a but for analyses at 0000 and 1200 GMT Feb 12 for TC Jason.

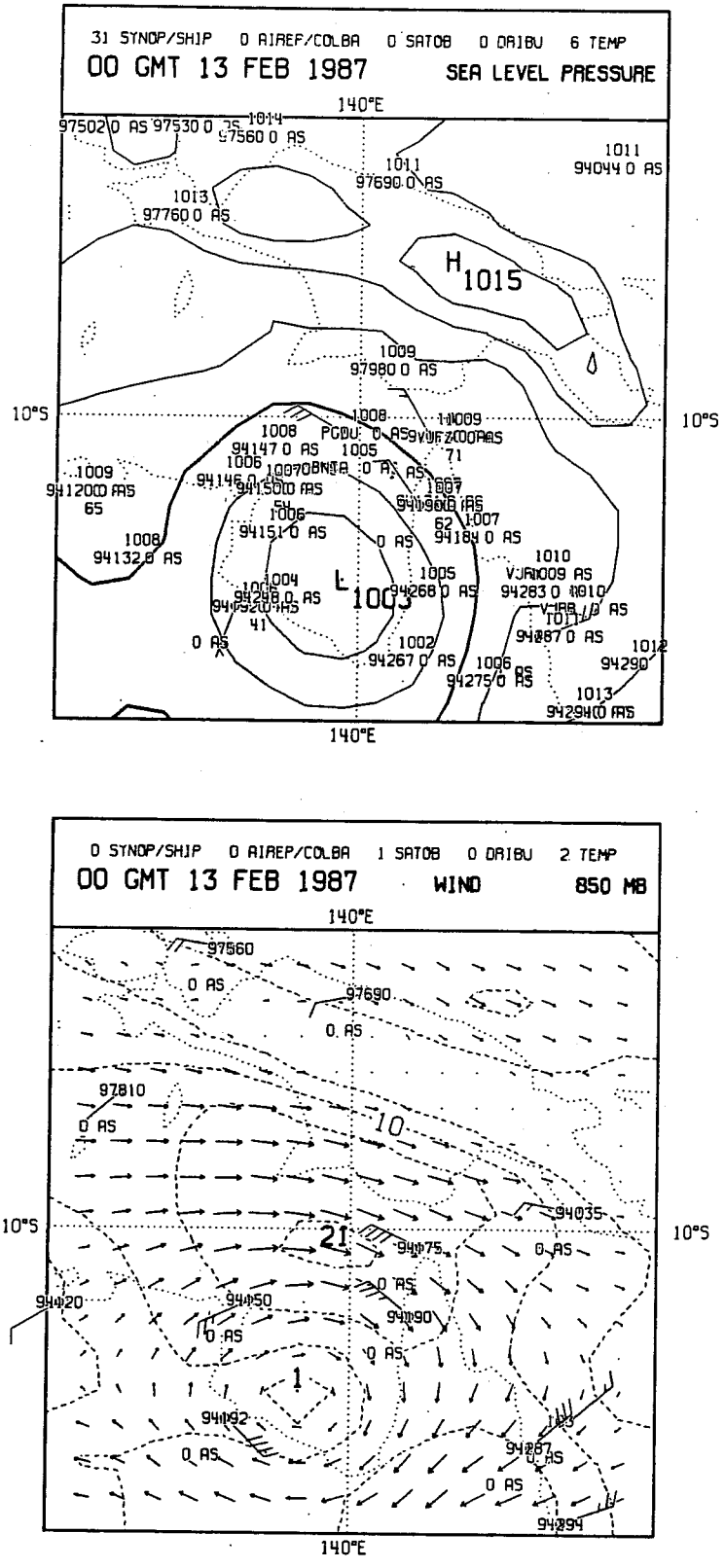

Fig. 31e As in Fig. 22a but for analyses at 0000 GMT Feb 13 for TC Jason.

The overall performance of the analysis system for most of the life cycle of Jason was poor. The cyclone was generally analysed to be too weak without a well developed circulation at certain stages so that it was not possible to define a location at these times. The analysed central pressures were too weak although there were observations which indicated lower pressures. However most of these observations were rejected as shown in Fig. 32. The rejection of the surface and 850 hPa wind observation at station 94150 on 1200 GMT Feb 10 for example is particularly notable as the cyclone was located very close to this location. The rejection of such an observation is a serious problem in the analysis of a tropical cyclone as these observations are vital not only to obtain the intensity but also to correctly locate the cyclone. The UKMO analysis system performed much better for the life cycle of Jason both with respect to position and intensity. An example of this is indicated in Fig. 33 which shows the UKMO analyses for 1200 GMT Feb 20. Part of the reason for the better performance of the UKMO analysis system is that bogus observations were used in the analyses of TC Jason although, as was noted for TCs Connie and Irma, the UKMO analyses tend to produce deeper lows than the ECMWF analyses even in the absence of bogus data.

To summarise the performance of the ECMWF system in analysing tropical cyclones, there are some encouraging features given that no particular attention has been paid to the problems of specifically handling tropical cyclones. The analysis system is able to define the gross features and locate three out of the four cyclones considered to within 1° to 1.5° of the BOM's location. Given that the analysis is performed on the Gaussian grid of the model, which for the T106 model has a resolution of approximately 1.125° in both zonal and meridional directions, this is close to the best that can be achieved by the current analysis forecast system. However, for TC Jason and at various times for the other cyclones there are location errors of 2° or more. Such errors can lead to serious errors in forecasting the future motion of the cyclones. The main reasons for location errors is lack of data close to the cyclones and rejection of useful data by the analysis system. One way of reducing the problem of data sparcity is to use bogus data such as done at operational centres such as the UKMO and Japan Meteorological Agency and more recently at ECMWF (Anderson and Hollingsworth, 1988). The estimated location and intensity of cyclones from satellite imagery can be used to generate bogus wind data around the cyclone. The use of such data has the potential of at least improving the location of the cyclone by the analysis system. However even when data is available (as for TC Irma and Jason) or when bogus data has been generated, there still remains the problem of rejection of data. There are several reasons for this; firstly the first guess could be inadequate because of deficiencies in model parametrization of physical processes and inadequate model resolution. Some of these factors are considered in Part II of this report. Secondly, the analysis system is not designed to handle tropical cyclones. Thus, for example, the first guess error variance used in the analysis system is probably too low for tropical cyclones and this could also

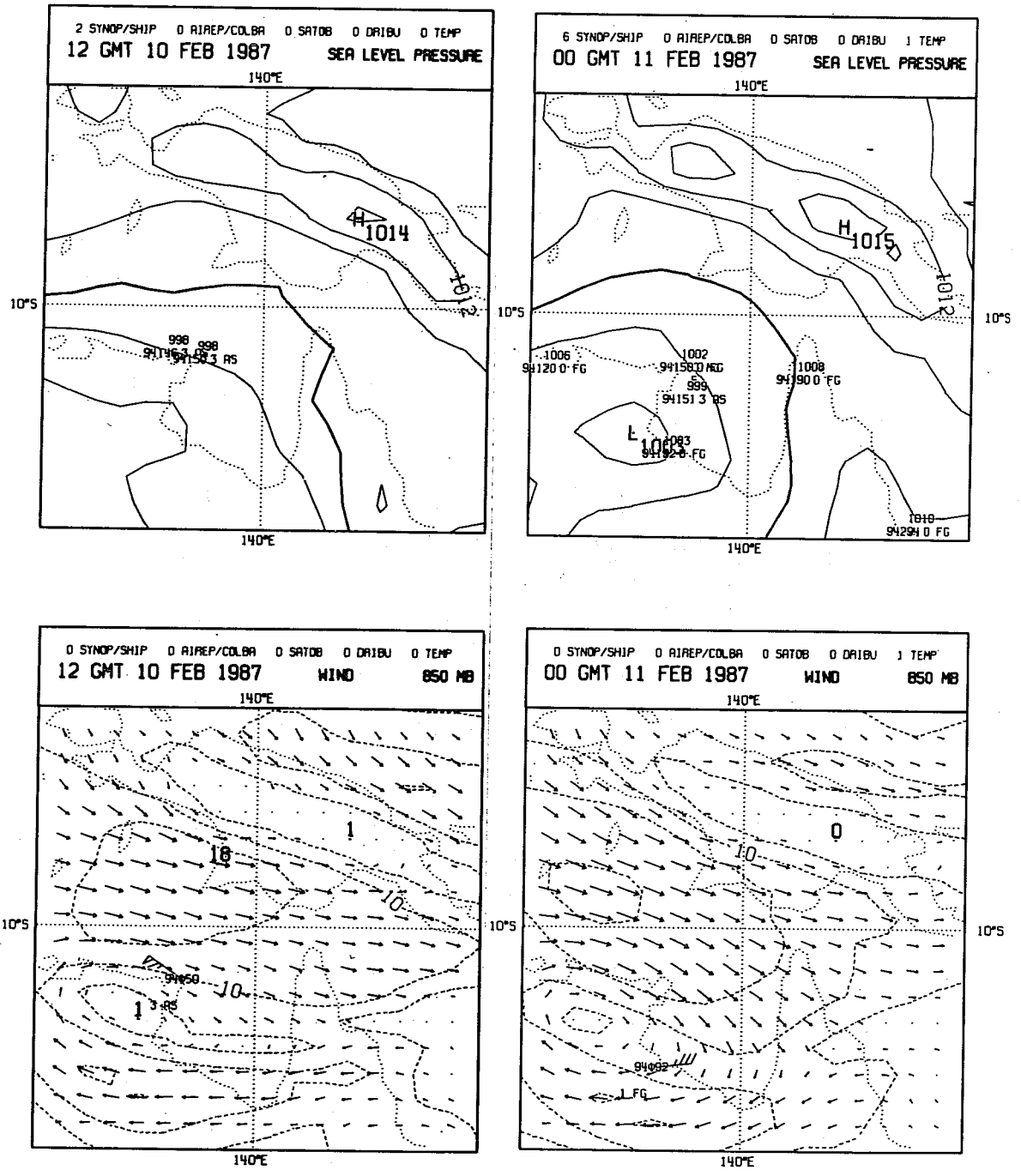

Fig. 32 As in Fig. 25 but for analyses at 1200 GMT Feb 10 and 0000 GMT Feb 11 for TC Jason.

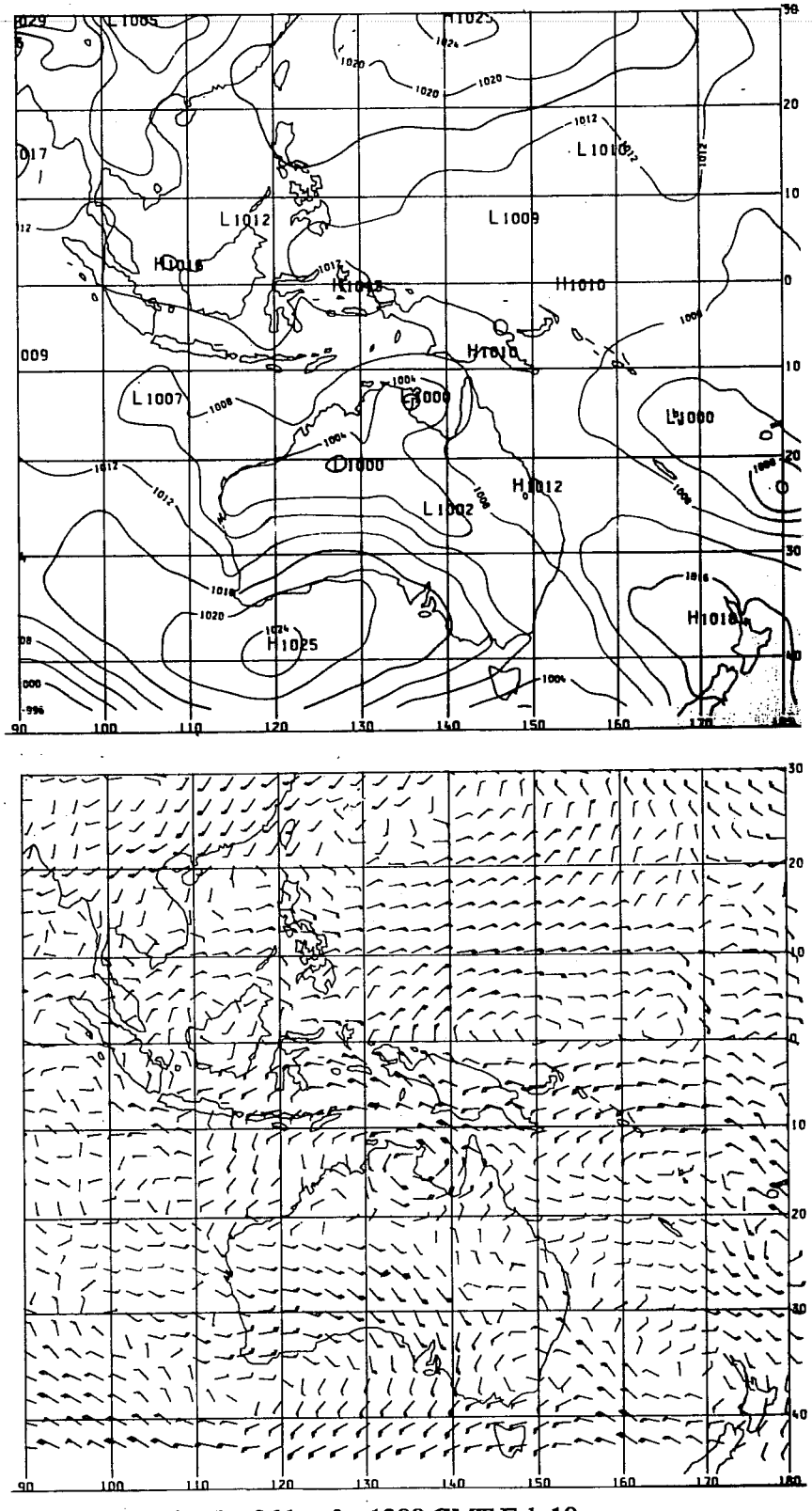

Fig. 33 As in Fig. 26 but for 1200 GMT Feb 10.

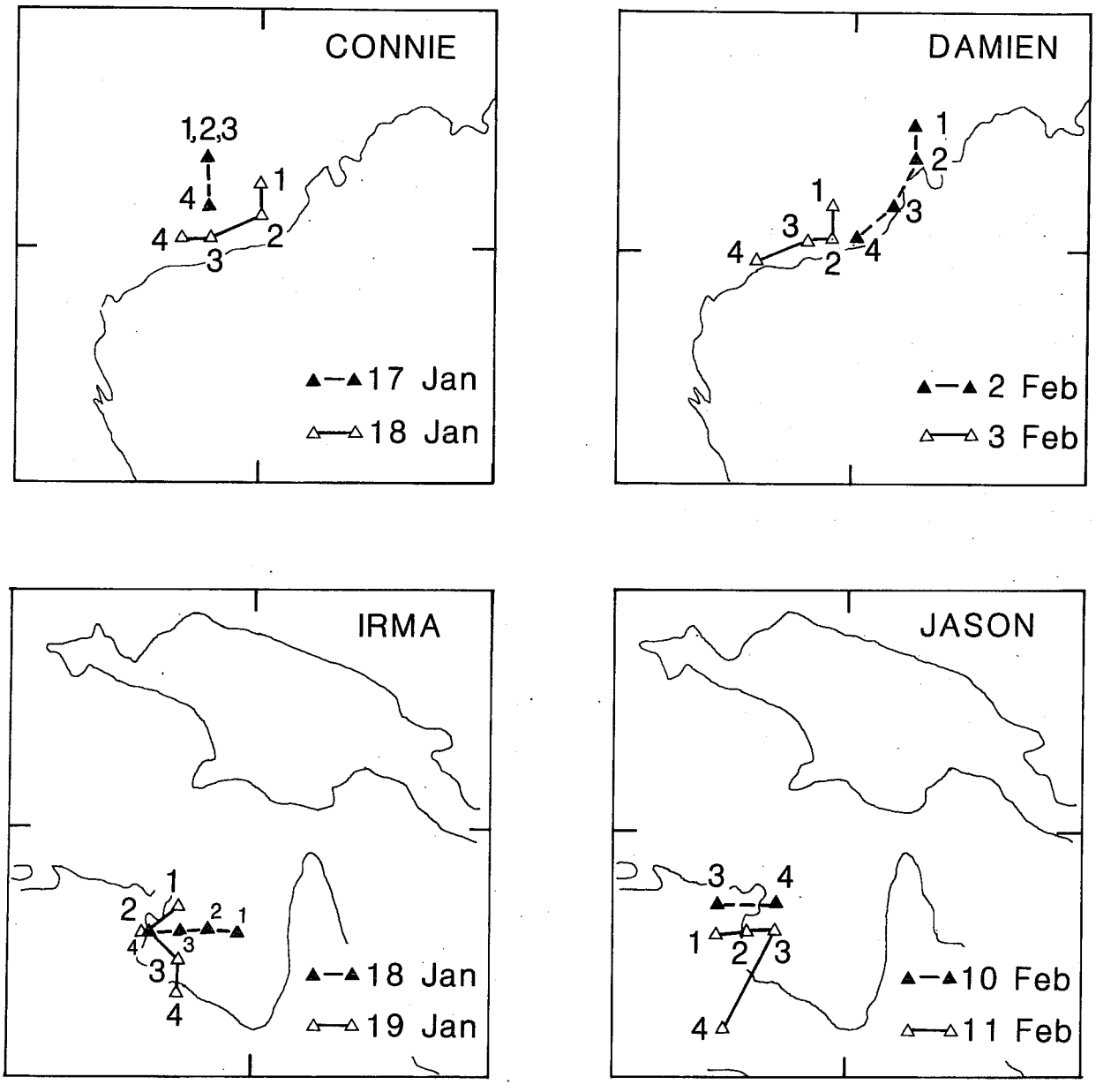

Fig. 34 Forecast tracks at 12 hr intervals for TCs Connie (starting times 1200 GMT Jan 17 and 18), Irma (starting times 1200 GMT Jan 18 and 19), Damien (starting times 1200 GMT Feb 2 and 3) and Jason (starting times 1200 GMT Feb 10 and 11).

lead to rejection of data. Furthermore the resolution of the horizontal and vertical structures used in the analysis system is probably inadequate for tropical cyclones. Some of these questions are addressed in Part III of this report. A consistent problem with the ECMWF analyses of the cyclones considered here is the underestimation of the central pressures. Although these can be improved, it should be noted that the ECMWF analysis-forecast system cannot resolve the inner structure of the cyclones and cannot simulate details of the structures of the cyclones. It therefore cannot analyse the full intensity of the cyclones such as indicated by BOM estimates of observations close to the cyclones.

3.2 Forecasts of tropical cyclones

In this section the performance of the forecast model in predicting the tracks of tropical cyclones will be described. The emphasis is on track prediction rather than detailed structure and intensification of the cyclones because the model does not have adequate resolution to resolve the detailed structure of the cyclones.

Fig. 34 shows the forecast tracks of the four cyclones considered in the previous section. In each case two forecasts are shown starting from analyses one day apart. The cyclones and the starting analyses are as follows:

Connie	1200 GMT	Jan 17 and Jan 18 1987
Irma	1200 GMT	Jan 18 and Jan 19 1987
Damien	1200 GMT	Feb 2 and Feb 3 1987
Jason	1200 GMT	Feb 10 and Feb 11 1987

The best tracks estimated by the BOM for each cyclone are shown in Fig. 21 and from the ECMWF analyses in Fig. 23. The main features to note are the considerable variability in two track forecasts for each cyclone and the significant position errors. Thus 1 day errors for TC's Connie, Irma and Damien for the two forecasts were 2.4° and 2.6°; 1.6° and 0.6°; 2° and 2.4° respectively. As with the analyses of TC Jason the forecasts throughout the life cycle of Jason were poor. The reason for the failure of the analyses-forecast system to handle Jason is due to a combination of factors. In the early stages of its life cycle Jason was a small scale cyclone which could not have been adequately resolved by the model. In the latter stages, as will be shown in Part II, the parametrization of cumulus convection in the model has a significant bearing.

In order to give further indication of the forecast performance, Figs. 35(a) to (d) show the one and two day forecasts for tropical cyclones Connie (initial date 1200 GMT Jan 18), Irma (initial date 1200 GMT Jan 18), Damien (initial date 1200 GMT Feb 2 and Jason (initial

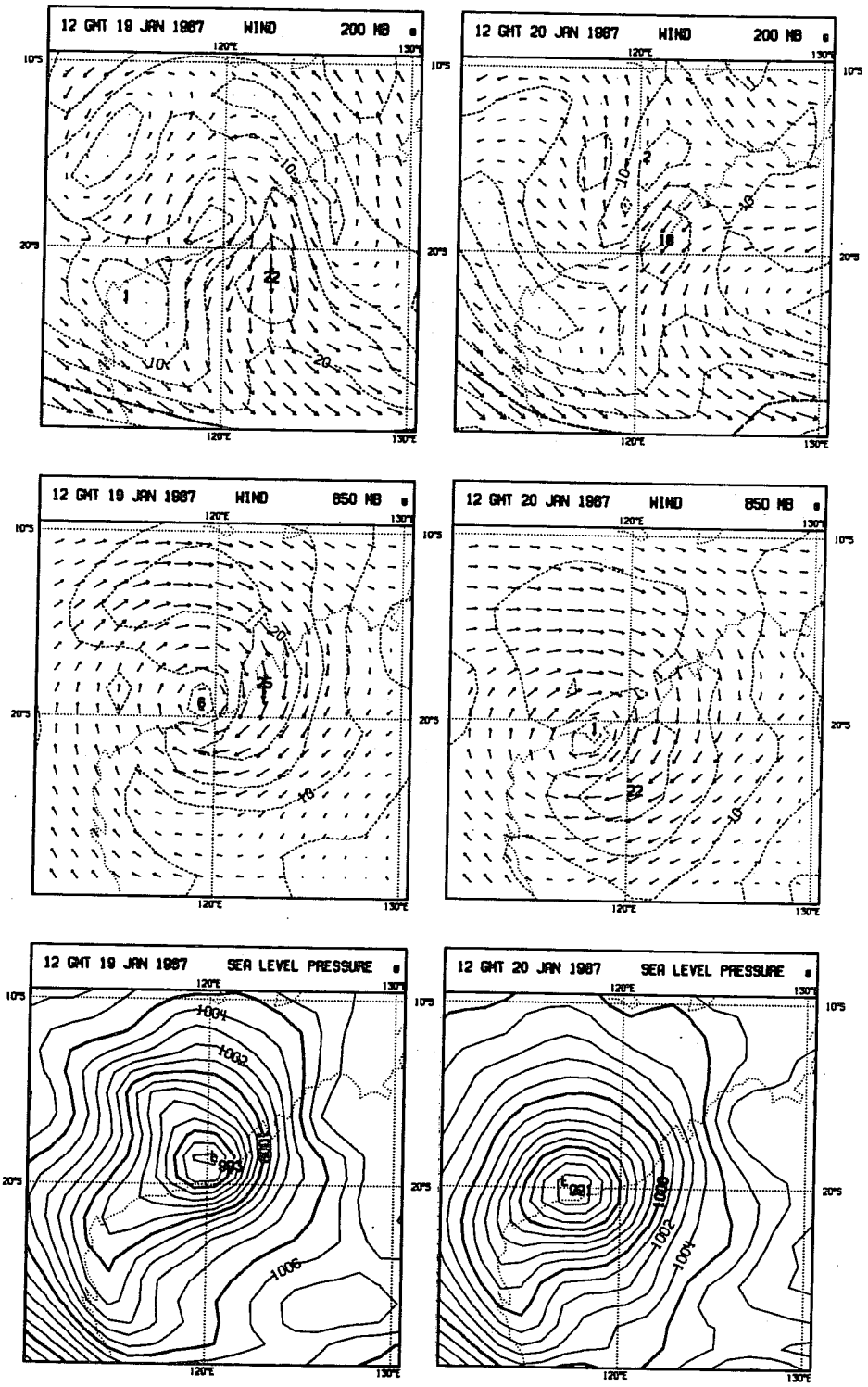

Fig. 35a 24 hr (left panels) and 48 hr (right panels) forecasts for TC Connie starting from 1200 GMT Jan 18 for MSLP (bottom in hPa), 850 hPa vector (middle in ms^{-1}). Contour intervals are 1 hPa for MSLP and 5 ms^{-1} for 850 hPa and 200 hPa isotachs.

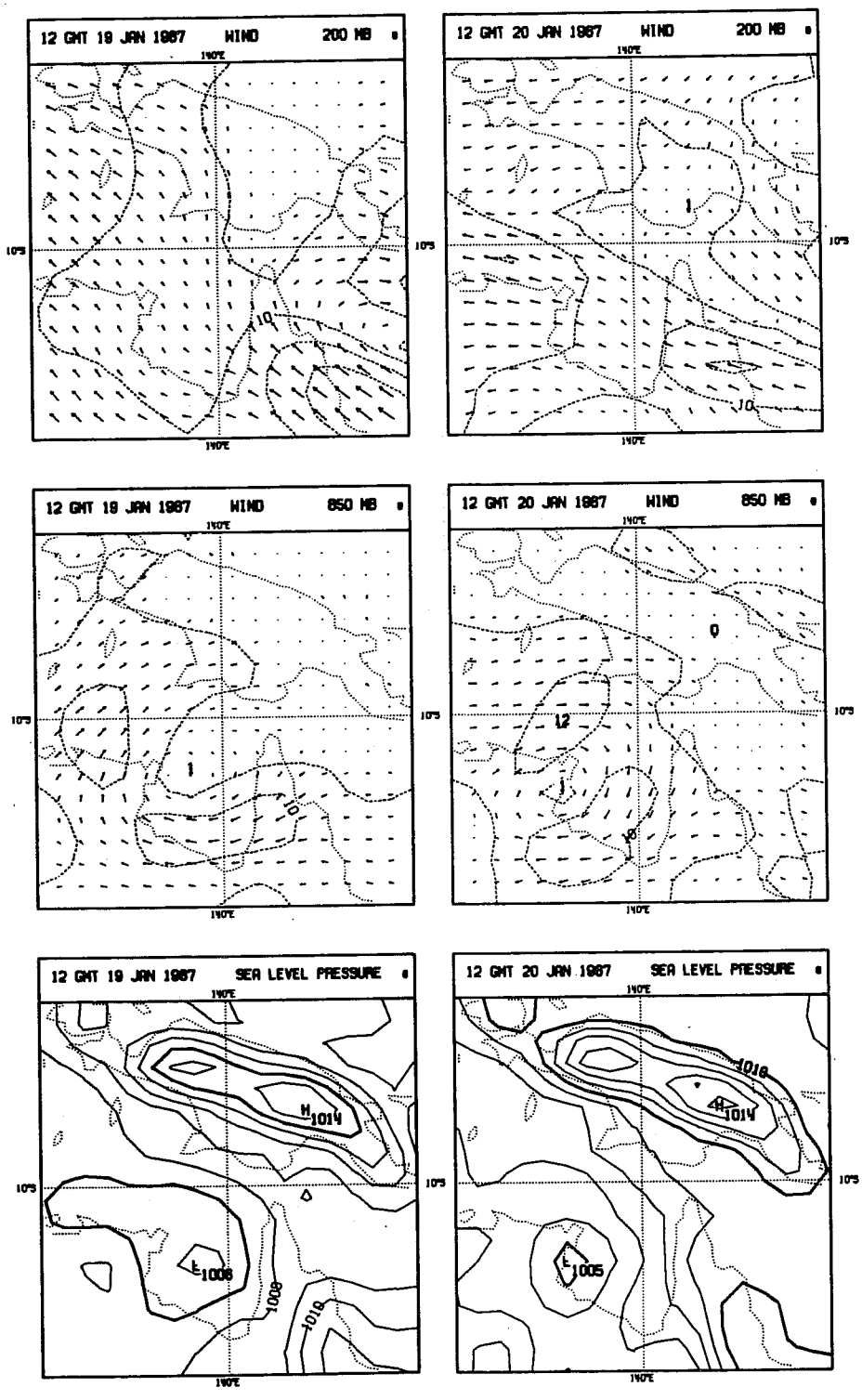

Fig. 35b As in Fig. 35a but for TC Irma starting from 1200 GMT Jan 18.

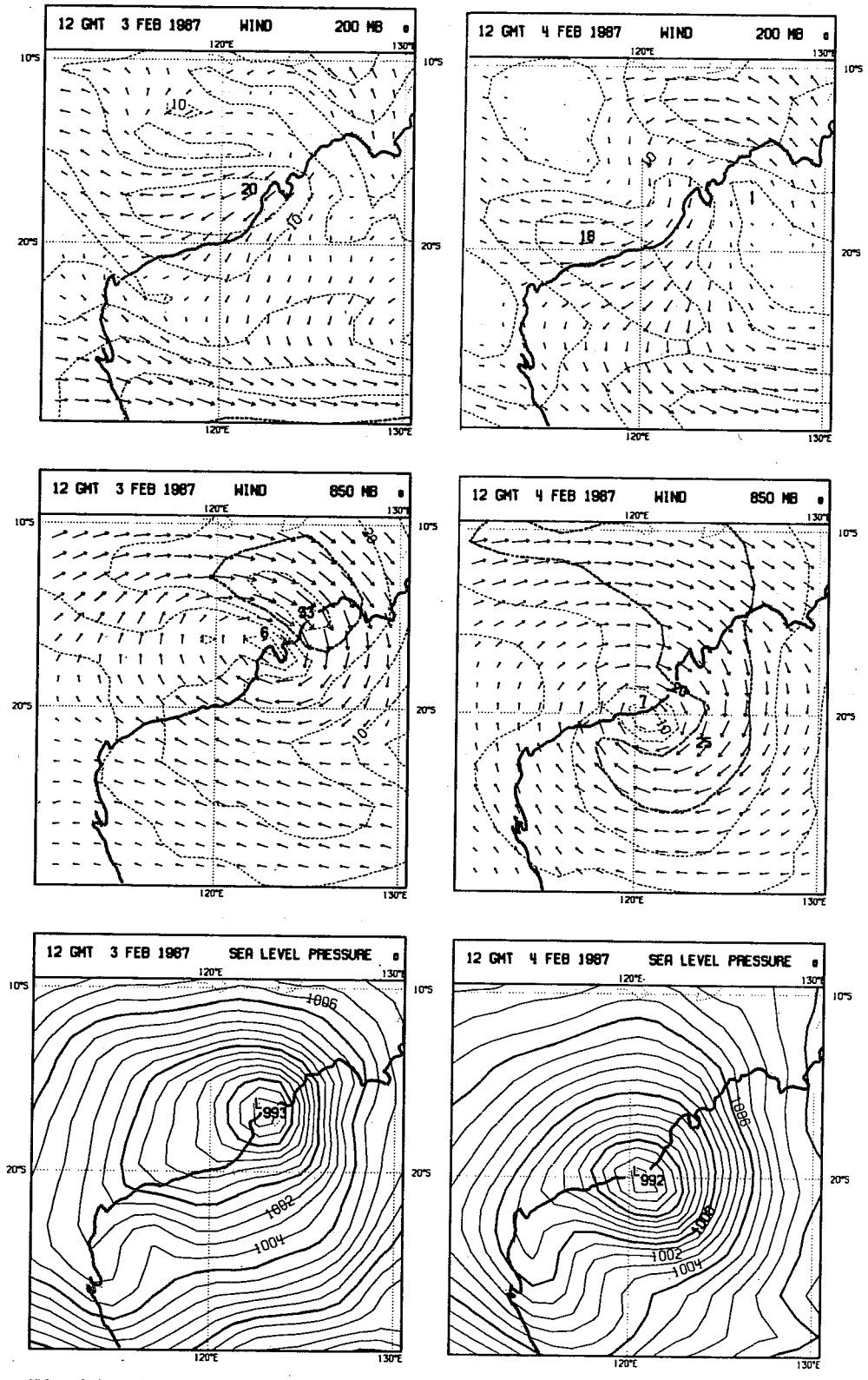

Fig. 35c As in Fig. 35a but for TC Damien starting from 1200 GMT Feb 2.

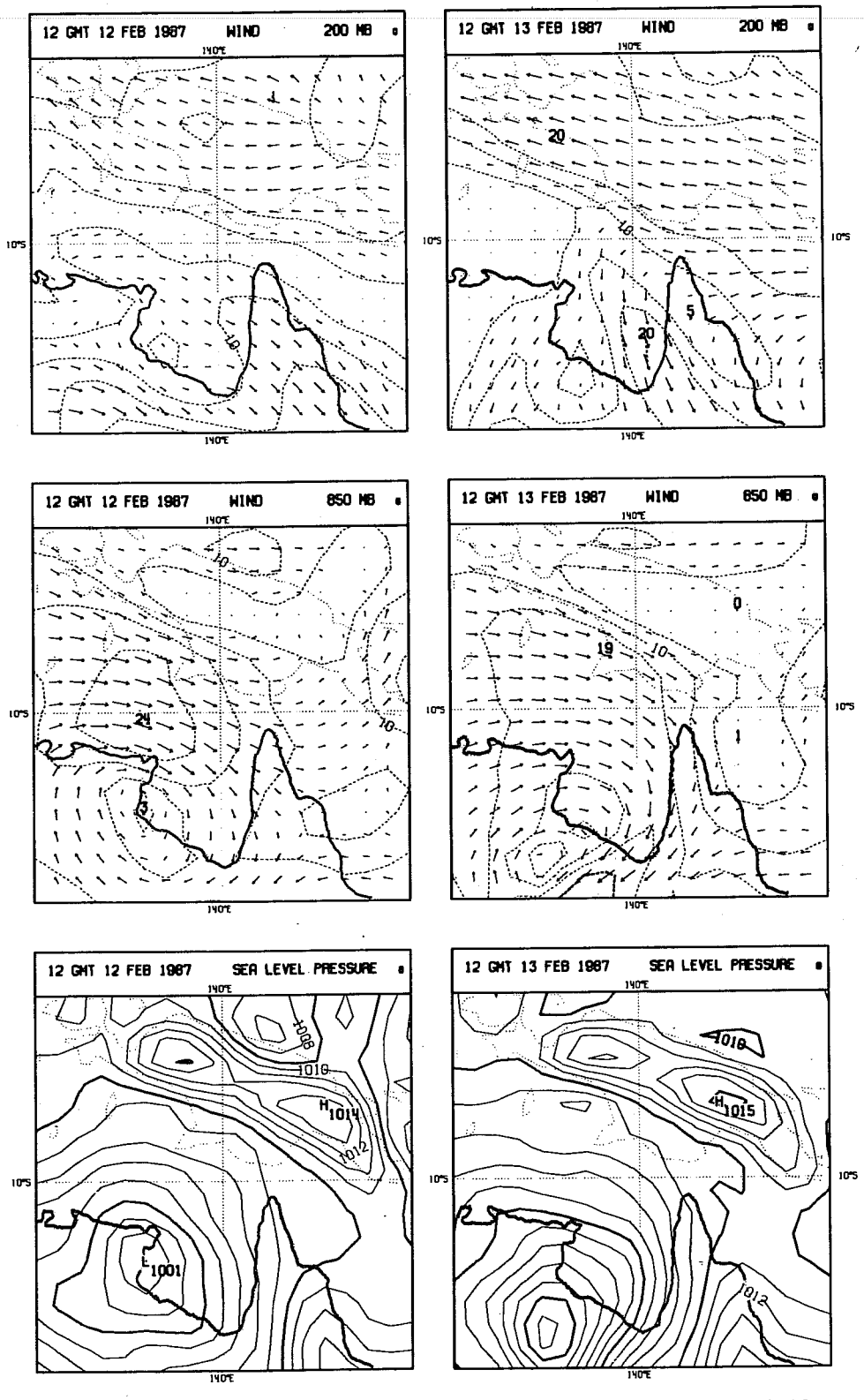

Fig. 35d As in Fig. 35a but for TC Jason starting from 1200 GMT Feb 10.

date 1200 GMT Feb 11). The model forecasts for day one are reasonable. Thus, for Connie and Damien inspite of the position error, most of the gross features in the verifying analysis (see Fig. 23c and 32b) are present in the forecast. The model deepens the central pressure and simulates strong low level winds of about 25 ms^{-1}. The one day forecast for Irma is in good agreement with the verifying analysis, (see Fig. 28a) although the low level winds are somewhat weak. Even for Jason where the initial analysis was poor leading to a poor forecast, the model intensifies the cyclone, moves it in the right direction and generates a reasonable low level circulation. By day two however, apart from Irma, there are large position errors. Thus for Connie the forecast keeps the cyclone over sea while it has gone a long distance overland. For Damien, the model moves the cyclone closer to the West Australian coast while the cyclone moves away from the coast. For both cyclones however, the model still maintains the cyclonic circulation and has a number of features present in the verifying analyses. The two day forecast for Irma is reasonable although it is weaker than analysed, particularly the low level wind field. The model correctly moves the cyclone towards the western coast of the Gulf of Carpentaria and subsequently moves it over land. The two day forecast for Jason on the other hand is poor with little correspondence with the analyses.

4. CONCLUSION

The aim of Part I of the report is to document the performance of the ECMWF analysis-forecast system in depicting the main features of the tropical circulation in the Australian region in the period January 10 to February 15 during which the Australian Monsoon Experiment was conducted. The features included the onset of the Australian summer monsoon, active and break periods in the monsoon and four tropical cyclones.

The model is successful in predicting the mean features during the period up to 3 days ahead. The major deficiency is a marked weakening of the upper level divergent circulation which appears to be related to the weakening in convective activity with time and underestimation of the outgoing longwave radiation in the model. The ECMWF analyses are in good agreement with independent BOM analyses in depicting the main changes during the period such as the onset and active/break periods in the monsoon. The model is able to forecast the monsoon onset correctly up to 24 hours ahead of time and provides impressive simulation of the subsequent episodes in the monsoon up to 48 hours ahead. The 24 hour model forecasts are also able to depict the dramatic changes in precipitation following the onset and during the active/break periods. The model however is unable to retain low level westerlies beyond 36-48 hours unless these westerlies are well established in the initial state. The reason for this is not clear and this aspect clearly needs further investigation. One possible reason could be the marked reduction in convective activity in the model with time.

There are a number of encouraging features in the analyses of tropical cyclones given that no particular attention has been paid to specifically handle TC's. The analysis system is able to define the gross features and locate three out of four cyclones to within 1° to 1.5°. However for TC Jason and at various times for the other cyclones there are location errors at 2° or more. Such errors can lead to serious errors in forecasting the future location of the cyclones. The main reason for location errors is lack of data close to the cyclones and rejection of useful data by the analysis system. Another consistent problem with the ECMWF analyses of tropical cyclones is the underestimation of central pressures. This is caused in large part by inadequate resolution which does not allow the inner structure of the cyclones to be resolved adequately, lack of data and errors in the first guess field. The forecasts for the cyclones mainly reflect errors in the initial analyses although this is not the sole cause of forecast errors. There is considerable variability in the track forecasts starting from initial conditions one day apart. Although the model forecasts the direction of motion of the cyclones in the first 24 hours there are significant position errors. The forecasts, as with the analyses, consistently underestimate the central pressures.

A number of factors contribute to the errors in the analyses and forecasts of tropical cyclones namely, inadequate data, deficiencies in the analysis scheme in its ability to handle tropical cyclones such as inappropriate first guess errors, insufficient resolution and inadequate parametrization of physical processes such as cumulus convection. The sensitivity of analysis-forecast system to cumulus parametrization is considered in Part II and the problem of data rejection and analysis resolution is considered in Part III of this report.

Finally, it should be noted that there is a considerable amount of ongoing work at ECMWF aimed at improving the performance of the analysis-forecast system in the tropics. Modifications in the analysis scheme to allow divergent analysis increments which resulted in significantly improved divergence analysis were implemented operationally in January 1988 (Undén, 1989). A revised filter for smoothing diabatic tendencies used in initialization was implemented operationally in November 1988. The net effect of this revision was to retain stronger diabatic forcing in the initialization (Puri, 1988). This, together with the use of divergent structure functions should result in improved retention of the analysed tropical divergent flow. A major change in the analysis scheme was implemented in July 1988. This change involved the use of higher resolution structure functions whose net effect was to increase the effective resolution of the analysis scheme from spherical wave number 24 to spherical wave number 48 (see Lönnberg, 1988 for details). This change resulted in significant improvement in the ECMWF analysis and forecasts and could have significant bearing on analysis of tropical cyclones (see Part III). Convective parametrization plays an important role in the tropics and two schemes namely the Betts-Miller adjustment scheme (Betts, 1986; Betts and Miller, 1986) and a mass-flux scheme (Tiedtke, 1989) have been developed which lead to improved model performance in the tropics compared to the current Kuo parametrization. The problems of underestimation of outgoing longwave radiation has been addressed by the development of a new radiation scheme (Morcrette, 1988). The mass-flux scheme and the new radiation scheme will be implemented operationally in mid-1989. In the absence of data, bogussing of TC data is one important means of reducing errors in the location of cyclones. A scheme to generate such data has been developed and tested at ECMWF (see Anderson and Hollingsworth, 1988) and will be implemented operationally. The overall impact of the above changes could lead to improved analyses-forecasts in the tropics.

References

Anderson, E. and A. Hollingsworth, 1988: Typhoon bogus observations in ECMWF data assimilation system. Tech. Memo. No. 148, ECMWF, Reading, UK, 25 pp.

Arpe, K., 1988: Planetary scale diabatic forcing errors in the ECMWF model. Proceedings on Workshop on diabatic forcing 30 November - 2 December 1987. ECMWF Workshop Proceedings, ECMWF, Reading, Berkshire, 103-149.

Betts, A.K., 1986: A new convective adjustment scheme. Part I: Observation and theoretical basis. Quart.J.Roy.Meteor.Soc., 112, 677-691.

Betts, A.K. and M.J. Miller, 1986: A new convective adjustment scheme. Part II: Single column tests using GATE wave, BOMEX, ATEX and Arctic air-mass data sets. Quart.J.Roy.Meteor.Soc., 112, 693-709.

Gunn, G.W., J.L. McBride, G.J. Holland, T.D. Keenan, N.E. Davidson and H.H. Hendon, 1989: The Australian Summer Monsoon circulation during AMEX Phase 2. Mon.Wea.Rev., 2554-2574.

Hall, C.D., 1987: Verification of global model forecasts of tropical cyclones during 1986. Meteor.Mag., 116, 216-220.

Heckley, W.A., 1985: Systematic errors of the ECMWF operational forecasting model in tropical regions. Quart.J.Roy.Meteor.Soc., 111, 709-738.

Holland, G.J., 1986: Interannual variability of the Australian Summer Monsoon at Darwin: 1952-1982. Mon.Wea.Rev., 114.

Holland, G.J., J.L. McBride, R.K. Smith, D. Jasper and T.D. Keenan, 1986: The BMRC Australian Monsoon Experiment: AMEX. Bull.Amer.Met.Soc., 67, 1466-1472.

Julian, P.R., 1984: Objective analysis in the tropics: A proposed scheme. Mon.Wea.Rev., 112, 1752-1767.

Kanamitsu, M., 1985: A study of the ECMWF operational forecast model in the tropics. ECMWF Tech.Rep. No. 49, ECMWF, Reading, UK, 73 pp.

Krishnamurti, T.N., N. Kanamitsu, W.J. Koss and J.D. Lee, 1973: Tropical east-west circulation during the northern winter. J.Atmos.Sci., 30, 780-787.

Krishnamurti, T.N., K. Ingles, S. Cocke, T. Kitade and Pasch, 1983: Details of low latitude medium range numerical weather prediction using a global spectral model II: Effects of orography and physical initialization. Florida State University, Report No. 83-11, Department of Meteorology, Tallahassee, Florida 32306, 45pp.

Lau, K.M. and C.P. Chang, 1987: Planetary scale aspects of the winter monsoon and atmospheric teleconnections. Monsoon Meteorology, C.P. Chang and T.N. Krishnamurti, Ed., Oxford Monographs on Geology and Geophysics No. 7, 203-231.

Manchur, W., 1987: The Australian tropical cyclone season 1986-87. Tropical cyclone; 551.515.2(94) Melbourne, Bur.Met.Aust.Met.Mag., Melbourne, 35, pp. 95-102.

McBride, J.L. and T.D. Keenan, 1982: Climatology of tropical cyclone genesis in the Australian region. J.Climatol., 2, 13-33.

Mohanty, U.C., A. Hollingsworth and S.K. Dash, 1985: Asian summer monsoon circulation statistics: 1979-1984.

Mohanty, U.C., J.M. Slingo and M. Tiedtke, 1985: Impact of modified physical processes on tropical simulation in the ECMWF model. ECMWF Technical Report No. 52, ECMWF, Reading, U.K., 44pp.

Puri, K., 1988: Specification of diabatic heating in the initialization of numerical weather prediction models. Proceedings on Workshop on diabatic forcing 30 November - 2 December 1987. ECMWF Workshop proceedings, ECMWF, Reading, Berkshire, 151-175.

Puri, K. and M.J. Miller, 1989: Use of satellite data in the specification of convective heating for diabatic initialization and moisture adjustment in numerical weather prediction models. Mon.Wea.Rev., 118, 67-93.

Reed, R.J., A. Hollingsworth, W.A. Heckley and F. Delsol, 1988: An evaluation of the performance of the ECMWF operational system in analyzing and forecasting tropical easterly wave disturbances over Africa and Tropical Atlantic. Mon.Wea.Rev., 116, 824-865.

Tiedtke, M., W.A. Heckley and J. Slingo, 1988: Tropical forecasting at ECMWF: The influence of physical parametrization on error structure of forecasts and analyses. Quart.J.Roy.Meteor.Soc., 114, 639-664.

Tiedtke, M., 1989: A comprehensive mass flux scheme for cumulus parametrization in large-scale models: Theoretical basis and verification on single column data sets from field experiments. Mon.Wea.Rev., 117, 1779-1800.

Undén, P., 1989: Tropical data assimilation and analysis of divergence. Mon.Wea.Rev., 117, 2495-2517.

PART II: SENSITIVITY OF ECMWF ANALYSES-FORECASTS OF TROPICAL CYCLONES TO CUMULUS PARAMETRIZATION

Kamal Puri and M.J. Miller

1. INTRODUCTION

In Part I of this report the main problems associated with analyses and forecasts of tropical cyclones were identified to be position errors and underestimation of the intensity of the cyclones. One of the factors contributing to the forecast errors and to analysis errors through inaccurate first guess is the parametrization of cumulus convection which is known to have a strong influence on model forecasts in the tropics (see Puri and Gauntlett, 1988). Another factor is insufficient model resolution. In this part the sensitivity of ECMWF analyses-forecasts of tropical cyclones to cumulus parametrization is considered. The sensitivity of two forecasts, one each for tropical cyclones Irma and Jason to increased model resolution will also be considered using a model truncated at triangular wave number 159 (T159). This model has a resolution of approximately 130 km compared with a resolution of 190 km for the T106 model. As in Part I only the cyclones which formed during the period covered by AMEX will be considered.

2. BRIEF DESCRIPTION OF CUMULUS CONVECTION PARAMETRIZATIONS USED

Two cumulus parametrization schemes are compared, namely the operational (in 1987) Kuo cumulus parametrization and the Betts-Miller parametrization (Betts, 1986; Betts and Miller, 1986). The Betts-Miller adjustment scheme is based on an adjustment towards quasi-equilibrium profiles of temperature (T) and moisture variable (q). Whereas most adjustment schemes such as the Manabe convective adjustment scheme (Manabe et al., 1965) adjust the (T, q) profiles to a saturated moist adiabat, the new scheme is designed to ensure adjustment to more realistic (and observed) structures (T_R, q_R) within a relaxation time scale of about one hour such that T_R is less stable than the wet adiabat in the lower part of the troposphere and more stable above. q_R is computed so as to maintain realistic sub-saturations in a convective atmosphere. The interested reader is referred to Betts and Miller (1986) for details of the scheme.

Results from the Betts-Miller scheme will be compared to the operational Kuo parametrization scheme. The latter scheme as used at ECMWF has the following modifications which are described in more detail in Slingo et al. (1988). Firstly the cloud base is defined as the condensation level for near-surface air rather than that for air with the mean characteristics of the well mixed layer which was used previously. The second change involves the

moistening parameter, B, which determines the partitioning between convective heating and moistening. B is assumed to depend on the mean saturation deficit of the whole layer i.e.

$$B = [1 - (\frac{\int_{p_T}^{p_B} RH \, dp}{p_B - p_T})]^n$$

where p_T and p_B are the pressures of the top and base of the cloud and RH the relative humidity. In its original form a linear dependency (n = 1) was used which tended to over-moisten the environment and to underestimate the latent heat release. In the modified scheme a cubic dependency on the environmental saturation deficit is used (n = 3).

3. RESULTS

The current study covered two time periods namely 1200 GMT Jan 17 to 1200 GMT Jan 21 and 1200 GMT Feb 2 to 1200 GMT Feb 13. For the Betts-Miller scheme this required data assimilation over the above periods. (The assimilation was in fact started two days prior to the start of each period in order to minimise spin up problems associated with using a different parametrization from an operational initial condition). Ten day forecasts were then performed from the subsequent analyses at one day intervals. In both the data assimilation and forecast steps, apart from the use of the Betts-Miller convection scheme, all other parameters were as in the operational suite.

The period covered by the study included the four TC's which formed in the Australian region during AMEX. Fig. 1 shows the best tracks and intensities of the cyclones as issued by the Australian Bureau of Meteorology (BOM). In the following, the operational system will be referred to as KUO and the experimental system using the Betts-Miller adjustment scheme as ADJ and the results will be presented in terms of the performance of the analyses and forecasts in handling the four tropical cyclones.

a. Comparison of analyses

Tables 1 to 4 show the positions and intensities of the four cyclones as a function of time as determined by the Bureau of Meteorology (BOM) and from KUO and ADJ analyses. Overall the position errors relative to the BOM best estimates for the two schemes are similar with the ADJ analyses providing marginally better locations for TC's Irma, Connie and Jason and the KUO scheme performing significantly better for TC Damien than the ADJ scheme which had errors at 2° or more for this cyclone. The major difference between the analyses from the two schemes is in the central pressures which (apart from TC Damien) are consistently deeper in the ADJ analyses. The differences are particularly marked for TC Connie where there are pressure differences of over 20 hPa between the two analyses. The differences

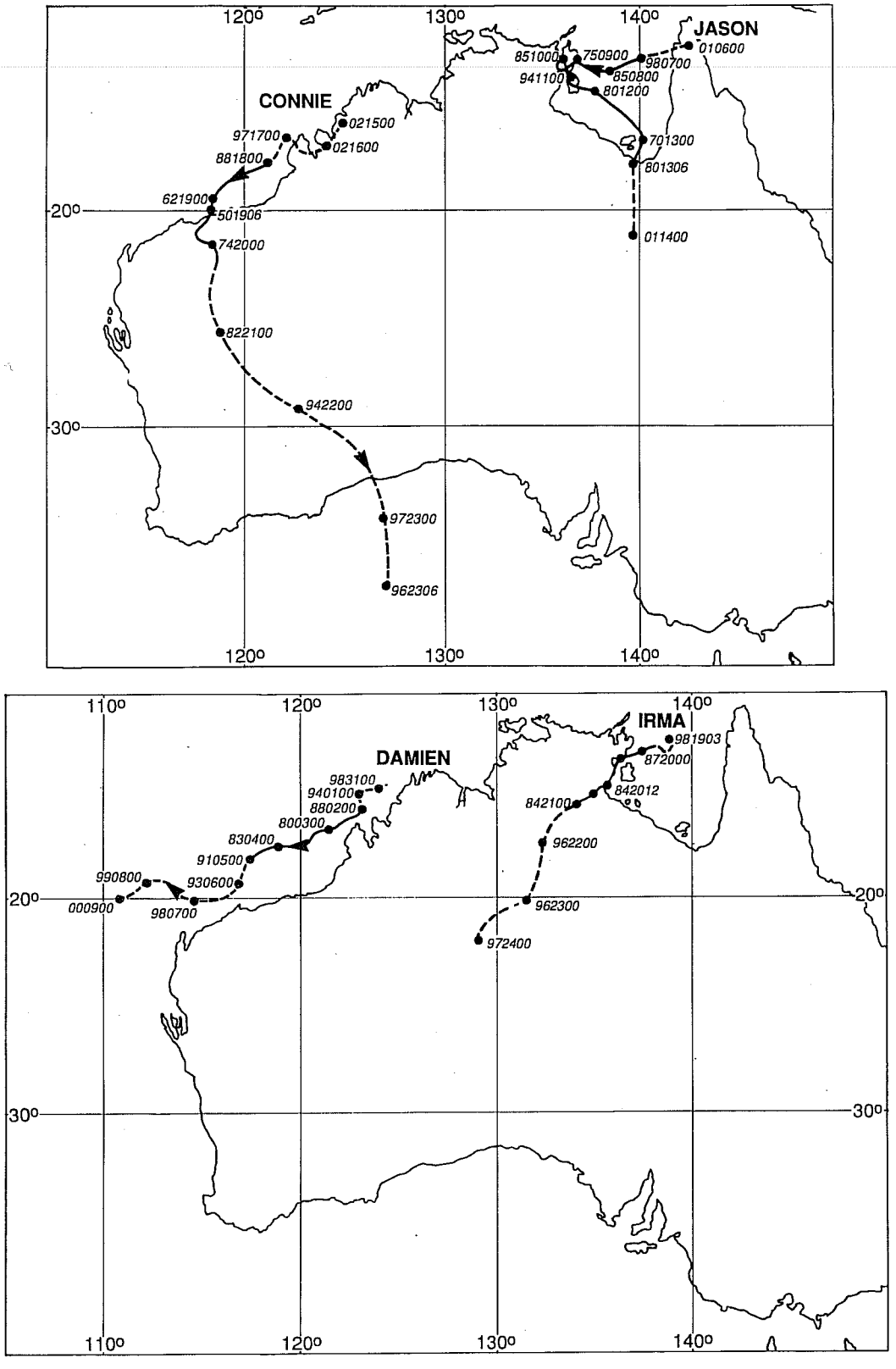

Fig. 1 Best tracks and intensities of TC's Irma, Connie, Damien and Jason issued by the Bureau of Meteorology. The legend is PPDDHH, where PP is central pressure, DD is day of month and HH is hour (GMT).

TROPICAL CYCLONE CONNIE - TRACKS

Jan	BOM			KUO Analysis			ADJ Analysis		
	Lat (S)	Long (E)	Press (hPa)	Lat (S)	Long (E)	Press (hPa)	Lat (S)	Long (E)	Press (hPa)
17/1200	17.1	121.9	994	17.4	121.9	997	17.4	121.4	993
18/0000	17.8	121.0	988	16.2	119.2	993	17.5	120.5	986
18/1200	18.5	119.2	976	17.3	120.4	990	17.4	120.4	981
19/0000	19.5	118.6	962	18.5	119.5	991	18.6	120.4	970
19/1200	20.5	118.4	955	19.6	119.2	994	19.7	119.2	975
20/0000	22.0	118.4	974	20.7	119.4	994	20.8	119.3	987
20/1200	23.5	118.2	980	23.0	118.1	995	22.9	119.2	991
21/0000	25.9	118.9	982	25.2	119.3	994	25.5	120.5	992

Table 1 Locations and central pressures for TC Connie obtained from BOM best estimates, KUO analyses and ADJ analyses. Central pressures are in hPa.

TROPICAL CYCLONE IRMA - TRACKS

Jan	BOM			KUO Analysis			ADJ Analysis		
	Lat (S)	Long (E)	Press (hPa)	Lat (S)	Long (E)	Press (hPa)	Lat (S)	Long (E)	Press (hPa)
19/0000	12.5	138.6	994	14.2	137.0	1004	13.0	138.2	1002
20/0000	12.8	137.4	987	13.0	137.0	1002	13.4	137.2	998
20/1200	13.6	135.9	984	15.4	135.9	1002	14.2	136.0	996
21/0000	15.4	134.1	984	16.5	134.5	999	16.5	135.0	994

Table 2 As in Table 1 but for TC Irma.

TROPICAL CYCLONE DAMIEN - TRACKS

Feb	BOM			KUO Analysis			ADJ Analysis		
	Lat (S)	Long (E)	Press (hPa)	Lat (S)	Long (E)	Press (hPa)	Lat (S)	Long (E)	Press (hPa)
02/0000	15.6	123.3	988	15.1	122.6	999	NA	NA	NA
02/1200	16.3	122.5	984	18.4	121.6	997	NA	NA	NA
03/0000	16.7	121.5	980	18.4	120.4	993	NA	NA	NA
03/1200	17.4	120.6	982	17.4	120.4	997	17.5	12.04	997
04/0000	17.5	118.9	983	17.3	119.2	997	17.4	120.4	997
04/1200	17.8	117.8	987	18.4	118.1	996	20.8	115.8	994
05/0000	18.1	117.6	991	17.3	117.0	998	18.6	118.1	998
05/1200	18.7	117.2	992	18.4	118.1	998	20.7	115.8	998

Table 3 As in Table 1 but for TC Damien.

NA Not Available

TROPICAL CYCLONE JASON - TRACKS

Feb	BOM			KUO Analysis			ADJ Analysis		
	Lat (S)	Long (E)	Press (hPa)	Lat (S)	Long (E)	Press (hPa)	Lat (S)	Long (E)	Press (hPa)
09/0000	12.9	136.8	977	13.1	135.9	1004	13.0	138.4	1003
09/1200	13.0	136.2	984	14.3	137.1	1003	13.1	138.2	1001
10/0000	12.6	136.1	990	14.3	137.2	1005	13.0	137.1	999
10/1200	13.1	136.2	992	*	*	*	14.2	138.2	999
11/0000	13.6	136.3	992	15.4	134.7	1003	14.2	138.3	998
11/1200	14.0	136.7	990	15.4	134.5	1002	15.4	137.0	1000
12/0000	14.2	137.8	980	14.2	135.9	1002	15.4	137.0	999
12/1200	15.5	139.0	965	15.4	138.3	1002	15.4	138.3	997

Table 4 As in Table 1 but for TC Jason.

* Centre not well defined

are better illustrated in Figs. 2(a) to (d) which show the MSLP and 850 hPa analyses at particular times for the four cyclones. The adjustment analyses tend to have better defined cyclonic circulations with deeper central pressures and stronger winds. Since the data base for the two analyses was identical, the deeper pressures must come from the first guess field in the assimilation cycle with the adjustment scheme. Although the adjustment analyses have deeper central pressures they are still too high compared to the BOM estimates. This is not surprising for a number of reasons. Firstly, the BOM estimates could have significant errors, secondly the analyses are consistent with the available observations which do not indicate much deeper pressures (except for TC Connie which had an observation of 968 hPa at 1200 GMT 19 Jan, which was rejected by both analyses) and thirdly the model and analysis resolutions are clearly not sufficient to resolve the inner core of tropical cyclones. The differences in analysed intensities of cyclones by the two schemes are also clearly evident in Figs. 3(a) to (c) which show the 1000 hPa and 850 hPa vorticity analyses for TC's Connie, Irma and Jason. The ADJ analyses are significantly stronger than the KUO analyses with localised cyclonic vorticity maxima in the region of the cyclones and also have better consistency between the two vertical levels shown. Thus if vorticity maxima were used to determine the location of the cyclone the results would be significantly different if 1000 hPa or 850 hPa KUO analyses were used while those from the ADJ analyses would be more consistent.

Figs. 4(a) to (d) show cross-sections of potential temperature-winds, vorticity and divergence for the ADJ and KUO analyses at latitudes 12°S and 15°S which are close to the analysed positions of TC's Irma (1200 GMT Jan 20) and Jason (1200 GMT Feb 10). These cross-sections also indicate the ability of the ADJ analyses to better isolate the tropical cyclones in terms of stronger vorticity in the region of the cyclone and improved consistency in the vertical of the vorticity and divergence. The divergence section for example indicates convergent flow (negative values) in the low levels and divergent flow at the higher levels for the ADJ analyses which is not as well defined in the KUO analyses. The divergence profile implied by the ADJ analyses is borne out by detailed observational studies of tropical cyclones (see McBride, 1981, for example).

A major problem with the KUO analyses noted earlier in Part I is the rejection of data in the vicinity of the cyclones. The same problem also occurs with the adjustment scheme. An example of this is shown in Fig. 5 which shows the ADJ analysis for MSLP and 850 hPa wind for TC Jason on 1200 GMT February 10. The analysis had a large position error at this stage and a major reason for this error was the rejection of sea level pressure data at station 94146 and 850 hPa wind field for station 94150 (Gove, 12°S; 130°E). These stations were very close to the centre of the cyclone and station 94150 was one of the stations in the enhanced data base where sondes were released every six hours and provided reliable and

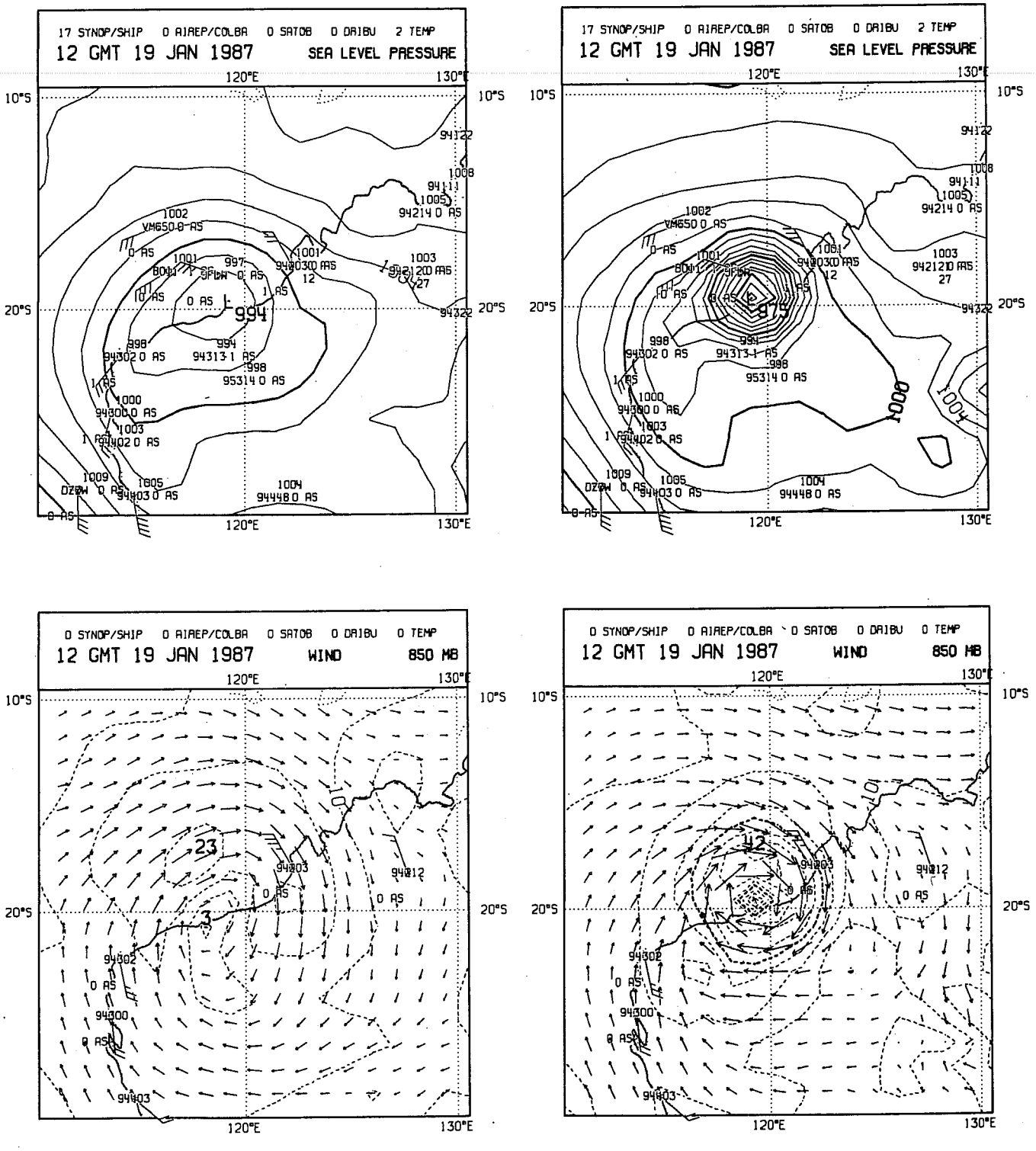

Fig. 2a MSLP (top in hPa) and 850 hPa vector wind (bottom in ms^{-1}) analyses for TC Connie at 1200 GMT Jan 19 1987 from the KUO (left panel) and ADJ (right panel) systems. Contour intervals are 2 hPa and 5 ms^{-1} respectively for MSLP and isotachs. The observations used by the analyses are also shown.

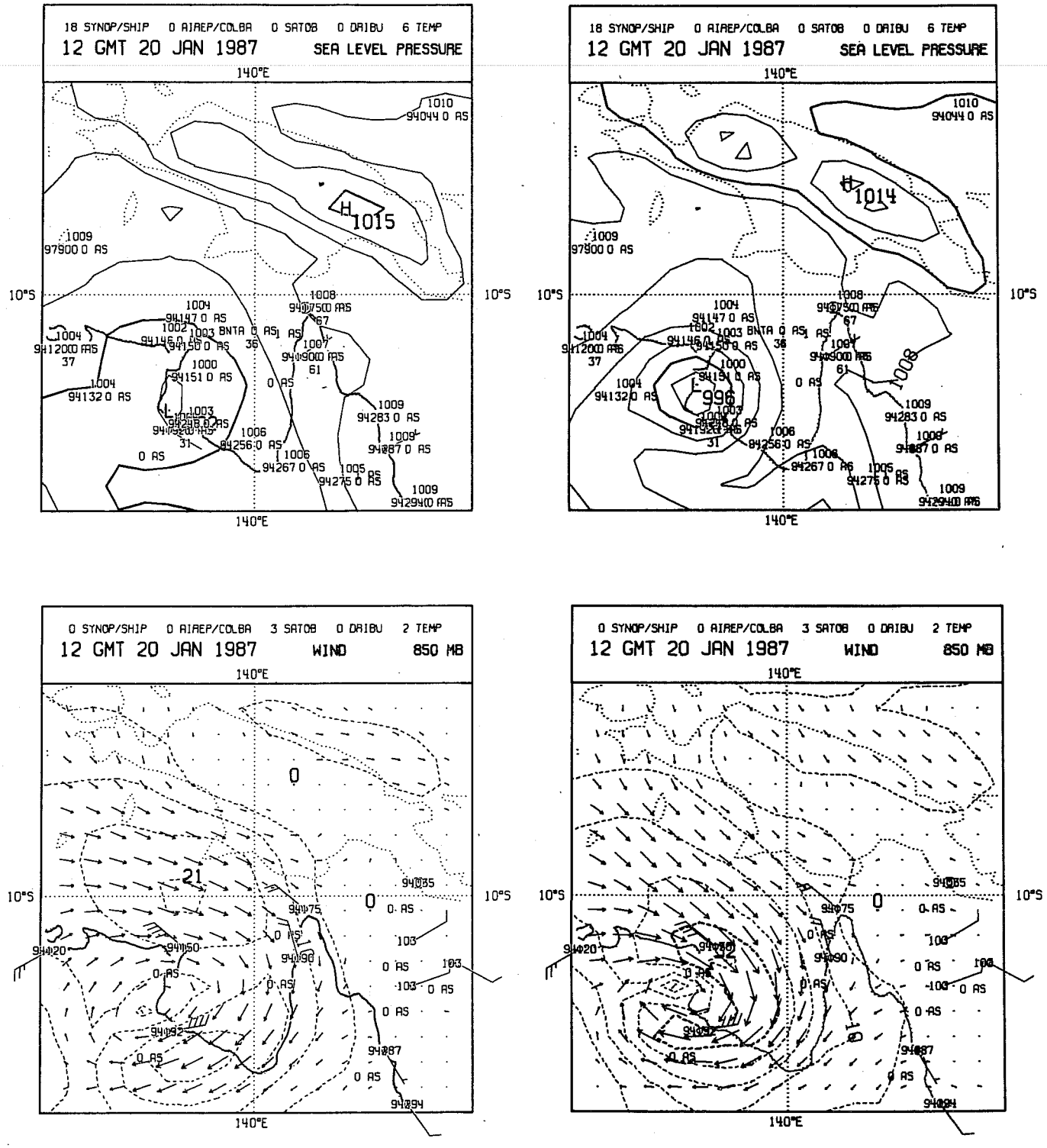

Fig. 2b As in Fig. 2a but for TC Irma at 1200 GMT Jan 20.

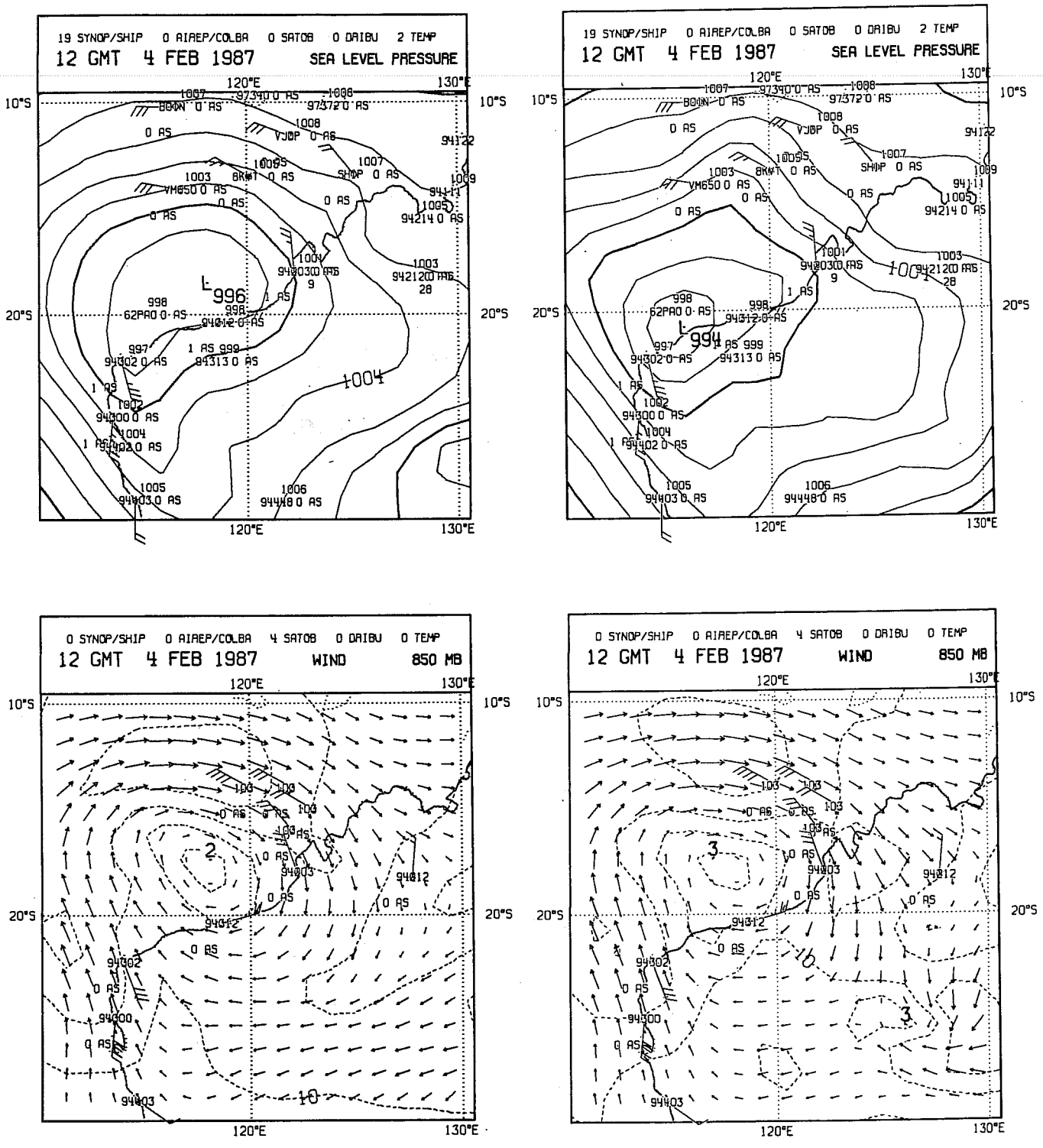

Fig. 2c As in Fig. 2a but for TC Damien at 1200 GMT Feb 4.

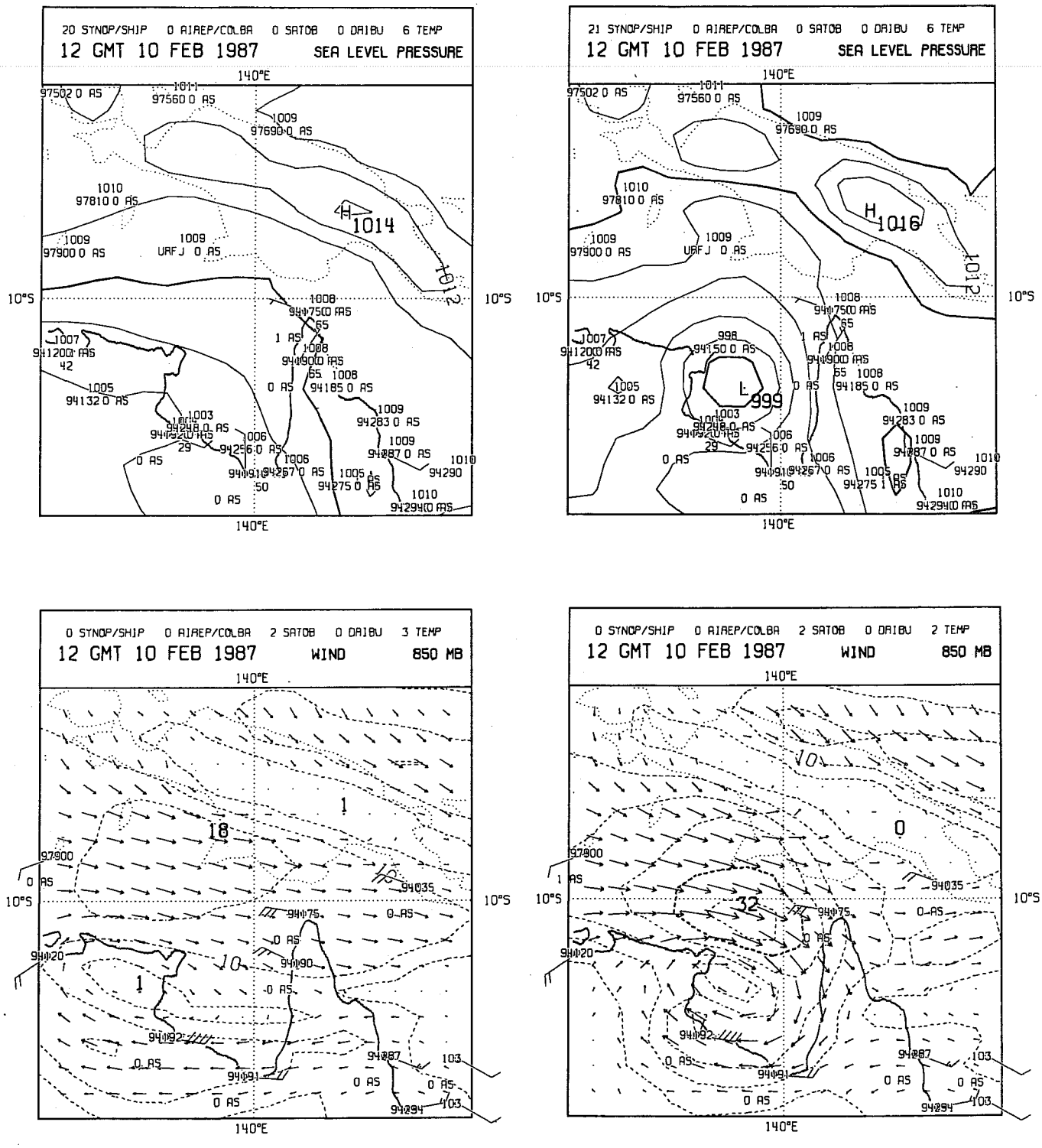

Fig. 2d As in Fig. 2a but for TC Jason at 1200 GMT Feb 10.

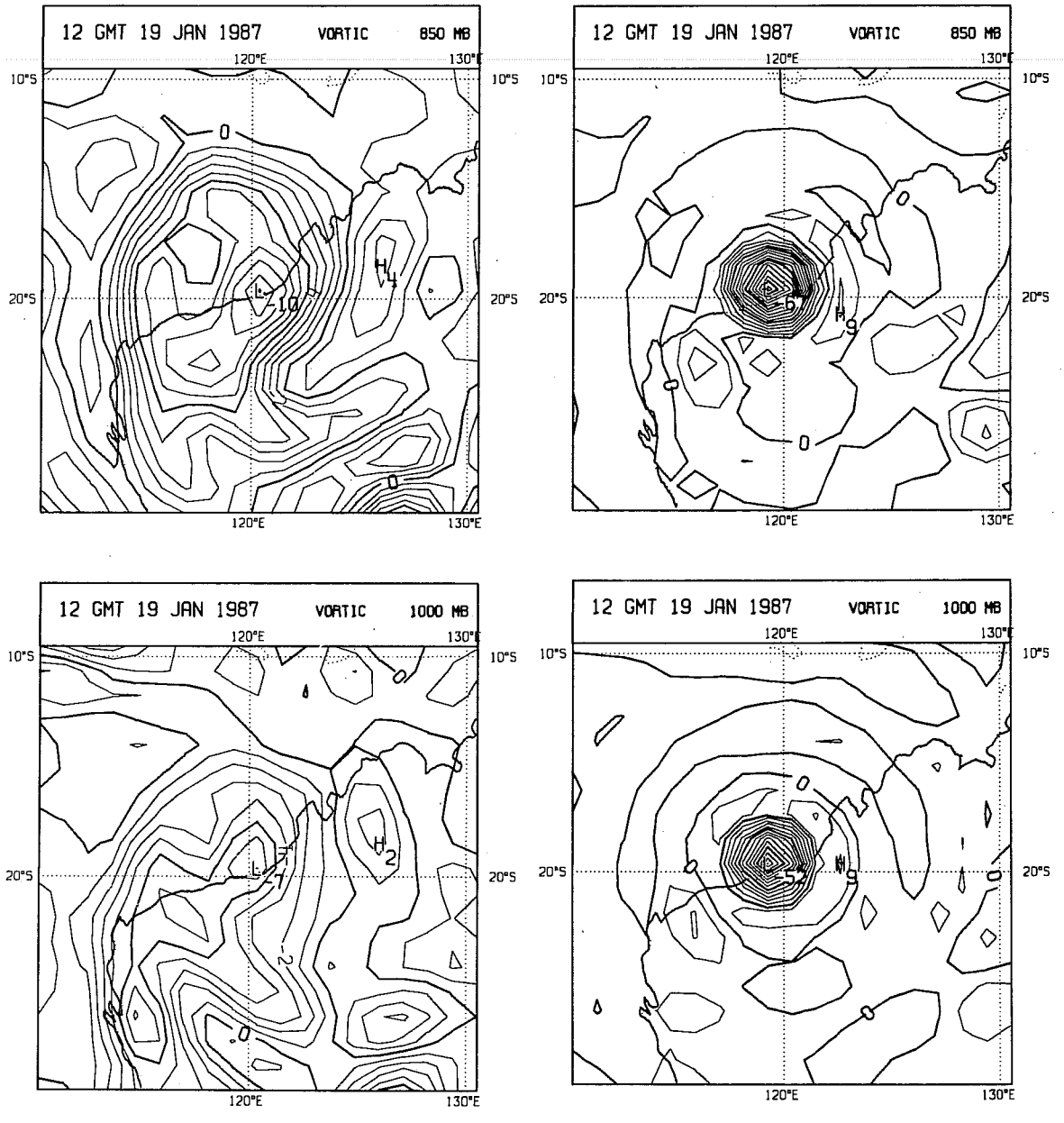

Fig. 3a 850 hPa (top) and 1000 hPa (bottom) vorticity analyses for TC Connie at 1200 GMT Jan 19 from the Kuo (left panel) and ADJ (right panel) systems. Contour intervals are 1 and 4 units respectively for the KUO and ADJ analyses.

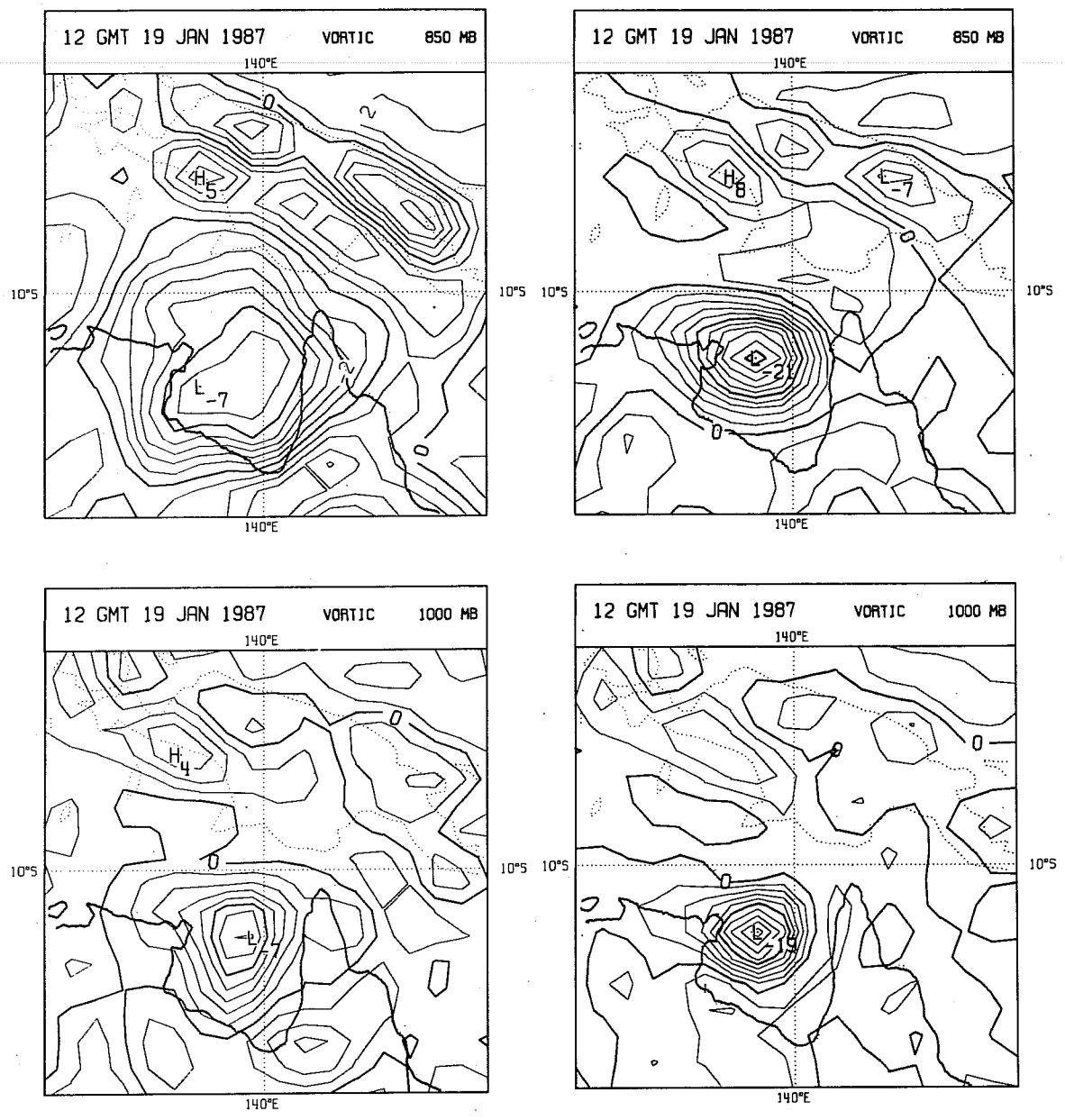

Fig. 3b As in Fig. 3a but for TC Irma at 1200 GMT Jan 19. Contour intervals are 1 and 2 units respectively for the KUO and ADJ analyses.

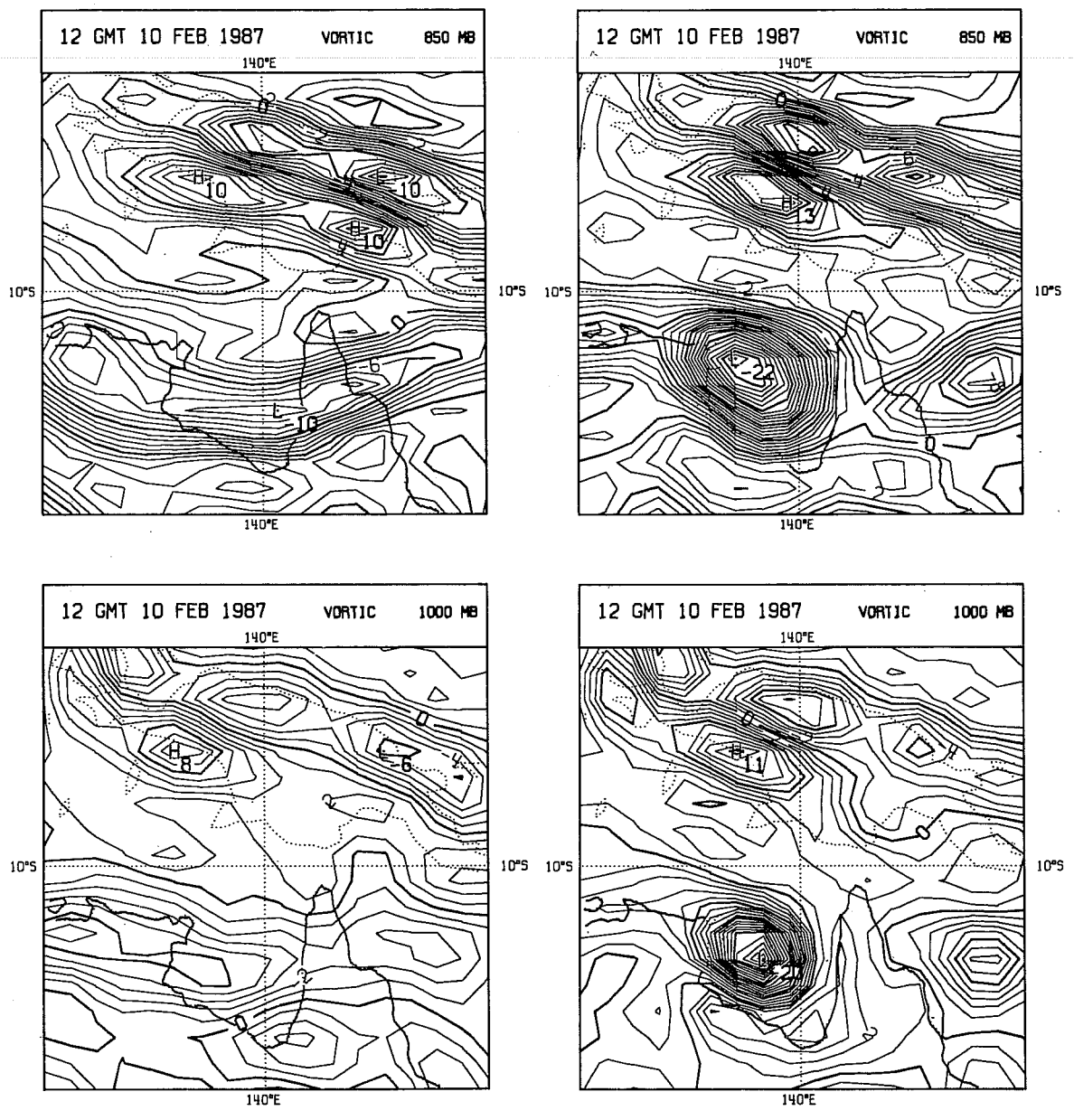

Fig. 3c As in Fig. 3a but for TC Jason at 1200 GMT Feb 10. Contour interval is one 1 unit.

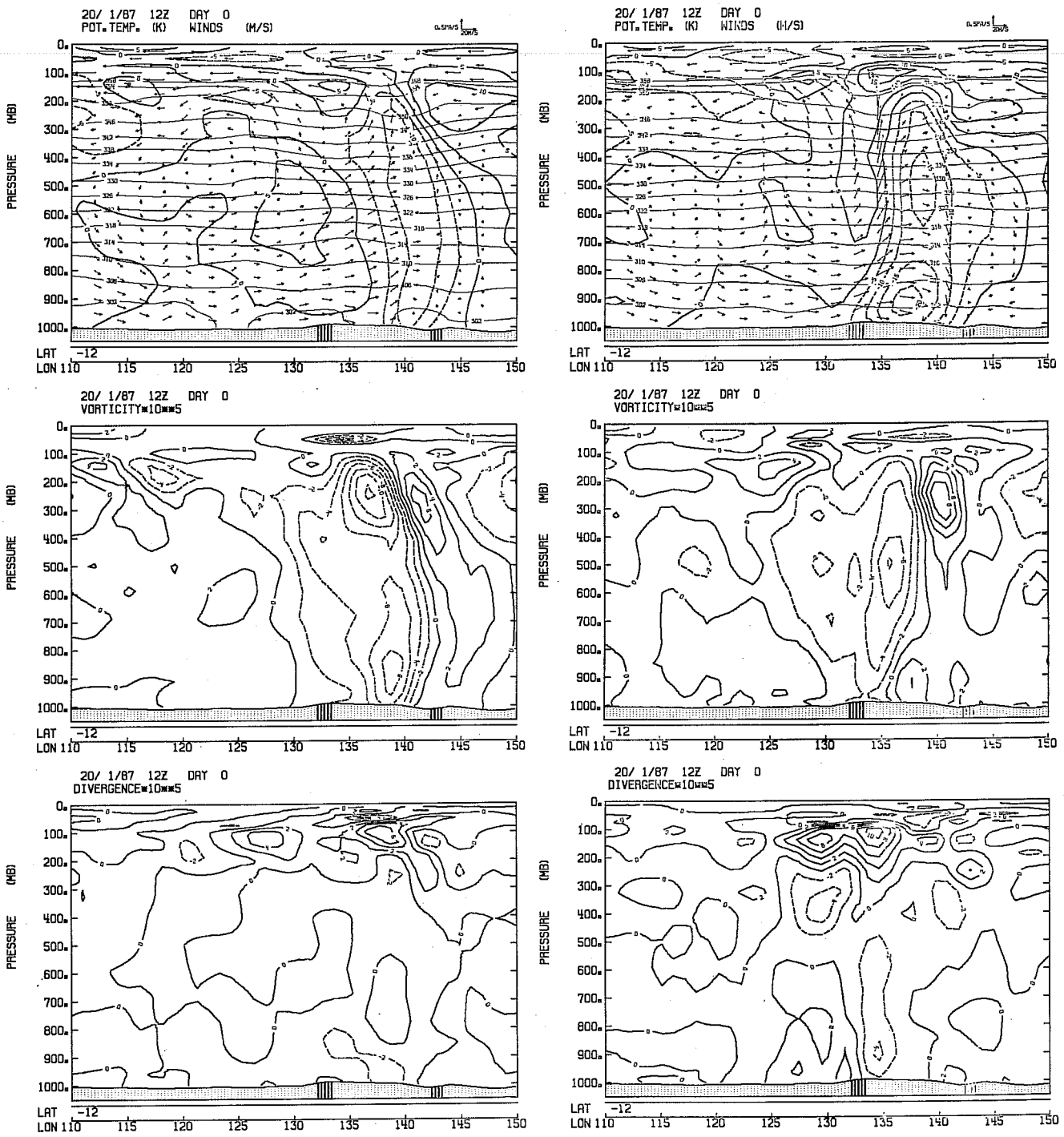

Fig. 4a Vertical sections at 12°S for potential temperature (K) - winds (ms^{-1}) (top), vorticity (middle, $x10^5$) and divergence (bottom, $x10^5$ at 1200 GMT Jan 20 for KUO (left panel) and ADJ (right panel) analyses. Contour intervals are 4K for pot. temp., 5 ms^{-1} for isotachs, 2 x 10^5 for vorticity and divergence.

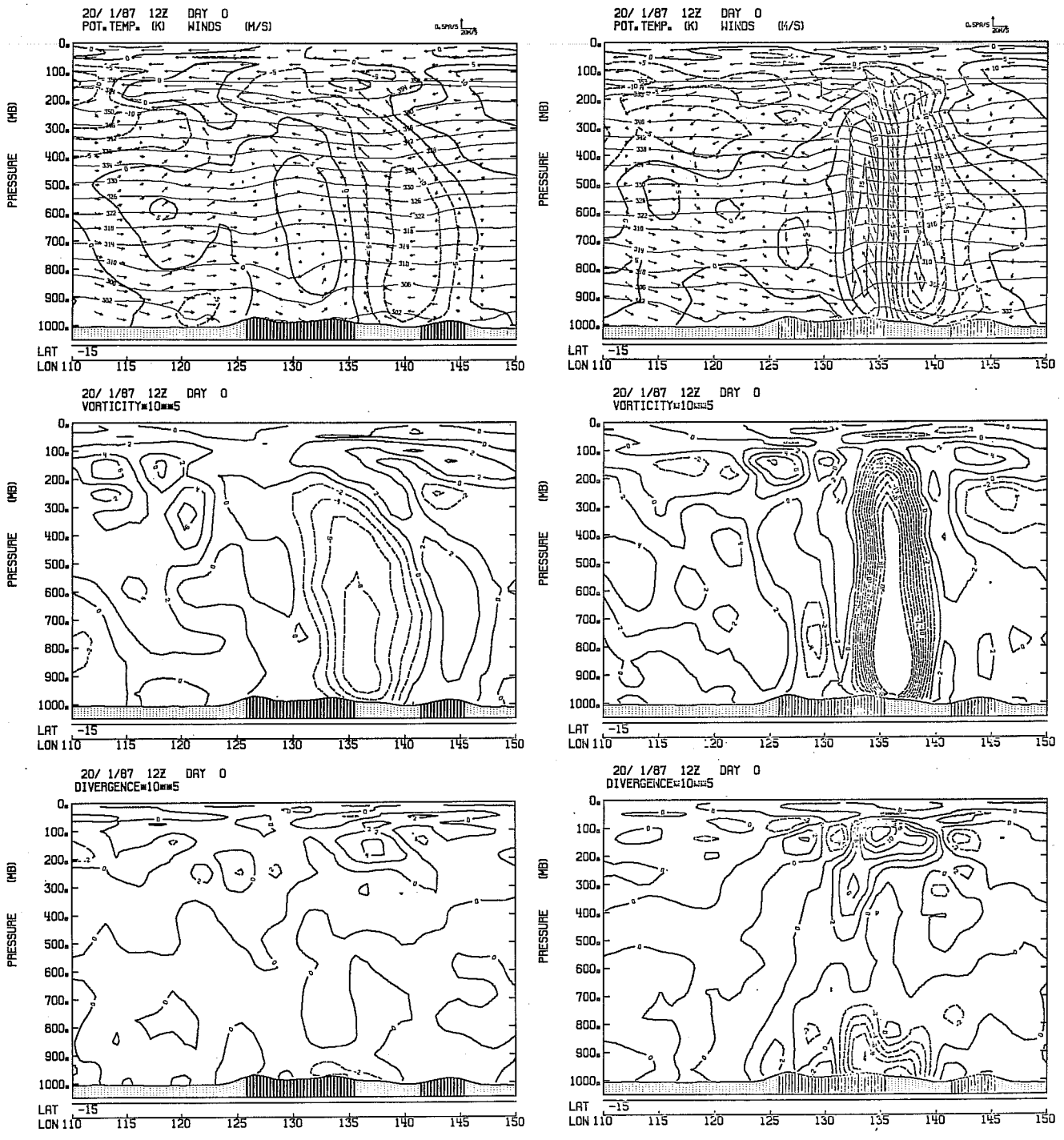

Fig. 4b As in Fig. 4a but at 15°S.

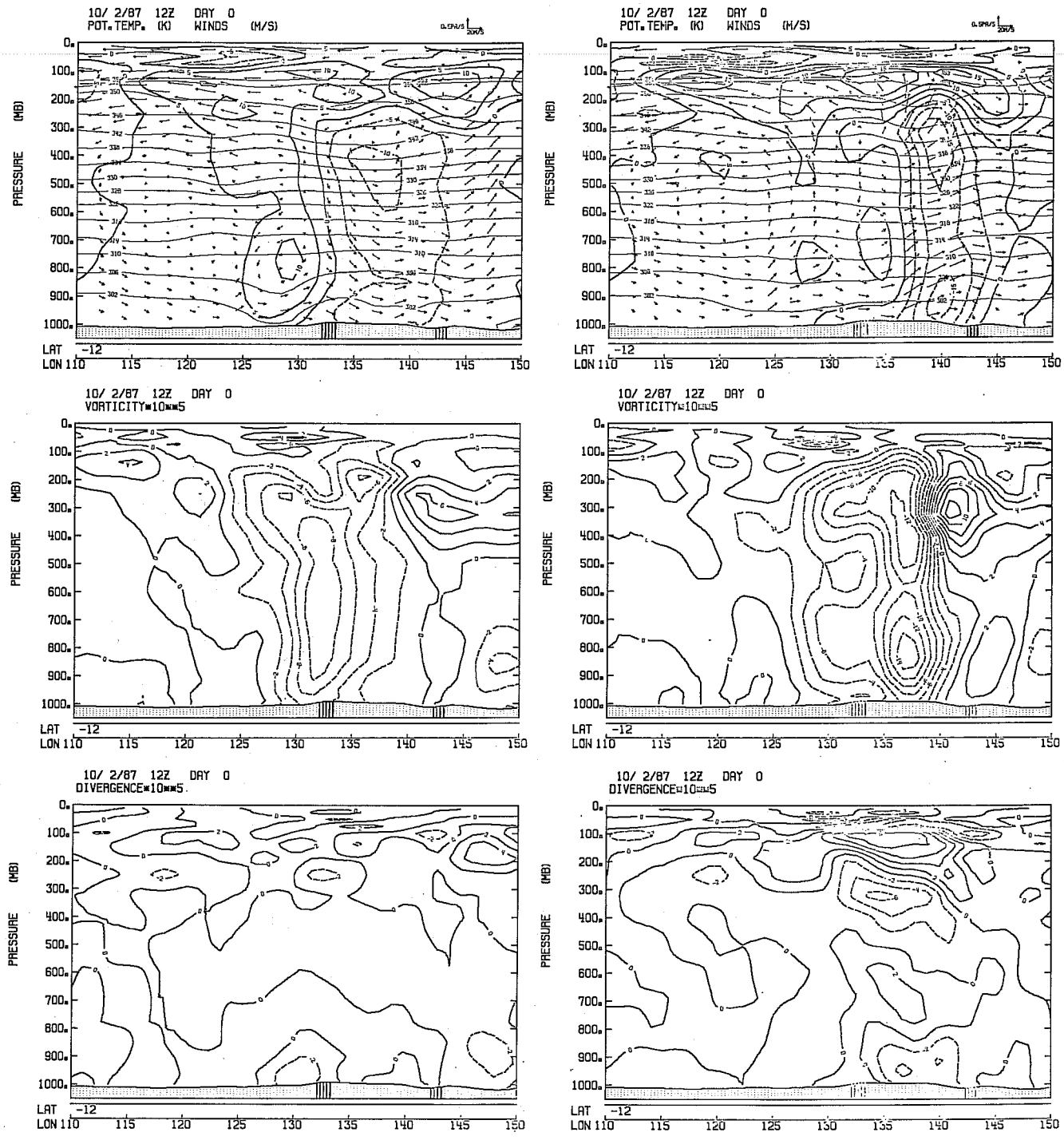

Fig. 4c As in Fig. 4a but at 1200 GMT Feb 10.

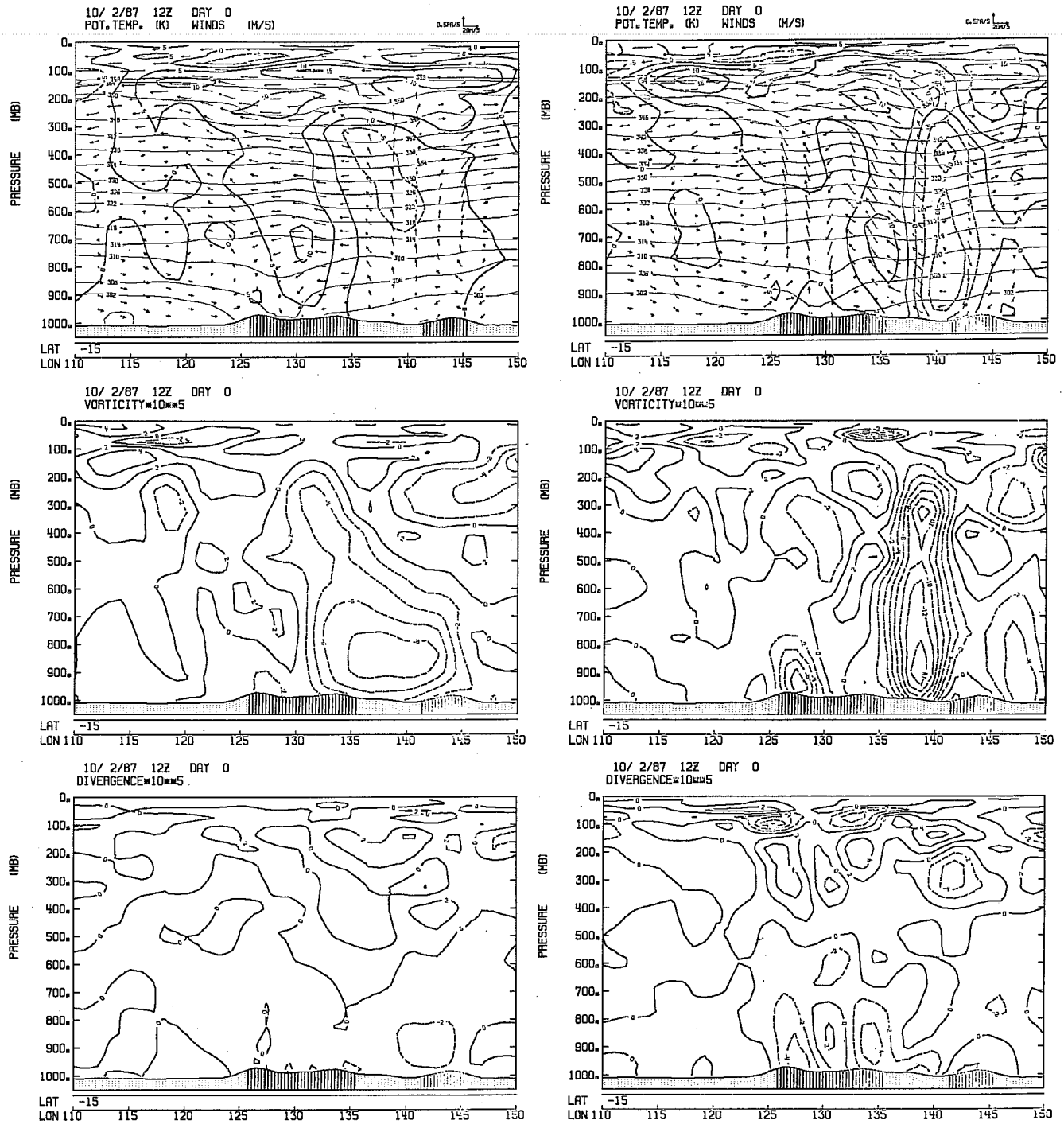

Fig. 4d As in Fig. 4b but at 1200 GMT Feb 10.

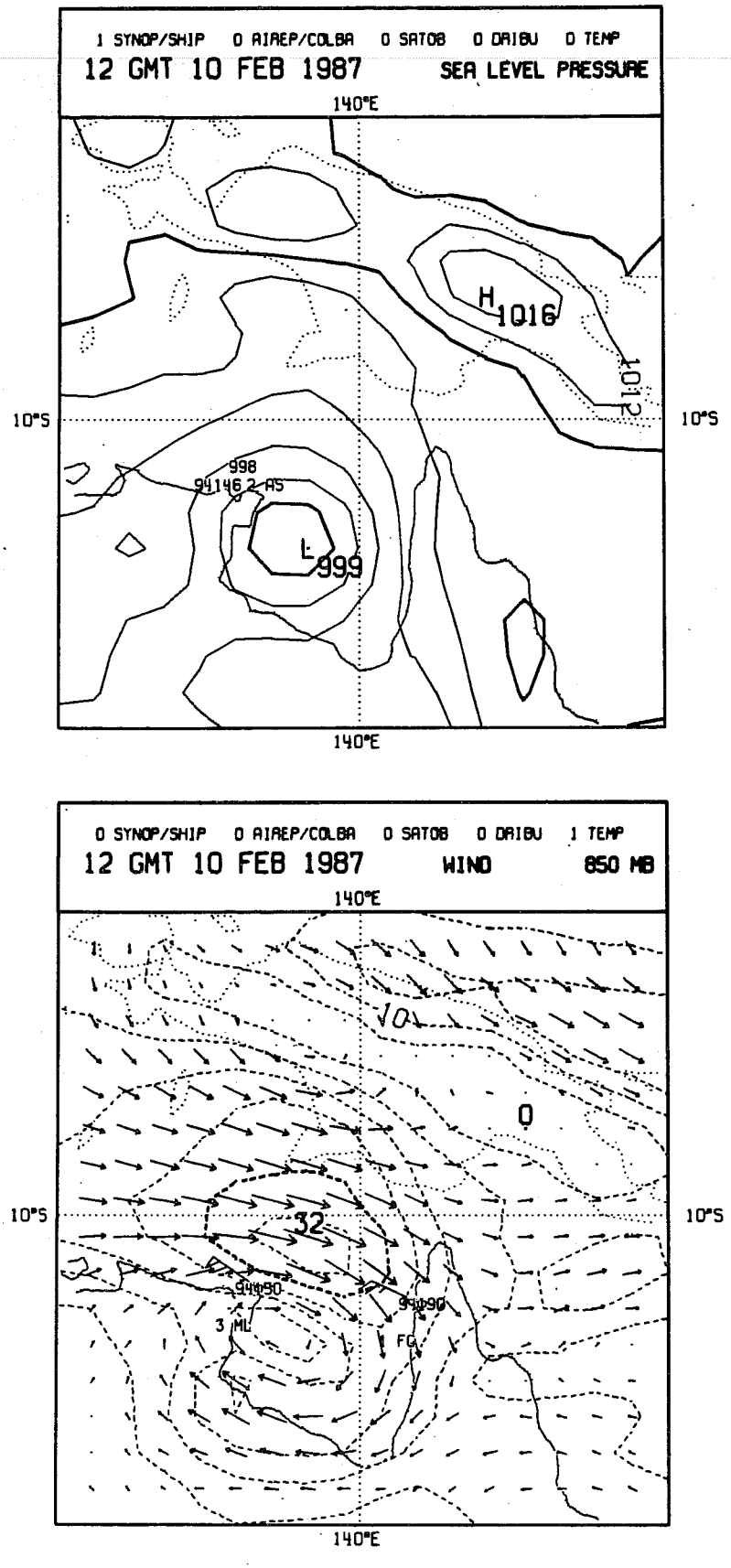

Fig. 5 MSLP (top in hPa) and 850 hPa vector wind (bottom in ms^{-1}) ADJ analyses for TC Jason at 1200 GMT Feb 10 showing observations rejected by the analysis.

useful data. A procedure to overcome the problem of rejection of useful data in the vicinity of the tropical cyclone will be described in Part III.

In summary, we note that the analyses of tropical cyclones show a marked sensitivity to the cumulus convection parametrization used in the forecast model. The analyses from the Betts-Miller adjustment system lead to stronger and better defined cyclonic circulations which have better vertical consistency than the operational analyses. Although both analyses are in general consistent with the observed data the gross features of the ADJ analyses are closer to the mean features reported in detailed composite studies of tropical cyclones (McBride, 1981).

b. Comparison of forecasts

The performance of the forecasts from the two schemes will be judged by comparing their ability to provide guidance on the genesis of tropical cyclones from initially weak or no cyclonic circulation and secondly to handle the motion of cyclones which were present in the initial conditions. As has been mentioned before, the model being used here does not have sufficient resolution to resolve the details of the cyclone structures and the inner core of the cyclones. Thus the comparison here will only be in terms of the gross features. Unless otherwise stated the forecasts referred to as KUO forecasts start from operational (i.e. KUO) analyses and use the KUO parametrization during the forecasts whereas the ADJ forecasts start from ADJ analyses and use the Betts-Miller adjustment scheme during the forecasts.

Figs. 6(a) to (d) show the one and two day KUO and ADJ forecasts starting from 1200 GMT January 17 and Figs. 7(a) and (b) shows the starting and verifying KUO and ADJ analyses for 1200 GMT January 17 and 19 respectively. The period corresponds to developments leading to the formation of tropical cyclone Irma on Jan 19 and the aim here was to determine whether the forecasts have the ability to generate and intensify cyclonic circulation in the Gulf of Carpenteria. The initial ADJ analysis has a low level cyclonic circulation in the Gulf while the KUO analysis has very weak circulation. Both verifying analyses are in reasonable agreement with respect to the location of TC Irma although the ADJ analysis has a significantly stronger cyclonic circulation. The adjustment forecast intensifies the cyclonic circulation in the Gulf during the two day period and deepens the surface pressure, both features being in reasonable agreement with the verifying analyses although the upper level flow is rather different. The KUO forecast however does not lead to any intensification and there is no indication of cyclonic development in the Gulf during the forecast period. One reason for the differences in the forecast performance of the two schemes can be seen in the forecasts for the lower and upper level velocity potentials and

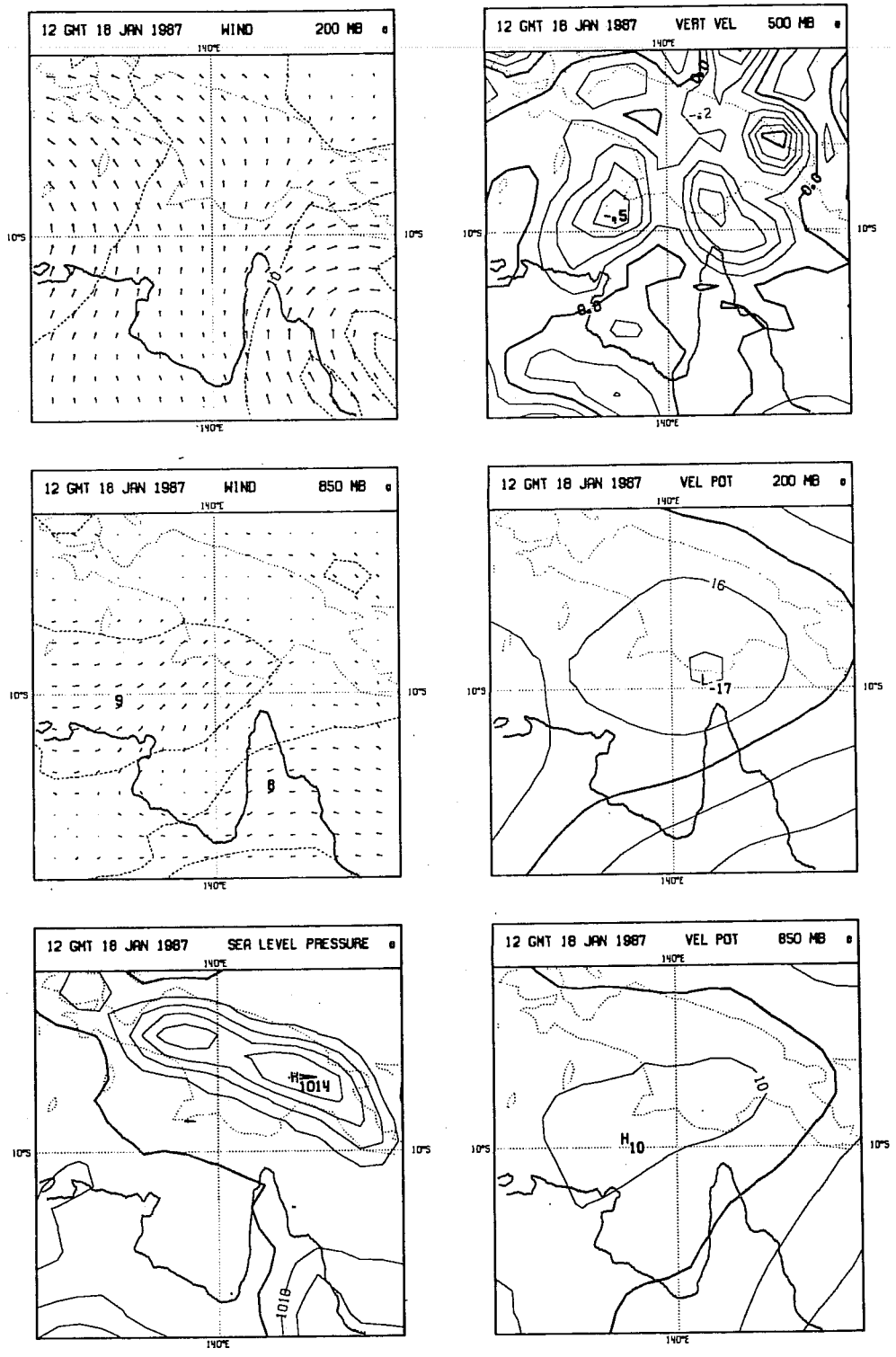

Fig. 6a Two day KUO forecast starting from 1200 GMT Jan 17 for MSLP (bottom left in hPa), 850 hPa vector wind (middle left in ms^{-1}), 200 hPa vector wind (top left in ms^{-1}), 850 hPa velocity potential (bottom right, in m^2s^{-1}), 200 hPa velocity potential (middle right, in m^2s^{-1}) and 500 hPa vertical velocity (top right, in hPa s^{-1}). Contour intervals are 1 hPa for MSLP, 5 ms^{-1} for isotachs, 1 m^2s^{-1} for velocity potentials and 0.1 hPa s^{-1} for vertical velocity.

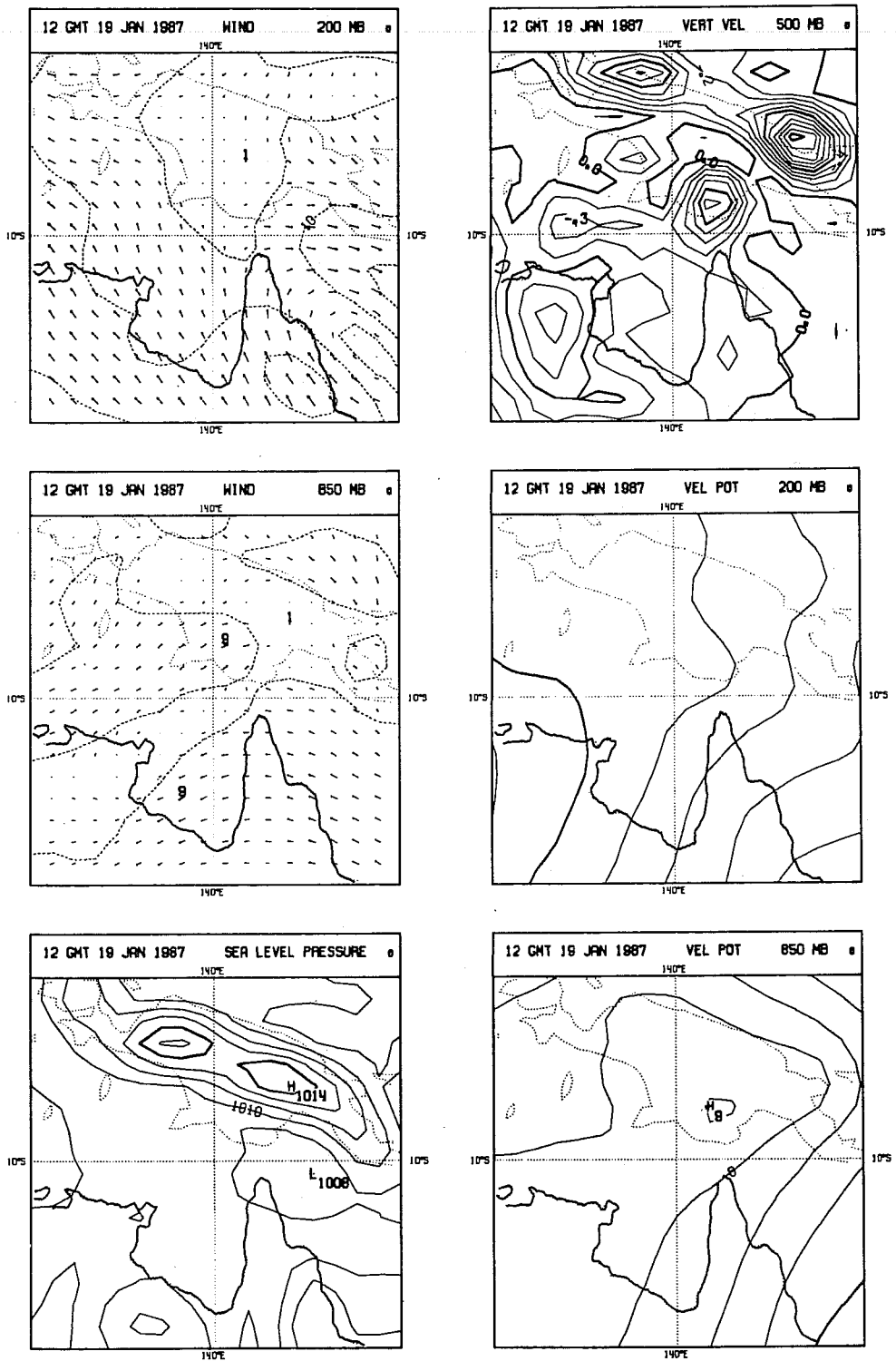

Fig. 6b As in Fig. 6a but for 2 day Kuo forecast.

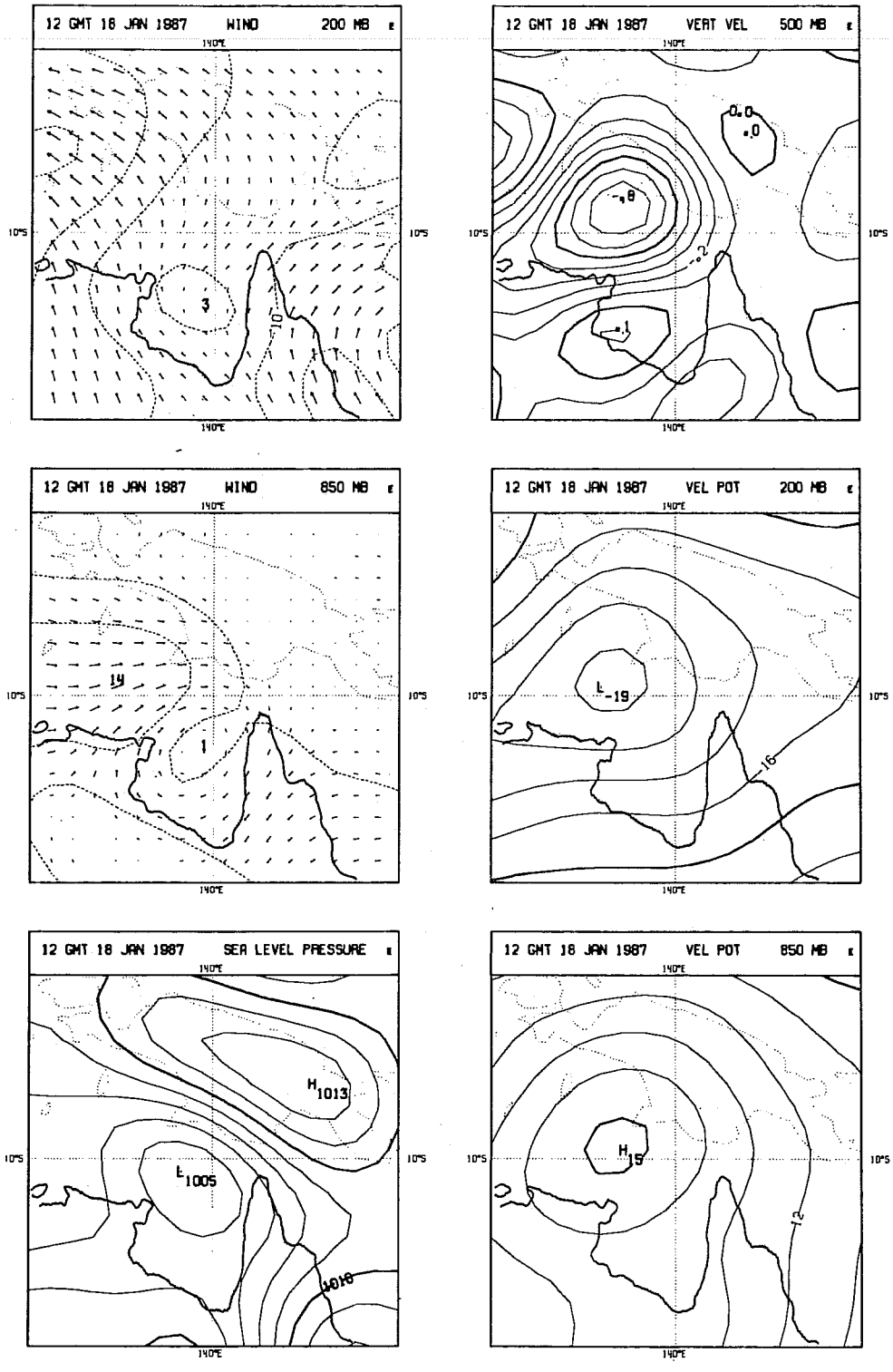

Fig.6c As in fig.6a but for ADJ forecast.

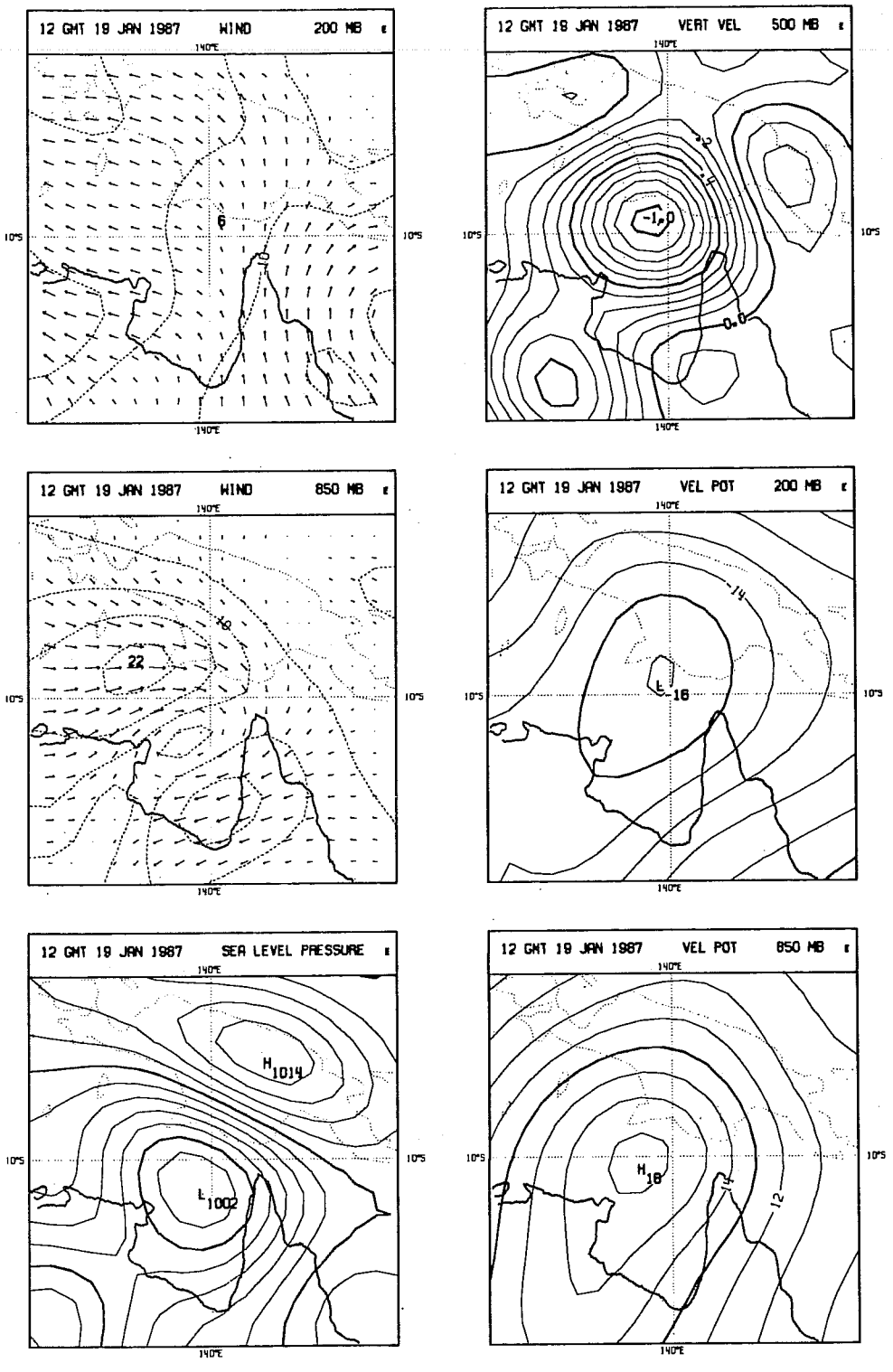

Fig.6d As in fig.6b but for ADJ forecast.

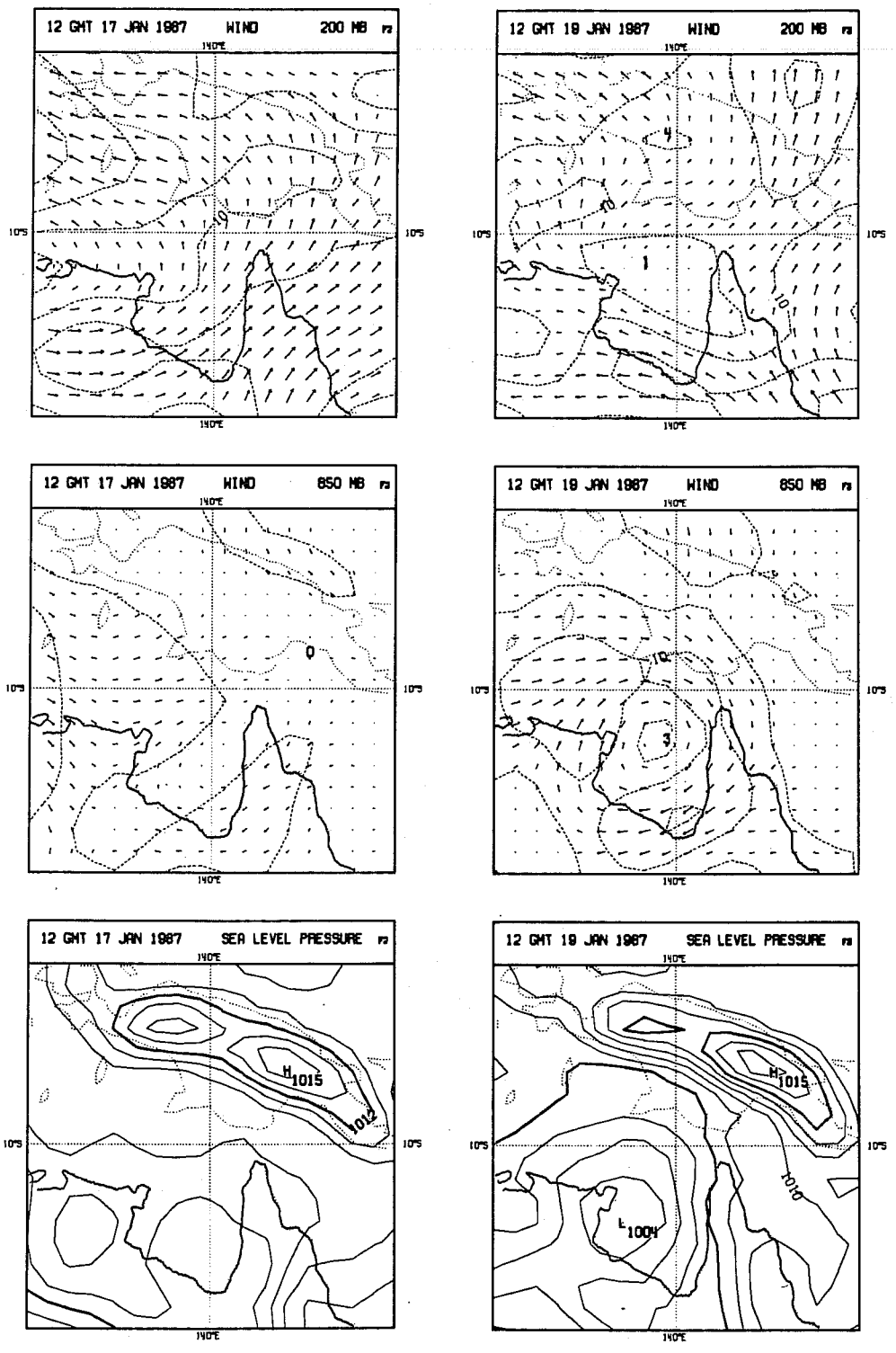

Fig. 7a MSLP (bottom), 850 hPa vector wind (middle) and 200 hPa vector wind (top) KUO analysis for 1200 GMT Jan 17 (left panel) and Jan 19 (right panel). Units and contour intervals are as in Fig. 6.

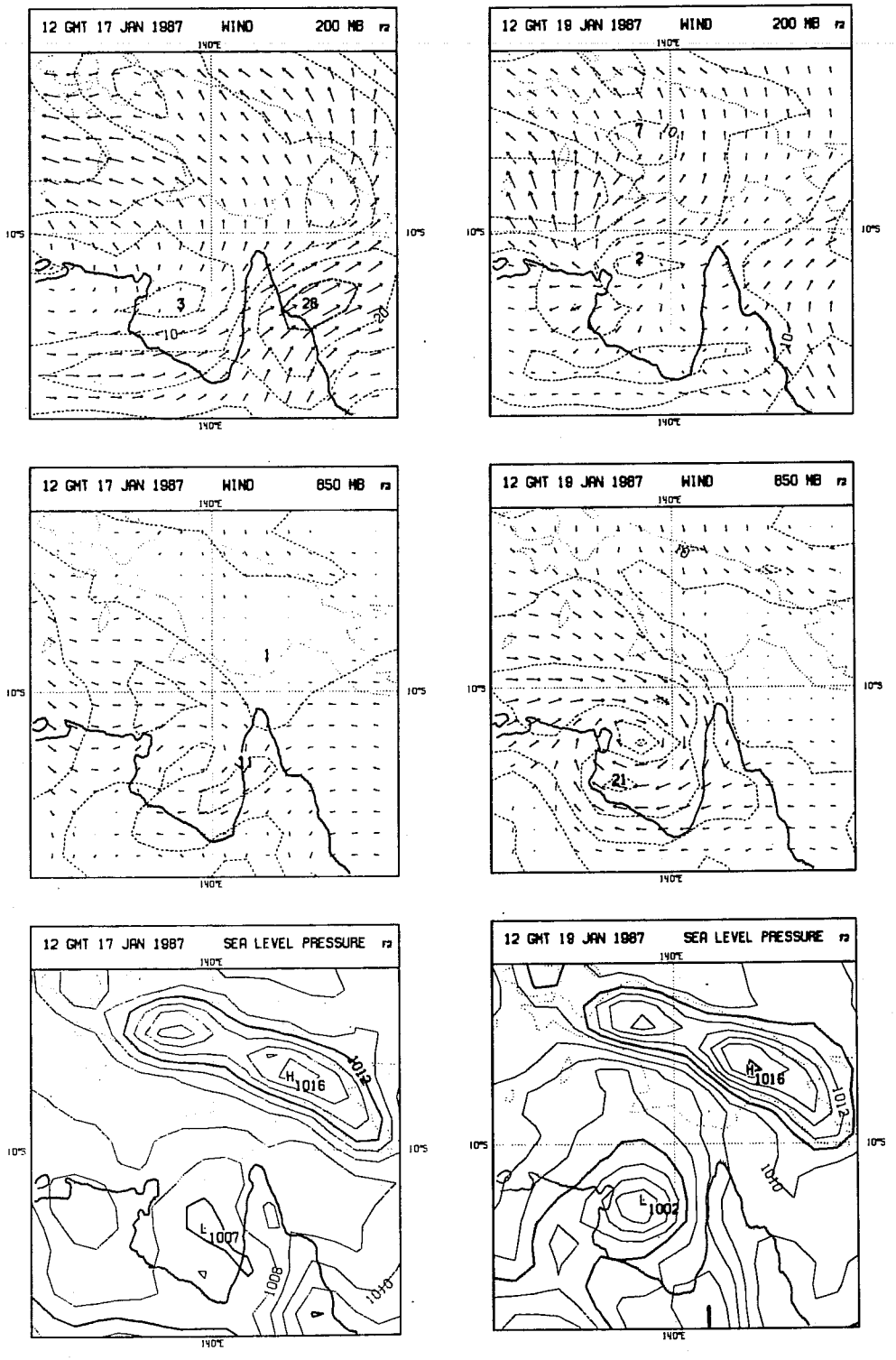

Fig. 7b As in Fig. 7a but for ADJ analyses.

the vertical velocity. The ADJ forecast generates good consistency of these fields in the vertical with significant upward motion (negative vertical velocity) in the region of the cyclonic circulation. The KUO forecasts on the other hand show little consistency in the vertical with a very weak divergent circulation. This important difference appears to be a systematic difference between the two systems for both analyses (not shown) and forecasts. The lack of vertical consistency appears to be a major deficiency in the KUO parametrization as used at ECMWF.

Another reason for differences in the forecasts could be due to differences in the initial conditions. Note that the ADJ analysis for 1200 GMT Jan 17 has stronger cyclonic circulation in the Gulf. These differences in analysis reflect the impact of the parametrization scheme on the analyses via the first guess. However in order to provide some indication as to which of the two factors (initial analysis or cumulus parametrization) exert a stronger influence on the forecasts, two further forecasts were carried out. The first one started from the KUO analyses for 1200 GMT January 17 and had the Betts-Miller adjustment scheme during the forecast (to be referred to as KUOADJ) and the second forecast started from ADJ analyses and used the KUO parametrization during the forecast to be referred to as ADJKUO). The two day forecasts are shown in Fig. 8. In both forecasts the circulation in the Gulf is weak although the KUOADJ generates the stronger circulation of the two forecasts providing some evidence of the stronger role of the cumulus parametrization on the forecasts.

Fig. 9 shows the two day forecast tracks for TC's Connie (starting date 1200 GMT 18 January), Irma (starting date 1200 GMT 18 January) and Jason (starting date 1200 GMT February 10) at 12 hour intervals and Figs. 10(a) to (f) show the maps for one and two day forecasts. When compared with the BOM best track estimates (see Fig. 1) the track for the ADJ forecasts for TC's Connie and Jason are better than the KUO forecasts whereas the latter forecast was significantly better for TC Irma. The ADJ forecast for TC Connie predicts landfall at approximately the observed time and a significantly better track for TC Jason which however still has large position errors that in large part appear to be related to the location error in the initial analysis. As with the analyses, a feature of the ADJ forecasts as evident in Fig. 10 is the stronger cyclonic circulation for all the cyclones with stronger winds and central pressures which are 5-7 hPa deeper than the KUO forecasts. Part of this is due to initial analyses having deeper central pressures; however, for TC Irma the ADJ forecast intensifies the cyclone compared to initial conditions. The KUO forecasts on the other hand appear to be unable to cause any significant intensification. Another notable feature in the forecasts from the two schemes is that the ADJ forecasts have marked consistency in the vertical between the divergent circulation and the vertical velocity whereas the KUO forecasts do not show this

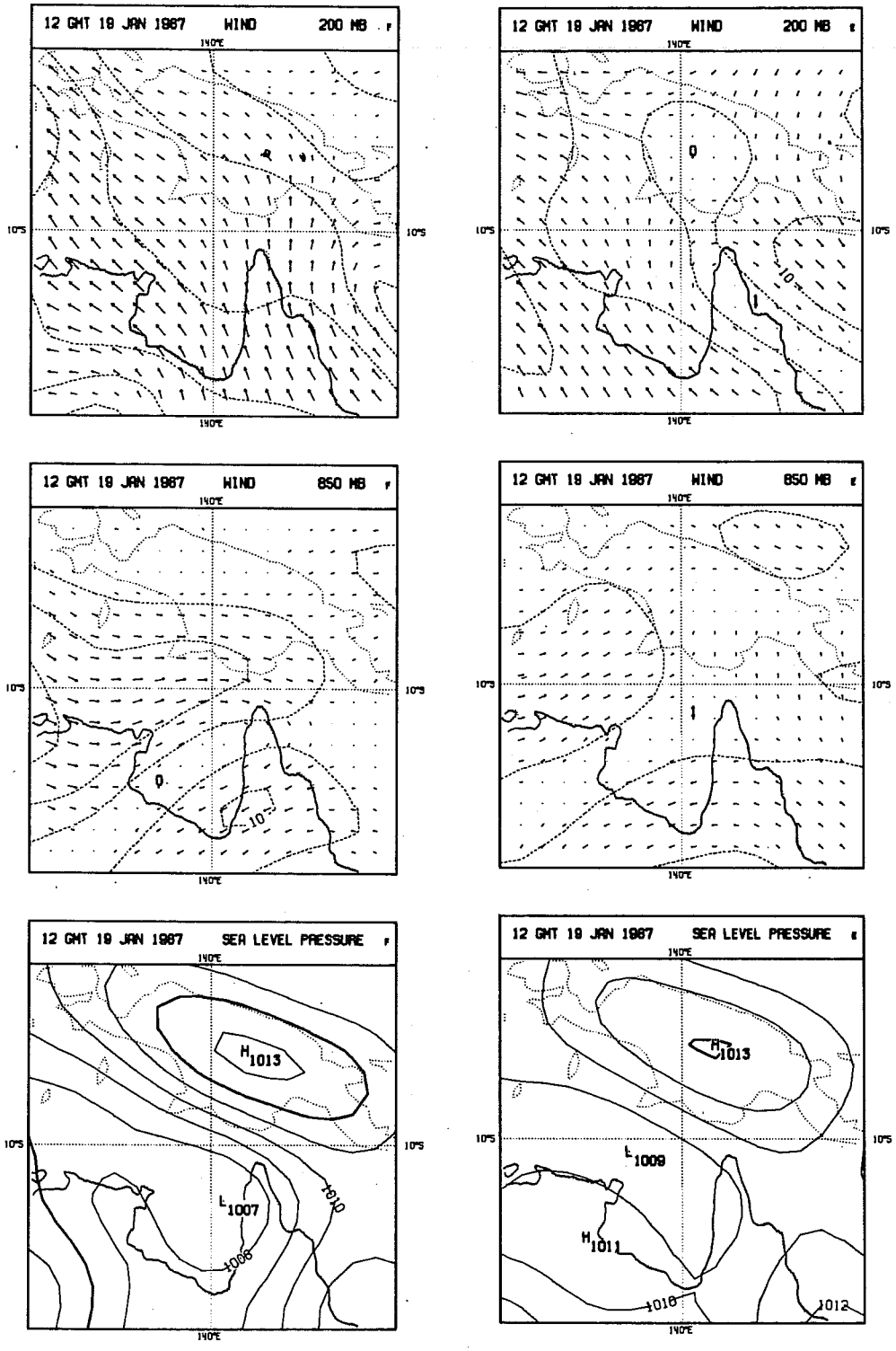

Fig. 8 As in Fig. 7 but for 2 day KUOADJ (left panel) and ADJKUO (right panel) forecasts from 1200 GMT Jan 17.

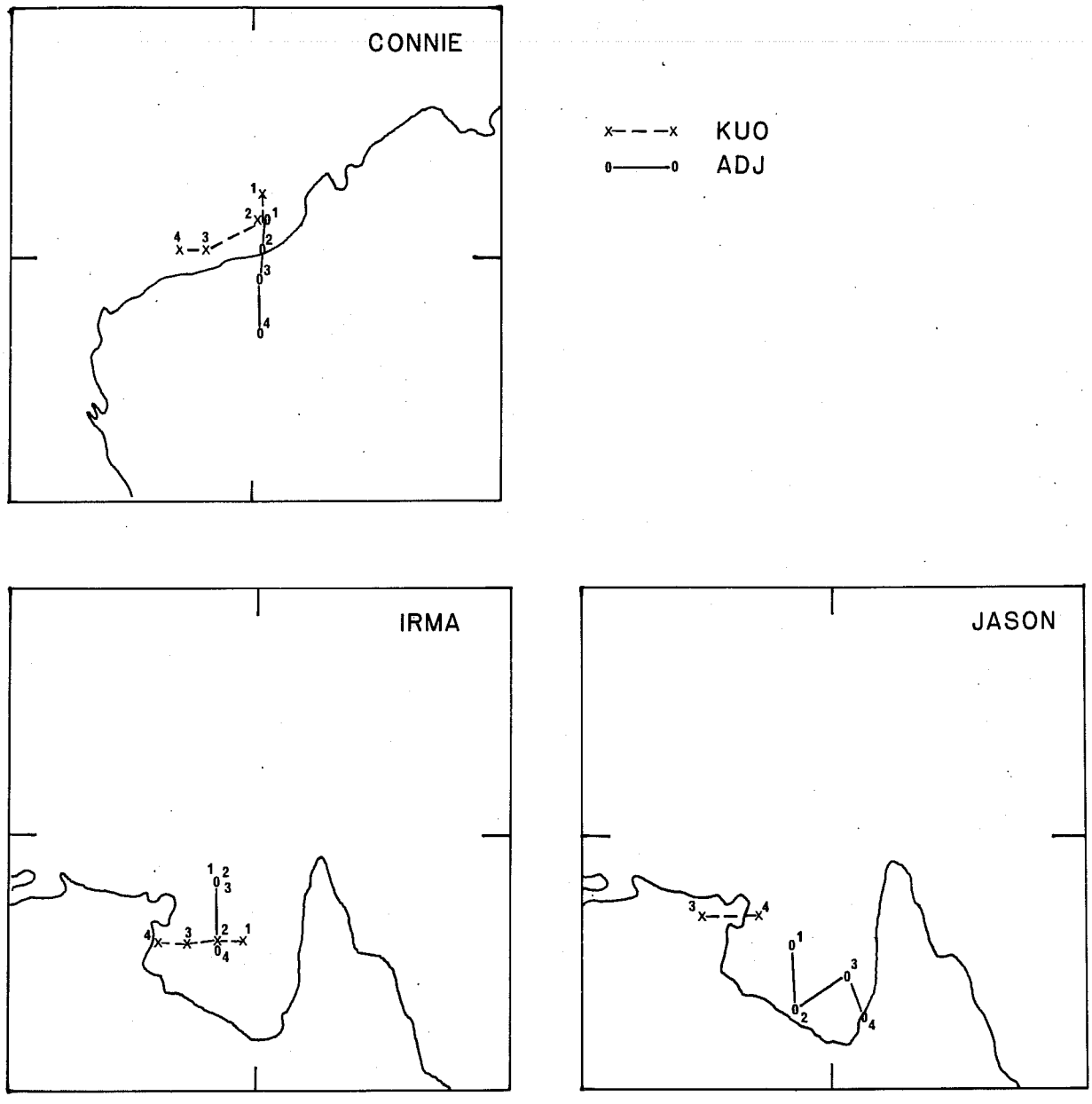

Fig. 9 Two day tracks for KUO (dashed) and ADJ (full line) forecasts for TC's Connie (starting date 1200 GMT Jan 18), Irma (1200 GMT Jan 18) and Jason (1200 GMT Feb 10). Numbers 1 to 4 indicate successive 12 hour intervals.

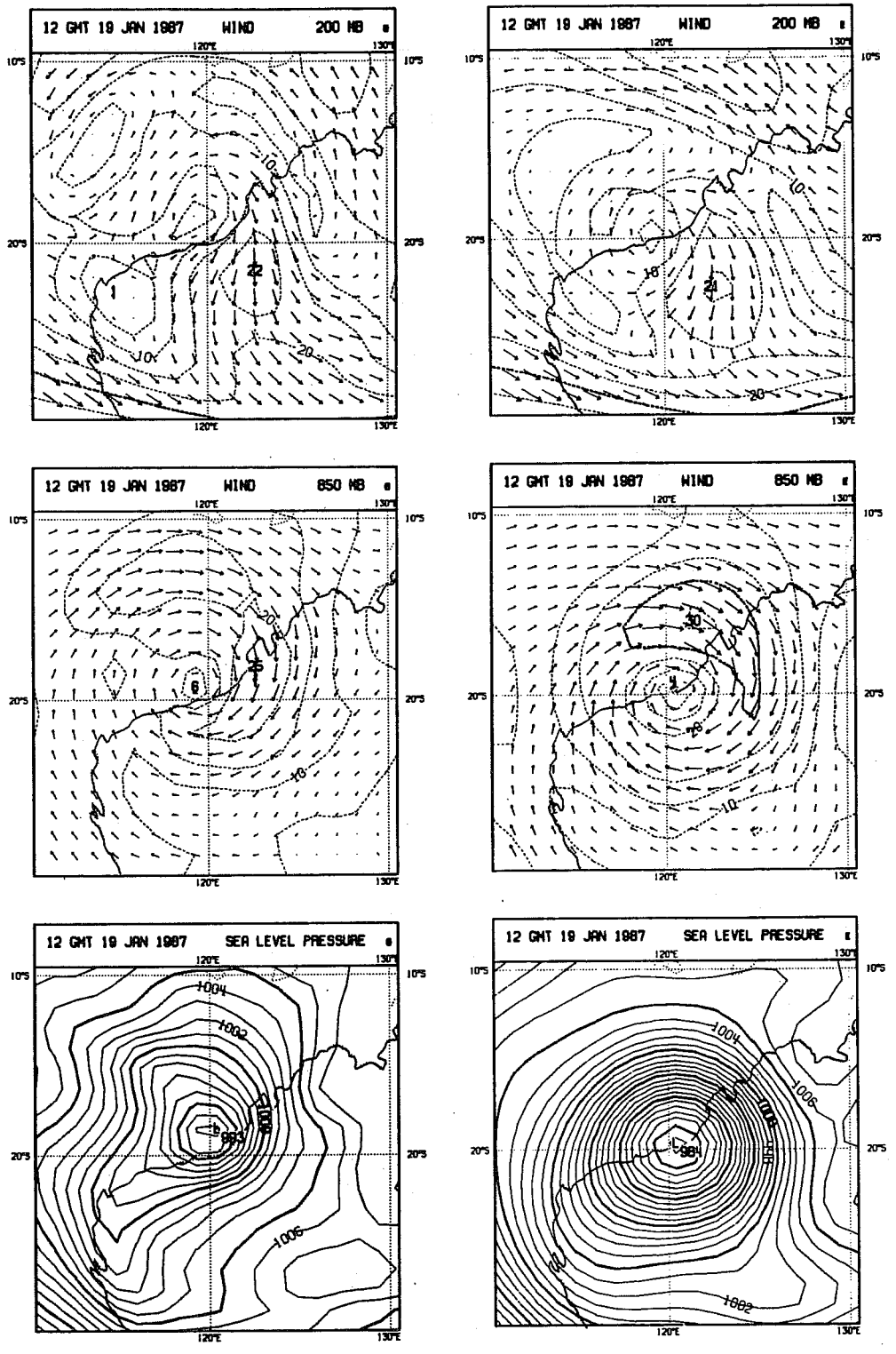

Fig. 10a One day KUO (left panels) and ADJ (right panels) forecasts for TC Connie starting from 1200 GMT Jan 18 for MSLP (bottom), 850 hPa vector wind (middle) and 200 hPa vector wind (top). Units and contour intervals are as in Fig. 6.

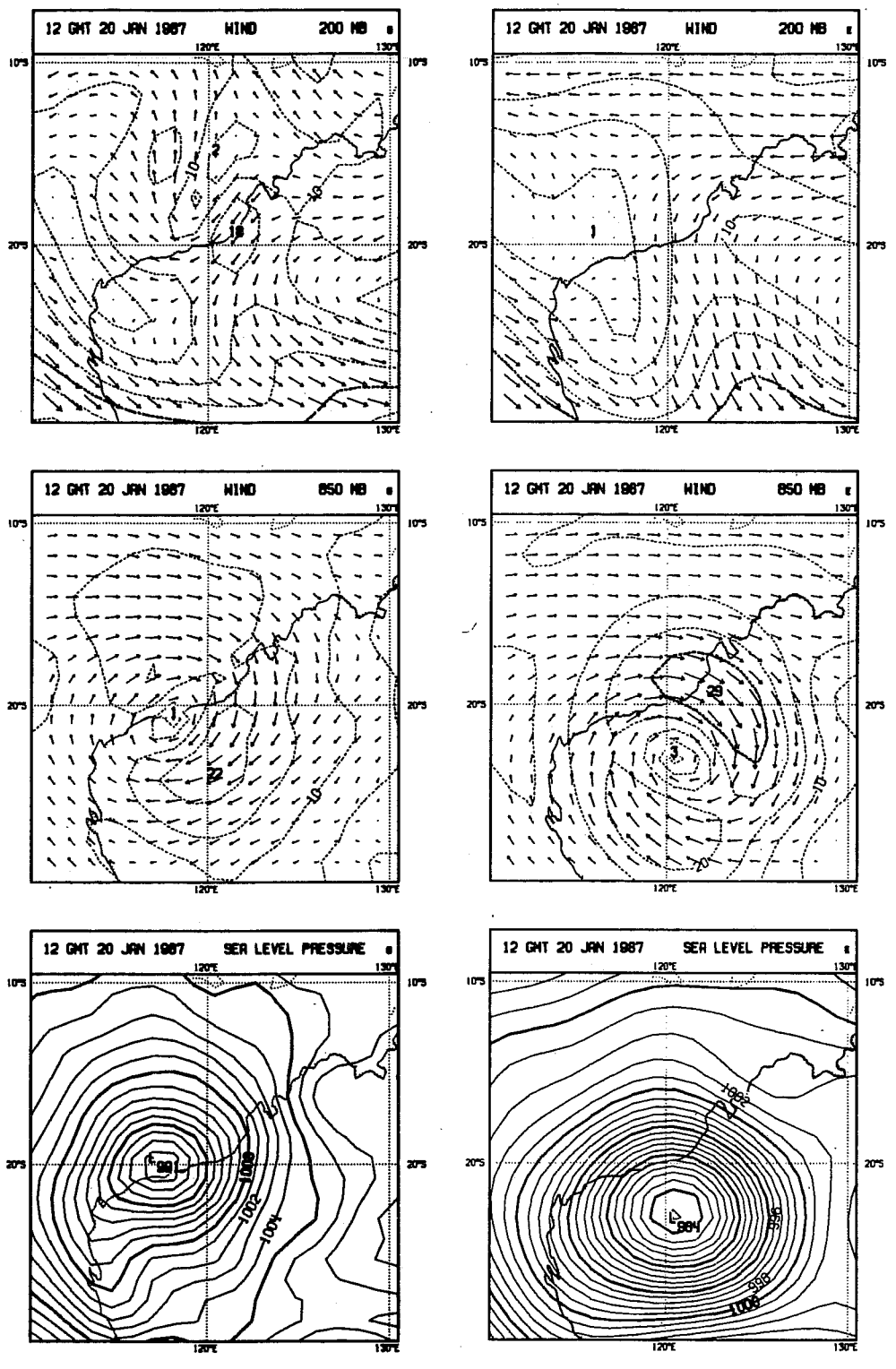

Fig. 10b As in Fig. 10a but for two day forecasts.

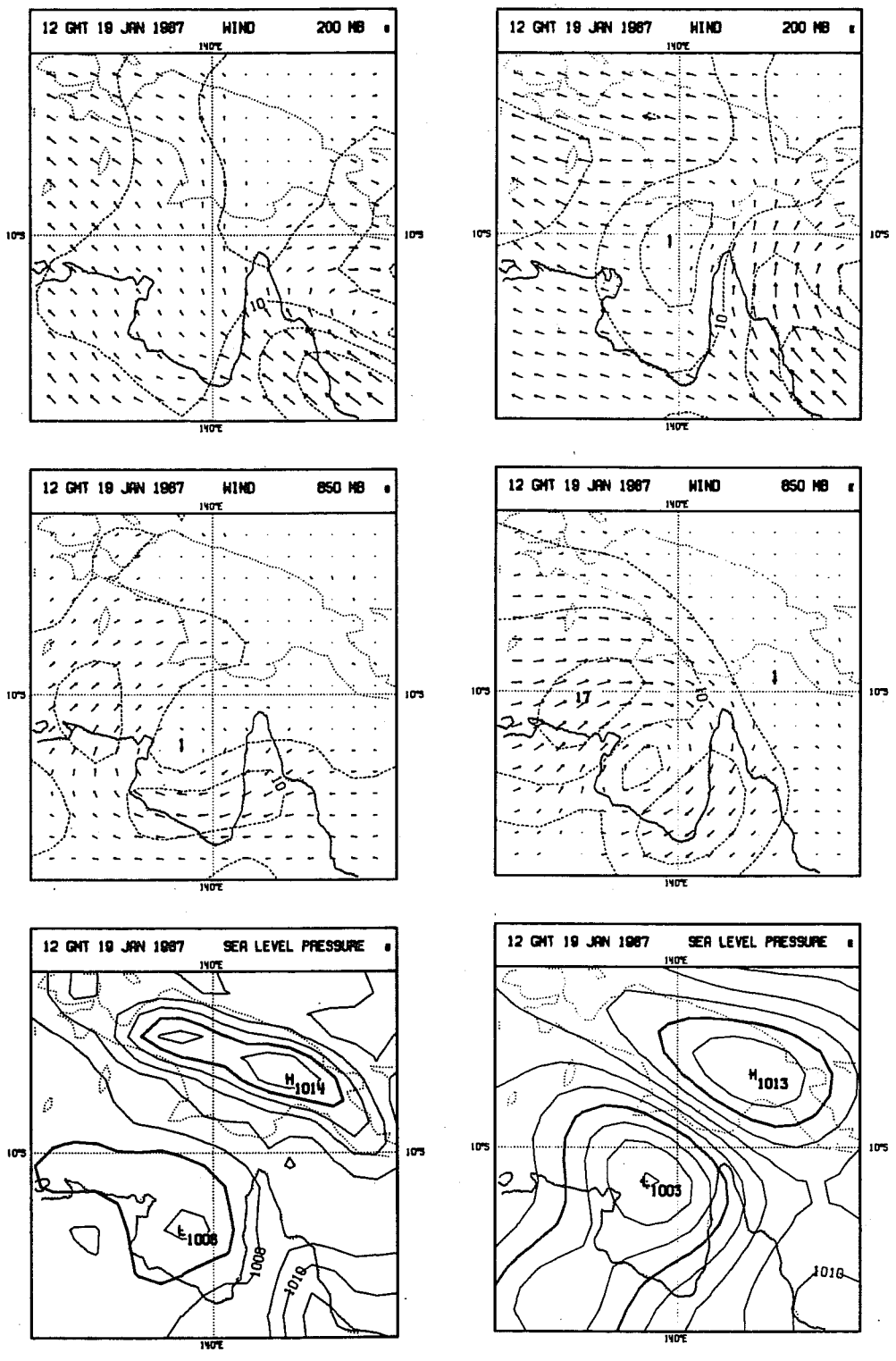

Fig. 10c As in Fig. 10a but for one day forecasts for TC Irma starting from 1200 GMT Jan 18.

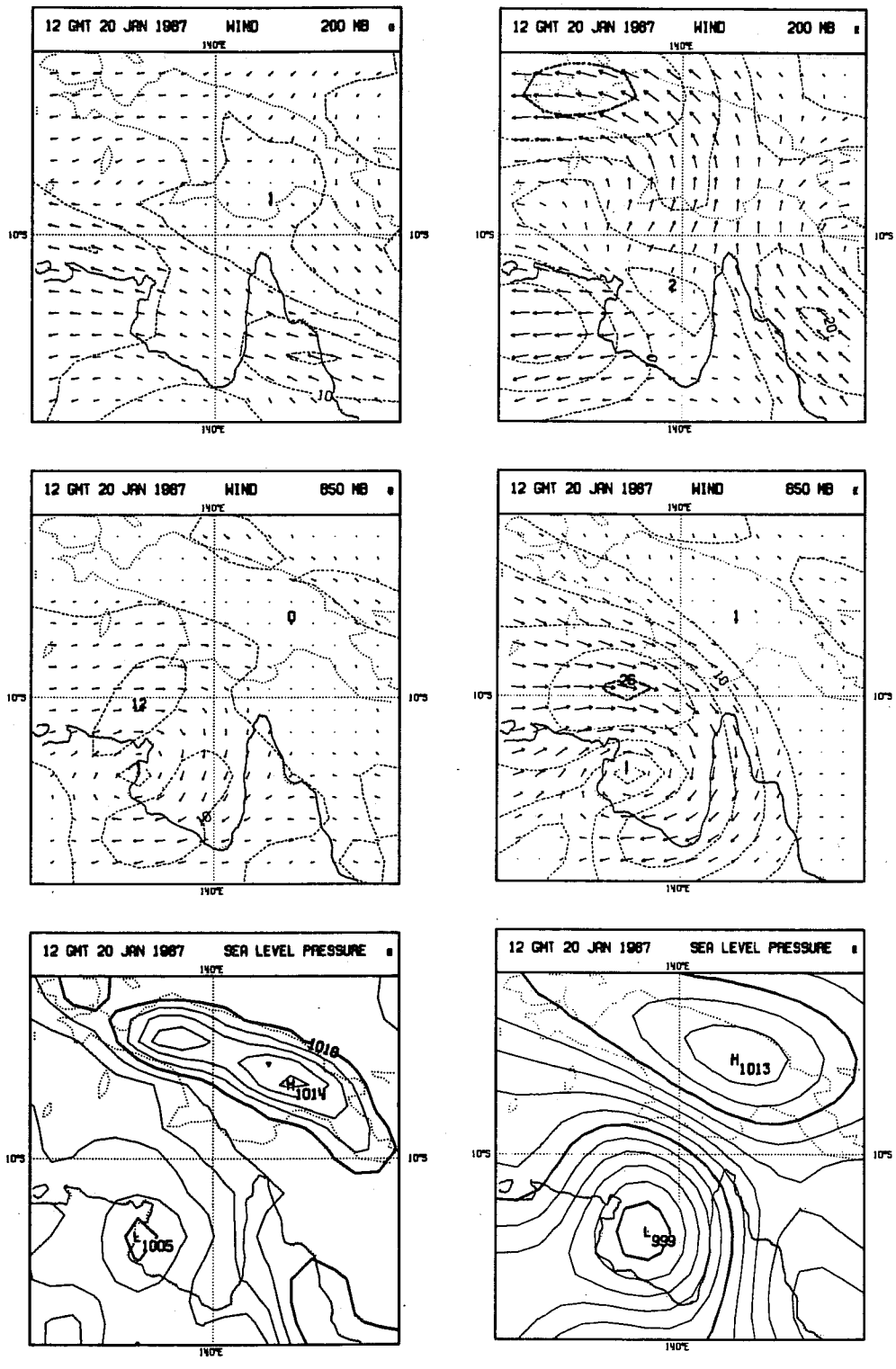

Fig. 10d As in Fig. 10c but for two day forecasts.

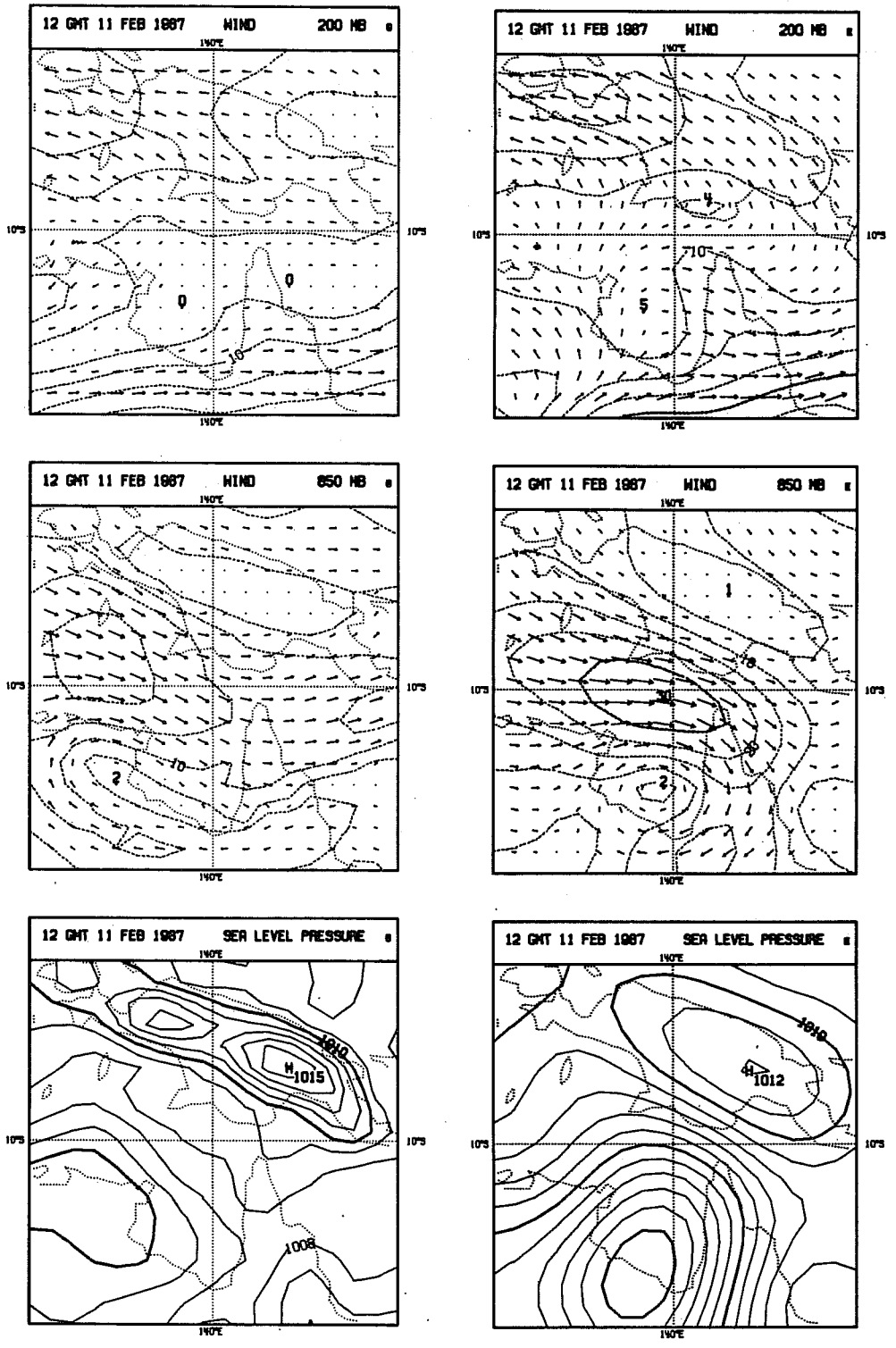

Fig. 10e As in Fig. 10c but for one day forecasts for TC Jason starting from 1200 GMT Feb 10.

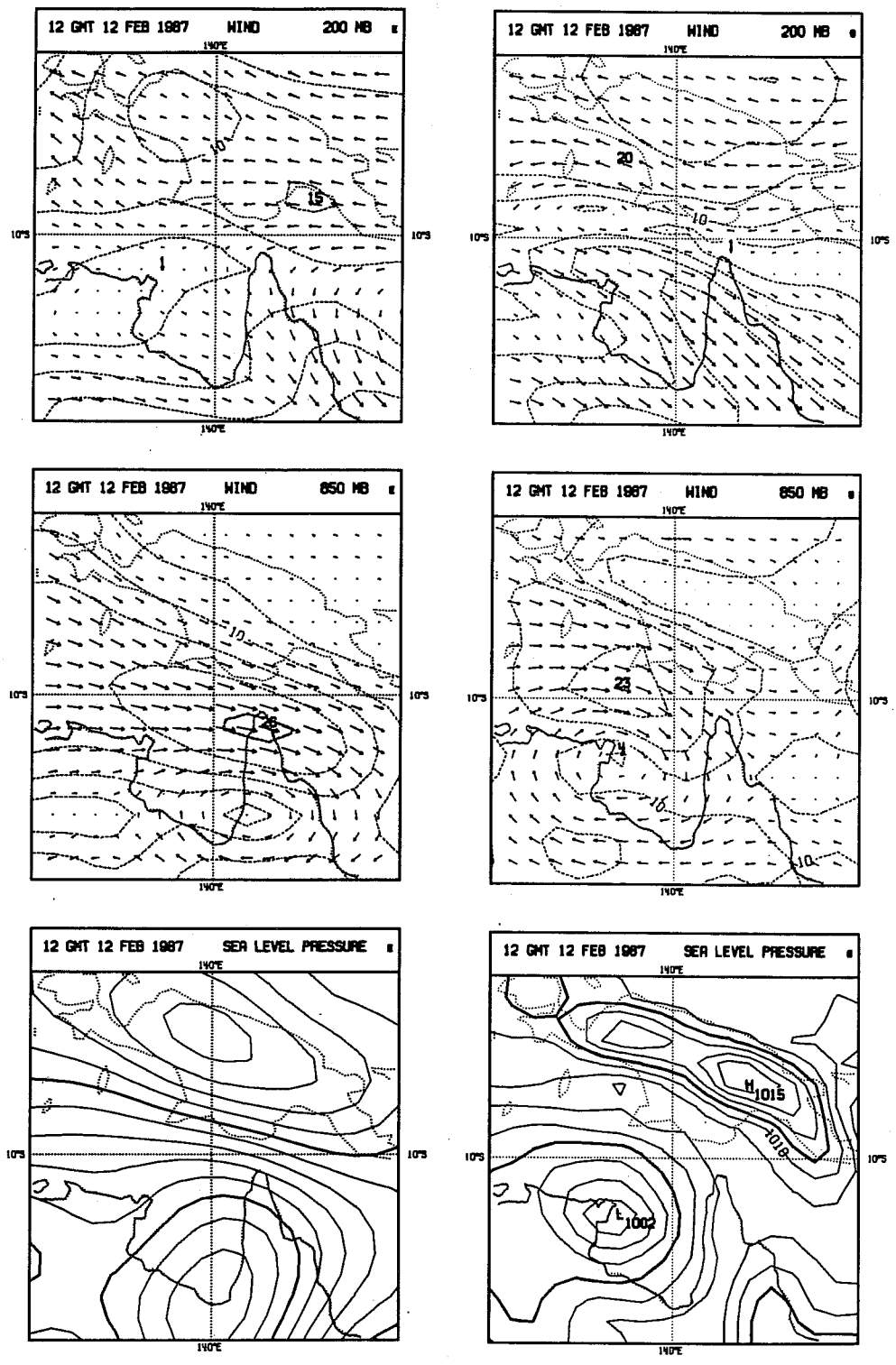

Fig. 10f As in Fig. 10e but for two day forecasts.

consistency and have a somewhat noisy vertical velocity. An example of this feature which was noted earlier for TC Irma (Fig. 6) is shown for the one day forecasts for TC's Connie and Jason in Figs. 11(a) and (b). These features are also indicated in the cross-sections for day 1 forecasts at latitudes close to the position of the TC's shown in Figs. 12(a) to (d). Note the stronger vorticity and divergent fields in the vicinity of the cyclone in the ADJ forecasts.

The results presented above, show that the forecasts for tropical cyclones show considerable sensitivity to the parametrization of cumulus convection. This was also evident in a limited number of forecasts run from the operational (KUO) analyses but using the recently developed mass flux cumulus parametrization scheme (Tiedtke, 1989). Two day forecasts for TC's Connie, Irma and Jason are shown in Figs. 13(a) to (c). Comparing with the KUO forecasts in Fig. 10 clearly confirms the sensitivity to cumulus parametrization; the mass flux forecasts produce somewhat more intense cyclonic systems and also show the marked consistency in the vertical between the velocity potential and vertical velocity which is also present in the ADJ forecasts. It should be noted that the forecasts with the mass flux scheme are shown mainly to indicate sensitivity of TC forecasts to cumulus convection and should not be interpreted in terms of the performance of this scheme. Such an assessment can only be made by starting from initial analyses which have been obtained through data assimilation using the mass flux scheme. Such a comparison is beyond the scope of this paper.

As was indicated earlier, the model resolution used in all the results presented above is not sufficient to resolve the details of tropical cyclones. A limited study to assess the impact of increased resolution was conducted by carrying out two forecasts using the ECMWF model truncated and triangular wave number 159 (T159). The first integration started from the operational analysis (KUO) of 1200 GMT Jan 18 and used the KUO parametrization during the forecast. The second integration was from the ADJ analysis of 1200 GMT Feb 10 and used the Betts-Miller parametrization during the forecast. The one and two day forecasts are shown in Figs. 14 and 15. The forecasts from Jan 18 for TC's Connie and Irma shows little sensitivity to increased resolution except for slight intensification in the cyclones. Part of the reason for this lack of sensitivity could be the systematic inability of the KUO scheme as used at ECMWF to intensify existing cyclonic systems in the tropics. The forecast from Feb 10 which used the Betts-Miller parametrization shows significant sensitivity. The T159 forecast intensifies the cyclone relative to the T106 forecast (see Fig. 10) and maintains a much better definition of the cyclonic circulation. Given that the initial condition of the forecast had a relatively large position error, the T159 forecast track is impressive with the position errors being mostly explained by the initial error. The T159 forecast also has considerably more detail. This is particularly the case for the upper level wind field

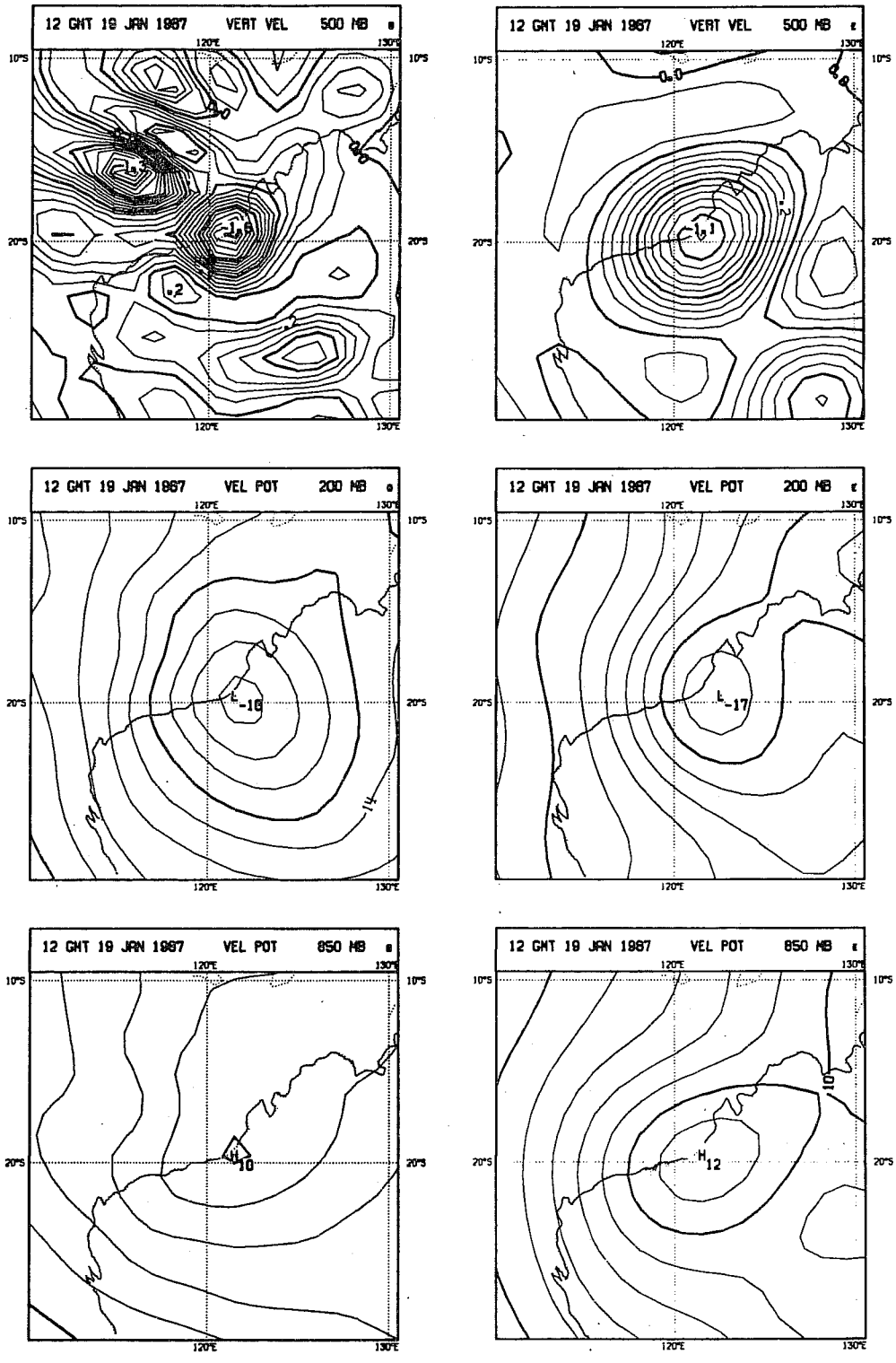

Fig. 11a One day KUO (left panels) and ADJ (right panels) forecasts starting from 1200 GMT Jan 18 for 850 hPa velocity potential (bottom), 200 hPa velocity potential (middle) and 500 hPa vertical velocity (top). Units and contour intervals are as in Fig. 6.

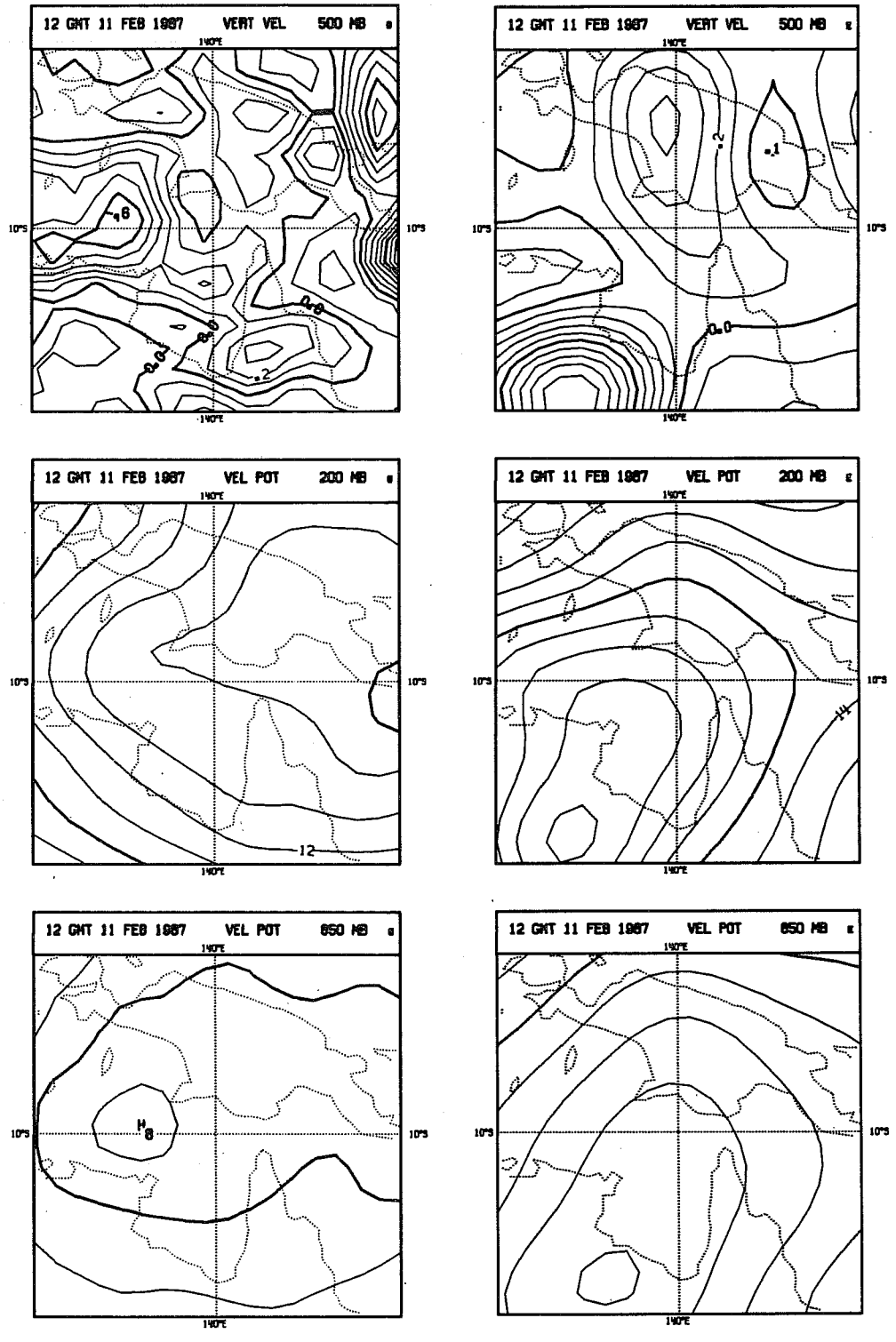

Fig. 11b As in Fig. 11a but for forecasts starting from 1200 GMT Feb 10.

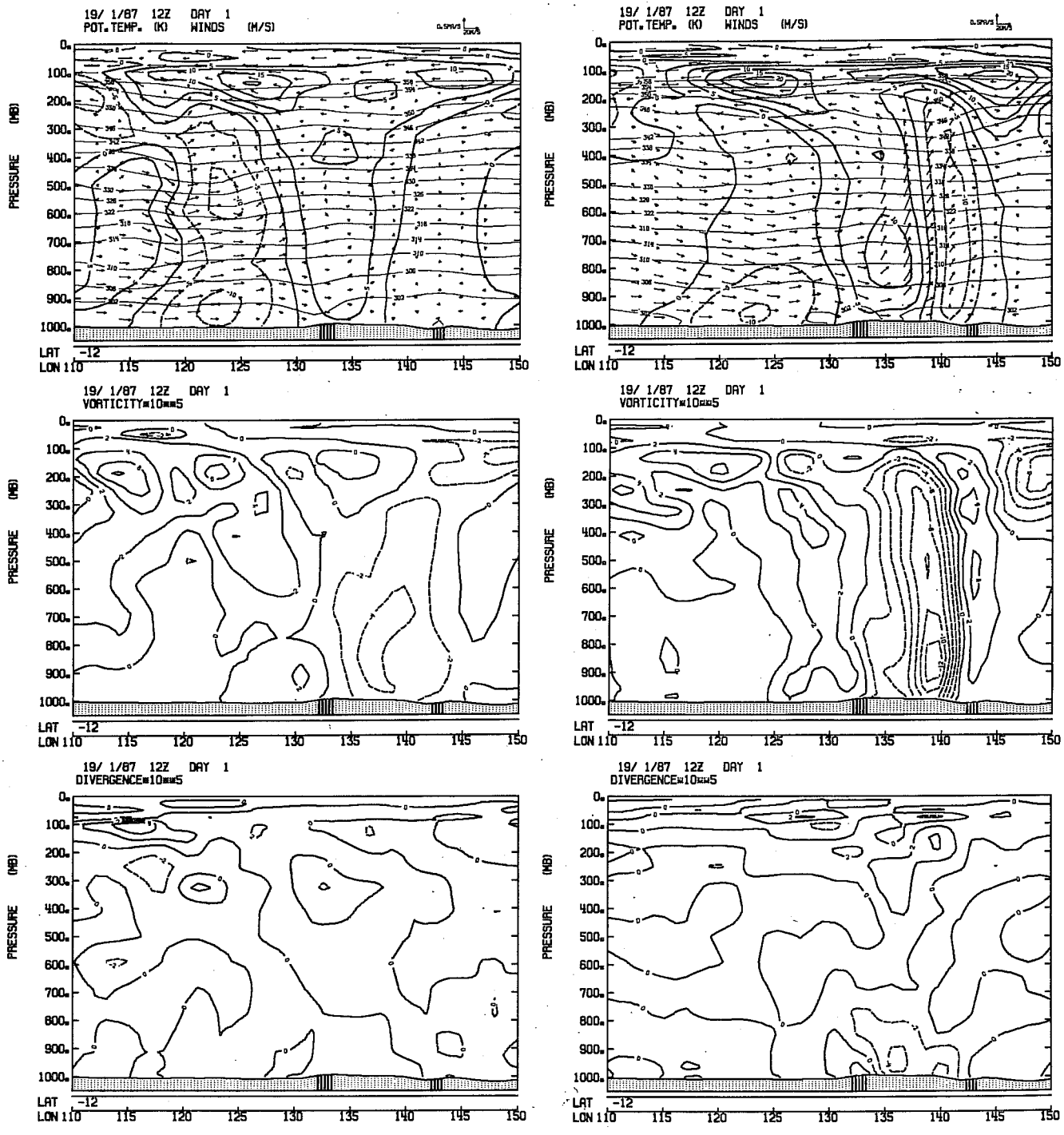

Fig. 12a As in Fig. 4a but for vertical sections at 12°S for one day forecasts from 1200 GMT Jan 18.

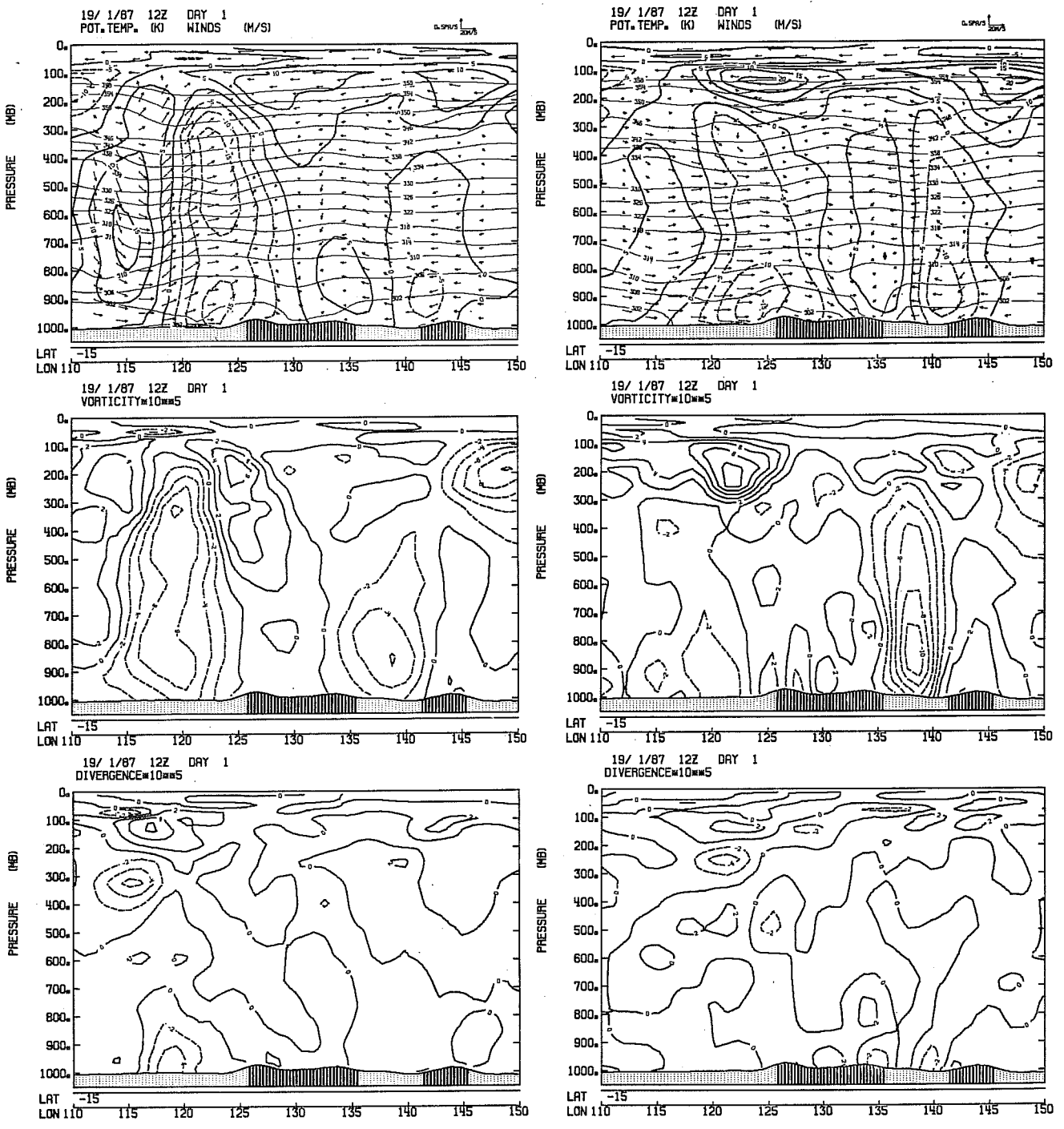

Fig. 12b As in Fig. 12a but at 15°S.

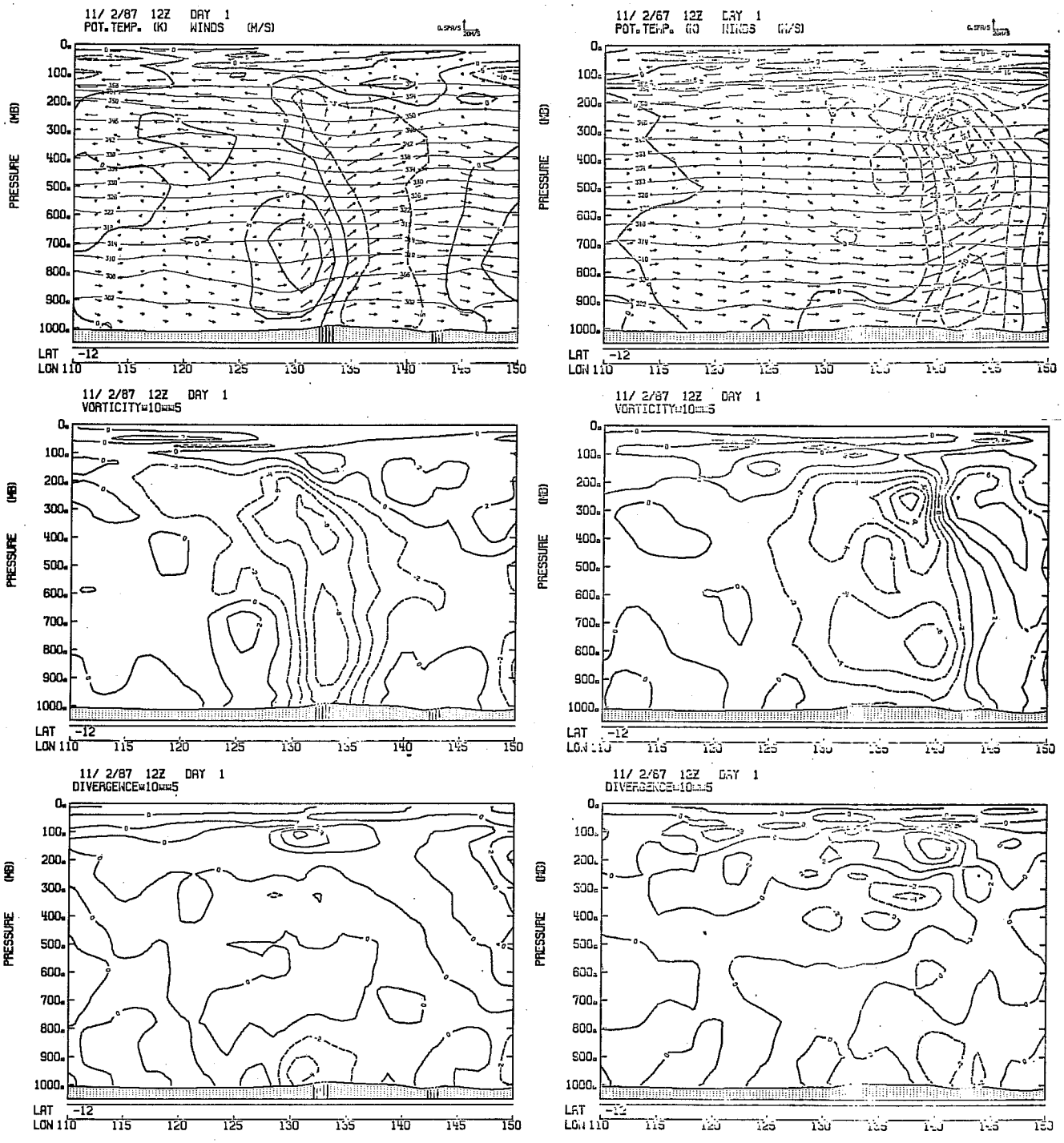

Fig. 12c As in Fig. 12a but for one day forecasts from 1200 GMT Feb 10.

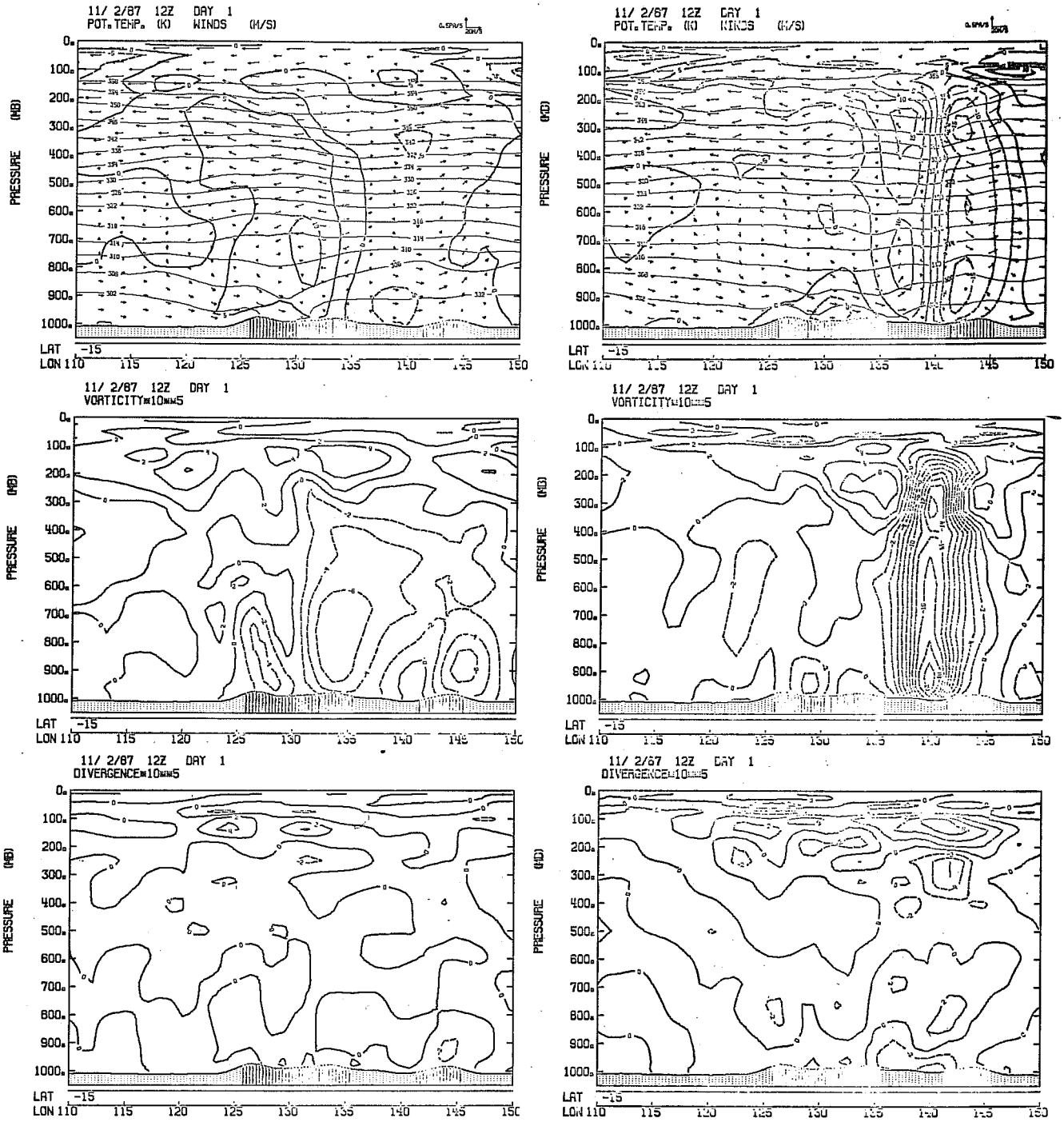

Fig. 12d As in Fig. 12c but at 15°S.

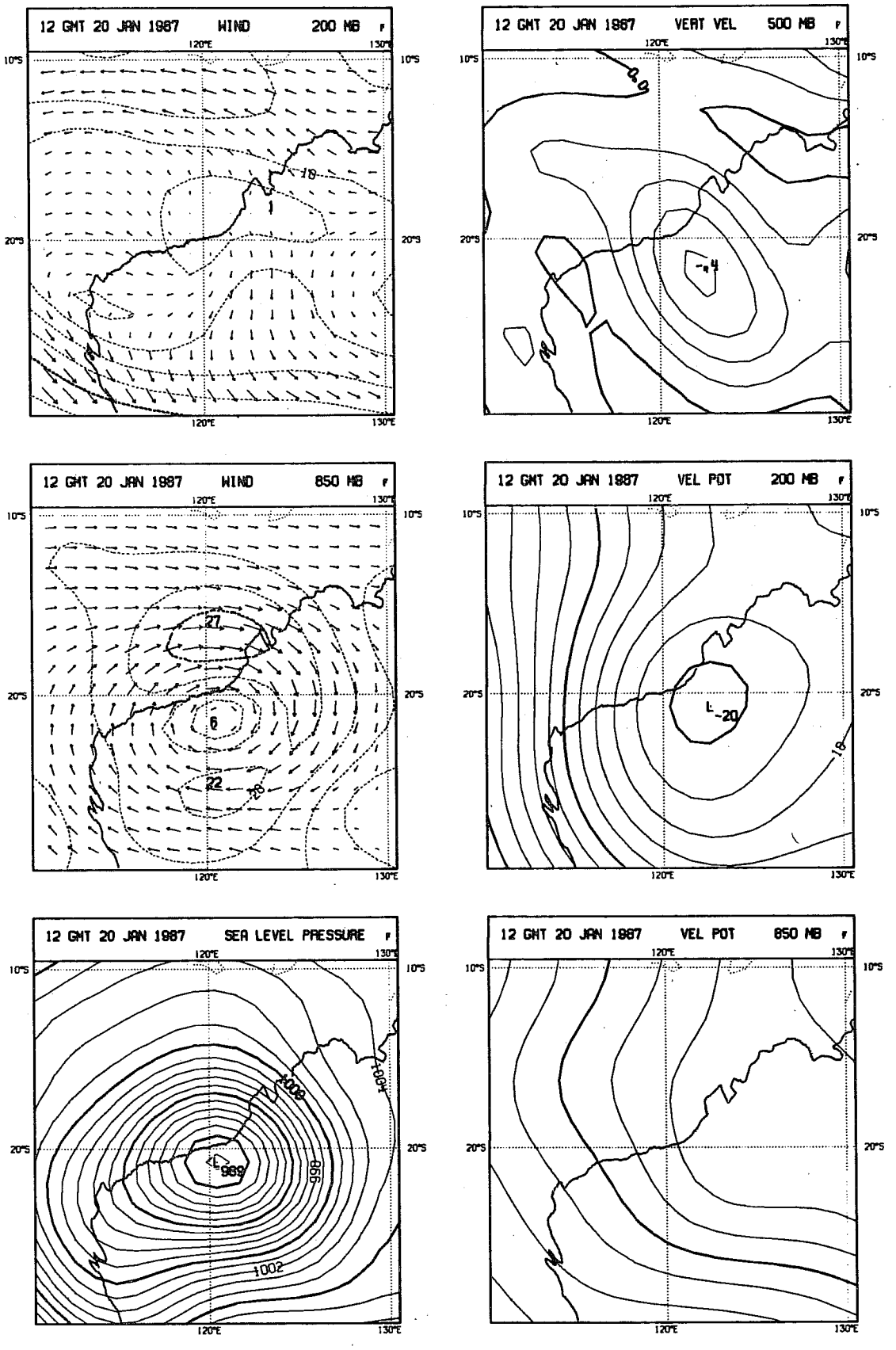

Fig. 13a As in Fig. 6a but for two day forecasts for TC Connie using the mass flux convective parametrization starting from KUO analysis of 1200 GMT Jan 18.

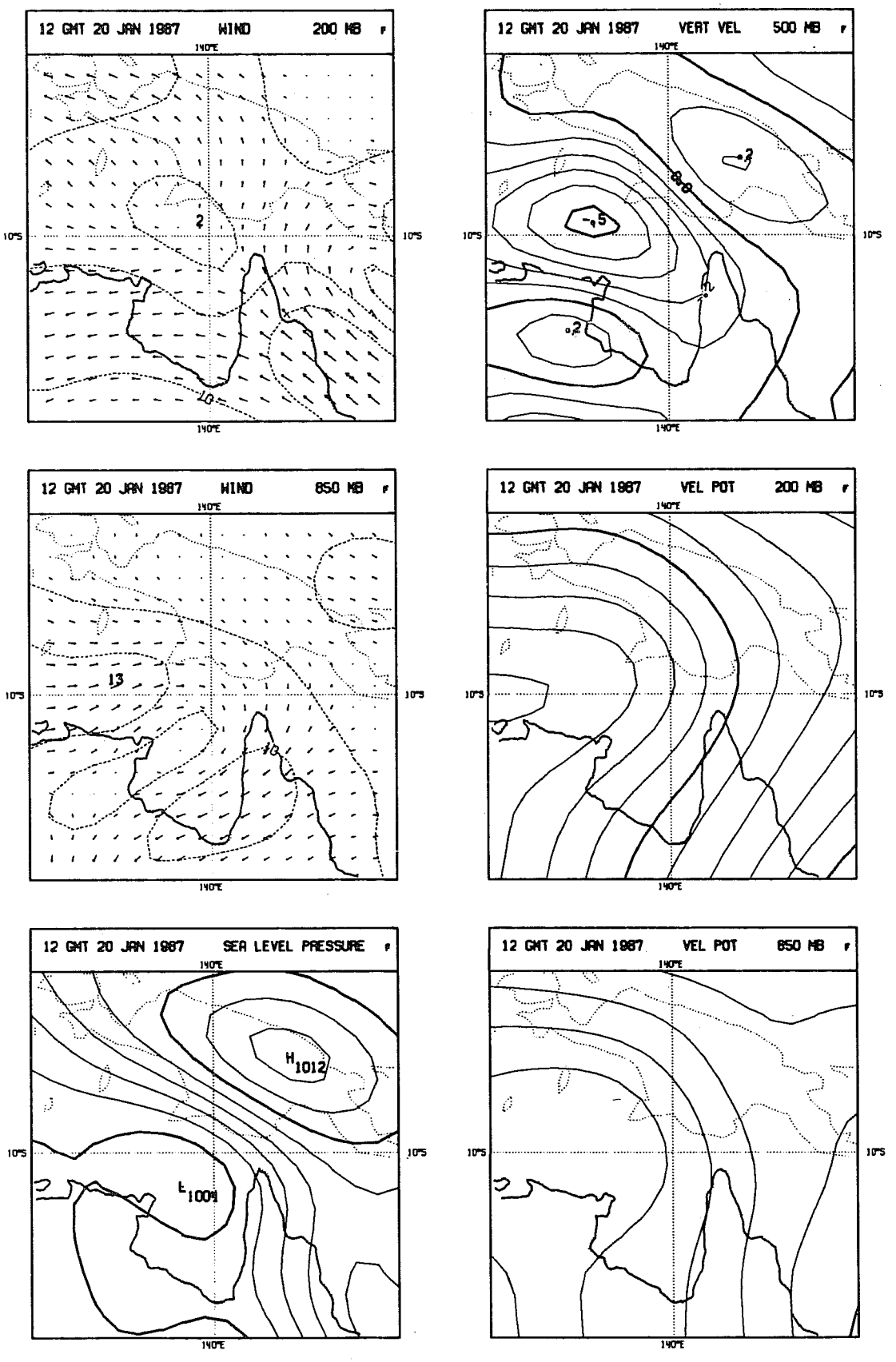

Fig. 13b As in Fig. 13a but for TC Irma.

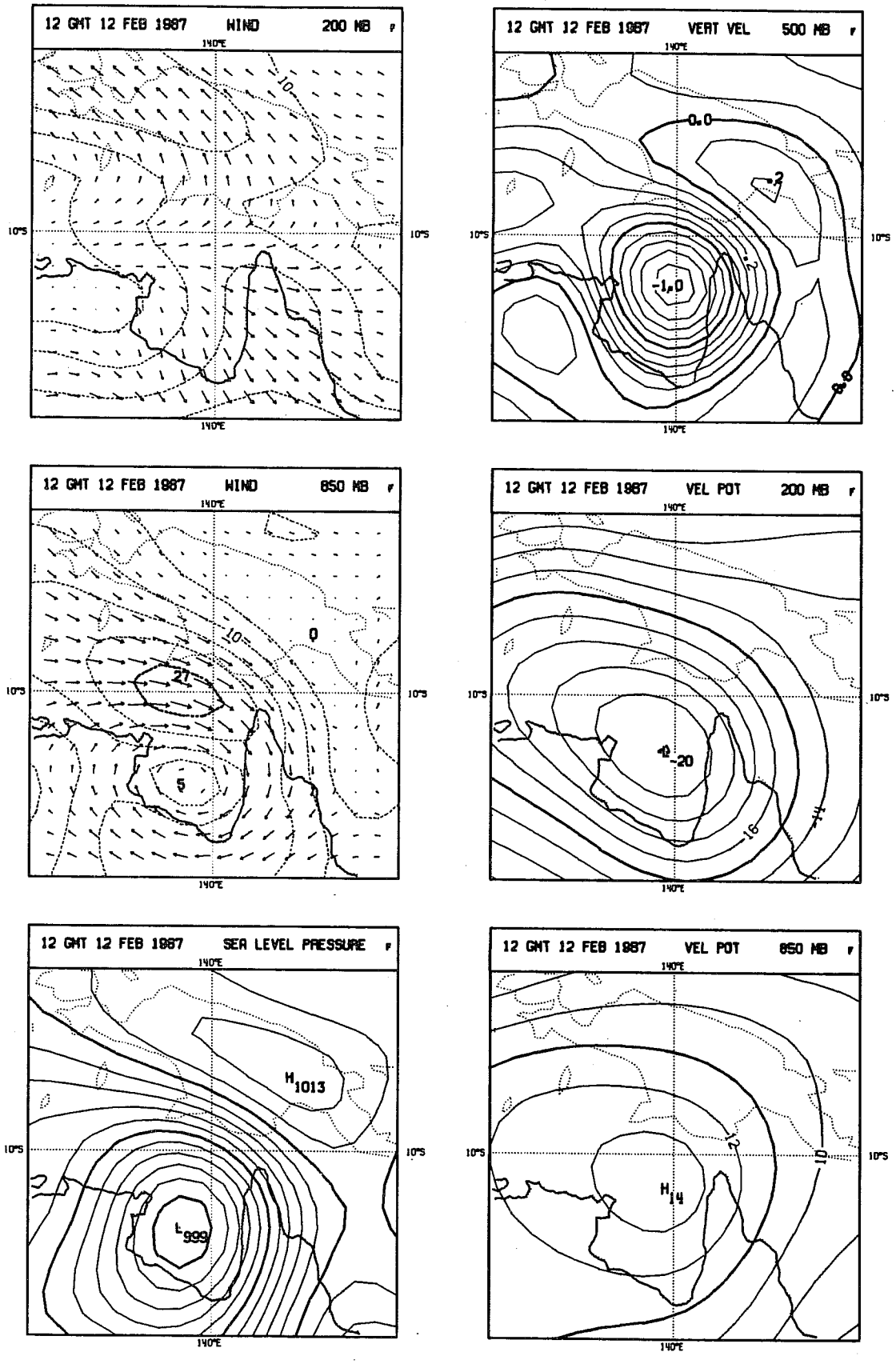

Fig. 13c As in Fig. 13a but for two day forecast for TC Jason starting from 1200 GMT Feb 10.

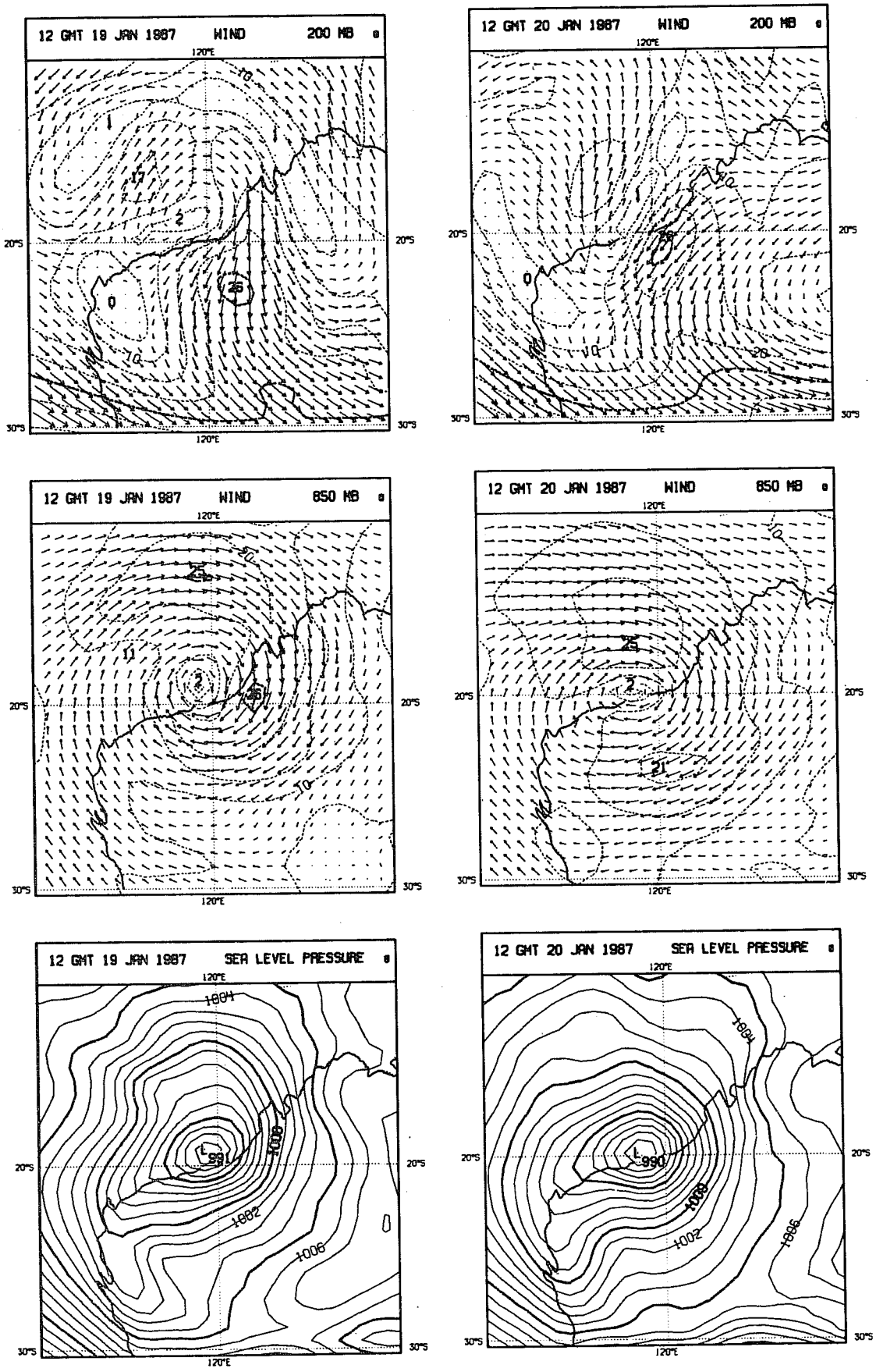

Fig. 14a One day (left panels) and two day (right panels) T159 forecasts for TC Connie starting from KUO analysis of 1200 GMT Jan 18 for MSLP (bottom), 850 hPa vector wind (middle) and 200 hPa vector wind (top). Units and contour intervals are as in Fig. 6.

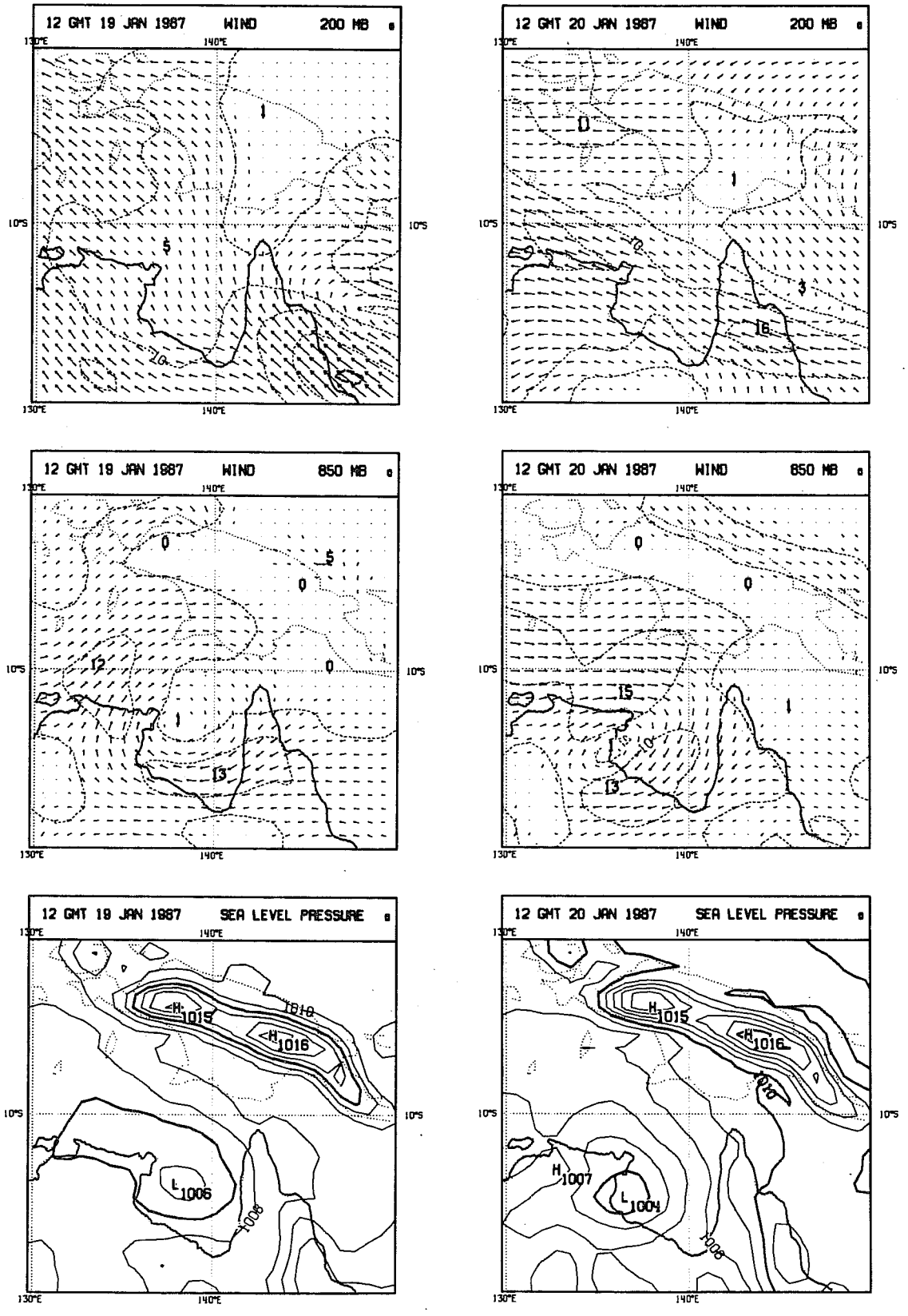

Fig. 14b As in Fig. 14a for TC Irma.

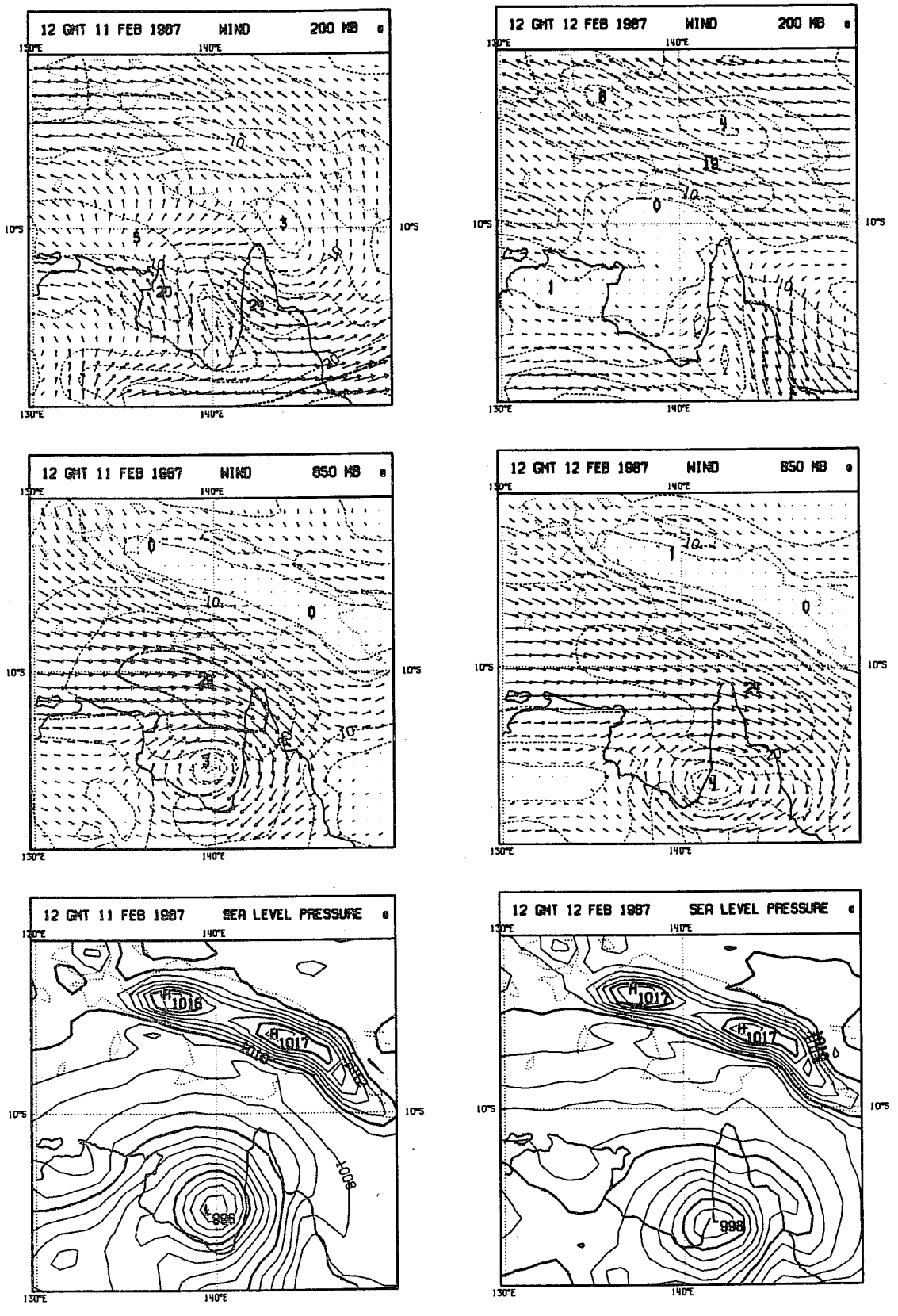

Fig. 15 As in Fig. 14 but for T159 forecasts for TC Jason from ADJ analysis of 1200 GMT Feb 10.

where, for example, there is a pronounced upper level trough at day 1 in the region of the cyclone which is not so evident in the lower resolution forecast. Such upper level troughs are considered to have a significant impact on the future development and motion of tropical cyclones (Holland, private communication). The greater amount of detail is also evident in the one day vorticity forecasts shown in Fig. 16(a) to (c) and precipitation forecasts shown in Figs. 17(a) and (b). Verification of precipitation forecasts is difficult because of lack of data. The GMS pictures for 1200 GMT Jan 19 and 1200 GMT Feb 11 are presented in Figs. 18(a) and (b) to indicate qualitatively regions of cloudiness during the forecast periods considered above. Both the T106 and T159 forecasts have most of the feature present in the GMS pictures and the ADJ forecasts appear to produce larger amount of precipitation compared to the KUO forecasts.

The limited case studies presented here indicate sensitivity of model forecasts to increased model resolution. However much more work needs to be carried out before any firm conclusions can be made. More case studies are clearly needed, possibly with analyses also generated using the high resolution model. Such work could probably be carried out with a limited area model although the role of large scale flow which is better handled by global models will need to be clarified.

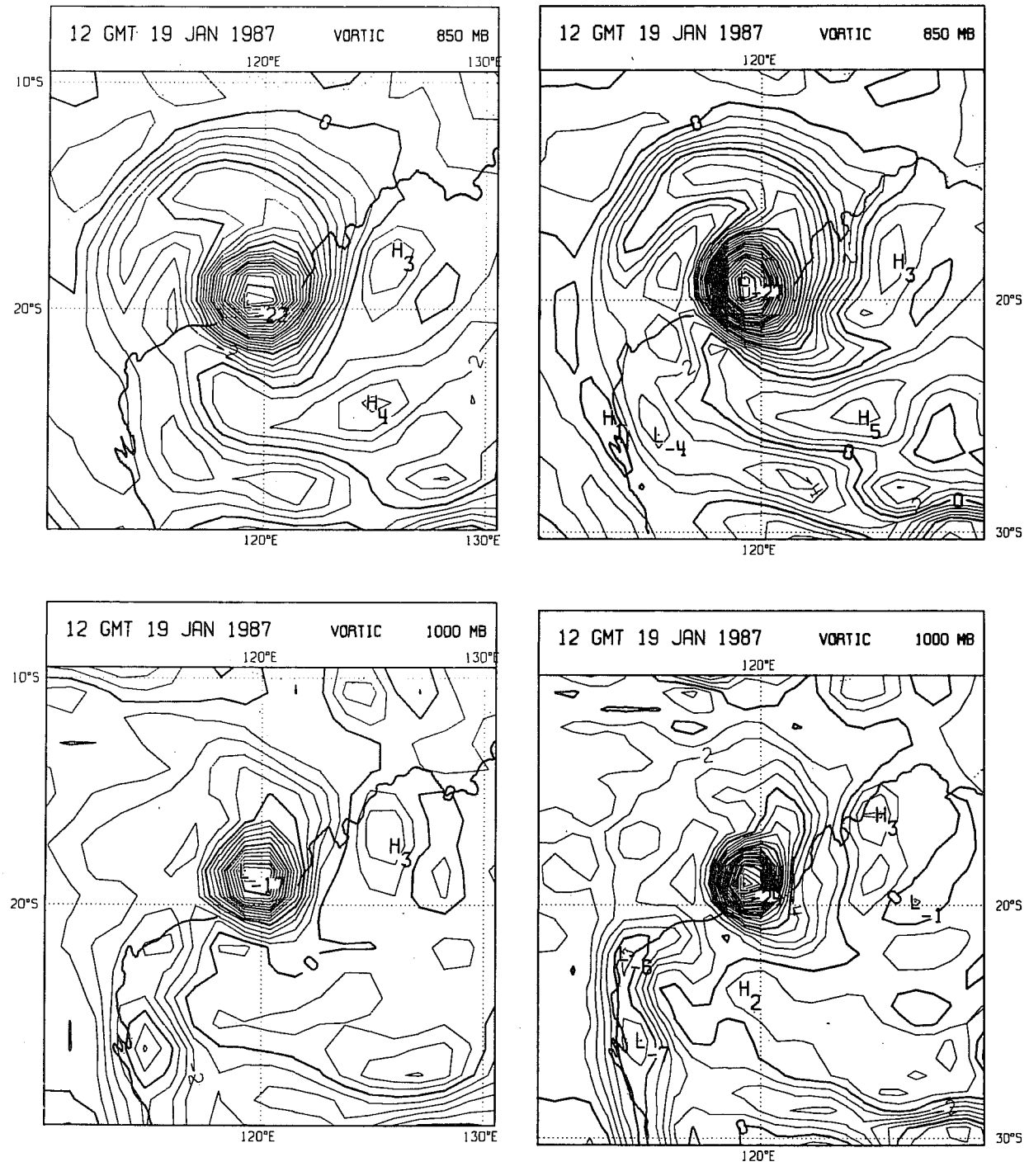

Fig. 16a One day T106 (left panels) and T159 (right panels) forecasts for TC Connie starting from KUO analysis of 1200 GMT Jan 18 for 850 hPa (top) and 1000 hPa (bottom) vorticity. Contour intervals are 1 unit.

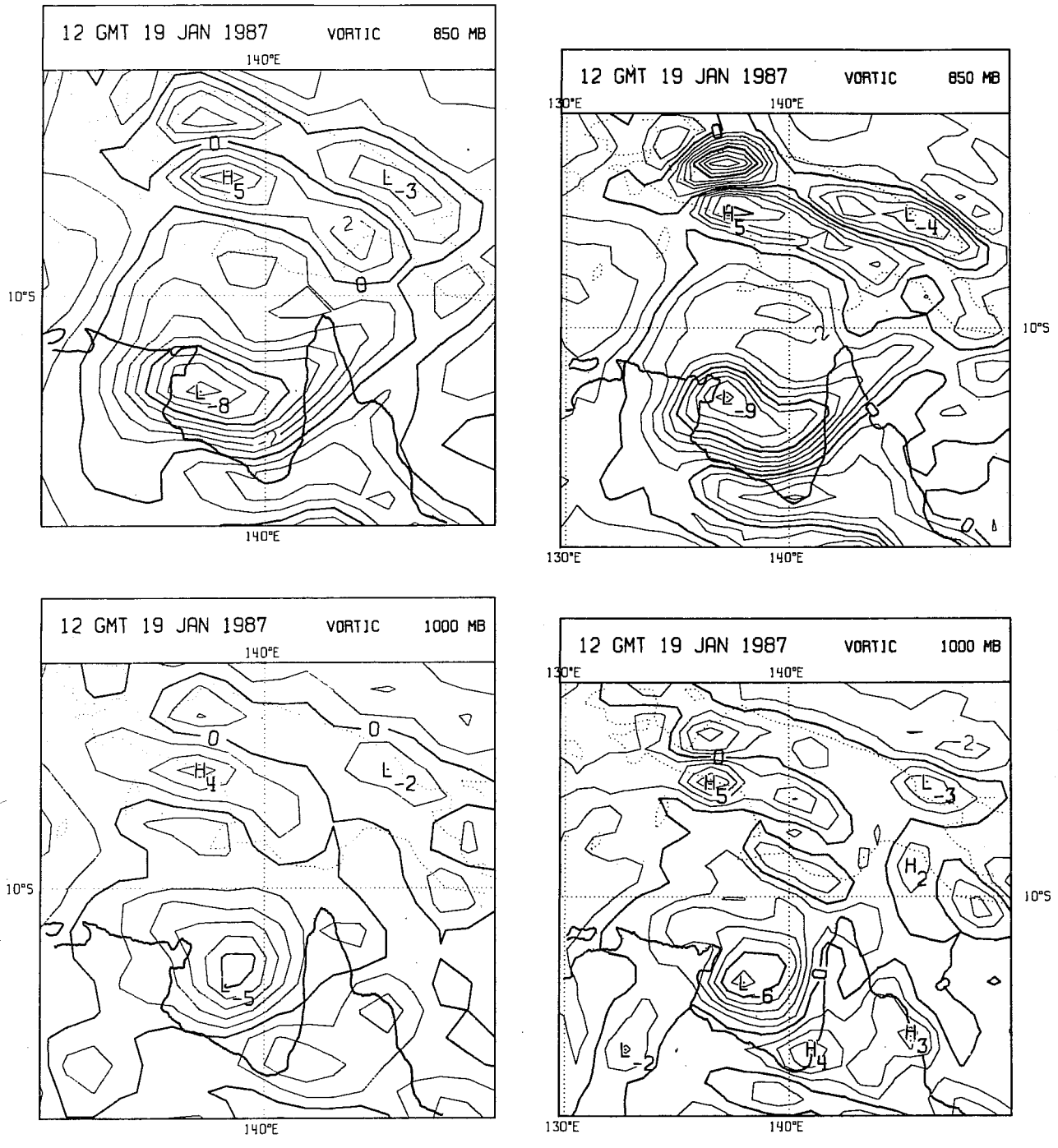

Fig. 16b As in Fig. 16a but for TC Irma.

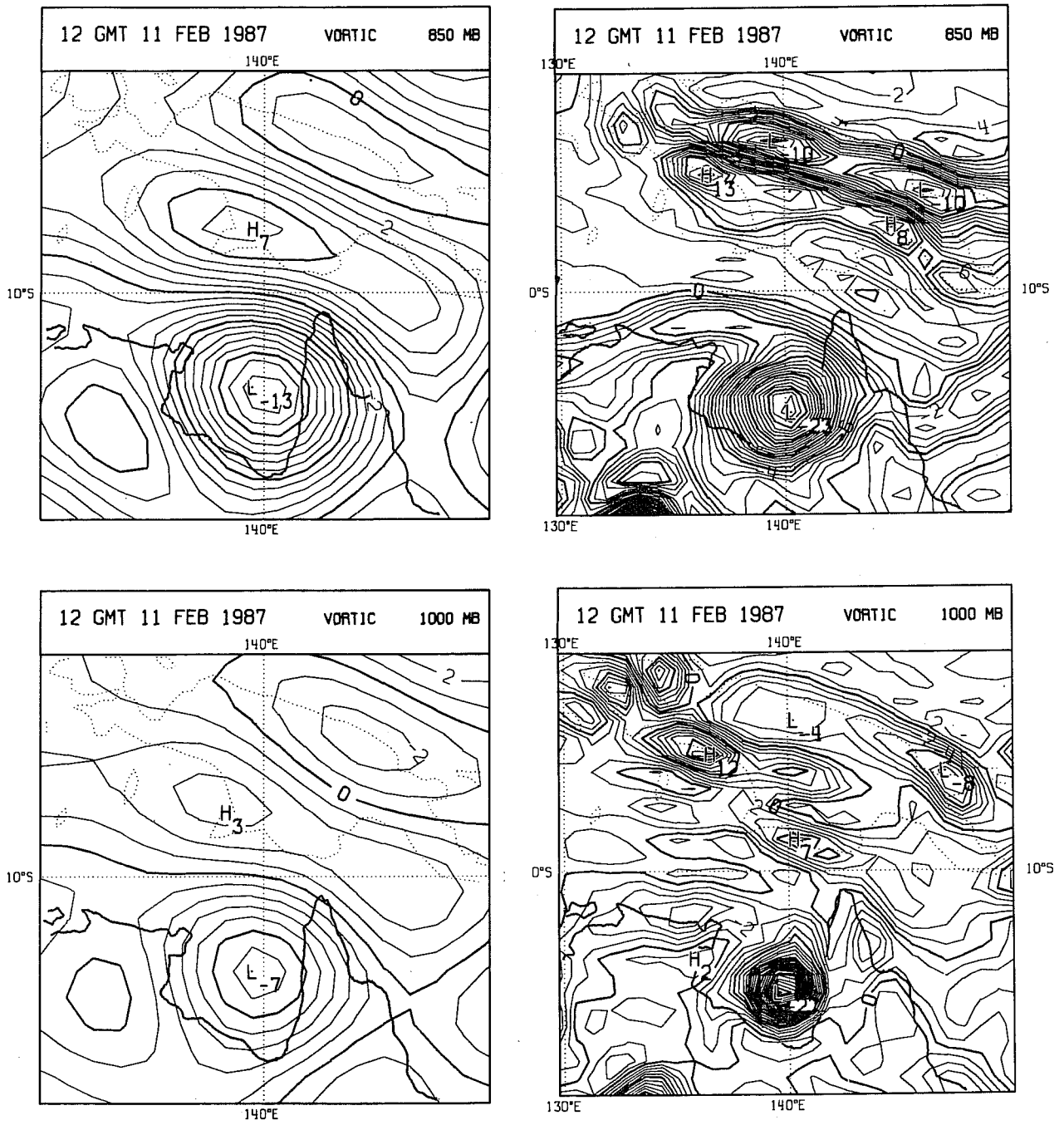

Fig. 16c As in Fig. 16a but for forecasts for TC Jason from ADJ analysis of 1200 GMT Feb 10.

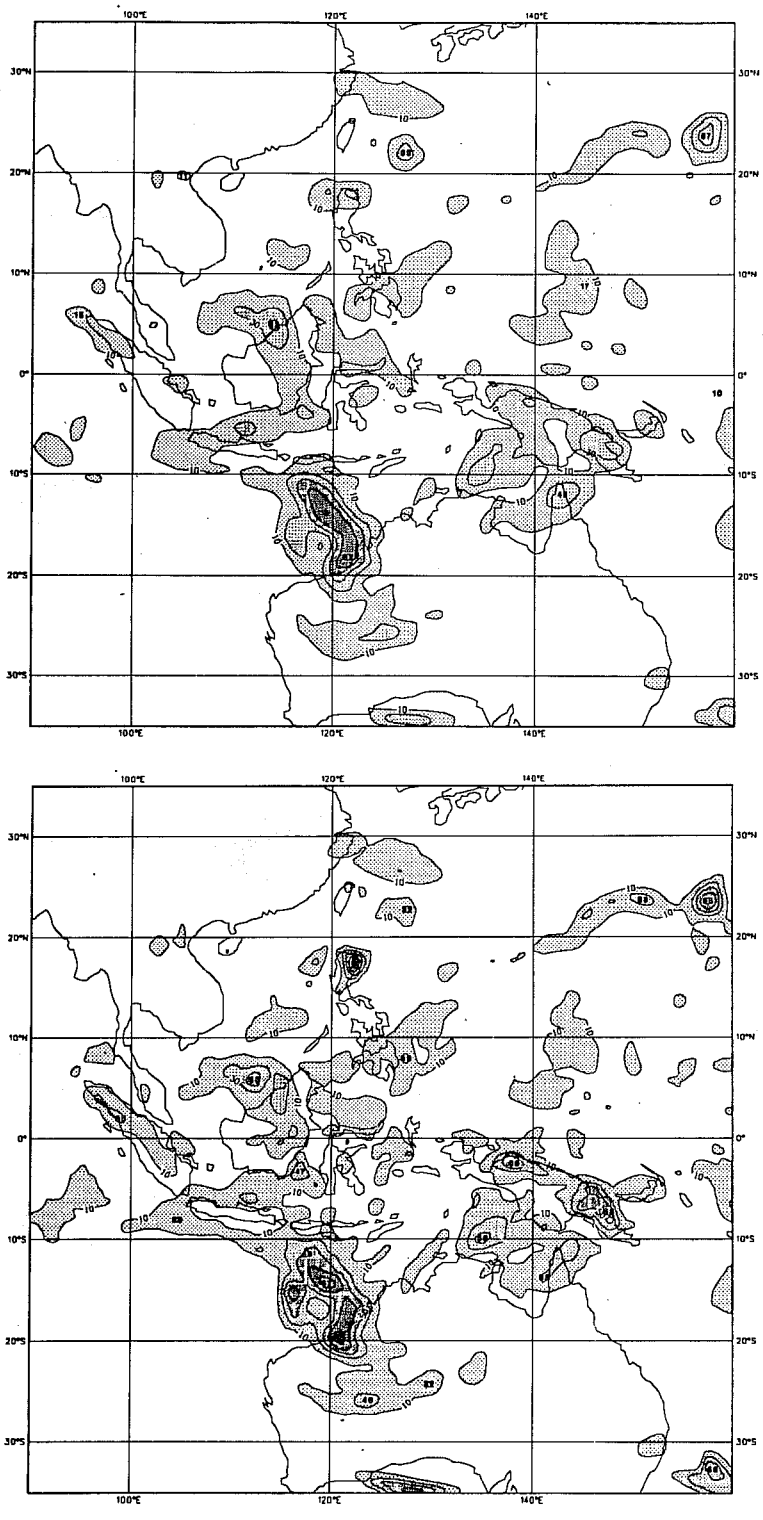

Fig. 17a One day T106 (top) and T159 (bottom) precipitation forecasts starting from KUO analysis of 1200 GMT Jan 18. Units are mm day^{-1} and contours plotted are 10, 30, 50, 70 and 100. Increasing shading levels denote increased precipitation.

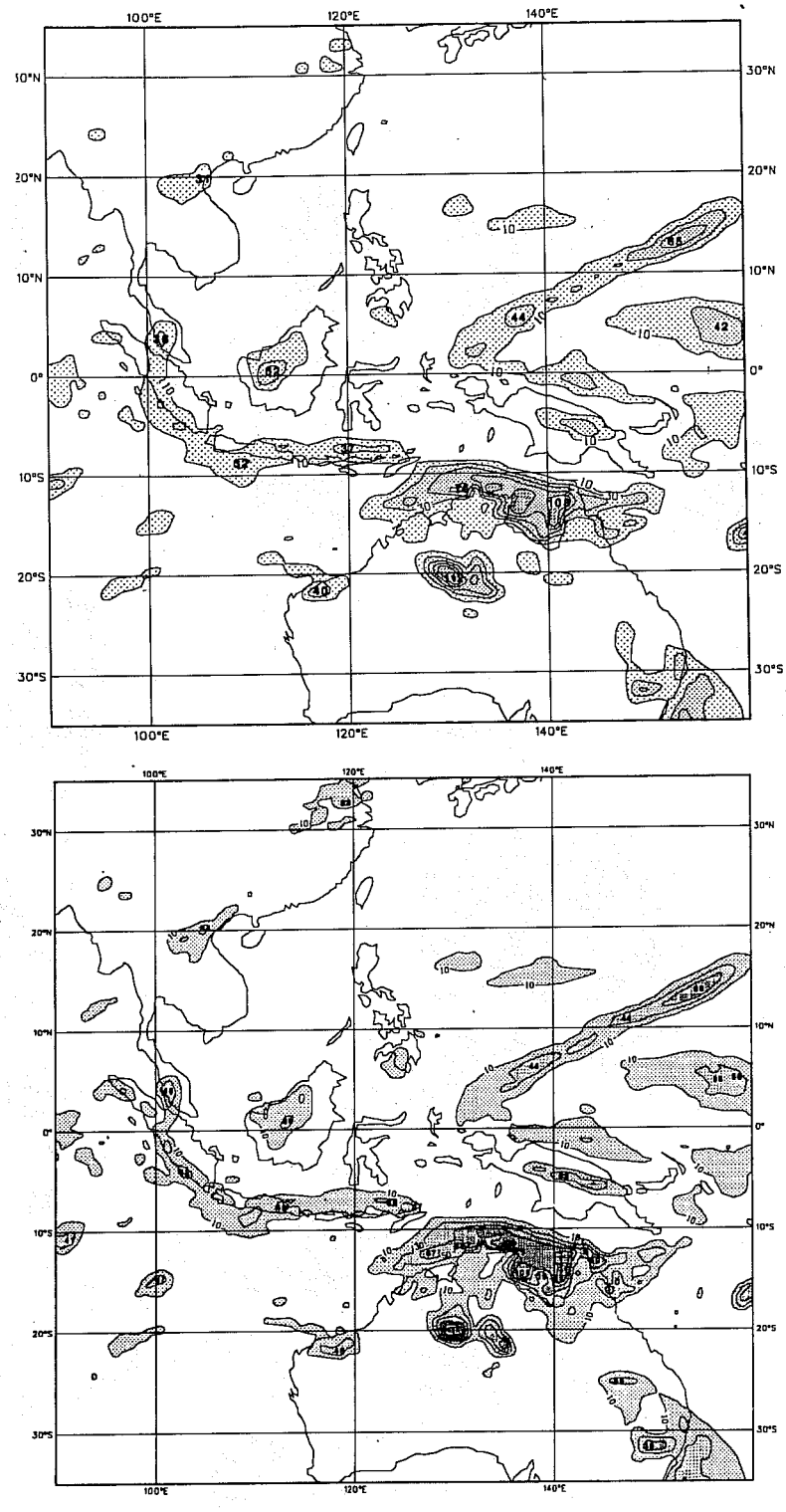

Fig. 17b As in Fig. 17a but for forecasts starting from ADJ analysis of 1200 GMT Feb 10.

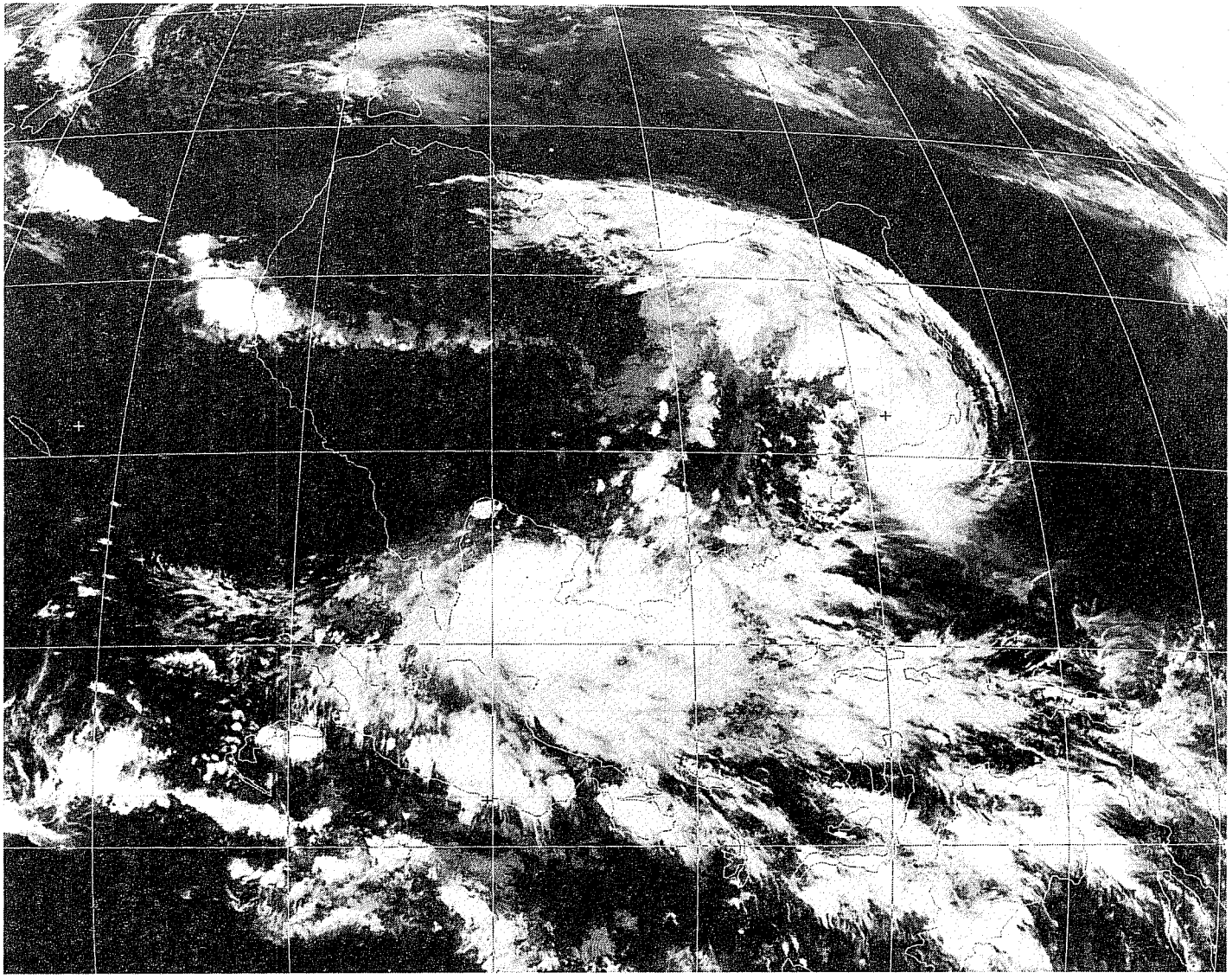

Fig. 18a Infra-red imagery from GMS satellite for 1200 GMT Jan 19.

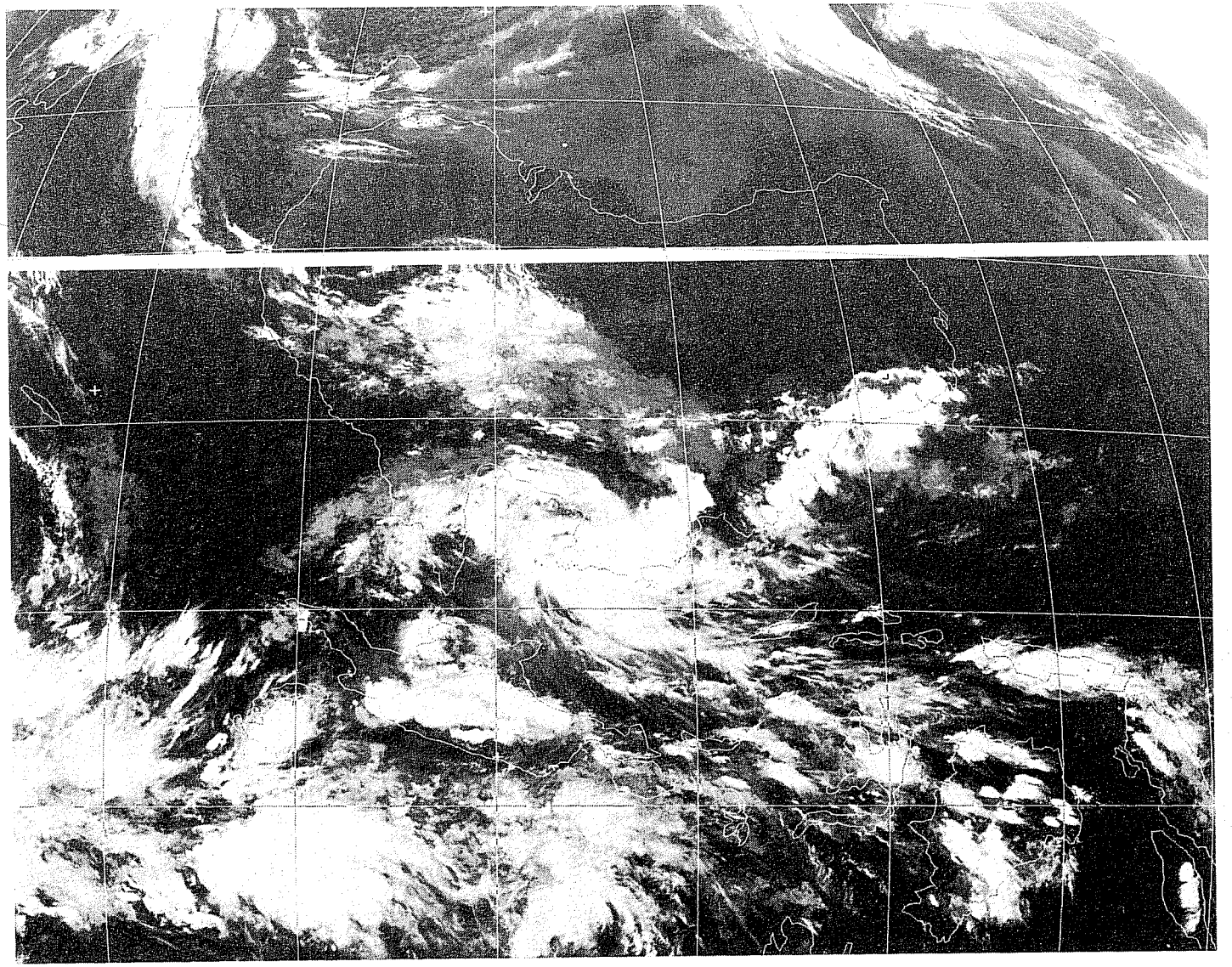

Fig. 18b As in Fig. 18a but for 1200 GMT Feb 11.

4. DISCUSSION

A major feature which emerges from this study is the marked sensitivity of both analyses and forecasts of tropical cyclones to cumulus convection parametrization. The Betts-Miller scheme leads to significantly stronger and better defined cyclonic circulations which have better vertical consistency than the operational analyses and forecasts based on KUO convective parametrization. The reason for these differences is not clear and needs further study. An obvious conclusion could be that the Betts-Miller scheme works well for tropical cyclones and points for future directions for cumulus parametrization research. However, there is another possible interpretation for the more intense analyses of tropical cyclones and short term forecasts. A feature of the Betts-Miller scheme as used at ECMWF is that it has a systematic spin-up signature where there is excessive precipitation in the first few hours of model integration. This should generate strong lower tropospheric convergence and hence given intensification of a pre-existing vortex. The Kuo scheme as used at ECMWF also has a typical spin-up signature which is rather different from the Betts-Miller scheme. In the Kuo scheme, there is an excess of precipitation over evaporation for the first 2-3 days although the precipitation does not reach its maximum till 1-2 days of integration. Thus for the six-hour analysis-forecast cycle and short range forecasts the Kuo scheme does not trigger sufficiently to impact significantly on any pre-existing vortex. This would also lead to the lack of vertical consistency noted for the Kuo based analyses and forecasts. It should however be noted that in addition to cumulus parametrization, the spin-up in numerical weather prediction models is a function of a number of factors such as the level of dynamic and thermodynamic consistency between variables such as divergence, temperature and moisture retained by the analysis scheme. These factors need to be considered in order to resolve the two different viewpoints mentioned above.

It should be emphasized that there are a large number of variations in the Kuo parametrizations as used at various institutes and the results presented here only apply to the Kuo scheme as used at ECMWF. The performance of the scheme is sensitive to a number of factors such as the moistening parameter B and the definition of the cloud base, for example. This sensitivity and its impact on the precipitation of the 1979 summer monsoon onset by the ECMWF model has been documented by Slingo et al. (1988). Akyildiz (Private communication) performed a limited study on the simulation of tropical cyclones in the ECMWF operational model during September to November 1986 (most of the physical parametrizations used were similar to the ones used in the current study, the main difference being that gravity wave drag was not included). He concluded that the model developed fewer and weaker tropical cyclones than the previous operational models (T63 spectral and the N48 grid point model) although the higher resolution T106 model would be expected to give a better representation of the storms. It was therefore suspected that the modifications in physical parametrizations made in 1985 inhibit the development of these intense tropical features. The features of the current study are therefore consistent with the earlier study.

5. CONCLUSION

In Part II the sensitivity of analyses and forecasts of tropical cyclones to cumulus parametrization and model resolution (forecasts only) was studied. Two parametrization schemes were compared, namely the operational Kuo scheme and the Betts-Miller adjustment scheme although a limited number of forecasts with the mass flux scheme of Tiedtke (1989) were also considered. The sensitivity of forecasts to model resolution was evaluated by comparing forecasts using T106 and T159 versions of the model.

Both analyses and forecasts of tropical cyclones considered here show considerable sensitivity to cumulus parametrization. The ADJ analyses and forecasts generated more intense cyclonic systems as indicated by maps of sea level pressure, low level winds and vorticities and cross-sections in the neighbourhood of the cyclones which are in closer agreement with the BOM estimates although, apart from TC Connie, analyses from both schemes are consistent with the observed data. For TC Connie there was an observations close to the centre of the cyclone which supported the BOM estimate. It should be noted, however, that both analyses rejected this observation. The cyclone location errors for both analyses systems are similar ranging from 1° to 2° and are larger for forecasts which show considerable variability with respect to initial conditions. The forecast position error strongly reflect errors in the initial conditions although this is not the sole cause of the forecast errors. Of the two cases considered here, the forecast for TC's Connie and Irma did not show much sensitivity to increased model resolution. TC Jason however showed significant sensitivity with the T159 model forecast showing considerable improvement; the main error of location in this forecast mainly reflected errors in the initial conditions.

Major problems however still remain which will need to be addressed before global systems such as the ECMWF analysis-forecast systems can provide satisfactory analyses and forecasts for tropical cyclones. The main problem lies in improving the location of the cyclones by the analysis system. A major contributing factor to this problem is the lack of adequate data in the region of the cyclone. One way of reducing this problem is to generate bogus data based on satellite imagery, for example, and information about wind profiles in tropical cyclones obtained from observational studies. Such procedures are already in use at operational centres such as the UKMO and Japan Meteorological Agency and have been studied for the ECMWF system by Andersson and Hollingsworth (1988). However even when data is available there is the problem of rejection of useful data in the vicinity of the cyclone by the analysis scheme. Examples of this rejection were given for TC's Connie and Jason which contribute to position errors. This rejection of data occurs because of errors in the first guess, the structure functions used in the analysis scheme not having sufficient resolution and the use of inappropriate parameters such as forecast error variances and quality control limits for tropical cyclones. The latter factors are considered

in Part III of this report. The first guess errors and the forecast errors are caused by analysis errors, inadequate parametrization of physical processes and insufficient model resolution. Some of these factors have been considered in this part of the paper which point to the need to improve the parametrization of cumulus convection and to increased model resolution. The rapid progress in computer engineering should allow considerable increases in model resolution while parametrization studies could benefit from more observational data such as collected during GATE and AMEX and through intercomparison studies with different parametrization schemes and models.

References

Anderson, E. and A. Hollingsworth, 1988: Typhoon bogus observations in the ECMWF data assimilation system. ECMWF Technical Memo. No. 148, ECMWF, Reading, UK, 25 pp.

Betts, A.K., 1986: A new convective adjustment scheme. Part I: Observational and theoretical basis. Quart.J.Roy.Meteor.Soc., 1123, 677-691.

Betts, A.K. and M.J. Miller, 1986: A new convective adjustment scheme. Part II: single column tests using GATE Wave, BOMEX, ATEX and arctic air-mass data sets. Quart.J.Roy.Meteor.Soc. 112, 693-709.

Manabe, S., J.S. Smagorinsky and R.F. Strickler, 1965: Simulated climatology of a general circulation model with a hydrologic cycle. Mon.Wea.Rev., 93, 769-798.

McBride, J.L., 1981: Observational analysis of tropical cyclone formation. Part I: Basic description of data sets. J.Atmos.Sci., 38, 1117-1131.

Puri, K. and D.J. Gauntlett, 1988: Numerical weather prediction in the tropics. J.Meteoro.Soc. Japan, Special Volume, Ed. T. Matsuno, 605-631.

Slingo, J.M., U.C. Mohanty, M. Tiedtke and R.P. Pearce, 1988: Prediction of the 1979 summer monsoon onset with modified parametrization schemes. Mon.Wea.Rev., 116, 328-346.

Tiedtke, M., 1989: A comprehensive massflux scheme for cumulus parametrization in large-scale models. Mon.Wea.Rev., 117, 1777-1798.

PART III: USE OF HIGH RESOLUTION STRUCTURE FUNCTIONS AND MODIFIED QUALITY CONTROL IN THE ANALYSIS OF TROPICAL CYCLONES

Kamal Puri and P. Lönnberg

1. INTRODUCTION

In Parts I and II of this report it was shown that the ECMWF analysis system has considerable problems in locating the position of tropical cyclones because of the rejection of reliable data. This rejection of data occurred because of errors in the first guess used by the analysis and partly because the structure functions used in the analysis did not have sufficient resolution to resolve small scale features such as tropical cyclones. The rejection of data is based on the notion that large observation-background departures are caused by gross observation errors. The rejection limits are tuned statistically to reflect average conditions and, consequently, certain atmospheric events which are poorly captured by the background field, can cause rejection of good data.

The errors in the first guess could have been caused by a number of factors, the main ones being deficiencies in the parametrization of cumulus convection and insufficient model resolution. These factors were considered in Part II. The aim of Part III is to firstly assess the impact of high resolution structure functions in the analysis of a tropical cyclone. A second aim is to assess the impact of forcing the analysis to accept data in a limited domain around the tropical cyclone. An obvious application of this would be the inclusion of bogus data for tropical cyclones in current data assimilation systems (see Andersson and Hollingsworth, 1988).

A description of some features of the high resolution structure functions together with the forcing of data is given in section 2 followed by results of various experiments in section 3 and a discussion in section 4.

2. BRIEF DESCRIPTION OF AN EXPERIMENTAL HIGH RESOLUTION ANALYSIS (HRA)

Only a brief description of the HRA scheme, which became operational in July 1988, will be given here. The interested reader is referred to Lönnberg (1988) for details. The effective analysis resolution has been enhanced by changing the response properties of the optimum interpolation (OI) scheme. Several modifications to the operational analysis have been made (Lönnberg, 1988), but only those which are of interest to the tropical analysis are discussed in the following.

The horizontal forecast error correlations are modelled by a series of Bessel functions:

$$\sum_{n=0}^{N} A_n J_0 (k_n r/D) \qquad (1)$$

where subscript n is the radial mode, A_n the amplitude of mode n, r the distance and D the maximum data selection radius. The wavenumbers k_n are chosen such that the derivative of J_0 is zero at r=D. Expansion (1) includes a constant term (mode 0) with k=0. The spectrum of the analysis response is controlled by D and N, and the spectrum A_n. The parameters D and N define the smallest wave that can be seen by the analysis. For a given value of D, an equivalent spherical wavenumber can be defined for every mode in (1).

The control runs, i.e. the operational (pre-July 1988) analysis, used N=5, while in the HRA runs N is set to 8. In the operational system, D is approximately 4400 km at 15°S which means that radial mode 5 corresponds to spherical wavenumber 24. In the HRA scheme, D is about 3400 km and mode 8 then corresponds to spherical wavenumber 48. The preferred response to wind data can be inferred from the forecast error correlations for wind. Figures 1a and 1b show the operational and HRA correlations for the longitudinal-longitudinal wind (L-L) and for transverse-transverse wind (T-T) respectively. The length scale of the correlations has been substantially reduced in HRA.

The other major change relative to the control runs is the retuning of the forecast error variances with the latest data assimilation statistics. A significant increase in the specified lower tropospheric wind forecast error leads to substantially larger weights being given to wind data. The vertical wind forecast error correlations have been subject to only a minor retuning in the tropics.

The ECMWF analysis scheme has two types of data quality control checks. The observation is, in both tests, compared to an independent estimate of the observed quantity at the observation position. If the difference between the observation and the independent

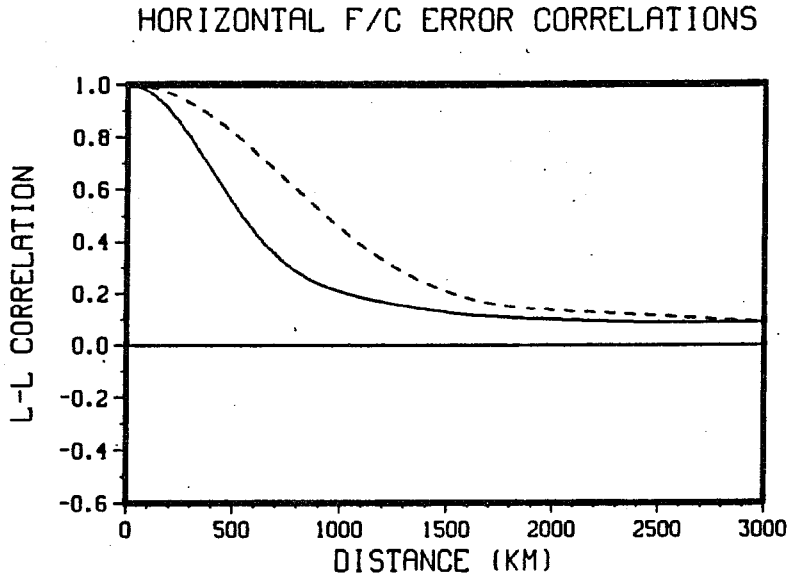

Fig. 1a Operational (dashed) and high resolution analysis (solid) correlations for the longitudinal - longitudinal wind (L-L) at 15°S.

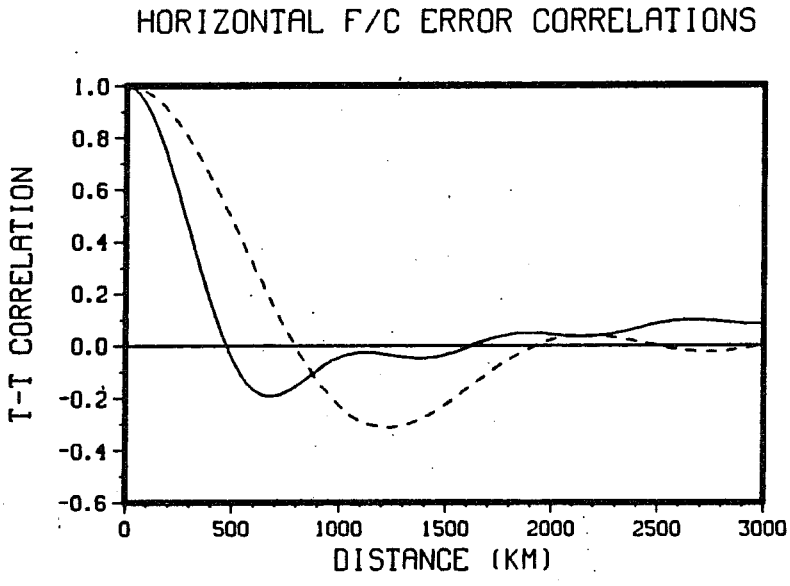

Fig. 1b As in Fig. 1a but for transverse - transverse wind (T-T).

estimate exceeds some predefined tolerance then the observation is assumed to be in error and rejected. These tests are, however, of little use when the error of the independent estimate is large relative to the observation error or when the estimated accuracy of the independent value is seriously in error. Proper tuning of the rejection limits is a necessary prerequisite for obtaining good analysis response to data.

The standard quality control limits are too stringent for observations in the vicinity of tropical cyclones. This would cause rejection of good data because of deficiencies in the first guess, for example. In the current study, the tropical cyclone under consideration (tropical cyclone Jason) formed in the Gulf of Carpentaria in Northern Australia. To avoid rejection of correct data, the quality control in the HRA scheme for observations in the region of the Gulf was relaxed and a very coarse check was made on the data. This ensured that all data, particularly wind data, in the vicinity of the cyclone were accepted by the analysis.

The check against the background value, i.e. the first-guess check, is intended to identify and reject observations with gross errors. Then the main burden of the quality control is carried by the test against an independent analysis using neighbouring observations. The usefulness of these checks is reduced by shortcomings in the forecast model in predicting extreme atmospheric events. A large departure caused by a poor background field might erroneously be regarded as a corrupt observation and rejected. Structures, like the core of a tropical cyclone, which cannot be resolved in the model can also not be resolved by the analysis as it tries to analyse data onto the model grid. Nor are these structures resolved in the independent analysis for quality control and therefore that test will reject many observations which represent shorter scales than can be resolved by the analysis. The analysis therefore rejects data on structures it cannot resolve on the model grid (Lorenc, 1981) consistent with its underlying assumptions.

Besides the use of HRA, the experiments reported here use the Betts-Miller adjustment scheme (Betts and Miller, 1984) to parametrize cumulus convection, rather than the Kuo parametrization used operationally. This scheme was used because it is found to produce better simulations of tropical cyclones in the Australian region (see Part II) than the operational scheme.

3. RESULTS

Two data assimilation experiments for the period 0000 GMT 8 February 1987 to 1200 GMT 13 February 1987 were carried out. In the control experiment (to be referred to as CNTL) the operational analysis scheme was used, whereas in the second experiment (to be referred to as HRES) the high resolution analysis together with the modified quality control was used to ensure that all wind data and most mass data in the region of the Gulf of Carpentaria were accepted by the analysis. Both experiments used the Betts-Miller adjustment scheme. The period of assimilation covered part of the life cycle of tropical cyclone Jason which formed in the Gulf of Carpentaria on 7 February and lasted until 13 February. During this period the cyclone was within the enhanced data network of AMEX and was well observed. Figure 2 shows the best track for the cyclone, issued by the Australian Bureau of Meteorology.

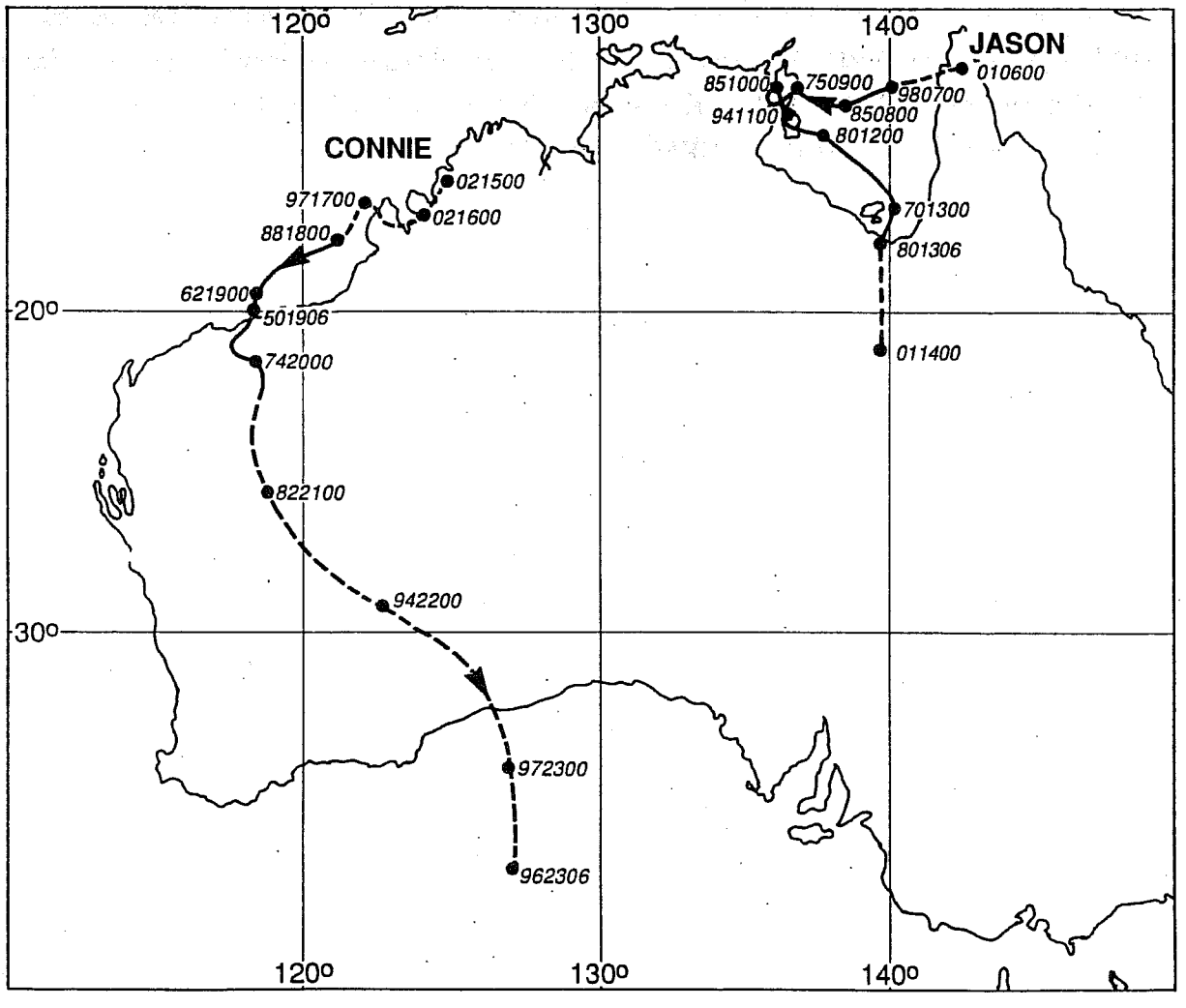

Fig. 2 Track of tropical cyclone Jason.

Figures 3 to 6 show the sea level pressure and 850 mb wind analyses from the two assimilations at 12 hour intervals starting from 1200 GMT 10 February 1987. The format of the figures is such that the left hand panels show the analyses from CNTL and the right hand panels from HRES. The upper panels indicate data not used by the analysis and the bottom panels show the data accepted unconditionally by the analysis. In the upper panels, flags of zero indicate that the data were not considered useful for the analysis, whereas flags greater than zero indicate rejection of data because of assumed poor quality. The main feature to note in the figures is that some sea level pressure data are flagged with zero because observations from the same station closer to the analysis time were available. No wind or mass data are rejected in HRES. On the other hand, in CNTL some mass and wind data in the vicinity of the cyclone are rejected. In particular, note the rejection (Fig. 3b) of the 850 mb wind at station 94150 (Gove; 12°S, 137°E) on 1200 GMT 10 February. From 1200 GMT 10 February to 1200 GMT 11 February the positions of the cyclone in HRES are much closer to the 'observed' best track than in CNTL which places the cyclone too far to the east. The position error in CNTL analyses, which can be as large as 3°, will have an impact both on the subsequent analyses (through errors in the first guess) and on forecasts of the cyclone track. The figures indicate that the use of HRA together with forced insertion of data have the potential to improve the analyses of the positions of tropical cyclones and suggest that using bogus data for tropical cyclone analyses, as done at institutes such as UKMO, could be beneficial.

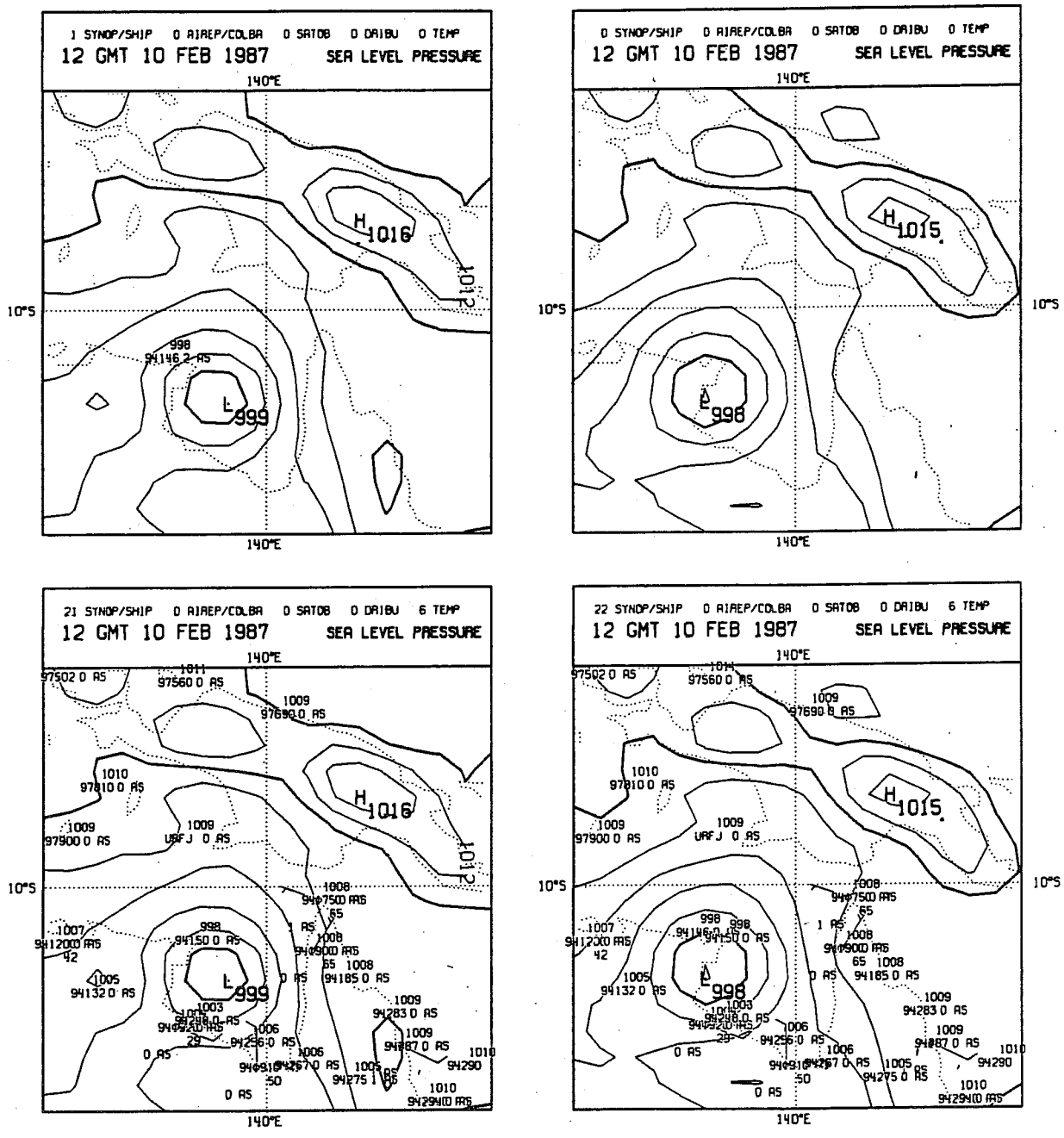

Fig. 3a Sea level pressure analyses from CNTL (left column) and HRES system (right column) for 1200 GMT February 10. Upper panels indicate data not used by analysis scheme and bottom panels show data accepted unconditionally by the analysis. Units are mb and contour interval is 2 mb. The surface pressure from station 94146 was used in HRES but not in CNTL. The observed sea level pressure (hPa) at a station is plotted on the first row. The second row contains station identifier, final flag and how far the datum reached in the analysis (FG = single level first-guess check, ML = multi-level first-guess check, AS = analysis check). For radiosonde, a third row containing the observed height of 1000 hPa is plotted. Only data indicated by AS and final flag value of 0 or 1 have been used by the analysis scheme.

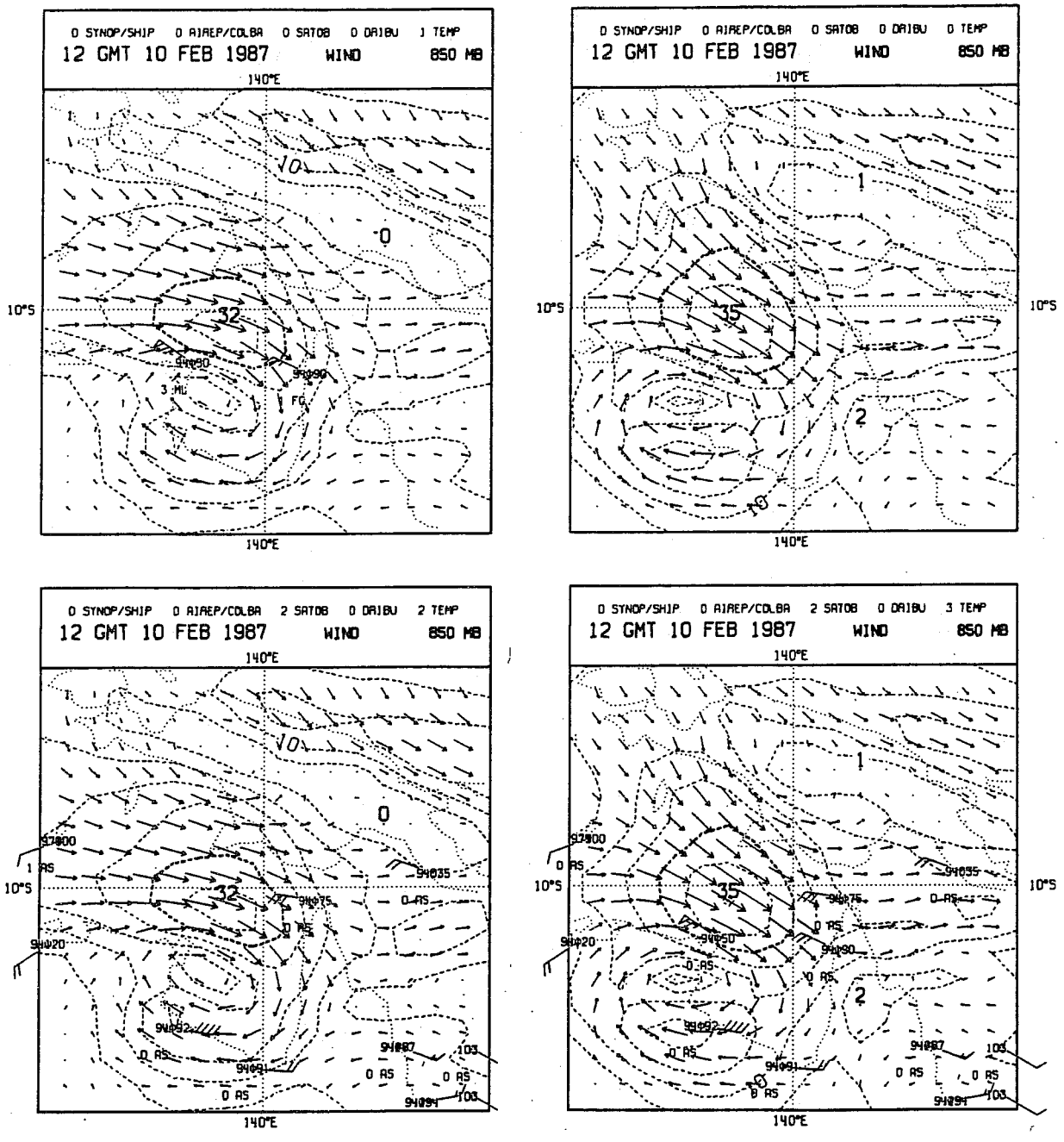

Fig. 3b As in Fig. 3a but for vector wind and isotachs at 850 mb. Units are ms^{-1} and contour interval for isotachs is 5 ms^{-1}. Winds from stations 94150 and 94190 used in HRES but not in CNTL. The station number, final flag and where it was set have been plotted for every wind observation.

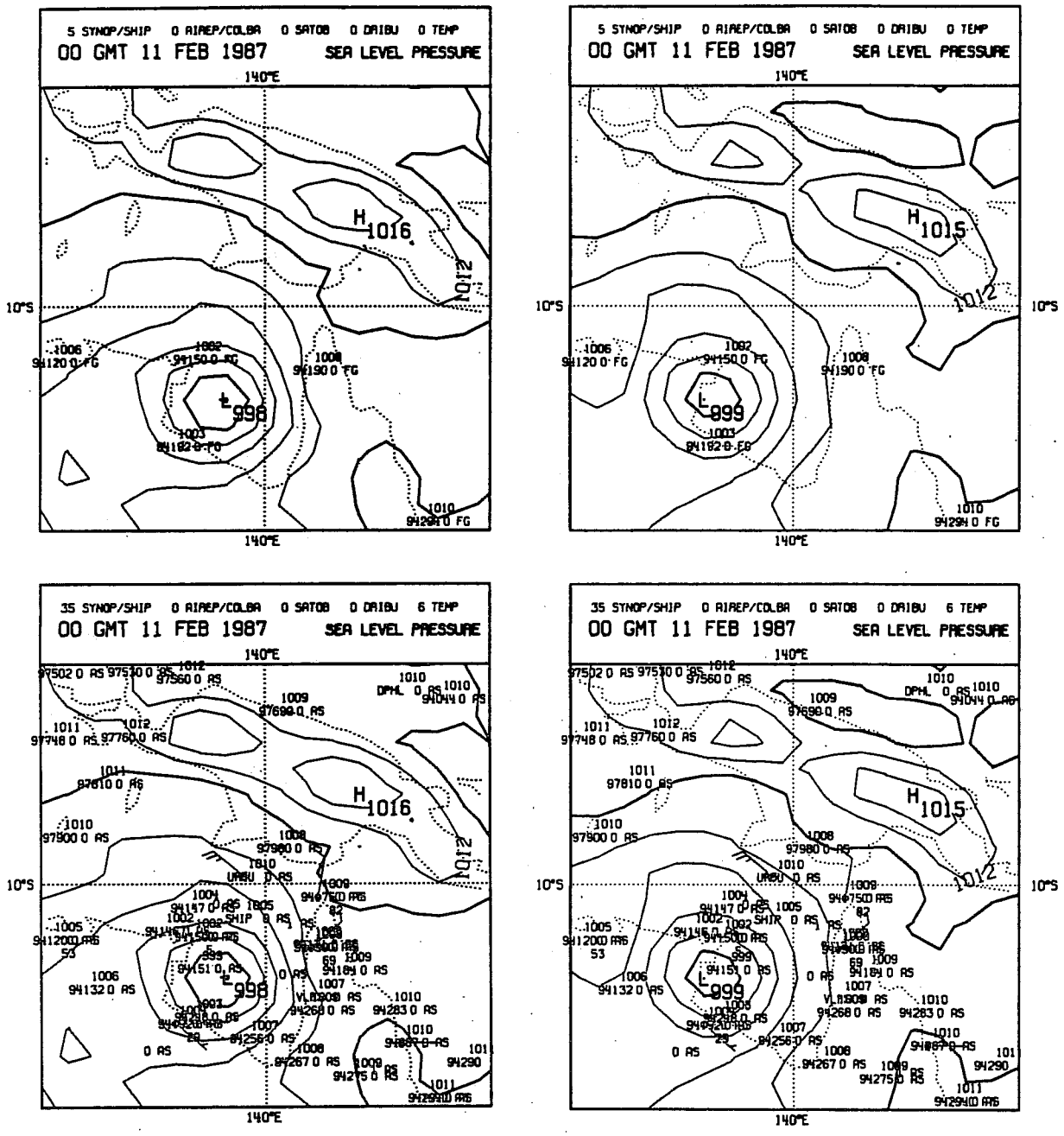

Fig. 4a As in Fig. 3a but for 0000 GMT February 11. No Quality Control differences.

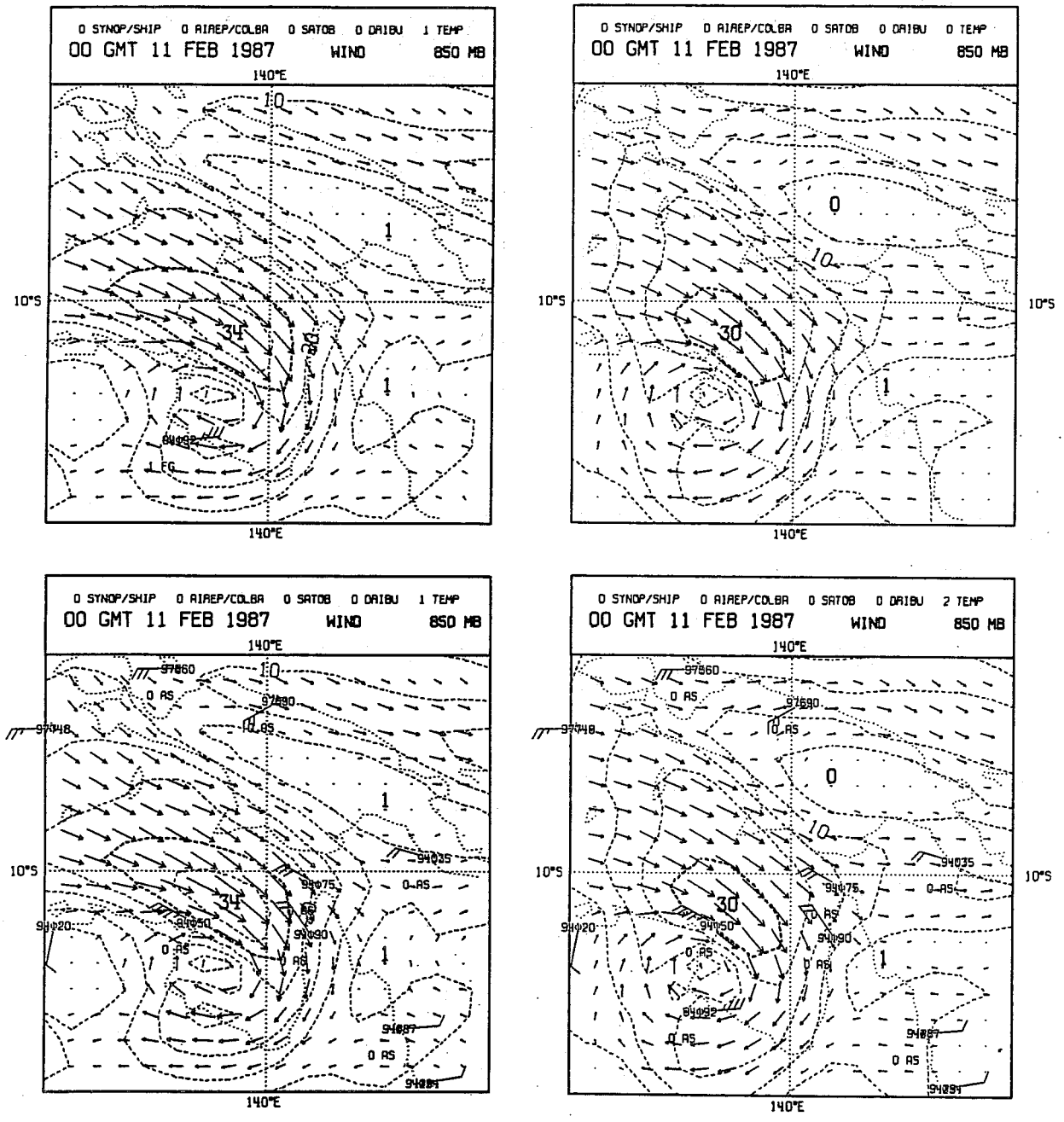

Fig. 4b As in Fig. 3b but for 0000 GMT February 11. The wind from station 94192 used in HRES but not in CNTL.

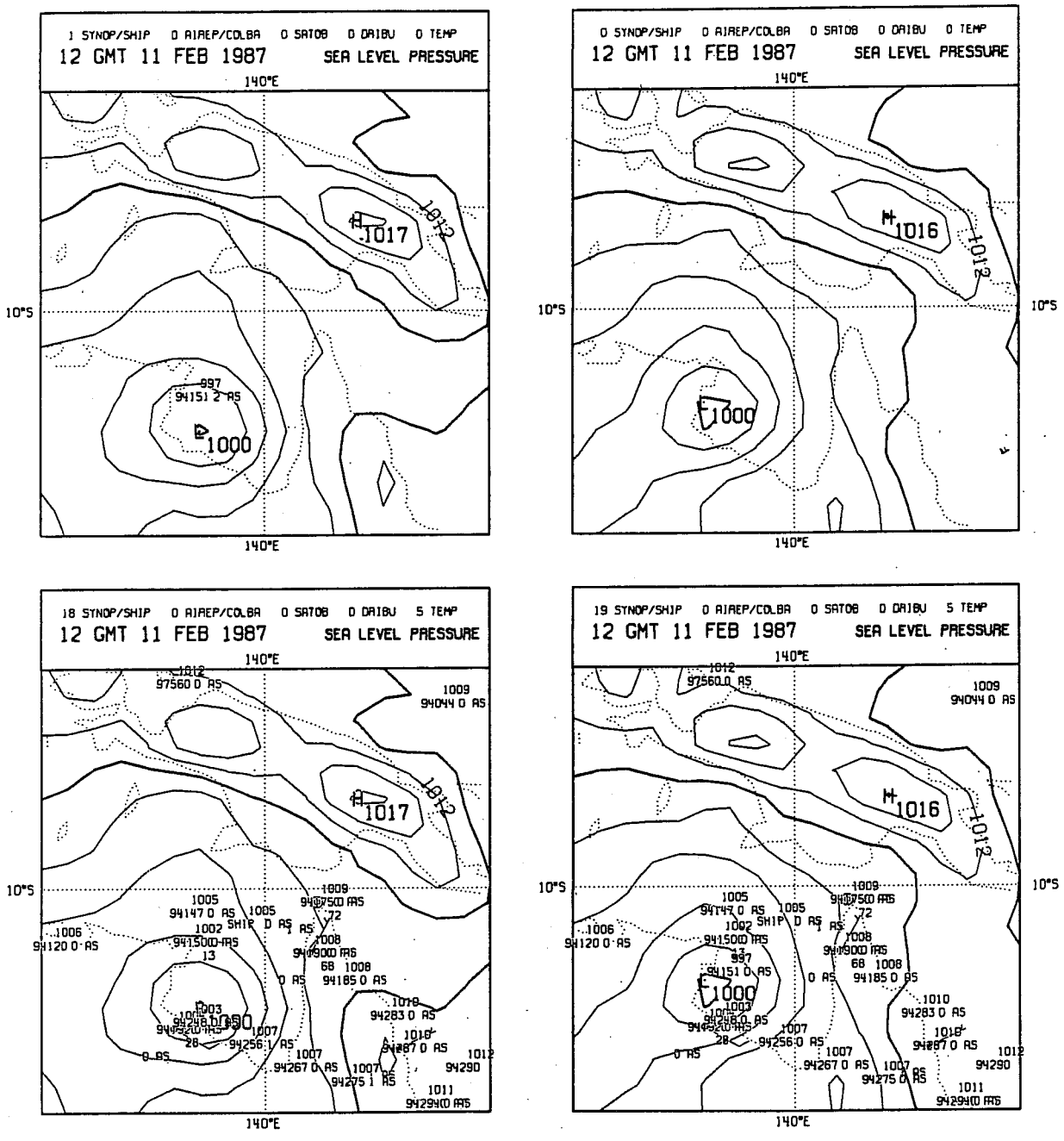

Fig. 5a As in Fig. 3a but for 1200 GMT February 11. Surface pressure from station 94151 used in HRES but not in CNTL.

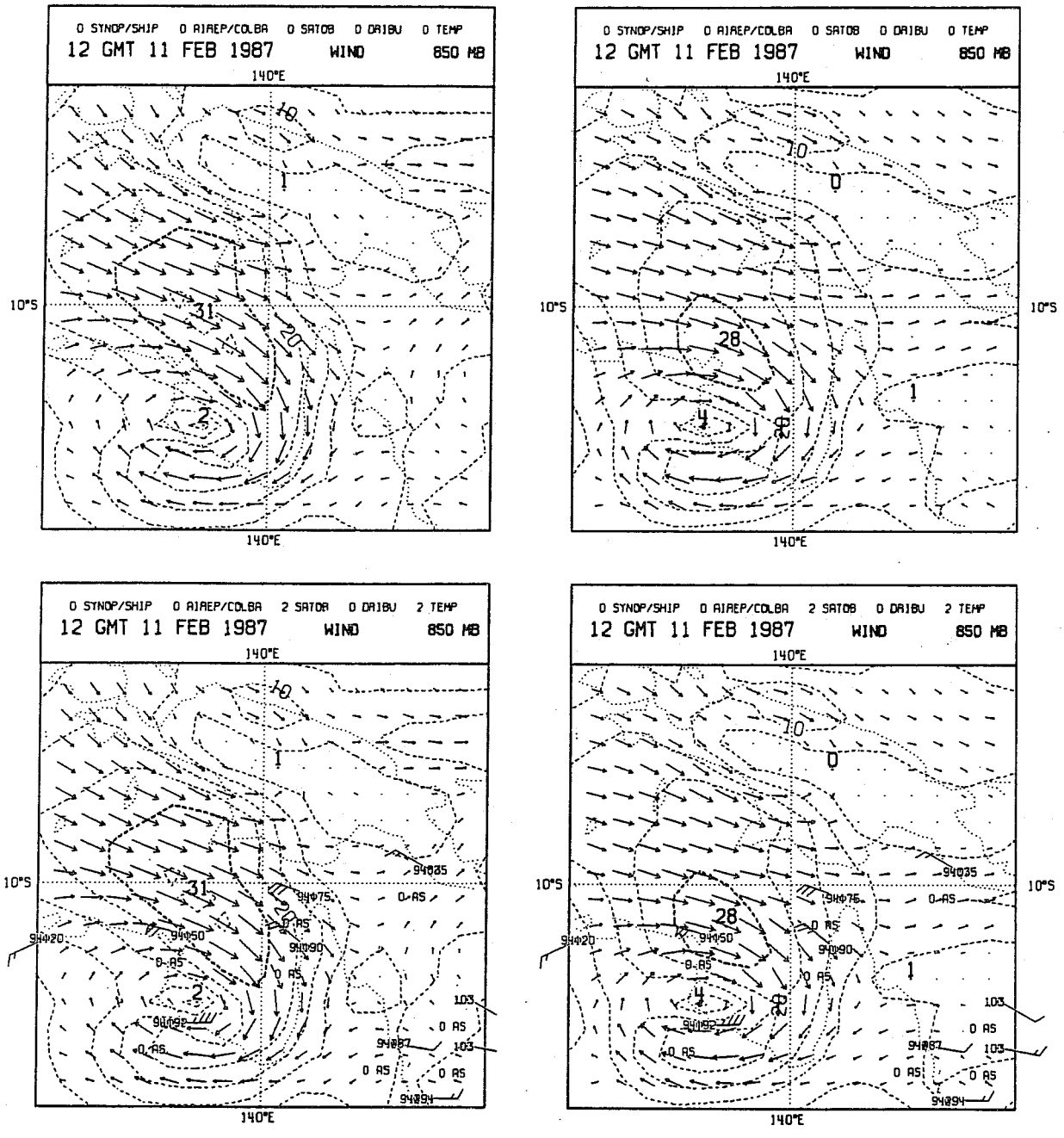

Fig. 5b As in Fig. 3b but for 1200 GMT February 11. No Quality Control differences.

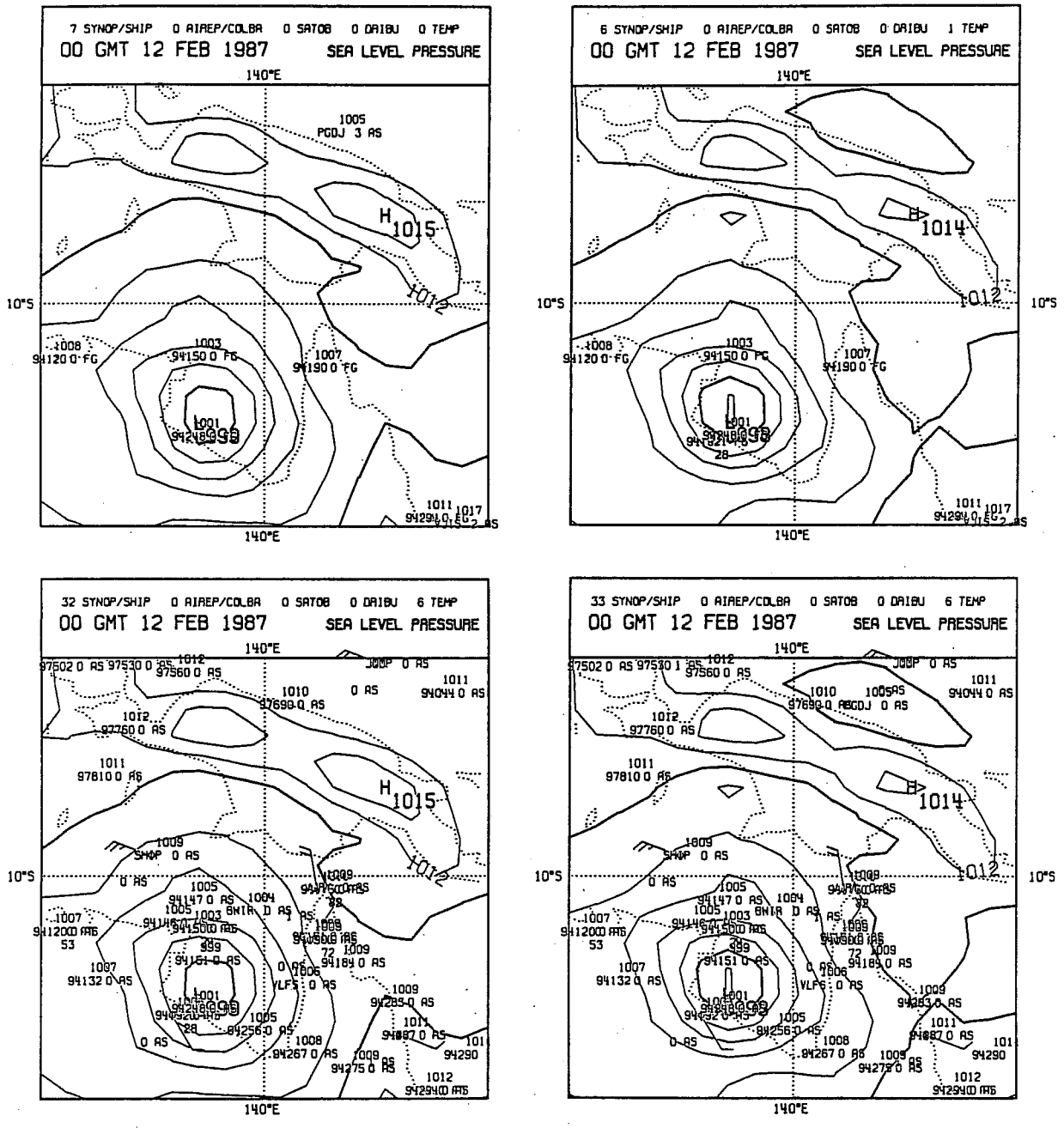

Fig. 6a As in Fig. 3a but for 0000 GMT February 12. Surface pressure from SHIP PGDJ used in HRES but not in CNTL.

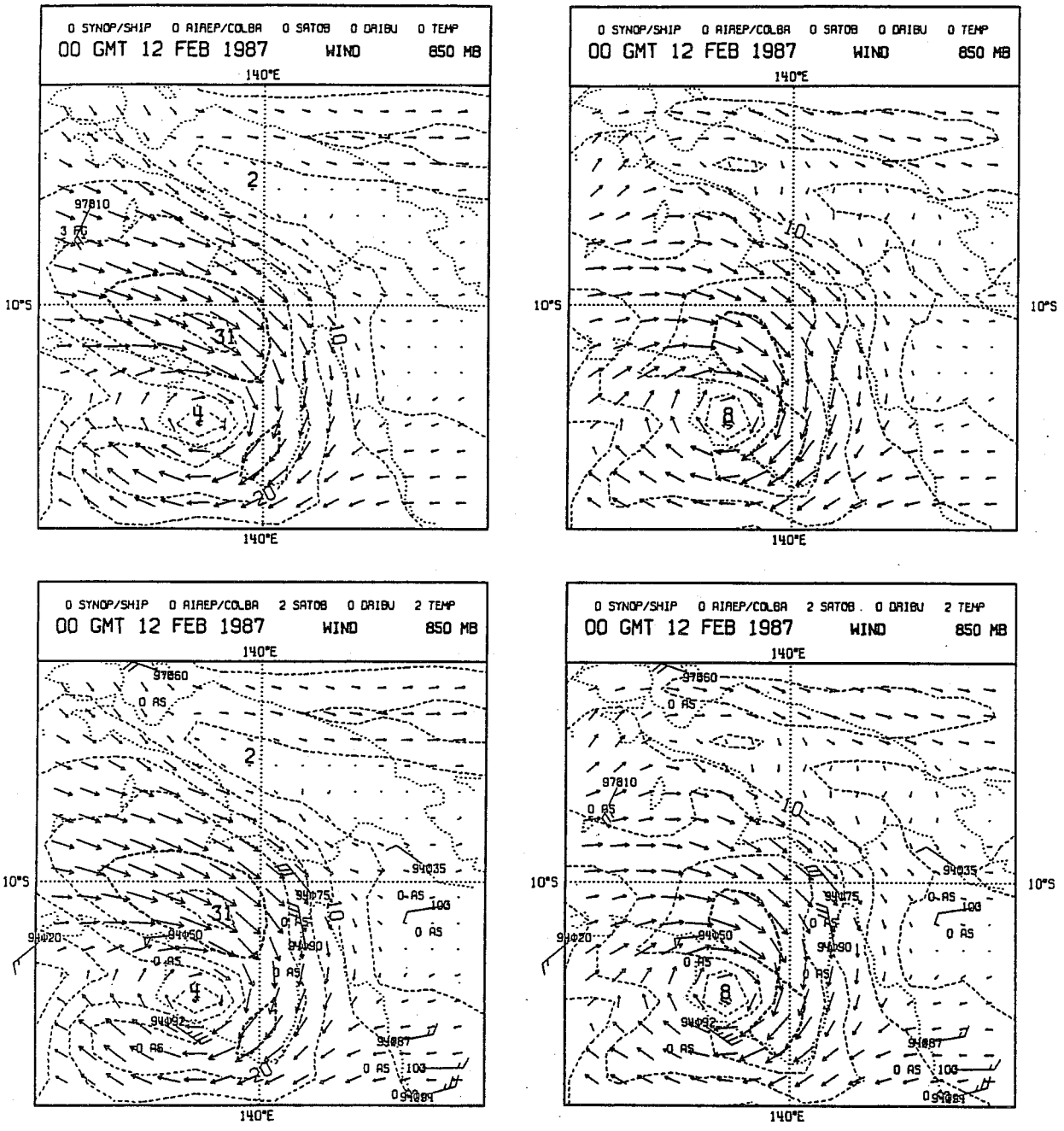

Fig. 6b As in Fig. 3b but for 0000 GMT February 12. Wind from station 97810 used in HRES but not in CNTL.

The HRA scheme is designed to give a more detailed description of the flow and it should show improved agreement between the observed and analysed wind field. Figs. 7a to 7c show the observed wind (magnitude and direction) together with the first guess, analysis and initialised analysis at three stations around the Gulf of Carpentaria. In general, the high resolution analysis is able to reduce the forecast errors (i.e. first guess errors) substantially and the analysed wind agrees reasonably well with the observations whereas the response of the CNTL analysis is not satisfactory. Although the HRA scheme draws to within the expected observation errors, it is still not able to cope adequately with strong vertical shears. This is evident for station 94150 (Fig. 7a) where the strongest flow is observed near the top of the boundary layer with a marked decrease of the wind speed above it. The first guess for the CNTL system shows a rather uniform structure of the wind field which is not significantly altered by the analysis. The first guess for this station in the HRA system has more structure in the boundary layer but overestimates the wind speed in the free atmosphere. The high resolution analysis in this case reduces the error substantially although it does not adequately handle the strong vertical shear.

The improved response by HRA to upper air data has a clearly positive impact on the assimilation of the cyclone when verified against observations from stations 94190 (Fig. 7b) and 94192 (Fig. 7c). In particular, the HRES short range forecast agrees well the observed wind speed and direction at station 94190. The CNTL short range forecast produces uniform wind profiles at stations 94190 (Fig. 7b) and 94192 (Fig. 7c) which verify poorly against the observed winds. In addition to the poor CNTL first-guess, the analysis response by the CNTL scheme is very weak at these stations, while the HRES scheme produces a satisfactory analysis of the wind profile.

A feature of the wind speed profiles shown in Fig. 7 is that the initialised analyses retain most of the information present in the uninitialised analyses indicating that the additional details present in the HRA scheme survive the initialisation step. This feature, which is consistent with geostrophic adjustment theory according to which the mass field should adjust to the wind field in the tropics, and on small vertical and horizontal scales, has implications for bogusing of tropical cyclone data. The results shown above suggest that this should be done for the wind field in preference to the mass field (see Andersson and Hollingsworth, 1988).

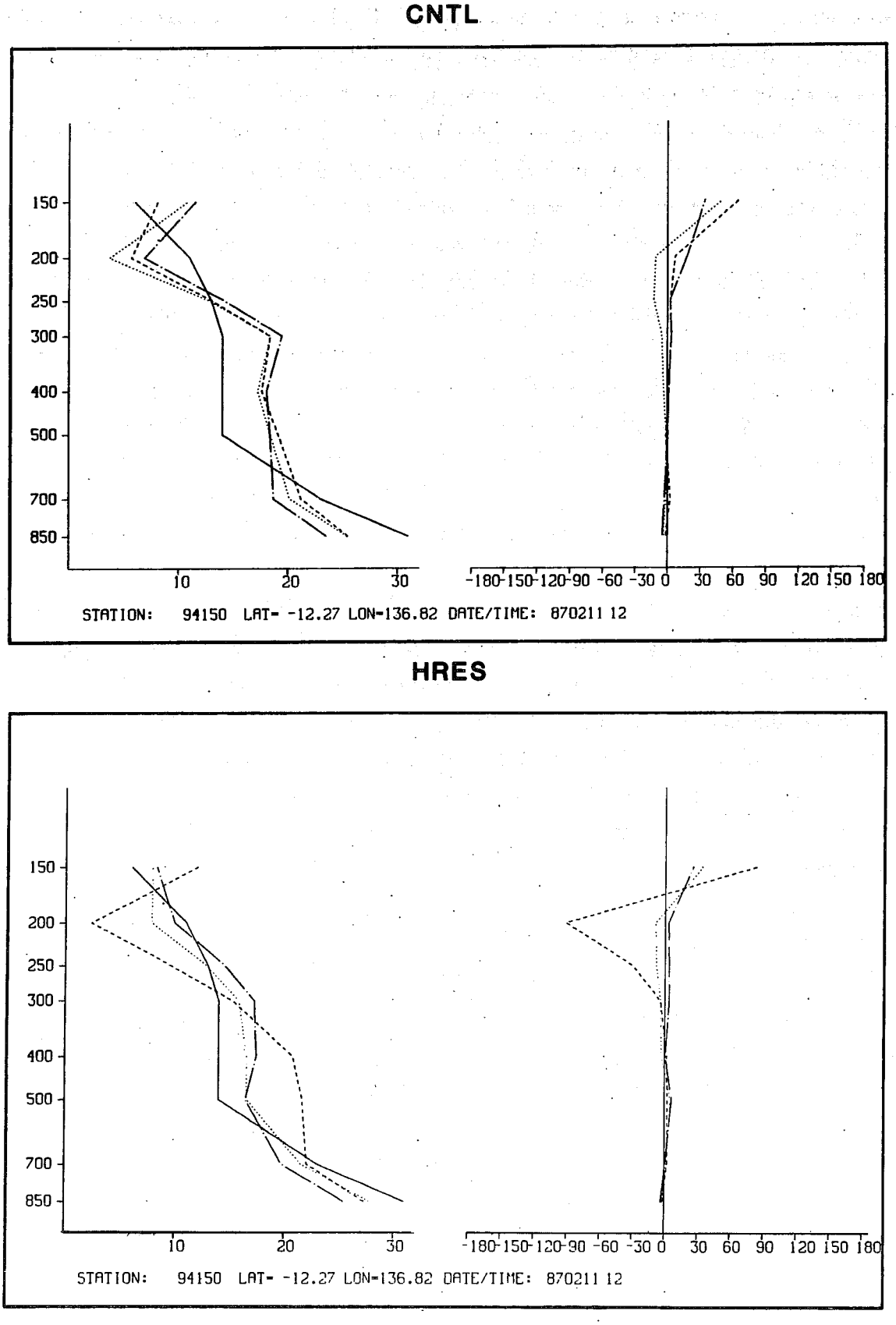

Fig. 7a Observed wind profile (full line) together with the profile for the first guess (dashed), analysis (dots) and initialised analysis (dash-dot) at station 94150 (12°S, 137°E) for 1200 GMT February 11. The wind magnitude (in ms^{-1}) and wind direction (relative to observed wind) are shown in the left and right hand panels respectively.

CNTL

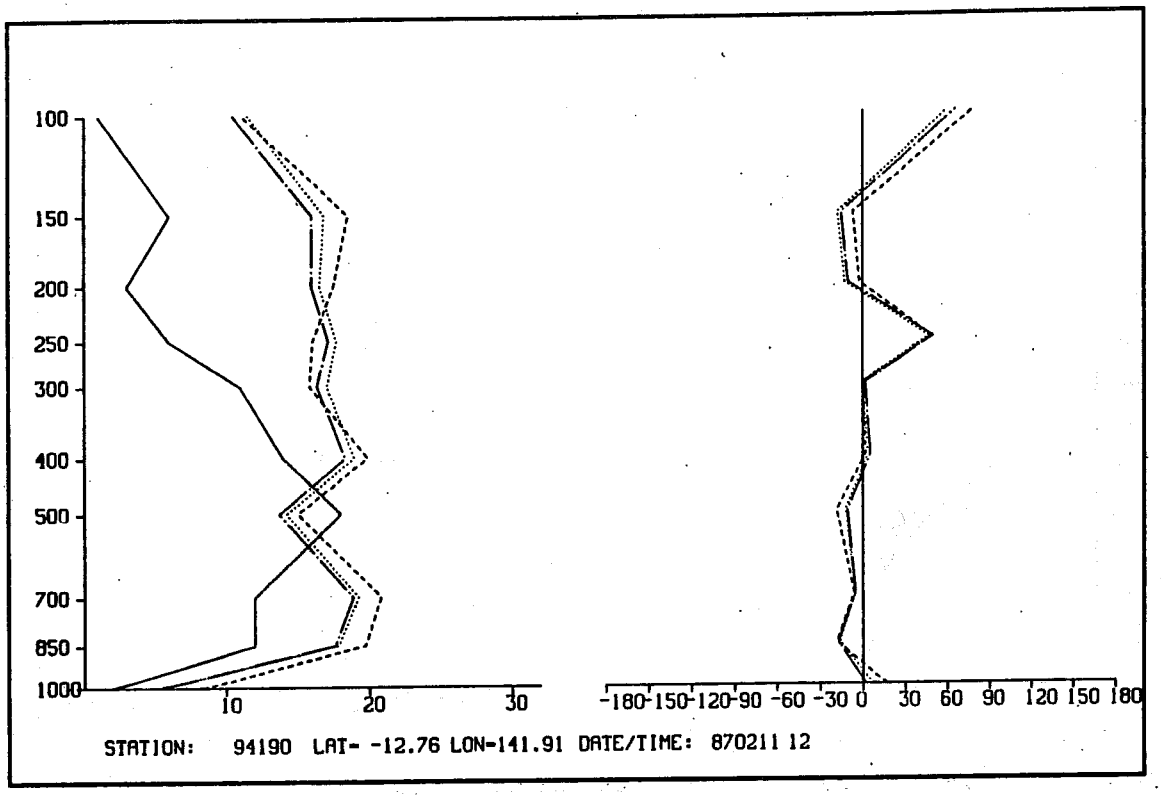

HRES

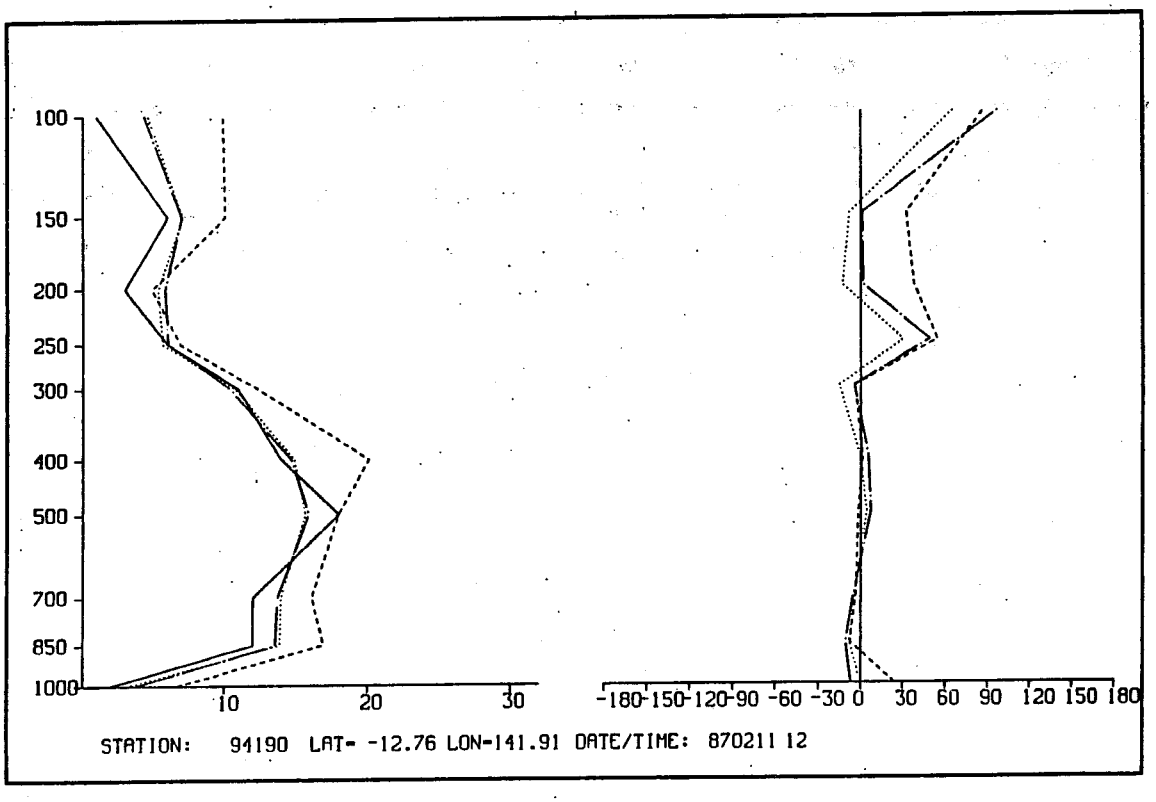

Fig. 7b As in Fig. 7a but for station 94190, 13°S, 142°E.

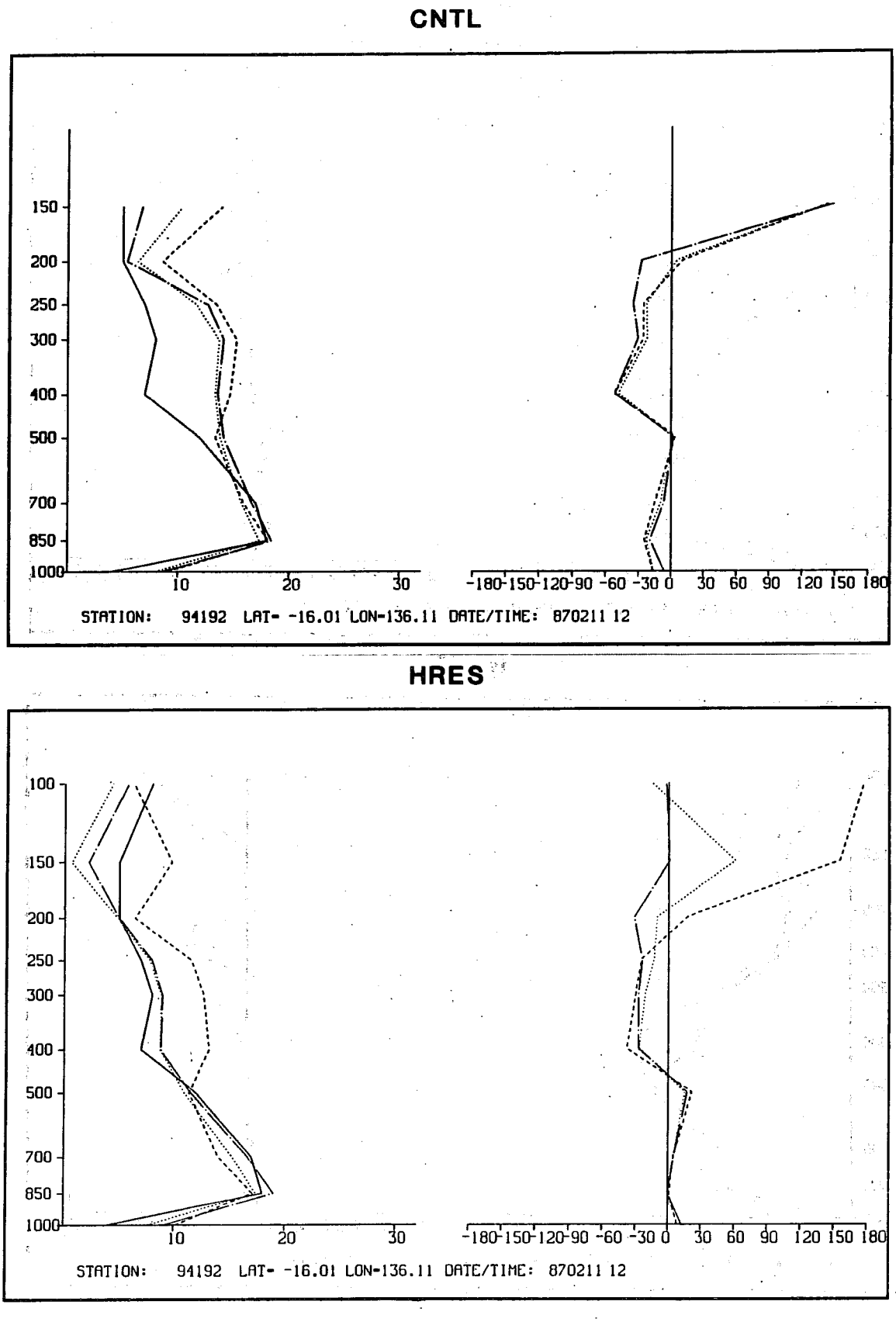

Fig. 7c As in Fig. 7a but for station 94192, 16°S, 136°E.

In order to indicate the impact of HRA analyses on model forecasts, Figs. 8a and 8b show 24 hour forecasts starting from 1200 GMT 10 February and 11 February 1987. The forecasts from the CNTL and HRES analyses are shown in the left and right hand panels respectively. The forecasted cyclone positions and depths can be verified against the best track shown in Fig. 2. The initial location of the cyclone for both days in the CNTL analyses was too far to the east with a position error of 2° to 3° as compared to the best track position. The initial location of the cyclone in the HRES analysis for 10 February is analysed to be somewhat south of the best track while the analysed location for 11 February agrees with the best track position fairly closely. The 24 hour forecasts from 10 February for both systems show significant position errors. The forecast from the HRES analysis of 11 February is much closer to the best track position than that from the CNTL analysis which is located too far to the south, a feature which again reflects the error in the initial condition. Forced insertion of critical radiosonde winds, which were rejected in CNTL, combined with improved analysis response to wind data in HRES produced a more accurate analysis of the cyclone in HRES than in CNTL.

The results presented above indicate some sensitivity of model forecasts of tropical cyclone motion to initial conditions, particularly the analysed location. The two forecasts from the HRES analyses show that the improved location does not necessarily lead to better forecasts. This is perhaps not surprising since there are other factors which also affect the motion of the cyclone. The wind profile in the region of the cyclone could affect the future development of the cyclone and the structure functions used here probably would filter the finer details of the observed profiles. Apart from analysis sensitivity, the motion of a cyclone is also sensitive to other factors in the model, namely resolution and parametrization of physical processes particularly cumulus convection. This sensitivity was described in Part II. All these factors will need to be considered before improved model forecasts of tropical cyclones can be made.

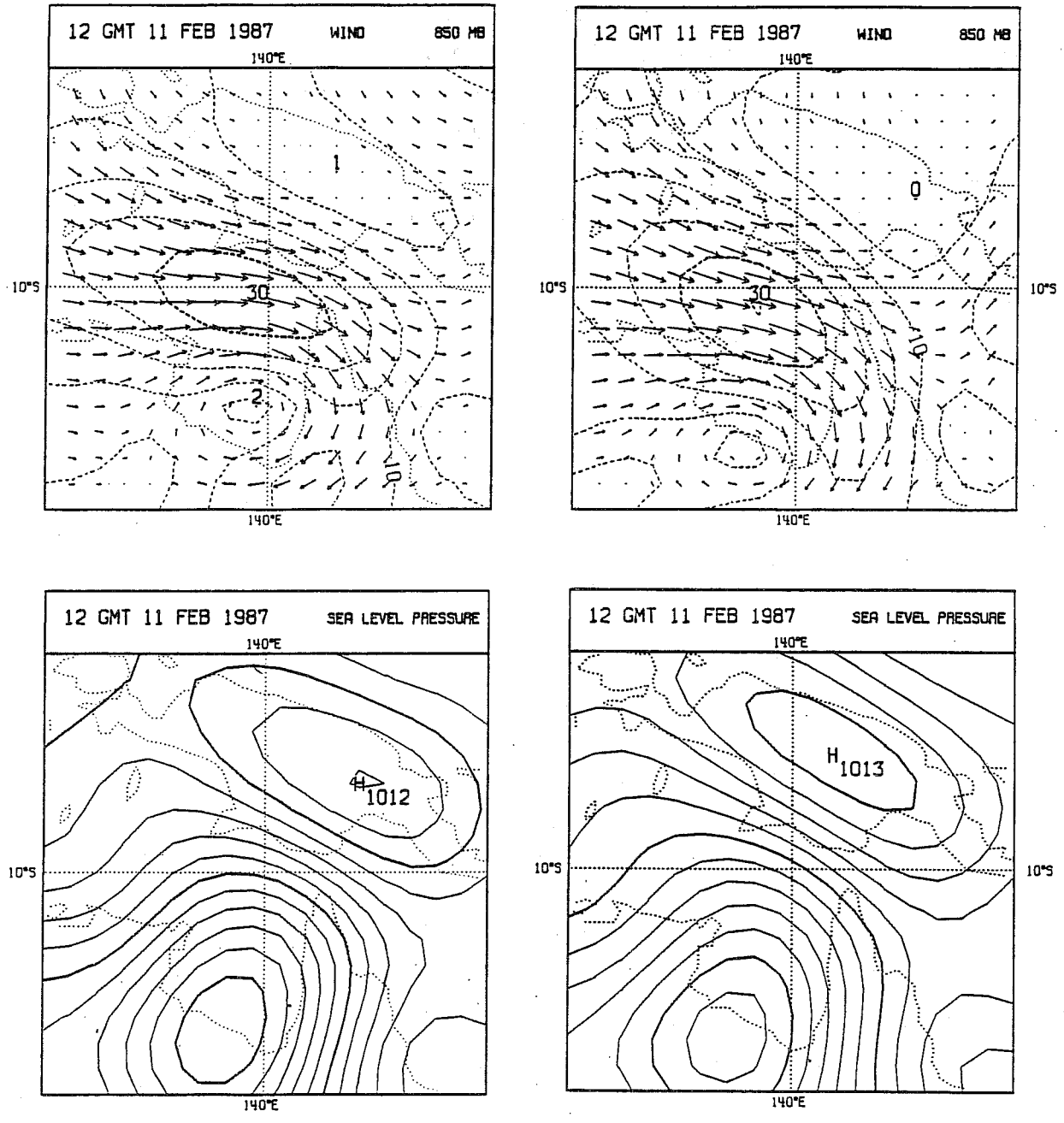

Fig. 8a 24 hour forecasts from 1200 GMT February 10 for CNTL (left column) and HRES (right column) analyses. Sea level pressure is shown in the bottom panels; units are mb and contour interval is 1 mb. Vector wind and isotachs at 850 mb are shown in the upper panels; units are ms^{-1} and contour interval for isotachs is 5 ms^{-1}.

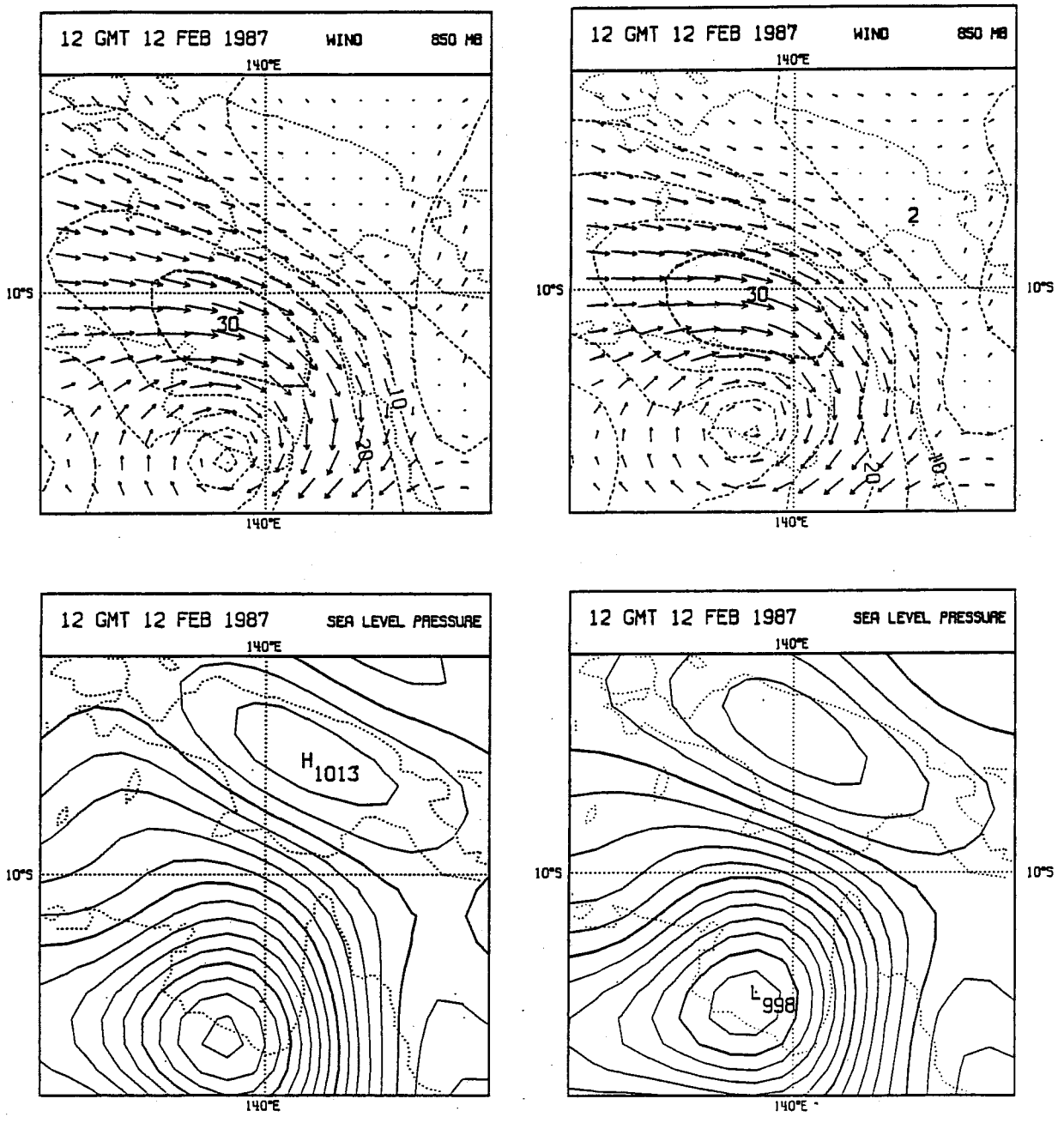

Fig. 8b As in Fig. 8a but for forecasts from 1200 GMT February 11.

4. DISCUSSION

With increasing resolution of global models used operationally and for research, special attention will have to be devoted to the treatment of tropical cyclones by the analysis-forecast systems. One important component is the analysis of tropical cyclones. Although the resolution of the models and the data base is clearly not adequate to define the detailed structure of the cyclones, the analysis system should be able to provide reasonable location of the cyclones and a reasonable description of the large scale environmental flow. The aim of the current study was to address this question for a tropical cyclone which was relatively well observed. It was shown that even with a reasonable data coverage the 1987 ECMWF operational analysis scheme performed poorly in locating the tropical cyclone. This was mainly due to i) rejection of good data because of inadequacies in the first guess and ii) the quality control limits being too stringent in the vicinity of the cyclone. In this study the problem of data rejection was overcome by altering the quality control checks to ensure that all data, particularly wind data, in the region of the cyclone were accepted by the analysis and by using high resolution structure functions to improve the response to these data. This procedure resulted in much improved location of the tropical cyclone. There was also greater detail in the analysed wind profile, in better agreement with the observed data. The greater detail was retained during initialisation, which is important as it suggests that the extra detail can be retained by the model.

The current study is based on a well observed tropical cyclone, which is not a typical situation. Apart from limited regions such as the eastern seaboard of the USA, cyclones in general tend to be poorly observed and the available information on location (and strength) is based on satellite imagery. Even this limited information could be usefully applied in correcting the location of the cyclone. Secondly, a set of bogus or synthetic data, particularly of the wind field could be generated in the region of the cyclones with the wind profiles based on results of previous studies of a large number of tropical cyclones (see for example Frank, 1977). The procedure suggested here is in fact used operationally at the UKMO, and has been tested successfully at ECMWF. In order to make optimal use of the generated bogus data, the high resolution analysis system described in the current study could be used to ensure that the data is not rejected, as was done by Andersson and Hollingsworth (1988).

5. CONCLUSION

Global models such as those used at ECMWF have attained resolutions where small scale systems such as tropical cyclones are beginning to be resolved. Because of the large diversity of the spatial scales and the scope of physical processes involved, tropical cyclone prediction using numerical models raises special problems which will need to be addressed. One such problem is the analysis of these small scale systems, particularly the location of these systems. In this study the sensitivity of analysis of a well observed tropical cyclone to higher resolution structure functions and forcing of data in the vicinity of the tropical cyclone is studied. It is shown that these changes in the analysis system lead to much improved location of the cyclone. The high resolution analysis structure functions are also able to depict more structure in the vertical, although strong wind shears are still not satisfactorily analysed. The procedure described here has obvious applications to using bogus data for tropical cyclone analysis in regions where the data base is inadequate.

References

Andersson, E. and A. Hollingsworth, 1988: Typhoon bogus observations in the ECMWF data assimilation system. ECMWF Technical Memo No. 148, ECMWF, Reading, U.K., 25 pp.

Betts, A.K. and M.J. Miller, 1984: A new convective adjustment scheme. ECMWF Technical Report No. 43, ECMWF, Reading, U.K., 62 pp.

Frank, W.M., 1977: The structure and energetics of the tropical cyclone I. Storm structure. Mon.Wea.Rev., 105, 1119-1135.

Hall, C.D., 1987: Verification of global model forecasts of tropical cyclones during 1986. Meteor. Mag., 116, 216-220.

Heckley, W.A., 1985: The performance and systematic errors of the ECMWF tropical forecasts (1982-1984). ECMWF Technical Report No. 53, ECMWF, Reading, U.K., 92 pp.

Holland, G.J., J.L. McBride, R.K. Smith, D. Jasper and T.D. Keenan, 1986: The BMRC Australian monsoon experiment: AMEX. Bull.Amer.Met.Soc., 67, 1466-1472.

Kanamitsu, M., 1985: A study of the ECMWF operational forecast model in the tropics. ECMWF Technical Report No. 49, Reading, U.K., 73 pp.

Lönnberg, P., 1988: Developments in the ECMWF analysis system. ECMWF Seminar 1988, Reading, U.K.

Lorenc, A.C., 1981: A global three-dimensional multivariate statistical interpolation scheme. Mon.Wea.Rev., 109, 701-721.

Reed, R.J., A. Hollingsworth, W.A. Heckley and F. Delsol, 1988: An evaluation of the performance of the ECMWF operational system in analyzing and forecasting tropical easterly wave disturbances over Africa and the Tropical Atlantic. Mon.Wea.Rev., 116, 824-865.

Tiedtke, M., W.A. Heckley and J. Slingo, 1988: Tropical forecasting at ECMWF: The influence of physical parametrization on the mean structure of forecasts and analyses. Q.J.R.Met.Soc., 114, 639-664.

TECHNICAL REPORTS

No. 1 A case study of a ten day prediction.
K. Arpe, L. Bengtsson, A. Hollingsworth and Z. Janjic. September, 1976

No. 2 The effect of arithmetic precision on some meteorological integrations.
A.P.M. Baede, D. Dent and A. Hollingsworth. December, 1976

No. 3 Mixed-radix fourier transforms without reordering.
C. Temperton. February, 1977

No. 4 A model for medium range weather forecasts - adiabatic formulation.
D.M. Burridge and J. Haseler. March, 1977

No. 5 A study of some parameterisations of sub-grid processes in a baroclinic wave in a two dimensional model.
A. Hollingsworth. July, 1977

No. 6 The ECMWF analysis and data assimilation scheme: analysis of mass and wind field.
A. Lorenc, I. Rutherford and G. Larsen. December, 1977

No. 7 A ten-day high-resolution non-adiabatic spectral integration; a comparative study.
A.P.M. Baede and A.W. Hansen. October, 1977

No. 8 On the asymptotic behaviour of simple stochastic-dynamic systems.
A. Wiin-Nielsen. November, 1977

No. 9 On balance requirements as initial conditions.
A. Wiin-Nielsen. October, 1978

No. 10 ECMWF model parameterisation of sub-grid scale processes.
M. Tiedtke, J-F. Geleyn, A. Hollingsworth, and J-F. Louis. January, 1979

No. 11 Normal mode initialization for a multi-level grid-point model.
C. Temperton and D.L. Williamson. April, 1979

No. 12 Data assimilation experiments.
R. Seaman. October, 1978

No. 13 Comparison of medium range forecasts made with two parameterisation schemes.
A. Hollingsworth, K. Arpe, M. Tiedkte, M. Capaldo, H. Savijarvi, O. Akesson and J.A. Woods. October, 1978

No. 14 On initial conditions for non-hydrostatic models.
A.C. Wiin-Nielsen. November, 1978

No. 15 Adiabatic formulation and organization of ECMWF's spectral model.
A.P.M. Baede, M. Jarraud and U. Cubasch. November, 1979

No. 16 Model studies of a developing boundary layer over the ocean.
H. Okland. November, 1979

No. 17 The response of a global barotropic model to forcing by large scale orography.
J. Quiby. January 1980.

No. 18 Confidence limits for verification and energetic studies.
K. Arpe. May, 1980

No. 19 A low order barotropic model on the sphere with orographic and newtonian forcing.
E. Kallen. July, 1980

No. 20 A review of the normal mode initialization method.
Du Xing-yuan. August, 1980

No. 21 The adjoint equation technique applied to meteorological problems.
G. Kontarev. September, 1980

No. 22 The use of empirical methods for mesoscale pressure forecasts.
P. Bergthorsson. November, 1980

No. 23 Comparison of medium range weather forecasts made with models using spectral or finite difference techniques in the horizontal.
M. Jarraud, C. Girard and U. Cubasch. February, 1981

No. 24 On the average error of an ensemble of forecasts.
J. Derome. February, 1981

No. 25 On the atmospheric factors affecting the Levantine Sea.
E. Ozsoy. May, 1981

No. 26 Tropical influences on stationary wave motion in middle and high latitudes.
A.J. Simmons. August, 1981

No. 27 The energy budgets in North America, North Atlantic and Europe based on ECMWF analysis and forecasts.
H. Savijarvi. November, 1981

No. 28 An energy and angular momentum conserving finite-difference scheme, hybrid coordinates and medium range weather forecasts.
A.J. Simmons and R. Strüfing. November, 1981

No. 29 Orographic influences on Mediterranean lee cyclogenesis and European blocking in a global numerical model.
S. Tibaldi and A. Buzzi. February, 1982

No. 30 Review and re-assessment of ECNET - A private network with open architecture.
A. Haag, F. Konigshofer and P. Quoilin. May, 1982

No. 31 An investigation of the impact at middle and high latitudes of tropical forecast errors.
J. Haseler. August, 1982

No. 32 Short and medium range forecast differences between a spectral and grid point model. An extensive quasi-operational comparison. C. Girard and M. Jarraud
August, 1982

No. 33 Numerical simulations of a case of blocking: The effects of orography and land-sea contrast.
L.R. Ji and S. Tibaldi. September, 1982

No. 34 The impact of cloud track wind data on global analyses and medium range forecasts.
P. Kallberg, S. Uppala, N. Gustafsson and J. Pailleux. December, 1982

No. 35 Energy budget calculations at ECMWF. Part 1: Analyses 1980-81.
E. Oriol. December, 1982

No. 36 Operational verification of ECMWF forecast fields and results for 1980-1981.
R. Nieminen. February, 1983

No. 37 High resolution experiments with the ECMWF model: a case study.
L. Dell'Osso. September, 1983

No. 38 The response of the ECMWF global model to the El-Nino anomaly in extended range prediction experiments.
U. Cubasch. September, 1983

No. 39 On the parameterisation of vertical diffusion in large-scale atmospheric models.
M.J. Manton. December, 1983

No. 40 Spectral characteristics of the ECMWF objective analysis system.
R. Daley. December, 1983

No. 41 Systematic errors in the baroclinic waves of the ECMWF model.
E. Klinker and M. Capaldo. February, 1984

No. 42 On long stationary and transient atmospheric waves.
A.C. Wiin-Nielsen. August, 1984

No. 43 A new convective adjustment scheme.
A.K. Betts and M.J. Miller. October, 1984

No. 44 Numerical experiments on the simulation of the 1979 Asian summer monsoon.
U.C. Mohanty, R.P. Pearce and M. Tiedtke. October, 1984

No. 46 Cloud prediction in the ECMWF model.
J. Slingo and B. Ritter. January, 1985

No. 47 Impact of aircraft wind data on ECMWF analyses and forecasts during the FGGE period, 8-19 November, 1979.
A.P.M. Baede, P. Kallberg and S. Uppala. March, 1985

No. 48 A numerical case study of East Asian coastal cyclogenesis.
Shou-jun Chen and L. Dell'Osso. May, 1985

No. 49 A study of the predictability of the ECMWF operational forecast model in the tropics.
M. Kanamitsu. September, 1985

No. 50 On the development of orographic cyclones.
D. Radinovic. June, 1985

No. 51 Climatology and system error of rainfall forecasts at ECMWF.
F. Molteni and S. Tibaldi. October, 1985

No. 52 Impact of modified physical processes on the tropical simulation in the ECMWF model.
U.C. Mohanty, J.M. Slingo and M. Tiedtke. October, 1985

No. 53 The performance and systematic errors of the ECMWF tropical forecasts (1982-1984).
W.A. Heckley. November, 1985

No. 54 Finite element schemes for the vertical discretization of the ECMWF forecast model using linear elements.
D.M. Burridge, J. Steppeler and R. Strüfing. January, 1986

No. 55 Finite element schemes for the vertical discretization of the ECMWF forecast model using quadratic and cubic elements.
J. Steppeler. February, 1986

No. 56 Sensitivity of medium-range weather forecasts to the use of an envelope orography.
M. Jarraud, A.J. Simmons and M. Kanamitsu. September, 1986

No. 57 Zonal diagnostics of the ECMWF 1984-85 operational analyses and forecasts.
C. Brankovic. October, 1986

No. 58 An evaluation of the performance of the ECMWF operational forecasting system in analysing and forecasting tropical easterly wave disturbances. Part 1: Synoptic investigation.
R.J. Reed, A. Hollingsworth, W.A. Heckley and F. Delsol. September, 1986

No. 59 Diabatic nonlinear normal mode initialisation for a spectral model with a hybrid vertical coordinate.
W. Wergen. January, 1987

No. 60 An evaluation of the performance of the ECMWF operational forecasting system in analysing and forecasting tropical easterly wave disturbances. Part 2: Spectral investigation.
R.J. Reed, E. Klinker and A. Hollingsworth. January, 1987

No. 61 Empirical orothogonal function analysis in the zonal and eddy components of 500 mb height fields in the Northern extratropics.
F. Molteni. January, 1987

No. 62 Atmospheric effective angular momentum functions for 1986-1987.
G. Sakellarides. February 1989

No. 63 A verification study of the global WAM model. December 1987 - November 1988.
L. Zambresky. May 1989

No. 64 Impact of changes to the radiation scheme in the ECMWF model.
J-J. Morcrette. November 1989.